AD_____

Award Number: DAMD17-98-1-8509

TITLE: Fluid Flow Sensitivity of Bone Cells as a Function of Age

PRINCIPAL INVESTIGATOR: Christopher R. Jacobs, Ph.D.

CONTRACTING ORGANIZATION: The M.S. Hershey Medical Center
Hershey, Pennsylvania 17033-0850

REPORT DATE: October 2000

TYPE OF REPORT: Annual

PREPARED FOR: U.S. Army Medical Research and Materiel Command
Fort Detrick, Maryland 21702-5012

REPORT DOCUMENTATION PAGE

Form Approved
OMB No. 074-0188

1. AGENCY USE ONLY (Leave blank)	2. REPORT DATE	3. REPORT TYPE AND DATES COVERED
	October 2000	Annual (1 Oct 99 - 30 Sep 00)

4. TITLE AND SUBTITLE
Fluid Flow Sensitivity of Bone Cells as a Function of Age

5. FUNDING NUMBERS
DAMD17-98-1-8509

6. AUTHOR(S)
Christopher R. Jacobs, Ph.D.

7. PERFORMING ORGANIZATION NAME(S) AND ADDRESS(ES)
The M.S. Hershey Medical Center
Hershey, Pennsylvania 17033-0850

E-MAIL:
cjacobs@psu.edu

8. PERFORMING ORGANIZATION REPORT NUMBER

9. SPONSORING / MONITORING AGENCY NAME(S) AND ADDRESS(ES)
U.S. Army Medical Research and Materiel Command
Fort Detrick, Maryland 21702-5012

10. SPONSORING / MONITORING AGENCY REPORT NUMBER

11. SUPPLEMENTARY NOTES

12a. DISTRIBUTION / AVAILABILITY STATEMENT
Approved for public release; Distribution unlimited

12b. DISTRIBUTION CODE

13. ABSTRACT *(Maximum 200 Words)*

In the second year of the project we have completed aim one and have completed half of aim two. For aim one we have demonstrated our hypothesis to be true, namely that gap junctional intercellular communication modulates the PGE2 response of bone cells to oscillating fluid flow. Interestingly, we found that PGE_2 release in response to oscillating flow does not appear to involve intracellular calcium. This has important implications because it indicates that other second messengers, such as the cyclic AMP pathway, may be important in transducing the fluid flow signal into the PGE_2 response. Additionally, the differential effect of oscillating fluid flow on intracellular calcium versus PGE_2 may prove to be a powerful tool in further investigations of the bone cell mechanotransduction pathway. We have begun work on our second task (aim 2) and have determined that while the $[Ca^{2+}]_i$ response to fluid flow does decrease as a function of age, gap junctional intercellular communication does not. These results have produced numerous scientific presentations and abstracts as well as one manuscript in review and two manuscripts in preparation. Finally, the results have been incorporated into two applications to the NIH which have been approved for funding.

14. SUBJECT TERMS
Key Words: Mechanotransduction, Osteoblasts, Osteocytes, Fluid Flow, Gap Junction, Adaptation, Remodeling, Mechanical Loading

15. NUMBER OF PAGES
113

16. PRICE CODE

17. SECURITY CLASSIFICATION OF REPORT	18. SECURITY CLASSIFICATION OF THIS PAGE	19. SECURITY CLASSIFICATION OF ABSTRACT	20. LIMITATION OF ABSTRACT
Unclassified	Unclassified	Unclassified	Unlimited

Table of Contents

Introduction

Bone cells are normally found in voids in the mineralized matrix known as lacunae. Small tubes in the matrix, known as canaliculi, interconnect the lacunae and are occupied by cellular processes. Gap junctions form where the processes of neighboring cells come into contact allowing for cell-cell communication via signaling substances. The extracellular space between the cell membrane and the mineralized matrix is filled with fluid which communicates with the bone's vascular supply. As the bone matrix is cyclically loaded due to physical activity, fluid flows in the lacunar-canalicular network from regions of high matrix strain to regions of low matrix strain and back again. Physiologic levels of this oscillating fluid flow has been shown to be a potent stimulator of bone cells *in vitro*. Additionally, we have shown that flow induced signals are transmitted from cell to cell such that cells that are not responding to flow directly can indirectly respond to flow-induced signals transmitted via gap junctions from adjacent cells. The consequence of this is that an ensemble of cells coupled via gap junctions is more sensitive to the effects of fluid flow than an equivalent collection of uncoupled cells. Our central hypothesis is that *there is an age-related decrease in the cellular responsiveness to fluid flow which is compounded by a decrease in cell-cell communication.*

In the prior funding period we had made the following key findings:

- Discovered that neither ROS cells nor the RCx16 and ROS/Cx45 transfectants of ROS cells exhibit increase $[Ca^{2+}]_i$ in response to oscillating fluid flow.
- Discovered that ROS cells as well as the RCx16 and ROS/Cx45 transfectants of ROS cells release PGE2 in response to oscillating fluid flow.
- Accumulated early evidence that cell-cell communication via gap junctions plays an important role in regulating bone cell anabolism.

In light of these findings, in the funding period just completed we have repeated these experiments with the MC3T3-E1 osteoblastic cell line known to respond to fluid flow with a $[Ca^{2+}]_i$ response. We utilized a recently created transfectant that employs a dominant-negative strategy to diminish gap junctional intercellular communication with time in culture.

Body

Aim 1: (Year 1) Demonstrate that the responsiveness of a cell ensemble is related to the degree of cell-cell communication. Three immortalized cell lines will be utilized in this aim; ROS (rat osteosarcoma), RCx16, and ROS/Cx45. Both RCx16 and ROS/Cx45 cells are ROS cells that have been transfected (but following different strategies) to limit cell-cell coupling. Previously we have shown that RCx16 and ROS/Cx45 cells are less coupled than ROS cells. The response of the cells will be quantified in terms of intracellular calcium concentration $[Ca^{2+}]_i$ and prostaglandin (PGE_2) release. Flow profiles will include oscillating flow at 0.5Hz, 1Hz and 2Hz as well as steady flow. In a parallel experiment the cell-cell coupling will be determined both in terms of injected dye spreading and calcium wave propagation.

Previously we had demonstrated that ROS, RCx16, and ROS/Cx45 cells release PGE2 in response to oscillatory fluid flow, but do not exhibit increased $[Ca^{2+}]_i$. In this last year we have further investigated the role of gap junctional intercellular communication in the release of PGE2 in response to flow in these cells. We confirmed inhibition of gap junction function by dye spreading in the RCx16 and ROS/Cx45 cell lines. We found that PGE2 release is diminished in cells with inhibited gap junctional communication (RCx16 and ROS/Cx45) relative to those with intact gap junctional communication (ROS) in response to flow. These findings are currently being prepared in manuscript form. However, since ROS cells now appear not to increase $[Ca^{2+}]_i$ in response to oscillatory flow, we elected to continue our work on this aim with the MC3T3-E1 cell line.

The detailed results of our MC3T3-E1 experiments are contained in the manuscript "Gap junctions and gap junctional intercellular communication in cell ensemble responsiveness to oscillatory fluid flow in

osteoblastic MC3T3-E1 cells" and has been submitted to the American Journal of Physiology for publication (appendix 1). In summary we demonstrated that gap junctional intercellular communication assessed by dye diffusion is diminished in the genetically manipulated cell line (DN-8) after 96 hours in culture, but not prior at 48 and 24 hours in culture. The control and DN-8 cells exhibited equivalent $[Ca^{2+}]_i$ responsiveness to flow, suggesting that $[Ca^{2+}]_i$ responsiveness to flow does not involve gap junctional intercellular communication. In contrast, we found dramatically diminished release of PGE2 in response to flow in the coupling deficient DN-8 cells (96 hours) suggesting that the PGE2 response to flow does depend on gap junctional intercellular communication.

These findings raised the possibility that the PGE2 response to flow does not involve a flow-induced increase in $[Ca^{2+}]_i$. To verify this interpretation we conducted an additional series of experiments using a blocker of intracellular cytosolic calcium mobilization. The results of these experiments demonstrate that PGE2 release in response to fluid flow can occur without a $[Ca^{2+}]_i$ increase. This conclusion is also consistent with our findings in the previous experiments utilizing ROS cells where we observed a PGE2 response to flow in a cell line that did not exhibit a $[Ca^{2+}]_i$ response to flow. This conclusion is highly significant since they suggest that the fluid flow response (and specifically oscillatory fluid flow) is unique in that PGE2 release can occur without the $[Ca^{2+}]_i$ response, which has not been previously observed for other physical and hormonal stimuli.

Aim 2: (Years 2 and 3) Quantify the responsiveness of bone cells as a function of age and cell-cell communication. Bone cells will be cultured from young, mature, and old rats and exposed to the fluid flow protocol of Aim 1.

We have demonstrated that confluent cultures of rat osteoblastic cells (ROB) from young, mature, and old animals display highly functional gap junctional intercellular communication. We found comparable functional communication in subconfluent ROB, from all three age groups, that were seeded on quartz microscope slides for calcium analysis.

Fluid flow induced shear stress was used as a mechanical stimulus to study intracellular calcium ($[Ca^{2+}]_i$) signaling in ROB that were isolated from young, mature, and old animals. Fura-2 was used to measure $[Ca^{2+}]_i$ in cells that were exposed to three minutes of oscillating fluid flow that produced shear stresses of 1 or 2 Pascals (Pa) at frequencies of 0.2, 1, or 2 Hz. Fluid flow caused an immediate and transient increase in $[Ca^{2+}]_i$. A significantly higher percentage of mature ROB displayed calcium transients than old ROB. Cells were more responsive to 0.2 Hz than to 1 or 2 Hz, and to 2 Pa than 1 Pa. These data suggest that intracellular calcium signaling is an important mechanotransduction response in rat osteoblastic cells and that there are age-related as well as frequency and shear stress amplitude dependent responses to oscillatory fluid flow.

Aim 3: (Years 3 and 4) Examine the effect of forskolin on fluid flow responsiveness in osteoblasts as a function of age. The protocol of Aim 1 will be applied to the cultures in the presence of forskolin or vehicle control to quantify its effects on both fluid flow responsiveness and cell-cell coupling. Ideally, a promising agent for osteoporosis intervention will be identified which can restore the responsiveness in cells cultured from old rats to that of cells cultured from young rats.

Work on this task has not yet begun.

Key Research Accomplishments

- Discovered that RCx16 and ROS/Cx45 gap junction deficient cells are less responsive to oscillatory fluid flow in terms of PGE2 release than ROS cells.

- Discovered that MC3T3-E1 cells exhibit an increase $[Ca^{2+}]_i$ in response to oscillating fluid flow, regardless of gap junctional intercellular communication.
- Discovered that MC3T3-E1 cells release PGE2 in response to oscillating fluid flow via a mechanism that involves gap junctional intercellular communication.
- Confirmed that the PGE2 response to oscillating fluid flow does not require a $[Ca^{2+}]_i$ response.
- Demonstrated that cell-cell communication via gap junctions plays an important role in regulating bone cell anabolism.
- Discovered that confluent and subconfluent cultures of rat osteoblastic cells have functional gap junctional intercellular communication that is not age dependent.
- Discovered that the percentage of cells displaying fluid flow induced intracellular calcium signaling in ensembles of rat osteoblastic cells was significantly greater in cells from mature rats (12 mos.) than in cells from old rats (24 mos.) for an array of functional loading regimes.

Reportable Outcomes

The following manuscripts and abstracts were supported either partially or fully by the project (reverse chronological order):

Manuscripts

"Gap junctions and gap junctional intercellular communication in cell ensemble responsiveness to oscillatory fluid flow in osteoblastic MC3T3-E1 cells." Saunders, MM, You, J, Trosko, JE, Yamasaki, H, Donahue, HJ, Jacobs, CR, Submitted, American Journal of Physiology. (appendix 1)

"Osteopontin gene regulation by oscillatory fluid flow via intracellular calcium mobilization and activation of mitogen-activated protein kinase in MC3T3-E1 osteoblasts" You, J, Reilly, GC, Zhen, X, Yellowley, CE, Chen, Q, Donahue, HJ, Jacobs, CR, Submitted, Journal of Biological Chemistry. (appendix 2)

"Substrate deformation levels associated with routine physical activity are less stimulatory to bone cells relative to loading-induced oscillatory fluid flow", You, J, Yellowley, CE, Donahue, HJ, Zhang, Y, Chen, Q, Jacobs, CR, Journal of Biomechanical Engineering **122:**387-393, 2000 (appendix 3).

"Functional gap junctions between osteocytic and osteoblastic cells", Yellowley, CE, Li, Z, Zhou, Z, Jacobs, CR, Donahue, HJ, Journal of Bone and Mineral Research **15:**209-217, 2000 (appendix 4).

"Mechanisms contributing to fluid-flow induced Ca^{2+} mobilization in articular chondrocytes", Yellowley, CE, Jacobs, CR, Donahue, HJ, Journal of Cellular Physiology **18:**402-408, 1999 (appendix 5).

Presentation Abstracts

"Oscillatory fluid flow-induced prostaglandin E2 production is dependent upon gap junctional intercellular communication in osteoblastic MC3T3-E1 cells" Saunders, MM, You, J, Trosko, J, Yamasaki, H, Donahue, HJ, Jacobs, CR, Accepted for presentation at the 2001 annual meeting of the Orthopaedic Research Society. (appendix 6)

"Mechanosensitivity of rat osteoblastic cells is a function of age, loading frequency, and shear stress" Donahue, SW, Jacobs, CR, Donahue, HJ, Accepted for presentation at the 2001 annual meeting of the Orthopaedic Research Society. (appendix 7)

"Oscillatory flow-induced prostaglandin E2 release involves protein kinase A and cyclooxygenase-2 in MC3T3-E1 osteoblasts" You, J, Saunders, MM., Yellowley, CE, Donahue, HJ, Jacobs CR, accepted for presentation at the Society for Physical Regulation in Biology and Medicine 2001 annual meeting. (appendix 8)

"Analysis of the glycocalyx of two bone cell types, in vitro, in order to investigate fluid flow effects" Reilly, GC, Yellowley, CE, Donahue, HJ, Jacobs CR, Accepted for presentation at the Society for Physical Regulation in Biology and Medicine 2001 annual meeting. (appendix 9)

"Oscillatory flow stimulates prostaglandin E2 release via protein kinase A in MC3T3-E1 osteoblasts involving cyclooxygenase-2" You, J, Saunders, MM, Yellowley, CE, Donahue, HJ, Jacobs, CR, Accepted for presentation at the 2001 annual meeting of the Orthopaedic Research Society. (appendix 10)

"The source of the intracellular calcium increase in the response of bone cells to oscillating fluid flow" Reilly, GC, You, J, Yellowley, CE, Donahue, HJ, Jacobs, CR, Submitted to the 2001 annual meeting of the Orthopaedic Research Society. (appendix 11)

"Manipulation of the bone cell glycocalyx reduces calcium responses to fluid flow" Reilly, GC, Yellowley, CE, Donahue, HJ, Jacobs, CR, Submitted to the 2001 annual meeting of the Orthopaedic Research Society. (appendix 12)

"Prostaglandin E2 (PGE2) response in MC3T3-E1 osteoblastic cells is dependent upon gap junction coupling" Saunders, M, You, J, Trosko, J, Yamasaki, H, Donahue, H, Jacobs, C, Presented at the 2000 annual fall meeting of the Biomedical Engineering Society, p S-86. (appendix 13)

"Prostaglandin E2 (PGE2) response to fluid flow is independent of intracellular calcium concentration in osteoblastic R)S 17/2.8 and RCx16 cells" Saunders, M, You, J, Trosko, J, Yamasaki, H, Donahue, H, Jacobs, C, Presented at the 2000 annual fall meeting of the Biomedical Engineering Society, p S-87. (appendix 14)

"Fluid flow induced intracellular calcium signalling is shear stress and frequency dependent in primary rat osteoblastic cells" Donahue, S, Donahue, H, Jacobs, C, Presented at the 2000 annual fall meeting of the Biomedical Engineering Society, p S-105. (appendix 15)

"Frequency dependent effects of oscillating fluid flow on bone cells" You, J, Saunders, M, Yellowley, C, Donahue, H, Jacobs, C, Presented at the 2000 annual fall meeting of the Biomedical Engineering Society, p S-105. (appendix 15)

"Investigation of the glycocalyx of cultured bone cells" Reilly, GC, Jacobs CR, Presented at the 2000 annual meeting of the American Society of Bone and Mineral Research, p S376. (appendix 16)

"Investigation of the signalling pathways involved in the calcium response of bone cells to oscillating fluid flow" Reilly, GC, Yellowley, CE, Donahue, HJ, Jacobs CR, Presented at the 2000 annual meeting of the American Society of Bone and Mineral Research, p S508. (appendix 17)

"Characterization of the glycocalyx of bone cells in order to investigate fluid flow effects" Reilly, GC, Yellowley, CE, Jacobs, CR, Presented at the 2000 meeting of the European Society of Biomechanics, p 320. (appendix 18)

"Mechanosensitivity of rat osteoblastic cells decreases with age" Donahue, SW, Jacobs, CR, Donahue, HJ, Presented at the 2000 International Sun Valley Hard Tissue Workshop. (appendix 19)

"Physiological levels of substrate deformation are less stimulatory to bone cells compared to fluid flow" You, J, Yellowley, CE, Donahue, HJ, Jacobs, CR, Presented at the 1999 International Mechanical Engineering Congress and Exposition, BED vol 43 "Advances in Bioengineering" p 161. (appendix 20)

"Differential effect of oscillating fluid flow on cytosolic calcium and prostaglandin in osteoblastic ROS 17/2.8 cells", Saunders, MM, You, J, Yellowley, CE, Jacobs, CR, Donahue, HJ, presented at the 2000 meeting of the Orthopaedic Research Society. (appendix 21)

"Mechanotransduction in bone via oscillating fluid flow", You, J, Zhen, X, Yellowley, CE, Chen, Q, Donahue, HJ, Jacobs, CR, presented at the 2000 meeting of the Orthopaedic Research Society. (appendix 22)

"Fluid flow induced calcium mobilization is frequency dependent", You, J, Yellowley, CE, Donahue, HJ, Jacobs, CR, presented at the 2000 meeting of the Orthopaedic Research Society. (appendix 24)

The following applications for funding were awarded by the NIH based on work supported this award:

"Mechanotransduction in bone via oscillating fluid flow", PI: C Jacobs, 1 R01 AR45989-01A1.

"Gap junctions and bone cell response to physical signals", PI: H Donahue, 2 R01 AG13087-06.

Conclusions

In summary, in the second year of the project we have completed aim one and have completed half of aim two. For aim one we have demonstrated our hypothesis to be true, namely that gap junctional intercellular communication modulates the PGE2 response of bone cells to oscillating fluid flow. Interestingly, we found that PGE_2 release in response to oscillating flow does not appear to involve intracellular calcium. This has important implications because it indicates that other second messengers, such as the cyclic AMP pathway, may be important in transducing the fluid flow signal into the PGE_2 response. Additionally, the differential effect of oscillating fluid flow on intracellular calcium versus PGE_2 may prove to be a powerful tool in further investigations of the bone cell mechanotransduction pathway. We have begun work on our second task (aim 2) and have determined that while the $[Ca^{2+}]_i$ response to fluid flow does decrease as a function of age, gap junctional intercellular communication does not. These results have produced numerous scientific presentations and abstracts as well as one manuscript in review and two manuscripts in preparation. Finally, the results have been incorporated into two applications to the NIH which have been approved for funding.

Gap junctions and gap junctional intercellular communication in cell ensemble responsiveness to oscillatory fluid flow in osteoblastic MC3T3-E1 cells

Saunders MM[†], You J[†], Trosko JE[‡], Yamasaki H[§], Donahue HJ[†], and Jacobs CR[†]
[†]Musculoskeletal Research Laboratory
Department of Orthopaedics and Rehabilitation
The Pennsylvania State University College of Medicine
The Milton S. Hershey Medical Center
Hershey, PA 17033

[‡]Michigan State University
Department of Pediatrics and Human Development
College of Human Medicine
East Lansing, MI 48824

[§]Kwansei Gakuin University
Uegahava, Nishinomiya, Japan

Running Heading: Osteoblastic flow-induced PGE_2 release is GJIC-dependent

Address for correspondence:
MM Saunders, Ph.D.
Department of Orthopaedics and Rehabilitation
The Pennsylvania State University College of Medicine
PO Box 850, 500 University Drive
Hershey, PA 17033-0850

Tel: (717) 531-6697
Fax: (717) 531-7583
msaunder@mrl.hmc.psu.edu

Figures: 6 Figures

ABSTRACT

In the current study, we examined the role of gap junctions in oscillatory fluid flow-induced changes in intracellular calcium concentration and prostaglandin release in osteoblastic cells. This work was completed in MC3T3-E1 cells with intact gap junctional communication as well as MC3T3-E1 cells rendered communication-deficient through expression of a dominant-negative connexin. Our results demonstrate that MC3T3-E1 cells with intact gap junctions respond to oscillatory fluid flow with significant increases in prostaglandin E_2 (PGE_2) release, whereas cells with diminished gap junctional communication do not. Furthermore, we found that cytosolic calcium ($Ca^{2+}{}_i$) response was unaltered by the disruption in gap junctional communication and was not significantly different between the cell lines. Thus, our results suggest that gap junctions contribute to the PGE_2 but not the $Ca^{2+}{}_i$ response to oscillatory fluid flow. These findings implicate gap junctional intercellular communication (GJIC) in bone cell ensemble responsiveness to oscillatory fluid flow and suggest that gap junctions and GJIC play a pivotal role in mechanotransduction mechanisms in bone.

KEYWORDS

Fluid flow, gap junctions, PGE_2, Ca^{2+}, mechanotransduction

INTRODUCTION

It is widely accepted that bone adapts to its physical loading milieu by optimizing mass and mechanical performance in a process known as bone remodeling. In a nonpathologic scenario, this process results in normal bone turnover whereby new bone formation is balanced by removal of existing bone. In a pathologic scenario, this process results in an imbalance whereby net bone formation (osteopetrosis) or net bone loss (osteopenia) ensues. Although the effects of remodeling have been histologically observed, the exact cellular pathways by which it occurs are incompletely understood. To this end, researchers have recently begun to investigate mechanotransduction mechanisms (15, 17, 32) in an attempt to better uncover the elusive signal transduction pathways by which physical stimuli can affect cellular responses in bone. These studies have found that bone cells can respond to a wide variety of endogenously occurring signals including mechanical stretch (41), streaming potentials, chemotransport, electrical effects (2, 6, 26, 33) and fluid flow (8, 17, 28, 41). In the latter area of research, it has been hypothesized that the fluid flow through the lacunar-canalicular network is pivotal to bone cell responsiveness. Although several hypotheses have been proposed, many believe that the osteocytes in the canalicular spaces sense the fluid flow (1) and in turn signal the osteoblasts to form bone.

While many accept the theory that osteoblast responsiveness to biophysical effects is linked to the osteocyte (1, 23), few have proposed a mechanism by which this may occur. We propose that bone cell responsiveness to fluid flow is aided by gap junctions which physically connect osteoblasts and osteocytes (39), as well as, osteoblasts to other osteoblasts. In this scenario, we hypothesize that gap junctions not only enable osteocytes to transfer signals to osteoblasts, but that the responsiveness of osteoblastic networks to the signal is amplified via gap junctions. By coupling the osteoblasts together, gap junctions enable the cells to respond in concert resulting in a more robust response than attained if an equal number of individual cell responses were achieved. This is the focus of our current work.

Gap junctions are transmembrane protein channels that enable neighboring cells to physically link thereby facilitating the rapid diffusion of small molecules and ions on the order of 1kDa in a process

known as gap junctional intercellular communication (GJIC). Gap junctions may be homospecific, uniting cells of the same type, or may be heterospecific, uniting cells of unlike type. With the exception of blood cells and muscle fibers, gap junctions have been found in most cells (30) with at least thirteen mammalian connexins identified to date and named with respect to molecular weight.

There is growing evidence to support a role for gap junctions in the cellular (and cell ensemble) response to physical stimuli. In bone, gap junctions have been linked to such functions as hormonal responsiveness (34), gene expression (25) and differentiation (7). Intercellularly, gap junctions have been linked to second messenger responses induced by physical stimuli such as Ca^{2+} release following membrane deformation (21). Interestingly, many fluid flow studies have shown that osteoblastic cells respond to flow *in vitro* with an increase in such second messengers as Ca^{2+} (13, 15), cAMP (28) and NO release (20) which have been shown to be physical regulators of gap junction channel opening.

GJIC has been linked to both normal and abnormal cell function. In normal cell function, GJIC has been linked to such processes as proliferation and differentiation, although the findings at times have been inconsistent. For instance, while GJIC is found to maintain cell differentiation status in cultured hepatocytes (40), it is decreased in differentiating keratinocytes in comparison to proliferating ones (12). Furthermore, we have recently demonstrated that gap junction function and expression parallel osteoblastic differentiation contributing to alkaline phosphatase expression (7). Thus, gap junction studies are widely dependent upon cell line, culture conditions and experimental environment and results must be interpreted within these contexts. In abnormal cell function, alterations in GJIC have been linked to disease (30, 36) suggesting that a status quo in gap junction function is crucial to homeostasis.

In the current study, we set out to examine the role of GJIC in transducing a mechanical stimulus to bone cells. That is, we exposed osteoblastic cells to levels of oscillatory fluid flow that occur *in vivo* due to habitual loading (35) and measured prostaglandin E_2 (PGE_2) release and cytosolic calcium concentration ($[Ca^{2+}]_i$), markers selected for their proposed role in the regulation of bone turnover (4, 10, 16, 19, 27). To correlate these findings with the role of GJIC, we utilized osteoblastic MC3T3-E1 (MC3T3) cells; MC3T3 cells expressing a dominant negative Cx43 (DN-8), the predominant gap junction

protein in bone, and a control transfectant (DN-VC). Comparisons of changes in PGE_2 release and $[Ca^{2+}]_i$ in the presence of oscillatory fluid flow in the three cell lines were then used to draw conclusions about the contribution of gap junctions and GJIC to bone remodeling.

MATERIALS AND METHODS

Cell Culture

Three immortalized osteoblastic cell lines were utilized in this study: MC3T3, DN-VC and DN-8. The MC3T3 is an immortalized, mouse osteoblastic cell line; the DN-8 is a neomycin-sustained transfectant of MC3T3 containing a mutant Cx43 and the DN-VC is a control for the transfection containing an empty plasmid. MC3T3 cells were cultured in minimal essential medium (MEM-α) (GIBCO BRL, Grand Island, NY) supplemented with 10% fetal bovine serum (FBS) (Hyclone, Logan, UT) and 1% penicillin/streptomycin (P/S) (GIBCO BRL, Grand Island, NY). The DN-8 and DN-VC cells were cultured in MC3T3 medium supplemented with neomycin (200μg/mL). All cell lines were maintained in an incubator at 37°C and 5% CO_2 with flow experiments conducted in the appropriate media supplemented with 2% FBS.

The DN-8 line was developed from a dominant-negative strategy as previously described (24). Briefly, a mutant gap junction protein (Cx43Δ) of Cx43 was developed by the deletion of residues in the internal cytoplasmic loop of the connexin structure. The goal of the strategy was to introduce this mutant gene into both protein channels of each linking cell such that the mutant could oligomerize with only a wild-type species. Unlike previous dominant-negative strategies where GJIC is obliterated and the resulting connexin oligomers are not transported to the membrane but remain in the cytoplasm, this novel mutation approach affects only permeability, leaving transport intact (24).

Cell Preparation

Experiments were conducted on two differently sized microscope slides. For the quantification of oscillatory fluid flow-induced Ca^{2+}_i mobilization, cells were plated on quartz slides (76mm x 26mm x 1.6mm) for imaging. These slides accomodated the relatively few cells needed to conduct the experiments and were made of quartz to allow for ultraviolet (UV) visualization. Cells were plated at $1.0x10^5$, $0.75x10^5$ or $0.5x10^5$ cells/slide and cultured for 24, 48 or 96 hours, respectively to achieve 85-90% confluence. For the quantification of oscillatory fluid flow-induced PGE_2 production, cells were plated on glass microscope slides (75mm x 38mm x 1mm). These slides were larger so that larger volumes of cells could be evaluated. Cells were plated at $3.5x10^5$, $2.75x10^5$ or $2.0x10^5$ cells/slide and cultured for 24, 48 or 96 hours, respectively to achieve 85-90% confluence. For quantification of GJIC, cells were plated as described above for the PGE_2 experiments. In addition, cells for double labeling were cultured in round (35mm-diam.) polystyrene petri dishes in the appropriate media for 24, 48 or 96 hours.

Gap Junctional Intercellular Communication Assays

GJIC assays were completed using epifluorescent microscopy and a double labeling technique, as previously described (39). In this technique, cells are loaded with the fluorescent dyes, calcein AM (Molecular Probes, Eugene, Oregon) and 1,1'-dioctadecyl-3,3,3',3'-tetramethylindocarbocyanine perchlorate ((DiI) Molecular Probes). The fluorescent dye calcein AM once in the cell is cleaved of its AM group and trapped within the cell. However, as a result of its small molecular size (< 1kDa), calcein is gap junction permeable and able to transfer to neighboring cells if functional (open) gap junctions are established. The fluorescent dye, DiI, is of a larger molecular size, intercalates within cell membranes and does not transfer to neighboring cells via GJIC. The loaded cells are then dropped onto unloaded cells in monolayer and cell transfer is quantified. If functional gap junctions are established, the calcein will transfer to neighboring cells which will then fluoresce green.

Coupling assays were completed to establish the extent of disruption of GJIC in DN-8 cells at 24, 48 and 96 hours in culture and compared to GJIC in the MC3T3 and DN-VC lines at the same time

points. Following quantification of GJIC, we assessed GJIC in the three cell lines at 96 hours in culture simultaneously with PGE_2 and $[Ca^{2+}]_i$ experiments to minimize passage variables. On the day of the experiments, the preconfluent cells ('donor' cells) plated in the petri dishes were removed from the incubator and washed twice with room temperature phosphate buffered saline (PBS) followed by aspiration. The donor cells were labeled with a BSA-enriched PBS-fluorescent dye mixture containing 20μL of calcein AM, 7μL of DiI and 20μL of pluronic acid (Molecular Probes) and incubated for 30min at 37°C. Following incubation, the dye mixture was aspirated and the donor cells washed twice in room temperature PBS. The donor cells were detached from the dishes by trypsinization, centrifuged at 200G for 8min and resuspended in fresh growth medium. The double-labeled (Calcein and DiI) donor cells were then dropped onto the glass slides containing confluent monolayers of unlabeled cells at a ratio of approximately 1:500 cells (labeled to unlabeled) and incubated for 90min at 37°C. Following the incubation period, the slides were removed from the dishes, washed twice with PBS and covered by round (25mm-diam) glass coverslips. The slides were placed on a Nikon fluorescent microscope (Nikon EFD-3, Optical Apparatus Co., Ardmore, PA) and visualized using fluorescein ($\lambda_{excitation}$ = 465-495nm; $\lambda_{emission}$ = 520nm) and rhodamine ($\lambda_{excitation}$ = 541-551nm; $\lambda_{emission}$ = 590nm) filters to locate the calcein and DiI loaded cells, respectively. Coupling was quantified by counting the number of neighboring cells fluorescing green, while the DiI was used to distinguish the labeled cells from those in the monolayer. Thirty cells were randomly selected and counted for each slide. Coupling was considered extensive if individual cells transferred calcein to more than fifteen cells and were not counted past this threshold number.

Parallel Plate Flow Chambers and Testing Machine

For PGE_2 and Ca^{2+} experiments, bone cells were placed in a parallel plate flow chamber and subjected to oscillatory fluid flow. This system has been previously characterized and we and others have employed it to expose endothelial cells (8), chondrocytes (37, 38) and bone cells (14, 15, 17, 41) to

physiologic levels of fluid flow. Briefly, the system imparts a laminar flow to the cells in monolayer exposing them to a shear stress governed by the equation (9),

$$\tau=6\mu Q/bh^2$$

where, τ is the shear stress, μ is the viscosity of the flow medium, Q is the flow rate and b and h are the width and height of the chamber, respectively. To accommodate the quartz and glass microscope slides, as previously noted, two differently sized chambers were employed. In general, the components for both chambers were the same and are shown in the exploded view of Figure 1. The chambers consisted of a polycarbonate manifold, a silastic gasket and a glass slide. This slide containing the cells in monolayer formed the bottom of the flow chamber when inverted on the manifold. For Ca^{2+} studies, an 18mL/min flow rate resulted in a shear stress of 20dyne/cm^2 and a rectangular flow volume of 38mm x 10mm x .28mm; for PGE_2 studies, a 43mL/min flow rate resulted in a shear stress of 20dyne/cm^2 and a rectangular flow volume of 56mm x 24mm x .28mm. In all flow experiments, flow rate was monitored with an ultrasonic flow probe (Transonic Systems Inc., Ithaca, NY) connected to the chamber inlet. For Ca^{2+} imaging, the flow chamber assembly was held together with vacuum pressure; for PGE_2 quantification, the flow chamber assembly was placed in a polycarbonate case bolted together to form an air-tight seal. For the latter experiments, the polycarbonate case containing the chamber enabled the system to be placed in an incubator for long-term flow periods (1hr) such that temperature and CO_2 levels could be precisely regulated. For both short- (Ca^{2+}) and long-term (PGE_2) experiments, the chamber was connected to a pneumatic, closed-loop feedback materials testing machine (EnduraTec, Minnetonka, MN) via tubing and syringes with oscillatory fluid flow delivered in the form of a 1Hz sine wave, Figure 1.

PGE_2 Quantification

PGE_2 accumulation in the supernatant was quantified with a commercially available, non-radioactive, competitive binding enzyme immunoassay system (BioTrak, Amersham Pharmaceuticals,

Piscataway, NJ). Following assaying, the optical densities of the samples were read at 450nm using a microplate reader (Dynex Technologies, Chantilly, VA). Manufacturer-supplied standards were also analyzed and used to construct a standard curve from which the sample concentrations were determined.

Oscillatory fluid flow-induced PGE_2 was quantified at the 48 and 96 hour time points. On the day of the experiments, preconfluent slides of cells were washed, placed in the parallel plate flow chamber, encased in the polycarbonate case, placed in the incubator and connected to the fluid flow delivery system. Cells were exposed to flow for 1hr following which 10mL medium from the inlet and outlet ports of the chamber and adjacent tubing were collected for PGE_2 analysis. These media are referred to throughout the manuscript as media collected immediately post-flow. In addition, the plates of cells were incubated in 10mL of fresh medium for 1hr post-flow and these media were also collected for PGE_2 analysis. These media are referred to throughout the manuscript as media collected 1-hour post-flow. Immediately following media collection, aliquots were frozen at –80°C. In addition, for some experiments, the ionophore, 4-Bromo-Calcium (50μM), was added to a plated slide from each cell line for 15 minutes at 37°C. The media from these collections were used as positive controls in the PGE_2 assays. On the day of assaying, samples were thawed at 4°C and vortexed. Assays were completed at room temperature within one month of collection and degradation assays were completed to ensure that this time period did not adversely affect the results.

The three cell lines were also subjected to oscillatory flow in the presence of thapsigargin, a drug used in our study to empty and prevent refilling of intracellular Ca^{2+} stores thus eliminating this source of Ca^{2+} contributing to changes in $[Ca^{2+}]_i$. PGE_2 experiments in the presence of thapsigargin were completed at the 96 hour time point following the exact protocol previously outlined with one exception, thapsigargin (50nM) was added to each petri dish of plated cells (30min prior to placing it in the flow chambers), the flow medium and the 10mL of fresh, 1 hour post-flow incubation medium.

Because total PGE_2 accumulation in the medium is dependent upon cell number, prostaglandin accumulation was normalized to total cell protein for each slide. Following the 1hr incubation and

collection of the additional 10mL of fresh medium, the cells were removed from each microscope slide by trypsinization, centrifuged at 200G for 8min and resuspended in 0.5mL of 0.05% Triton X 100 detergent. The suspended cells were placed in 1mL centrifuge tubes and lysed using three cycles of rapid freezing (-80°C) and thawing. The lysate was frozen at –80°C until analysis with a commercially available assay kit (BioRad, Hercules, CA). Following assaying, the optical densities of the samples were read at 405nm using a microplate reader. Manufacturer-supplied standards were analyzed and used to construct the standard curve from which the sample concentrations were determined. Frozen cells and media were assayed at room temperature within one month of collection.

Calcium Imaging

Ca^{2+} imaging was completed with fluorescent microscopy and the dual-wavelenth ratiometric dye, fura-2 AM (Molecular Probes, Eugene, OR). This indicator was selected for its ability to exhibit two distinct spectra and two distinct wavelengths based upon the presence or absence of Ca^{2+} binding to the indicator (31). The indicator is loaded in the fura-2 AM form which allows it to easily enter the cells. Following loading, the AM groups are cleaved in an enzymatic process leaving the indicator trapped within the cell.

$[Ca^{2+}]_i$ was quantified in the three cell lines at the 96 hour time point. On the day of the experiments, preconfluent slides of cells were loaded with 10μM fura-2 AM in 1mL of fresh media and incubated at 37°C for 45 minutes. Following incubation, the cells were washed in the appropriate flow medium (2% FBS), placed on the parallel plate flow chamber, transferred to a fluorescent microscope and connected to the loading machine. To allow the cells to settle and ensure that the AM hydrolizing process was complete, the cells were allowed to equilibrate on the microscope stage for 30min immediately prior to testing. Cells were subjected to 3min of oscillatory flow preceded by a 3min no flow baseline. An image acquisition and analysis software package (Metafluor) was used to capture the images for $[Ca^{2+}]_i$ determination.

Data Analyses

Ca^{2+} results were analyzed with a Rainflow counting technique (18). This technique, adapted from the field of mechanical fatigue, enables individual responses to be extracted from data containing multiple responses and has generally been employed to determine the contribution of a particular loading cycle to the overall lifetime of a structure. Rainflow applied to our research enabled individual cell responses to be isolated and separated from background noise with a threshold response defined as a change in $[Ca^{2+}]_i$ of 20nM or larger.

PGE_2 results were analyzed using a microplate reader and normalized to total protein with total PGE_2 accumulation in the medium given in pg/μg. GJIC was quantified by counting cell fluorescence transfers, as previously described. All Ca^{2+}, PGE_2 and GJIC data obtained were expressed as mean ± SEM. To compare results between the cell lines, GLM ANOVAs with SNK post-hoc comparisons were completed using a commercially available software program (Instat, GraphPad Software Inc., San Diego, CA) with an a priori significance level of 0.05.

RESULTS

Osteoblastic Cell Line GJIC as a Function of Time in Culture

GJIC was qualitatively evaluated at 24, 48 and 96 hour time points in the three cell lines with typical dye transfers shown (Figure 2). In these double exposed photographs, the green (calcein) fluorescence indicates the coupled cells in monolayer while the yellow (calcein and DiI) fluorescence indicates double-labeled donor cells. Quantitative results for the 24, 48 and 96 hour time points (Figure 3) depict number of donor cells coupled to individual acceptor cells in monolayer. We found that the MC3T3 and DN-VC cell line coupling was not dependent upon time in culture up to 96 hours. At 24 and 48 hours, the three cell lines did not exhibit a significant difference in coupling compared to each other.

However, at the 96 hour time point, DN-8 cells exhibited a significant decrease in coupling in comparison to the MC3T3 ($p<0.001$) and DN-VC ($p<0.001$) lines at 96 hours, as well as in comparison to themselves at the 24 ($p<0.001$) and 48 ($p<0.001$) hour time points.

PGE_2 Accumulation in Response to Fluid Flow

Since GJIC was decreased in DN-8 cells only after 96 hours in culture, we first examined PGE_2 response to fluid flow at this time point (Figure 4a). Media from MC3T3 and DN-VC from cells collected 1 hour post-flow accumulated significantly more PGE_2 than cells not exposed to flow ($p<0.0005$ and $p<0.0001$, respectively). However, media from poorly coupled DN-8 cells did not accumulate more PGE_2 than control cells. Similar results were obtained when media was collected immediately post-flow (not shown).

We also examined the effect of fluid flow on PGE_2 accumulation in DN-8 cells cultured at 48 hours, a period after which DN-8 cells are as well coupled as MC3T3 cells (Figure 4b). Whereas exposure to fluid flow did not increase PGE_2 accumulation in media collected 1 hour post-flow from DN-8 cells cultured for 96 hours it did in media from DN-8 cells cultured 48 hours ($p<0.005$ vs no flow controls). Similar results were obtained when media was collected immediately post-flow (data not shown).

Calcium Response to Oscillatory Fluid Flow

In cells cultured for 96 hours there was a 7.9-fold increase ($p<0.0007$ vs. no flow) in percentage of MC3T3-E1 cells responding to three minutes of oscillatory fluid flow with an increases in $[Ca^{2+}]_i$; an 8.9-fold increase in DN-VC cells ($p<0.0001$) and a 9.3-fold increase in DN-8 cells ($p<0.0003$) (Figure 5). The fold increases were not statistically different between the three cells lines. No significant differences in $[Ca^{2+}]_i$ amplitude within or between groups were observed (data not shown); a finding also made in our previous work in human fetal osteoblastic (hFOB) cells (41).

PGE_2 Accumulation in the Presence of Thapsigargin

One interpretation of our findings that GJIC contributed to the PGE_2 but not the $[Ca^{2+}]_i$ response to fluid flow in DN-8 cells is that cytosolic Ca^{2+} mobilization may not be critical to fluid flow-induced PGE_2 accumulation. To address this issue, we examined the effect of thapsigargin on fluid flow-induced PGE_2 accumulation. In the presence of thapsigargin, media from MC3T3 and DN-VC cells collected 1 hour post-flow had a 92.1% and 278%, respectively, increase in PGE_2 accumulation relative to no flow control. Once again, fluid flow did not increase PGE_2 accumulation in DN-8 cells cultured 96 hours and thus poorly coupled. Therefore, thapsigargin did not significantly alter the PGE_2 response to fluid flow in any of the cell lines examined (Figure 6).

DISCUSSION

In this study we set out to investigate the role of gap junctions and GJIC in mechanotransduction mechanisms in bone. We applied a novel dominant-negative genetic intervention strategy to MC3T3-E1 osteoblastic parent cells to render them communication deficient. We subjected the resulting cell line to oscillatory fluid flow and measured flow-induced PGE_2 release and changes in $[Ca^{2+}]_i$. This is the first study examining GJIC in bone cell ensemble responsiveness to fluid flow and, while only the second study examining the effects of oscillatory fluid flow on $[Ca^{2+}]_i$ in osteoblastic cells, it is the first to quantify the PGE_2 response. We found that a breakdown in gap junction coupling had no effect upon changes in $[Ca^{2+}]_i$ but resulted in a significant inhibition of oscillatory fluid flow-induced PGE_2 release suggesting that gap juctions play a pivotal role in the mediation of oscillatory fluid flow-induced PGE_2 production in osteoblastic cells.

To verify the effectiveness of the dominant-negative strategy used to render the DN-8 cells communication-deficient, we quantified the extent of coupling in the DN-8 cells at 24, 48 and 96 hours in culture. These results were compared to coupling experiments conducted at the same time points in the communication-intact, control-transfectant DN-VC cell line. We found an 80.1% decrease in coupling in

the DN-8 cells between 48 and 96 hours in culture, whereas no significant change was noted in the DN-VC cells over the same time period. These results indicate that GJIC in only the DN-8 cell line was dependent upon time in culture. Therefore, because the cells are genetically identical and cultured under the same culture conditions, these cells provide a novel model system in the analysis of GJIC in bone cell responsiveness to fluid flow.

To address the role that gap junctions play in the oscillatory fluid flow-induced PGE_2 response, we subjected the cell lines to 1hr of oscillatory fluid flow and measured PGE_2 accumulation in the media compared to PGE_2 accumulation in media from no-flow controls. At the 48 hour time point, when intact GJIC was exhibited in the DN-8 cell line, the application of oscillatory fluid flow resulted in significant increases in PGE_2 accumulation. However, at the 96 hour time point, when GJIC was inhibited, no increase in oscillatory fluid flow-induced PGE_2 accumulation resulted. In contrast, the DN-VC cell line responded at both time points with significant increases in PGE_2 accumulation. Thus,we found that a breakdown in coupling was accompanied by a significant decrease in PGE_2 responsiveness to oscillatory fluid flow. These findings strongly suggest that gap junctions and GJIC are necessary in the signal transduction pathway whereby osteoblastic cells increase production of PGE_2 in response to oscillatory fluid flow and that a GJIC-dependent pathway exists.

To address the role that gap junctions play in the mediation of oscillatory fluid flow-induced changes in $[Ca^{2+}]_i$, we subjected the cell lines to 3min of oscillatory fluid flow and measured $[Ca^{2+}]_i$ compared to $[Ca^{2+}]_i$ of no-flow controls. At the 96 hour time point, DN-8 and DN-VC cells responded to oscillatory fluid flow with significant increases in $[Ca^{2+}]_i$. Moreover, differences in flow-induced $[Ca^{2+}]_i$ were not significantly different in the DN-8 and DN-VC lines at this time point. Thus, we found that a breakdown in coupling was not accompanied by a significant change in $[Ca^{2+}]_i$ and that the Ca^{2+} responses of the cell lines, regardless of degree of coupling, were equally responsive. These findings strongly suggest that gap junctions and GJIC are not necessary in the signal transduction pathway whereby osteoblastic cells increase $[Ca^{2+}]_i$ in response to oscillatory fluid flow and that a GJIC-independent pathway exists.

In this study we found that while coupling-deficient osteoblastic cells responded to the application of oscillatory fluid flow with significant increases in PGE_2 release, changes in $[Ca^{2+}]_i$ were not found due to changes in coupling. These findings suggest that the PGE_2 and $[Ca^{2+}]_i$ responses elicited via oscillatory fluid flow may be unlinked in these osteoblastic cells, a notion contradictory to prevailing opinion. To address this issue, we subjected the cell lines to oscillatory fluid flow in the presence of thapsigragin. We found that the introduction of thapsigargin did not significantly affect PGE_2 production whereas the Ca^{2+} response was completely annihilated (data not shown). Furthermore, because we have data indicating that the only source of Ca^{2+} in the MC3T3-E1 cells is from intracellular stores (pending publication) (42) which are emptied by the thapsigargin, our findings provide concrete evidence to suggest a separation of pathways involved in Ca^{2+} wave propagation and PGE_2 production in osteoblastic cells.

In this study we set out to investigate the role of gap junctions in mediating oscillatory fluid flow-induced PGE_2 response in osteoblastic cells. Inasmuch as this was our goal, we were largely interested in whether the application of oscillatory fluid flow resulted in significant increases in PGE_2 production in the cell lines. However, studies have shown that the exact PGE_2 timecourse has yet to be elucidated and that flow-induced PGE_2 production is not obliterated with the cessation of the stimulant (22). To address the time-dependent response of oscillatory fluid flow-induced PGE_2 release in these cell lines, PGE_2 accumulation in the media was measured at two time points after cessation of flow. In the first approach, the flowed media was collected immediately following flow exposure; in the second approach, the flowed cells were placed in an equivalent volume of fresh media immediately post-flow and incubated for 1hr. We found that in the coupling-intact DN-VC cells, flow-induced levels of PGE_2 accumulation in media from cells incubated for 1 hour post-flow were significantly higher compared to media from cells collected immediately post-flow. Similarly, PGE_2 levels in media from no-flow control cells incubated for 1 hour post-flow were significantly elevated compared to levels from no-flow contol cells collected immediately post-flow. These findings were similar to those observed in the DN-8 line at 48 hours when coupling was still intact suggesting that a comparison of baseline PGE_2 accumulation levels from media

collected from incubated post-flow cells is more appropriate than in media collected immediately post-flow and may be more sensitive to extracellular regulation.

Curiously we found that basal PGE_2 levels were elevated in the DN-8 cells at the 96 hour time point. While we are unable to definitively explain this result, it is unlikely that the elevation was a result of the transfection process since the control transfectant DN-VC cells did not exhibit a similar trend. To further address this issue, we added the ionophore, 4-Bromo-Calcium (50μM for 15min) to confluent slides of DN-8 cells and measured PGE_2 accumulation levels in excess of those shown in Figure 4 (data not shown) indicating that increases beyond these basal levels were indeed possible. In any case, we do not feel that these findings detract from the main finding of this paper, namely that GJIC-deficient cells do not respond to oscillatory fluid flow with an increase in PGE_2 release.

It is also possible that factors other than GJIC are invovled in the responsiveness of a cell ensemble to oscillatory flow by affecting the inherent responsiveness of the individual cells. For instance, it is possible that membrane permeability or morphological changes in the membrane are important and could lead to sensitivity changes in protein receptors, ion channels and cytoskeletal elements. This may help to explain the increase we observed in basal PGE_2 production levels in the DN-8 cells at the 96 hour time point. Furthermore, it is also possible that GJIC may affect such changes in cellular sensitivity. For instance, it has previously been shown that GJIC contributes indirectly to morphological changes by contributing to extracellular matrix organization (3).

Although a substantial body of evidence exists linking GJIC and cellular responsiveness to physical stimuli, the work to date has provided only indirect evidence. For instance, several studies have shown that the application of physical stimuli *in vitro* results in increased Cx43 expression in both osteoblasts (43) and osteocytes (29), a finding paralleling those in smooth muscle (5) and endothelial cells (11). However, these studies did not address changes in coupling or that changes in coupling influences the sensitivity of the cell ensemble. Thus, it is important to distinguish between connexin formation and functional coupling which would provide direct evidence to suggest that gap junctions are important in mechanotransduction.

In this study we investigated the role of GJIC in oscillatory fluid flow-induced PGE_2 production and changes in $Ca^{2+}{}_i$ signalling. We found direct evidence to indicate that the PGE_2 response was dependent upon gap junctions as demonstrated by the lack of PGE_2 released in the gap junction-deficient DN-8 cell line in comparison to the DN-VC cell line. In addition, by investigating real-time $Ca^{2+}{}_i$ responses in these cell lines we found that all three cell lines were able to respond to oscillatory fluid flow with an immediate increase in $[Ca^{2+}]_i$. Finally, by blocking the $Ca^{2+}{}_i$ response with thapsigargin, we demonstrated that the PGE_2 response in MC3T3 –E1 cells to oscillatory fluid flow does not depend upon an increase in $[Ca^{2+}]_i$. Taken together, these findings strongly suggest an important role for gap junctions and GJIC in bone cell mechanotransduction mechanisms.

ACKNOWLEDGMENTS

The authors thank Dr. Zhiyi Zhou for maintenance of the cell lines and technical assistance with the double labeling assays. This work was supported by Army grant DAMD17-98-1-8509, NIH AR45989 and AG15107, and the Whitaker Foundation and NCI Grant [CA-21104]2JET.

REFERENCES

1. Ajubi, N. E., J. Klein-Nulend, P. J. Nijweide, T. Vrijheidlammers, M. J. Alblas, and E. H. Burger. Pulsating fluid flow increases prostaglandin production by cultured chicken osteocytes - A cytoskeleton-dependent process. *Biochemical & Biophysical Research Communications* 225: 62-68, 1996.

2. Binderman, I., Z. Shimshoni, and D. Somjen. Biochemical pathways involved in the translation of physical stimulus into biological message. *Calcified Tissue International* 36: S82-5, 1984.

3. Bowman, N. N., H. J. Donahue, and H. P. Ehrlich. Gap junctional intercellular communication contributes to the contraction of rat osteoblast populated collagen lattices. *Journal of Bone and Mineral Research* 13: 1700-1706, 1998.

4. Brown, E. M., M. Pollak, C. E. Seidman, J. G. Seidman, Y. H. Chou, D. Riccardi, and S. C. Hebert. Calcium-ion-sensing cell-surface receptors. *N Engl J Med* 333: 234-40, 1995.

5. Cowan, D. B., S. J. Lye, and B. L. Langille. Regulation of vascular connexin43 gene expression by mechanical loads. *Circulation Research* 82: 786-93, 1998.

6. Donahue, H. J., Z. Li, Z. Zhou, and B. Simon. Pulsed electromagnetic fields affect steady state levels of Cx43 mRNA in osteoblastic cells. *Journal of Bone & Mineral Research* 10: S207, 1995.

7. Donahue, H. J., Z. Li, Z. Zhou, and C. E. Yellowley. Differentiation of human fetal osteoblastic cells is partially dependent on gap junctional intercellular communication. *American Journal of Physiology (Cell) (in press)*:, 2000.

8. Frangos, J. A., S. G. Eskin, L. V. McIntire, and C. L. Ives. Flow effects on prostacyclin production by cultured human endothelial cells. *Science* 227: 1477-1479, 1985.

9. Frangos, J. A., L. V. McIntire, and S. G. Eskin. Shear stress induced stimulation of mammalian cell metabolism. *Biotechnology and Bioengineering* 32: 1053-1060, 1988.

10. Fuller, K., and T. J. Chambers. Effect of arachidonic acid metabolites on bone resorption by isolated rat osteoclasts. *J Bone Miner Res* 4: 209-15, 1989.

11. Gabriels, J. E., and D. L. Paul. Connexin43 is highly localized to sites of disturbed flow in rat aortic endothelium but connexin37 and connexin40 are more uniformly distributed [see comments]. *Circulation Research* 83: 636-43, 1998.

12. Gibson, D. F., D. D. Bikle, J. Harris, and G. S. Goldberg. The expression of the gap junctional protein Cx43 is restricted to proliferating and non differentiated normal and transformed keratinocytes. *Experimental Dermatology* 6: 167-74, 1997.

13. Hung, C. T., F. D. Allen, S. R. Pollack, and C. T. Brighton. Intracellular Ca2+ Stores and Extracellular Ca2+ Are Required In the Real-Time Ca2+ Response Of Bone Cells Experiencing Fluid Flow. *Journal of Biomechanics* 29: 1411-1417, 1996.

14. Hung, C. T., F. D. Allen, S. R. Pollack, and C. T. Brighton. What Is the Role Of the Convective Current Density In the Real-Time Calcium Response Of Cultured Bone Cells to Fluid Flow. *Journal of Biomechanics* 29: 1403-1409, 1996.

15. Hung, C. T., S. R. Pollack, T. M. Reilly, and C. T. Brighton. Real-time calcium response of cultured bone cells to fluid flow. *Clinical Orthopaedics & Related Research* 313: 256-69, 1995.

16. Imamura, K., H. Ozawa, T. Hiraide, N. Takahashi, Y. Shibasaki, T. Fukuhara, and T. Suda. Continuously applied compressive pressure induces bone resorption by a mechanism involving prostaglandin E2 synthesis. *J Cell Physiol* 144: 222-8, 1990.

17. Jacobs, C. R., C. E. Yellowley, B. R. Davis, Z. Zhou, and H. J. Donahue. Differential effect of steady versus oscillating flow on bone cells. *Journal of Biomechanics* 31: 969-976, 1998.

18. Jacobs, C. R., C. E. Yellowley, D. V. Nelson, and H. J. Donahue. A novel application of rainflow counting to time-varying biophysical data. *Computer Methods in Biomechanics and Biomedical Engineering* 2: 1-10, 1999.

19. Jee, W. S., K. Ueno, Y. P. Deng, and D. M. Woodbury. The effects of prostaglandin E2 in growing rats: increased metaphyseal hard tissue and cortico-endosteal bone formation. *Calcif Tissue Int* 37: 148-57, 1985.

20. Johnson, D. L., T. N. McAllister, and J. A. Frangos. Fluid Flow Stimulates Rapid and Continuous Release Of Nitric Oxide In Osteoblasts. *American Journal of Physiology - Endocrinology & Metabolism* 34: E 205-E 208, 1996.

21. Jorgensen, N. R., S. T. Geist, R. Civitelli, and T. H. Steinberg. ATP- and gap junction-dependent intercellular calcium signaling in osteoblastic cells. *Journal of Cell Biology* 139: 497-506, 1997.

22. Klein-Nulend, J., E. H. Burger, C. M. Semeins, L. G. Raisz, and C. C. Pilbeam. Pulsating fluid flow stimulates prostaglandin release and inducible prostaglandin G/H synthase mRNA expression in primary mouse bone cells. *Journal of Bone & Mineral Research* 12: 45-51, 1997.

23. Klein-Nulend, J., C. M. Semeins, N. E. Ajubi, P. J. Nijweide, and E. H. Burger. Pulsating fluid flow increases nitric oxide (NO) synthesis by osteocytes but not periosteal fibroblasts--correlation with prostaglandin upregulation. *Biochemical & Biophysical Research Communications* 217: 640-8, 1995.

24. Krutovskikh, V. A., H. Yamasaki, H. Tsuda, and M. Asamoto. Inhibition of intrinsic gap-junction intercellular communication and enhancement of tumorigenicity of the rat bladder carcinoma cell line BC31 by a dominant-negative connexin 43 mutant. *Mol Carcinog* 23: 254-61, 1998.

25. Lecanda, F., D. A. Towler, K. Ziambaras, S. Cheng, M. Koval, T. H. Steinberg, and R. Civitelli. Gap junctional communication modulates gene expression in osteoblastic cells. *Molecular Biology of the Cell* 9: 2249-2258, 1998.

26. McLeod, K. J., H. J. Donahue, P. E. Levin, M. A. Fontaine, and C. T. Rubin. Electric fields modulate bone cell function in a density-dependent manner. *Journal of Bone & Mineral Research* 8: 977-84, 1993.

27. Pilbeam, C. C., H. Kawaguchi, Y. Hakeda, O. Voznesensky, C. B. Alander, and L. G. Raisz. Differential regulation of inducible and constitutive prostaglandin endoperoxide synthase in osteoblastic MC3T3-E1 cells. *Journal of Biological Chemistry* 268: 25643-25649, 1993.

28. Reich, K. M., C. V. Gay, and J. A. Frangos. Fluid shear stress as a mediator of osteoblast cyclic adenosine monophosphate production. *Journal of Cellular Physiology* 143: 100-104, 1990.

29. Su, M., J. L. Borke, H. J. Donahue, Z. Li, N. M. Warshawsky, and C. M. Russell. Expression of connexin 43 in rat mandibular bone and PDL cells during experimental tooth movement. *Journal of Dental Research* 76: 1357-1366, 1997.

30. Trosko, J., and R. Ruch. Cell-cell communication in carcinogenesis. *Frontiers in Bioscience* 3: d208-236, 1998.

31. Tsien, R. Y., T. J. Rink, and M. Poenie. Measurement of cytosolic free Ca2+ in individual small cells using fluorescence microscopy with dual excitation wavelengths. *Cell Calcium* 6: 145-57, 1985.

32. Turner, C. H., and F. M. Pavalko. Mechanotransduction and function response of the skeleton to physical stress: The mechanisms and mechanics of bone adaptation. *Journal of Orthopaedic Science* 3: 346-355, 1998.

33. Vander Molen, M. A., H. J. Donahue, C. T. Rubin, and K. J. McLeod. Osteoblastic networks with deficient coupling: differential effects of magnetic and electric field exposure. *Bone* 27: 227-31, 2000.

34. Vander Molen, M. A., C. T. Rubin, K. J. McLeod, L. K. McCauley, and H. J. Donahue. Gap junctional intercellular communication contributes to hormonal responsiveness in osteoblastic networks. *J. Biol. Chem.* 271: 12165-12171, 1996.

35. Weinbaum, S., S. C. Cowin, and Y. A. Zeng. A model for the excitation of osteocytes by mechanical loading induced bone fluid shear stresses. *Journal of Biomechanics* 27: 339-360, 1994.

36. White, T. W., and D. L. Paul. Genetic diseases and gene knockouts reveal diverse connexin functions. *Annu Rev Physiol* 61: 283-310, 1999.

37. Yellowley, C. E., C. R. Jacobs, Z. Li, Z. Zhou, and H. J. Donahue. Effects of fluid flow on intracellular calcium in bovine articular chondrocytes. *American Journal of Physiology - Cell Physiology* 273: C30-C36, 1997.

38. Yellowley, C. E., C. R. Jacobs, Z. Zhou, and H. J. Donahue. Pulsatile fluid flow-induced shear stress increases intracellular calcium concentration in bovine articular chondrocytes. *Biophysical Journal* 70: A365, 1996.

39. Yellowley, C. E., Z. Li, Z. Zhou, C. R. Jacobs, and H. J. Donahue. Functional gap junctions between osteocytic and osteoblastic cells. *J Bone Miner Res* 15: 209-17, 2000.

40. Yoshizawa, T., S. Watanabe, M. Hirose, A. Miyazaki, and N. Sato. Dimethylsulfoxide maintains intercellular communication by preserving the gap junctional protein connexin32 in primary

cultured hepatocyte doublets from rats. *Journal of Gastroenterology & Hepatology* 12: 325-30, 1997.

41. You, J., C. E. Yellowley, H. J. Donahue, Y. Zhang, Q. Chen, and C. R. Jacobs. Substrate deformation levels associated with routine physical activity are less stimulatory to bone cells relative to loading-induced oscillatory fluid flow. *J Biomech Eng* 122: 387-93, 2000.

42. You, J., X. Zhen, C. E. Yellowley, Q. Chen, H. J. Donahue, and C. R. Jacobs . Mechanotransduction in bone cells via oscillating flow. (Abstract) *Orthop. Trans.* 46: 293, 2000.

43. Ziambaras, K., F. Lecanda, T. H. Steinberg, and R. Civitelli. Cyclic stretch enhances gap junctional communication between osteoblastic cells. *Journal of Bone & Mineral Research* 13: 218-228, 1998.

FIGURE LEGENDS

Figure 1. Schematic of oscillatory fluid flow delivery system. a) Oscillatory fluid flow was delivered via a sinusoidal waveform generated by a materials testing machine connected to the flow chamber using tubing and syringes. b) The flow chamber consisted of a parallel plate design. Cells in monolayer on the glass slide were inverted on the flow chamber on a silastic gasket. During fluid flow, the assembly was held together with either a vacuum seal or encased in a polycarbonate case (not shown).

Figure 2. Qualitative results of double labeling assay at 24 and 96 hours in the three cell lines examined. MC3T3-E1 (a,b), DN-VC (c,d) or DN-8 (e,f) cells were grown in monolayer for 24, 48 (not shown) or 96 hours and subjected to homospecific GJIC analysis. Donor cells double labeled with the fluorescent dyes calcein and DiI were placed in contact with unloaded like cells in monolayer. Cell transfer was visualized after 90 minutes. In the dual exposure photographs, the cells fluorescing green (calcein) are the unlabeled cells in monolayer demostrating functional coupling; the cells fluorescing yellow (calcein and DiI) are the dual labeled donor cells (magnification 400x).

Figure 3. Quantitative results of double labeling assay at 24, 48 and 96 hours in the three cell lines examined. MC3T3-E1 and DN-VC cell lines were highly coupled at all time points. No significant differences in coupling were found within or between these two lines at the various time points. The DN-8 cell line was well coupled at 24 and 48 hours and not significantly different from the other cell lines at these time points. At 96 hours, coupling in the DN-8 line was significantly diminished in comparison to the DN-8 line at 24 hours and 48 hours ($p<0.001$), as well as in comparison to the MC3T3-E1 and DN-VC lines at this time point ($p<0.001$). Each bar is representative of a minimum of 60 cells (maximum 110) and is plotted as mean ± SEM with individual cell transfers not counted past a maximum of fifteen cells. * - significantly different from 24 and 48 hour time points within group; + - significantly different from 96 hour time points in MC3T3 and DN-VC cell lines

Figure 4. Results of PGE_2 quantification in the three cell lines examined. The numbers are representative of total PGE_2 accumulation in the media normalized to total protein and collected immediately (0-hour) and after an additional 1 hour incubation period (1-hour). (Top) At 48 hours, the DN-8 cell line displayed an increase in PGE_2 accumulation in response to oscillatory fluid flow with more accumulation obtained from the 1-hour post-flow samples. At 96 hours, the DN-8 cell line responded to flow with no significant increases in PGE_2 accumulation from either the 0-hour or 1-hour collections. (Bottom) At 96 hours, the MC3T3 and DN-VC cell lines responded to fluid flow with an increase in PGE_2 accumulation, while the DN-8 cell line did not respond to fluid flow. Although results are shown for the 1-hour collections only, similar trends were exhibited in the 0-hour collections (data not shown). Interestingly, baseline levels were elevated in this line at this time point. All results are shown plotted as mean ± SEM with each value representative of at least ten experiments. * - significantly different from no-flow control within group; ** - significantly different from media collected 1-hour post-flow at same time point in DN-VC and DN-8; *** - significantly different from media collected 1-hour post-flow at same time point in MC3T3

Figure 5. Results of $[Ca^{2+}]_i$ imaging at 96 hours. In all cell lines examined, oscillatory fluid flow induced a significant increase in the percentage of cells responding with an increase in $[Ca^{2+}]_i$ ($p<0.0003$, at least). Significant differences were not observed between the groups when comparing the no-flow controls or the flowed samples. All results are shown plotted as mean ± SEM with each value representative of at least four experiments (MC3T3) or six experiments (DN-VC and DN-8). * - significantly different from no-flow control within group

Figure 6. Results of PGE_2 quantification in the presence of thapsigargin at 96 hours in the three cell lines examined. At 96 hours, the PGE_2 response of the cell lines to oscillatory fluid flow was not altered by the presence of thapsigargin. All results are shown plotted as mean ± SEM with each value representative of a minimum of two experiments.

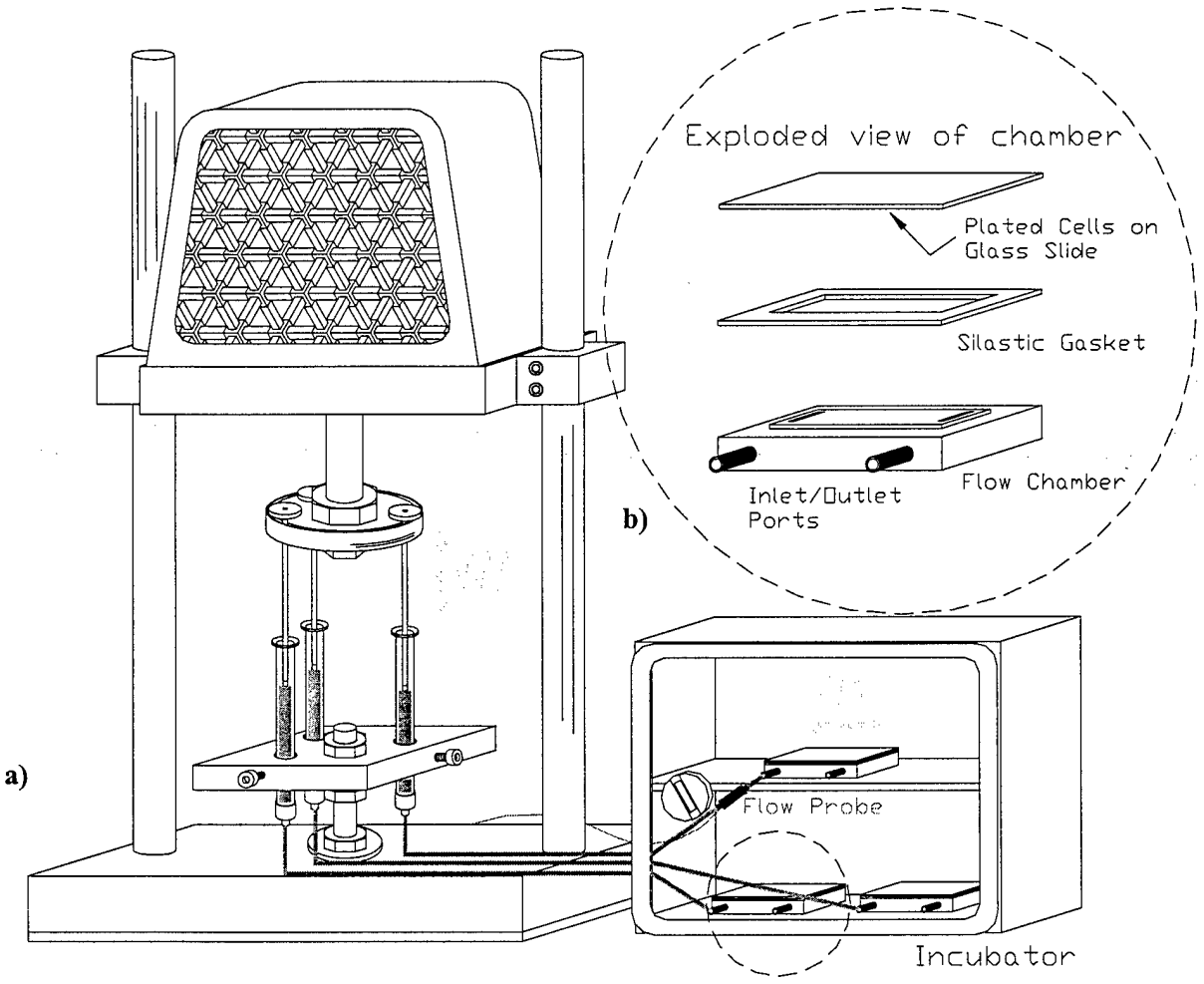

Figure 1 (Saunders, M., et al)

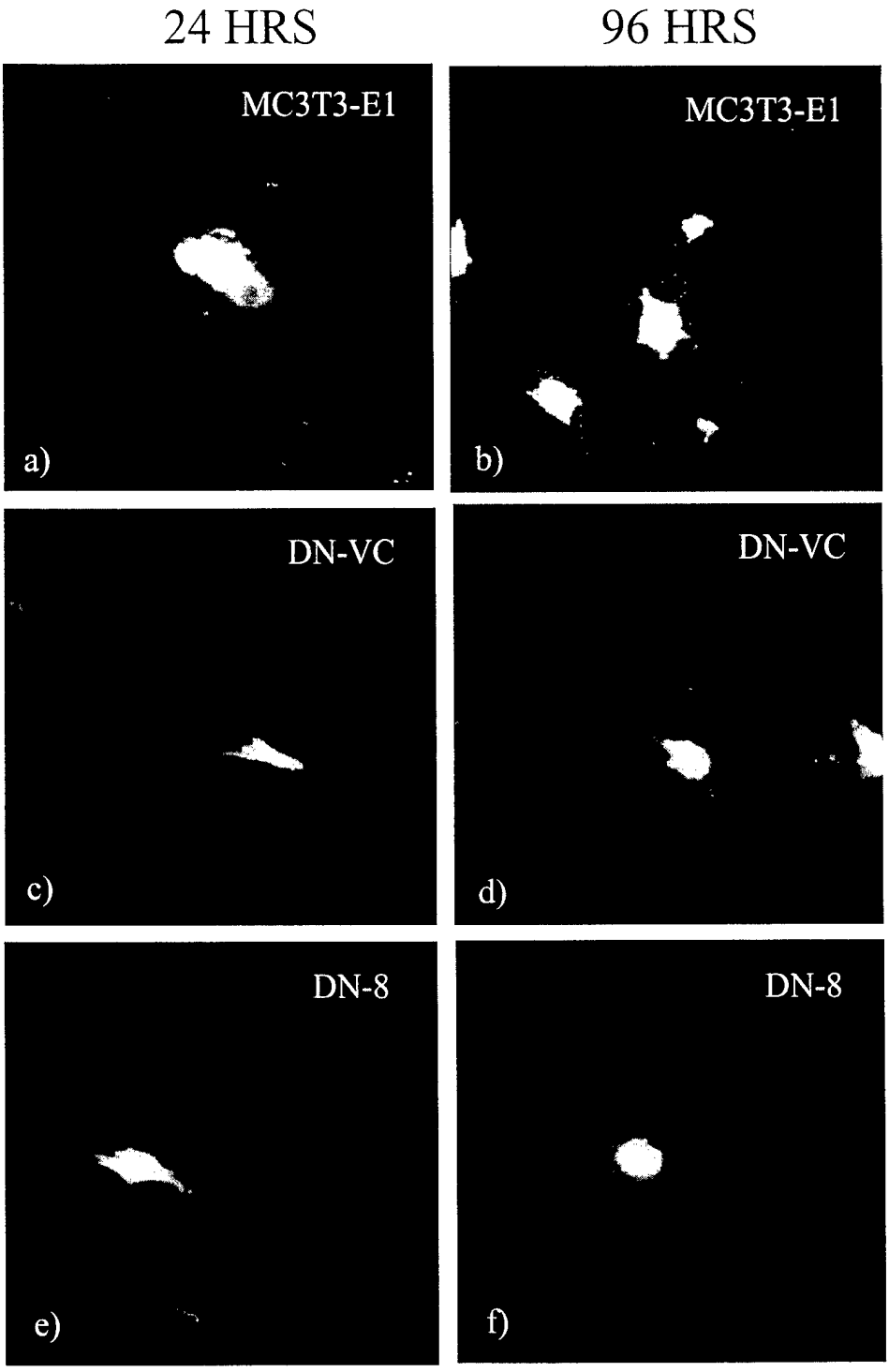

Figure 2 (Saunders, M., et al)

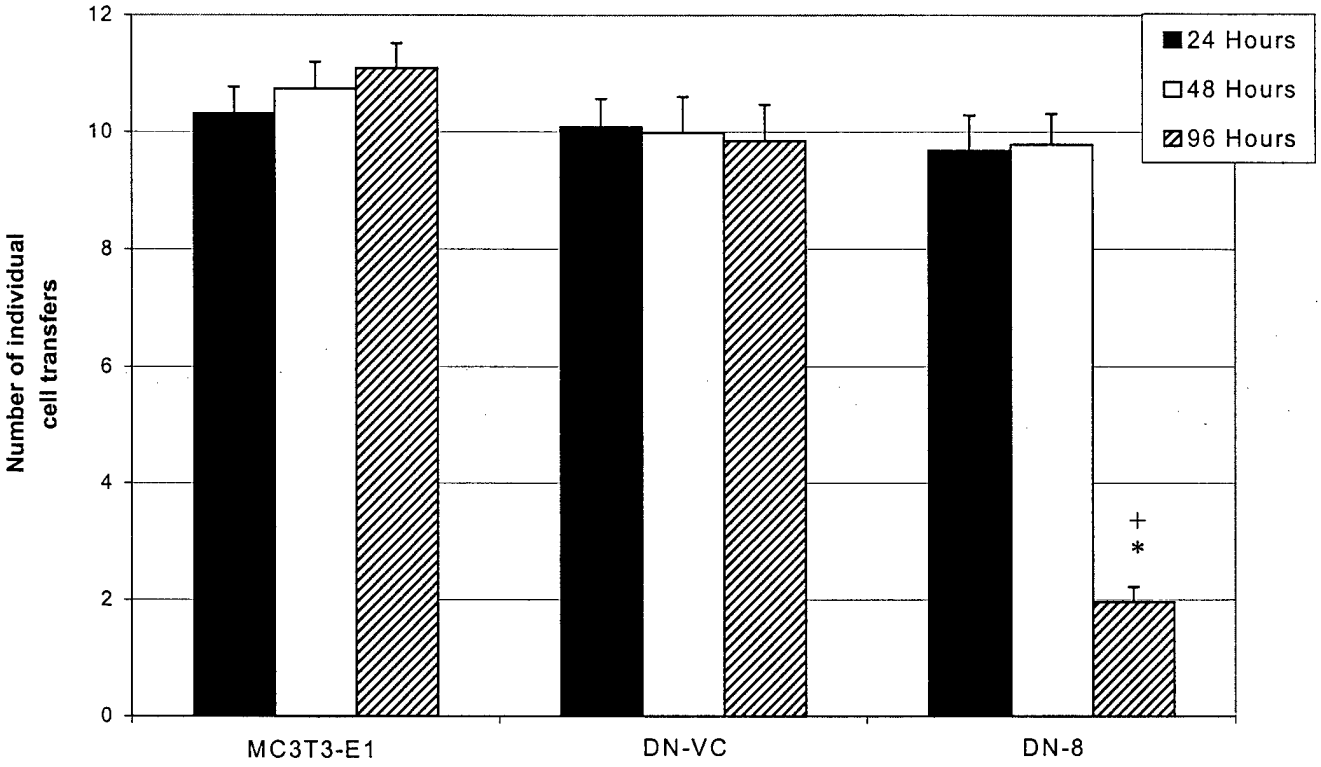

Figure 3 (Saunders, M., et al)

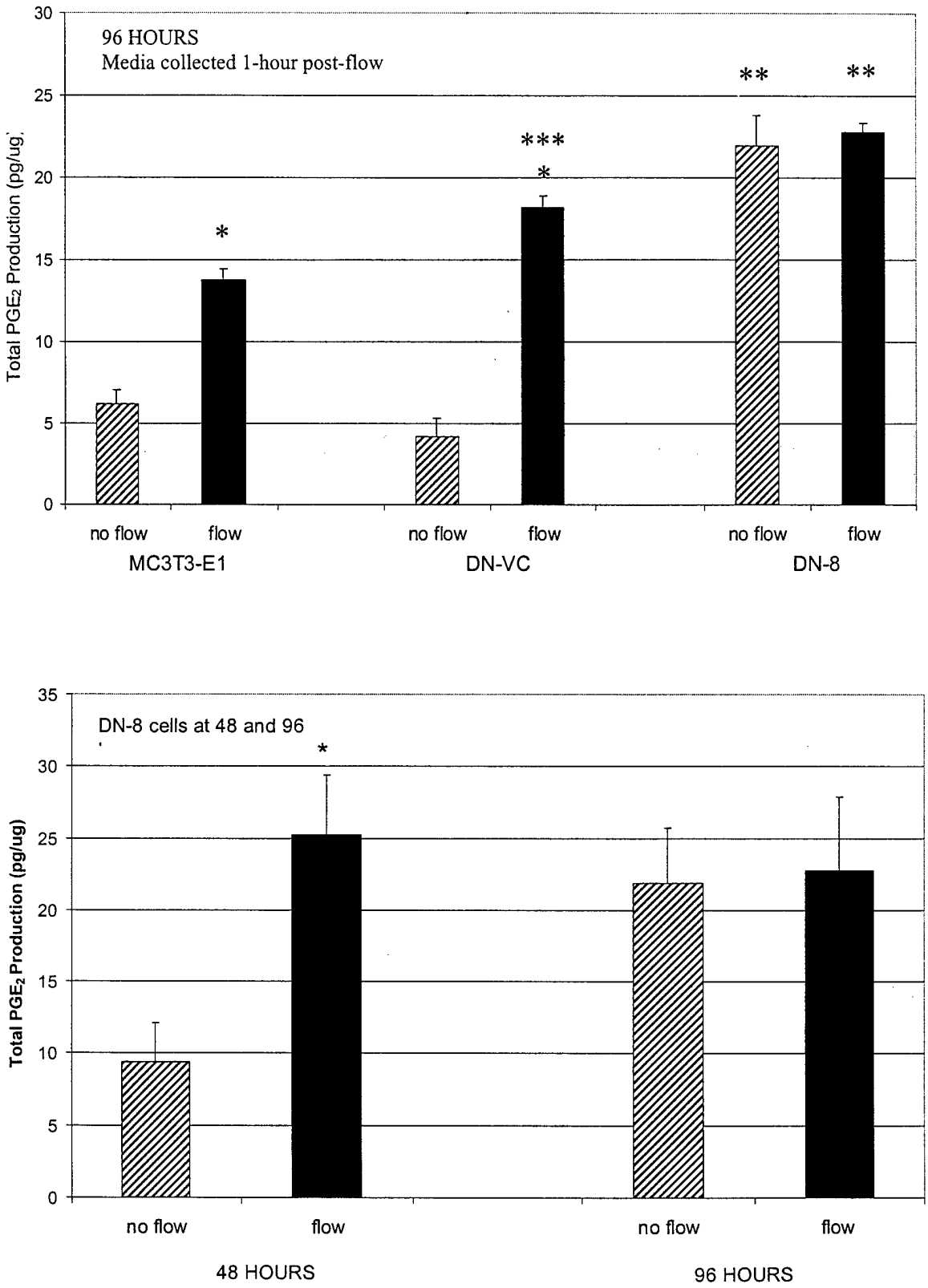

Figure 4 (Saunders, M., et al)

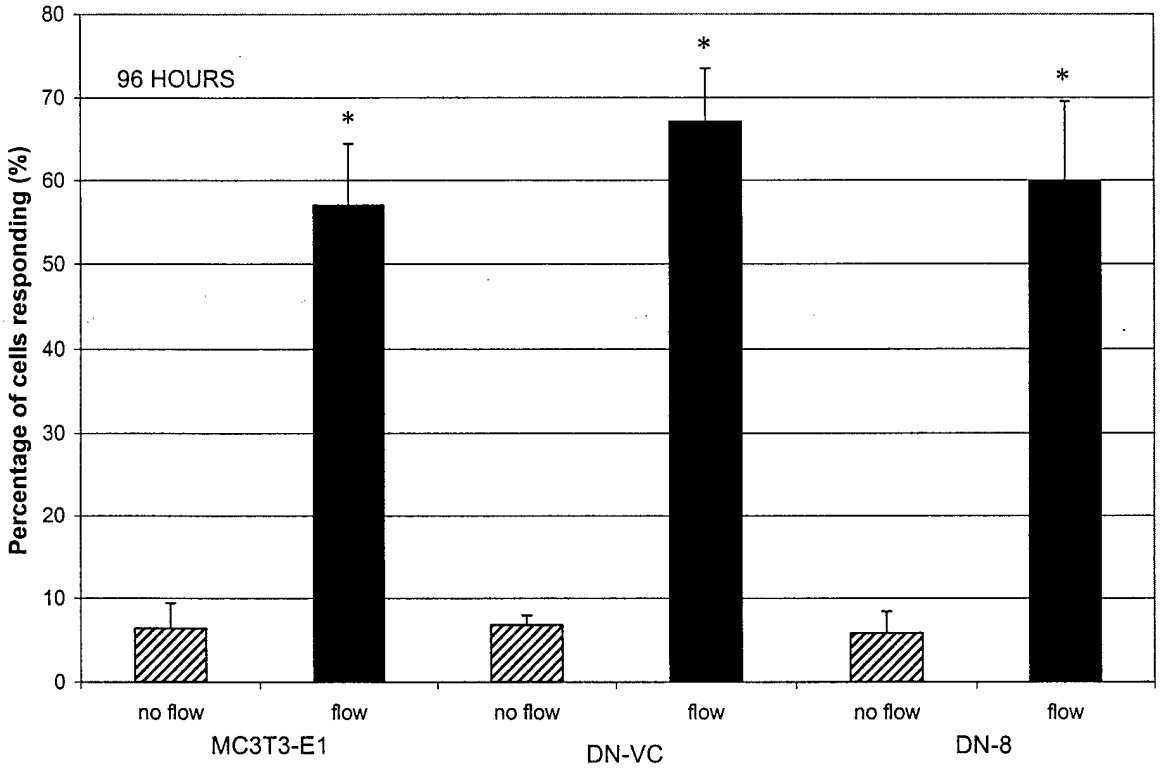

Figure 5 (Saunders, M, et al)

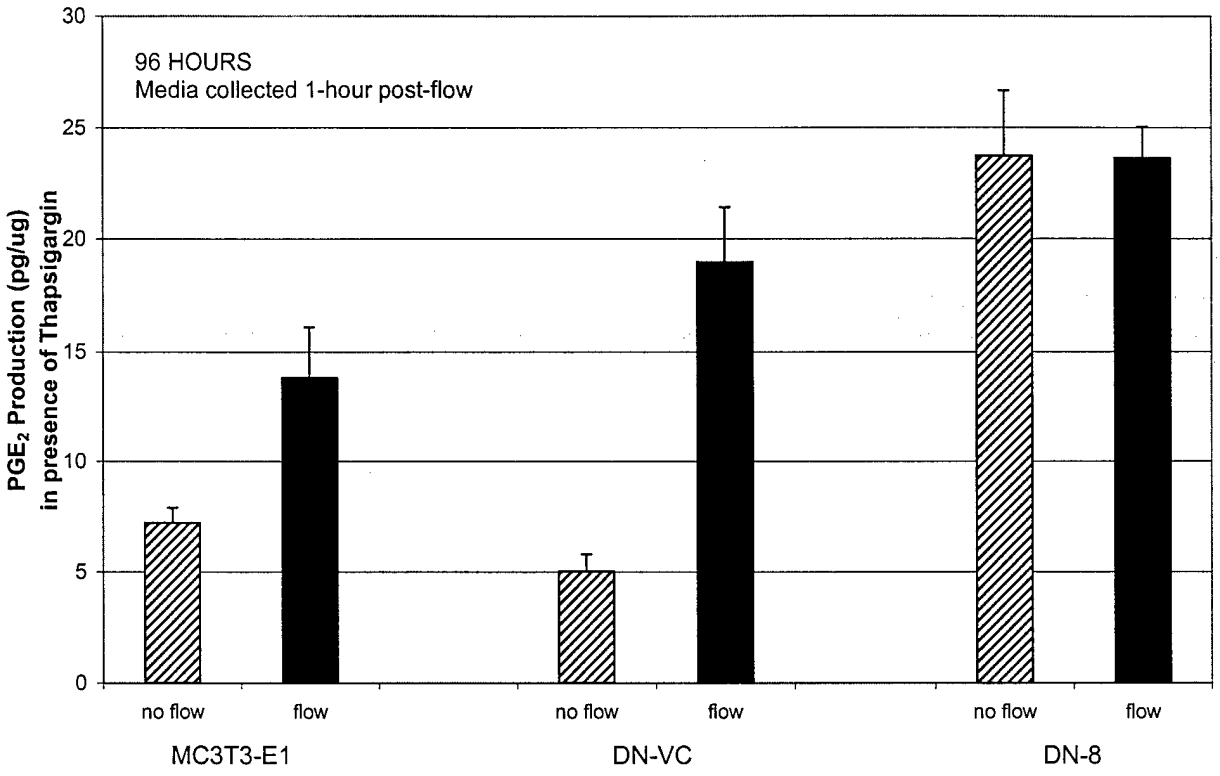

Figure 6 (Saunders, M, et al)

OSTEOPONTIN GENE REGULATION BY OSCILLATORY FLUID FLOW VIA INTRACELLULAR CALCIUM MOBILIZATION AND ACTIVATION OF MITOGEN-ACTIVATED PROTEIN KINASE IN MC3T3-E1 OSTEOBLASTS

Jun You[a §], Gwendolen C. Reilly[a], Xuechu Zhen[b], Clare E. Yellowley[a], Qian Chen[a], Henry J. Donahue[a], and Christopher R. Jacobs[a]

[a] Musculoskeletal Research Laboratory
Department of Orthopaedics and Rehabilitation
The Pennsylvania State University College of Medicine
Hershey, PA 17033

[b] Department of Pharmacology & Physiology
MCP-Hahneman School of Medicine
Drexel University
Philadelphia, PA 19129

* This work was supported by NIH AR45989, AG13087, AG00811 and AG17021, the Whitaker Foundation, Arthritis Foundation, and The US Army Medical Research and Materiel Command award number DAMD 17-98-1-8509

§ **To whom correspondence should be addressed**:
J. You, Ph.D.
Musculoskeletal Research Laboratory
Department of Orthopaedics and Rehabilitation
Penn State University College of Medicine
The Milton S. Hershey Medical Center
Hershey, PA 17033, USA
E-mail: jxy118@psu.edu
Tel: 717-531-4819
Fax: 717-531-7583

Figures: 4 figures.

Running title: Oscillatory flow activated Ca^{2+}_i, MAP kinases and osteopontin

SUMMARY

Recently fluid flow has been shown to be a potent physical stimulus in the regulation of bone cell metabolism. However, most investigators have applied steady or pulsing flow profiles rather than oscillatory fluid flow, which occurs *in vivo* due to mechanical loading. Here oscillatory fluid flow was demonstrated to be a potentially important physical signal for loading-induced changes in bone cell metabolism. We selected three well-known biological response variables including intracellular calcium (Ca^{2+}_i), mitogen-activated protein kinase (MAPK) activity and osteopontin (OPN) mRNA levels to examine the response of MC3T3-E1 osteoblastic cells to oscillatory fluid flow with shear stresses ranging from $2N/m^2$ to $-2N/m^2$ at 1Hz, which is in the range expected to occur during routine physical activities. Our results showed that within 1 minute, oscillatory flow induced cell Ca^{2+}_i mobilization, while two MAPKs (ERK, p38) were activated over a two hour time frame. However, there was no activation of JNK. Furthermore two hour oscillatory fluid flow increased steady-state OPN mRNA expression levels by approximately four-fold, 24 hours after exposure to fluid flow. The presence of both ERK and p38 inhibitors, and thapsigargin completely abolished the effect of oscillatory flow on steady-state OPN mRNA levels. In addition, experiments using a variety of pharmacological agents suggest that oscillatory flow induces Ca^{2+}_i mobilization via the L-type voltage operated calcium channel and the IP_3 pathway.

INTRODUCTION

Mechanical loading plays an important role in regulating bone metabolism. Increased mechanical loading increases bone formation and decreases bone resorption (1). The absence of mechanical stimulation causes reduced bone matrix protein production, mineral content and bone formation, as well as an increase in bone resorption (2). However, the mechanism by which bone cells sense and respond to their physical environment is still poorly understood. In this study we examine a novel physical stimulus, loading induced oscillatory fluid flow, and demonstrate that when applied to cultured osteoblastic cells at levels expected to occur *in vivo* it regulates mRNA levels for an important bone matrix protein, osteopontin (OPN). Furthermore, this regulation occurs via an increase in intracellular calcium (Ca^{2+}_i) and mitogen-activated protein kinases (MAPKs).

The sensitivity of bone tissue to mechanical loading has been proposed to involve a variety of cellular biophysical signals including loading-induced electric fields, matrix strain, and fluid flow. The latter effect of loading, originally described by Piekarski et al. (3), has recently been proposed to directly regulate bone cell metabolism *in vivo* (4,5). Furthermore, relative to other loading-induced biophysical signals applied to cells *in vitro*, fluid flow appears to be significantly more potent at physiological levels (6-10). The origin of loading-induced fluid flow is a consequence of the fact that a significant component of bone tissue is unbound fluid. Bone tissue contains an extracellular fluid compartment that has been demonstrated to communicate with the vascular compartment and mechanical loading has been shown to enhance fluid exchange between the two spaces (11).

When bone is exposed to mechanical loading fluid in the matrix is pressurized and tends to flow into haversian canals. As loading is removed (e.g. during the gait cycle) the pressure gradients, and consequently the direction of fluid flow, are reversed resulting in a flow time-history experienced by the cells that is oscillatory in nature. *In vitro* experiments have shown fluid flow to have a number of effects on bone cells including Ca^{2+}_i mobilization (12), production

of nitric oxide (NO) and prostaglandin E_2 (PGE_2) (8,13), and regulation of the expression of genes for OPN, cyclooxygenase-2, and c-fos (14,15). However, it is important to note that only one study to date utilized a reversing flow profile and found significantly different results when contrasted with non-reversing flow (16). Thus, the aim of this study is to detail important aspects of the biochemical response pathway including immediate, intermediate, and long term effects of oscillatory fluid flow on bone cells, as well as their interrelationships.

To achieve this goal, we first investigated three well-known biological osteogenic response variables. $Ca^{2+}{}_i$, a known second messenger transducing extracellular signals to the cell interior, was our immediate response variable. Activity of MAPKs is important for regulating cell differentiation and apoptosis by transmitting extracellular signals to the nucleus (17,18) and was our intermediate response variable. OPN is characterized as one of the predominant noncollagenous proteins that accumulate in the extracellular matrix of bone (19,20) and is also believed to be an important factor associated with bone remodeling caused by mechanical stress *in vivo* (21). Recently, strong evidence suggests that OPN is an important factor in loading induced bone cell metabolism (22-24). Therefore, we quantified steady-state OPN mRNA levels as a long-term response to oscillatory flow.

Recently MAPK family members including extracellular signal-regulated kinase (ERK), N-terminal Jun kinase (JNK) and p38 MAP kinase have been shown to be important signaling components linking mechanical stimuli to cellular responses, including cell growth, differentiation, and metabolic regulation, in endothelial cells, smooth muscle cells, and myocytes (25-28). However, the role of MAPKs in bone cell mechanotransduction has not been determined. Moreover the role of $Ca^{2+}{}_i$ in osteogenic gene transcription is unclear, especially in the case of oscillatory fluid flow. Therefore, the second goal of this study is to elucidate the roles of $Ca^{2+}{}_i$ and the three major MAPKs in bone cell osteopontin gene expression induced by oscillatory flow.

Finally, the mechanism responsible for fluid-flow induced $Ca^{2+}{}_i$ mobilization has not been

fully established, particularly for the oscillatory flow profiles expected to occur *in vivo*. Yellowley et al. (29) demonstrated that the steady flow-induced $Ca^{2+}{}_i$ responses in bovine articular chondrocytes involved both influx of external Ca^{2+} and release of internal Ca^{2+} from IP_3-sensitive stores and that the mechanism is G-protein activated. Similar results were observed in bone cells stimulated by steady fluid flow (14,30). However there is evidence to suggest that steady and oscillatory fluid flow may have different biophysical effects on bone cells (16). Therefore, the third goal of this study is to elucidate the mechanism contributing to oscillatory flow-induced $Ca^{2+}{}_i$ mobilization in bone cells. Steady flow (30), substrate stretch (31) and whole bone loading experiments (32) suggest that either stretch activated (SA) mechanosensitive channels and/or L-type voltage operated calcium channels (L-type VOCCs) may be involved. Additionally, it is not known whether the involvement of the IP_3 sensitive stores is as important in the response to oscillatory fluid flow and whether other internal pathways (the ryanodine-sensitive pathway) may be involved in $Ca^{2+}{}_i$ mobilization.

MATERIALS AND METHODS

Cell Culture

The mouse osteoblastic cell line MC3T3-E1 was cultured in minimal essential medium (MEM-α) (GIBCO, Grand Island, NY) containing 10% fetal bovine serum (FBS) (Hyclone, Logan, UT), 1% penicillin and streptomycin (GIBCO BRL, Grand Island, NY) and maintained in a humidified incubator at 37°C with 5% CO_2. All cells were subcultured on glass slides for two days prior to experiments, with the exception of cells cultured for $Ca^{2+}{}_i$ studies, for which quartz slides were used, for UV transparency. $3x10^5$ cells were seeded on the glass slides (75mm x 38mm x 1.0mm), and $0.85x10^5$ cells on the quartz slides (76mm x 26mm x 1.6mm). There are no significant differences observed in the behavior of MC3T3-E1 cells grown on normal glass slides versus quartz slides (unpublished data). Cells were exposed to oscillatory fluid flow in MEM-α and 2% FBS for calcium imaging experiments, and in MEM-α and 10% FBS for long term 2 hour experiments.

Oscillatory Fluid Flow Device

Two different parallel plate flow chamber sizes were utilized. Larger chambers with a rectangular fluid volume of 56mm x 24mm x 0.28mm were employed for long term flow in order to accommodate the larger glass slides. This size of slide was necessary to obtain adequate amounts of cell protein and mRNA. The smaller chamber design, fluid volume 38mm x 10mm x 0.28mm, was employed in the calcium imaging studies where total cell number is not an issue. The oscillatory flow device was described in our previous study (16). Briefly, a Hamilton glass syringe was mounted in a small servopneumatic loading frame (EnduraTec, Eden Prairie, MN). The flow rate was monitored with an ultrasonic flowmeter with a 100Hz frequency response (Transonic Systems Inc., Ithaca, NY).

Calcium Imaging

Intracellular calcium ion concentration ($[Ca^{2+}]_i$) was quantified with the fluorescent dye

fura-2. Fura-2 exhibits a shift in absorption when bound to Ca^{2+} such that the emission intensity when illuminated with ultraviolet light increases with calcium concentration at a wavelength of 340nm, and decreases with calcium concentration at 380nm. The ratio of light intensity between the two wavelengths corresponds to calcium concentration. A calibration curve of intensity ratio and calcium concentration was obtained using fura-2 in buffered calcium standards supplied by the manufacturer (Molecular Probes, Inc., Eugene, OR).

Preconfluent (80%) cells were washed with MEM-α and 2% FBS at 37°C, incubated with 10μM fura-2-acetoxymethyl ester (Molecular Probes, Eugene, OR) solution for 30 min at 37°C, then washed again with fresh MEM-α and 2% FBS prior to experiments.

Cell ensembles were illuminated at wavelengths of 340 and 380nm in turn. Emitted light was passed through a 510nm interference filter and detected with an ICCD camera (International LTD., Sterling, VA). Images were recorded, one every two seconds, and analyzed using image analysis software (Metafluor; Universal Imaging, West Chester, PA). Basal $[Ca^{2+}]_i$ was sampled for 3 minutes and followed by 3 minutes of oscillatory fluid flow (peak shear stress: $2N/m^2$, 1Hz).

MAPK activity assay

There are three major MAPKs, p38 MAPK, ERK (extracellular signal regulated protein kinase) and JNK (Jun-N-terminal kinase). 100μg lysate protein from either control or flowed cells was immunoprecipitated with anti-p38 MAPK, anti-ERK1/2 or anti-JNK antibody (Santa Cruz Biotech. Inc., Santa Cruz, CA) overnight. Following addition of 15μl of protein A/G for 2 hours, the immunocomplex was collected by centrifugation and the kinase reaction was then conducted in a kinase reaction buffer containing substrates myelin basic protein (MBP, for p38 MAPK or ERK) or c-Jun GSK (for JNK) in presence of $[\gamma\text{-}^{32}P]$ ATP as described before (33). The reaction mix was subjected to SDS-PAGE and phosphorylation of substrates was determined by autoradiography.

Osteopontin mRNA Analysis

Steady-state osteopontin mRNA level was quantified by quantitative real-time reverse transcription PCR (QRT RT-PCR) (9). Briefly, this technique is based on the detection of a fluorescent signal produced by an OPN-specific oligonuleotide probe during PCR primer extension (Prism 7700 Sequence Detection System, Applied Biosystems, Frost City, CA). The RNeasy Mini Kit (Qiagen Inc., Valencia, CA) was used to extract total RNA after lysis and homogenization with the QIAshredder mini column system (Qiagen Inc., Valencia, CA). Mouse osteopontin cDNA primers and probes were designed using sequence data from Miyazaki et al. (34) (GenBank Accession No. X51834) and the QRT RT-PCR probe/primer design software Primer Express (v1.0 Applied Biosystems, Frost City, CA). The fluorogenic oligonucleotide probe for mouse osteopontin was 5'-CGG TGA AAG TGA CTG ATT CTG GCA GCT C-3' (Synthetic Genetics, San Diego, CA). The forward and reverse PCR primers were 5'-GGC ATT GCC TCC TCC CTC-3', and 5'-GCA GGC TGT AAA GCT TCT CC-3' respectively. These sequences were synthesized and PCR conditions optimized with respect to concentrations of Mg^{2+}, probe and both primers. Relative changes in the levels of OPN mRNA and 18S rRNA were quantified 24 hours after mechanical stimulation.

Pharmacological agents

A series of pharmacological agents were used to examine the mechanism of calcium mobilization: thapsigargin (50nM), gadolinium chloride (10μM), nifedipine (20μM), ryanodine (1μM and 20μM), 2-aminoethoxydiphenyl borate (2APB) (100mM), U73122 and U73343 (4 or 5μM). Thapsigargin is an inhibitor of the ATP-dependent Ca^{2+} pump of intracellular Ca^{2+} stores which causes Ca^{2+} discharge (35) and was used to empty the intracellular calcium stores. Gadolinium chloride (10μM) (Aldrich Chem. Co., Milwaukee, WI), is a putative stretch-activated channel blocker (36). Nifedipine is a blocker of the L-type VOCC (37). Ryanodine, which affects ryanodine sensitive channels in intracellular calcium stores, was used in two concentrations: 1μM, which is expected to hold the channel open and 20μM which is expected to

block the channel (38,39). U73122 inhibits the action of phospholipase C (PLC) and possibly phospholipase A_2 (PLA_2), and thereby the production of inositol 1,4,5 triphosphate (IP_3). Thus, it inhibits the release of calcium through IP_3 sensitive intracellular calcium stores (14,40). U73343, an isoform of U73122 that does not inhibit IP_3 production, was used as a control. 2APB is a specific inhibitor of the IP_3 receptor and does not affect ryanodine sensitive or membrane calcium channels (41,42). Cells were pretreated with media containing the required drug for 30-60 min prior to flow and the drug remained present during the flow experiments.

Nifedipine, ryanodine and 2APB were dissolved in 100% ethanol to give a final concentration of ethanol in the flow media of 0.1% (v/v), vehicle controls were conducted with the same concentration of ethanol. Thapsigargin, U73122 and U73343 were dissolved in DMSO to give a final concentration of DMSO in the flow media of 0.0032%, 0.17% and 0.17% (v/v) respectively. Gadolinium chloride was directly dissolved in medium.

Thapsigargin and gadolinium chloride were also used in long-term flow experiments to examine the role of $[Ca^{2+}]_i$ in downstream responses. For the MAPK investigations, cells were incubated with MAPK inhibitor for 2 hours before the fluid flow experiments were performed. The p38 inhibitor SB203580 (10μM) or the ERK inhibitor PD98059 (10μM) (Calbiochem-Novabiochem Co., La Jolla, CA) was also present in the flow media. All pharmacological agents were from Sigma (St. Louis, MO) unless indicated.

Data Analysis

We used a numerical procedure from mechanical analysis, known as Rainflow cycle counting, to identify calcium oscillations (43). Briefly, this technique identifies complete cycles or oscillations in the time history data even when they are superimposed upon each other, and therefore can be used to distinguish and quantify $[Ca^{2+}]_i$ responses from background noise. We defined a response as an oscillation in $[Ca^{2+}]_i$ at least two-fold greater than that of the average baseline level of non-treated cells. Baseline $[Ca^{2+}]_i$ data were recorded for each slide for 3 min prior to the application of oscillatory fluid flow.

Data were expressed as mean ± SEM. To compare observations from no flow and flow responses a two-sample Student t-test was used in which sample variance was not assumed to be equal. To compare observations from more than two groups, a one-way analysis of variance was employed followed by a Bonferroni selected-pairs multiple comparisons test (Instat, GraphPad Software Inc., San Diego, CA). $p<0.05$ was considered statistically significant. For calcium experiments all controls were combined as no effect of vehicles was found (one way ANOVA).

RESULTS

$Ca^{2+}{}_i$ responses to oscillatory fluid flow

Typical cell $Ca^{2+}{}_i$ responses are shown in figure 1A. The fraction of MC3T3-E1 cells responding with an increase in $Ca^{2+}{}_i$ to oscillatory fluid flow (peak shear stress $2N/m^2$, 1Hz) is shown in figure 1B. The data were obtained from 6 individual experiments (slides) and a total of 334 cells. Within thirty seconds of starting oscillatory flow, 59.1±4.6% of cells increased $[Ca^{2+}]_i$ which was significantly different from no flow periods (8.9±1.6%). However the responding cell $[Ca^{2+}]_i$ amplitudes (65.5±17.5nM) for flow periods was not statistically different from those for no flow periods (86.5±18.3nM).

MAPK responses to oscillatory fluid flow

The time courses of activation of three major MAPKs in MC3T3-E1 cells are shown in figure 2. At each time point cells from two slides were combined to yield sufficient protein for the MAPK activity assay. In the absence of flow there was minimal p38, ERK1/2, and JNK activity. However, dramatic responses for p38 and ERK1/2 activities were observed beginning at 15 min after applying oscillatory flow. p38 activity reached a maximum at 30 min and returned to initial levels 90 min after the onset of oscillatory flow (figure 2). ERK1/2 activity reached a maximum at 60 min and returned to its pre-flow value at 90 min. In contrast, there was no change in JNK activity during a 90 min flow period, indicating a selective activation of p38/ERKs in response to flow.

OPN responses to oscillatory fluid flow

The long time frame biological response, steady-state OPN mRNA level, was quantified in response to oscillatory fluid flow at 1Hz, resulting in a wall shear stress of $2N/m^2$, utilizing QRT RT-PCR. The cells that experienced oscillatory flow or no flow for 2 hours were then incubated for an additional 24 hours prior to collection. Our results show oscillatory fluid flow increased steady-state osteopontin mRNA levels by 3.96±0.76 fold over no-flow control (figure

3, $p<0.05$).

Role of $Ca^{2+}{}_i$ and MAPK activities in the OPN mRNA response to oscillatory fluid flow

To assess role of $Ca^{2+}{}_i$ in the OPN mRNA response to oscillatory fluid flow, cells were subjected to oscillatory fluid flow in the presence of 50nM thapsigargin. Interestingly thapsigargin completely blocked the oscillatory flow effect on steady-state OPN mRNA levels (0.93±0.08 times no flow levels) which were not statistically different from those for no flow period (figure 3). However, gadolinium chloride ($GdCl_3$, 10μM) did not attenuate the flow effect on steady-state OPN mRNA levels (4.19±0.21 times no flow levels) which were not statistically different from those for flow control case.

Based on the MAPK activation results, two MAPK inhibitors were employed to block the activity of ERK1/2 and p38. Cells were exposed to 10μM of the p38 inhibitor SB203580 (SB) for 2 hours prior to and for the duration of oscillatory fluid flow. SB reduced the effect of fluid flow on steady-state OPN mRNA levels to 1.61±0.50 times no-flow levels. Similar results of ERK1/2 inhibitor PD98059 (PD) (10μM) were obtained with a reduction of steady-state OPN mRNA to 1.76±0.21 times no-flow levels. Moreover the presence of both inhibitors (SB+PD) completely abolished the effect (0.84±0.05 times no-flow levels, not statistically different). Those results suggest that activation of p38 MAPK and ERKs are synergistically involved in flow-mediated OPN expression.

Sources of Ca^{2+} mobilization in response to oscillatory fluid flow

The number of cells that responded to oscillatory fluid flow with a change in intracellular calcium in the presence of $GdCl_3$ was not significantly different from control (62.2±3.4%, figure 4A). In contrast to the results for $GdCl_3$, nifedipine, an L-type VOCC blocker, did reduce the number of cells responding to flow. The number of cells responding in the presence of nifedipine (29.3±13.6%) was as low as in the no flow case and the mean increase in $[Ca^{2+}]_i$ over baseline (35.6±2.9nM) was lower than in flow controls.

On application of thapsigargin, which emptied intracellular stores, there was a significant ($p<0.05$) decrease in the percentage of cells responding to oscillatory flow. U73122, which inhibits production of IP_3 via the PLC pathway and does not affect membrane channels, reduced the number of cells responding to 18.0±9.0%, compared with 48.0±9.5 in the control group. 2ABP which acts directly on IP_3 receptors (42), rather than on IP_3 catalysis, blocked the response completely. Ryanodine at 1μM had a small, but statistically significant effect on number of cells responding, which was reduced to 41.6±9.9%. It also had a small effect on the mean increase in $[Ca^{2+}]_i$ over baseline, which was reduced to 37.4±5.5nM. At 20μM, at which concentration the ryanodine sensitive channel should have been blocked, there was a very small and not statistically significant reduction in the number of cells responding, to 55.1±10.4%. Although there were some differences in the mean response amplitudes (figure 4B), these were not found to be statistically significant. Some drug-treated cells (nifedipine and ryanodine) showed higher responses in the no flow period compared to controls (data not shown) because the drugs caused increased spontaneous calcium oscillations and increased drift in the baseline levels.

DISCUSSION

While a large number of *in vitro* studies have been aimed at discovering the regulatory effect of mechanical loading in bone adaptation, little consensus can be found in the literature regarding the appropriate biophysical signals. For example, bone cells have been shown to respond with metabolic changes to deformation induced by stretching of the substrate to which they are attached (22,44-46). However, these studies either employed hyperphysiologic levels of strain or systems known to induce mechanical effects other than pure strain (47). More recent studies have suggested that bone cells are more responsive to the fluid flow induced by mechanical strain than directly to the strain in the tissue (7-9). However, loading-induced fluid flow *in vivo* involves a reversal of flow direction associated with the cyclical unloading that occurs in the vast majority of physical activities. To date, the ability of the resulting oscillatory flow profiles to regulate bone cell behavior *in vitro* has not been investigated, beyond its ability to mobilize cytosolic calcium (16). In this study a novel oscillatory fluid flow system was designed to demonstrate that oscillatory fluid flow is capable of regulating bone cell gene expression via ERK and p38 MAPK activity and intracellular calcium signaling involving IP_3 mediated calcium release. Additionally, we were able to demonstrate some important differences in the characteristics of the response of bone cells to oscillatory flow when contrasted with published experiments on steady/pulsatile flow. The study of the effects of oscillatory fluid flow on bone cells will allow us to more accurately understand the mechanism of mechanotransduction in bone cells *in vivo*, for which the other *in vitro* systems may not be as suitable.

Our experimental data have shown that oscillatory fluid flow induced three biological responses that are believed to be important in the response of bone tissue to mechanical load. In the short term, within two minutes of the start of oscillatory flow, 59.1±4.6% of cells increased $[Ca^{2+}]_i$ which was significantly different from the no flow period. This is consistent with prior observations of the $Ca^{2+}{}_i$ response of bovine aortic endothelial cells (48), articular chondrocytes (49) and bone cells (12,16) to steady/pulsatile fluid flow. However, oscillatory flow appears to be

significantly less stimulatory than steady/pulsatile flow for bone cells (16). This suggests that the mechanotransduction pathways induced by oscillatory flow are different in part or in whole than those activated by steady/pulsatile flow.

Recently MAPK activity has been shown to be modulated by various external stimuli such as growth factors, cytokines and physical stresses (ultraviolet radiation, hyperosmolarity, hypoxia and fluid flow shear stress) (17,18,50), and is known to play a pivotal role in a variety of cell functions. Our results are the first to examine the regulation of MAPK activity in response to biophysical stimulation in bone cells. We show that fluid flow induces an increase in the activity of two of three major MAPKs (ERKs and p38) over a period of 2 hours for bone cells. p38 activity started to increase at 15 min and reached a maximum at 30 min, then returned to initial levels 90 min after the onset of oscillatory flow. A similar pattern was observed for ERK1/2 activity, with some delay, at 60 min it reached a peak and returned to its pre-flow value at 90 min. JNK activity was unchanged during 90 min of oscillatory fluid flow stimulus. Our biphasic time course ERK1/2 and p38 activity results are consistent with previous studies in endothelial cells and smooth muscle cells (25,26). However, our time to peak ERK1/2 activity (60 min) is slower than observed for steady fluid flow (5 min), possibly due to the different mechanical stimuli. Another difference is that oscillatory fluid flow did not induce JNK activity in bone cells, however steady fluid flow is capable of activating JNK in endothelial cells within 60 min (25). Although possibly due to differences between the cell types, it may be a result of differences in the effects of the physical signals applied. This suggests the possibility that oscillatory fluid shear stress may stimulate different mechanotransduction pathways from steady/pulsatile fluid shear stress.

It was suggested previously that the ERK pathway is involved in the regulation of cell proliferation and differentiation while p38 and JNK are important signaling pathways in the regulation of cell apoptosis (51). However, recent information demonstrated that p38 MAPK may also play a critical role in the regulation of differentiation (52,53). In this study, both the

p38 inhibitor SB203580 (SB) and the ERK1/2 inhibitor PD98059 (PD) were applied to determine if the increased MAPK activity we observed was required for the effect of oscillating flow on steady-state OPN mRNA levels. Either MAPK inhibitor alone was found to greatly attenuate (80%) the flow effect on steady-state OPN mRNA, while the presence of both inhibitors (SB+PD) completely abolished the effect of flow on steady-state OPN mRNA levels. This indicates that oscillatory flow-induced OPN expression involves both ERK and p38 MAPK activity with mild redundancy, but does not require JNK activity. It is interesting to note that JNK activity has been observed in endothelial cells in response to steady flow associated with apoptosis (25). In contrast, bone cells experiencing more moderate oscillatory shear stress exhibit increased ERK1/2 activity associated with proliferation and differentiation, but no change in JNK activity. These findings support the view that oscillatory fluid flow may be a potent cellular physical signal in bone remodeling *in vivo*.

Our results also suggest that the biochemical mechanism of $Ca^{2+}{}_i$ mobilization is different between non-reversing steady/pulsatile fluid flow and oscillatory flow. The results of the calcium experiment using nifedipine show that the L-type VOCC membrane channel is involved in the calcium response to oscillatory flow in contrast to steady flow experiments in primary bone cells (30), and in the same cell line (14). However our data is in agreement with substrate stretch experiments on primary osteoblasts in which the calcium response was inhibited by nifedipine (31). In those experiments fluid flow may have been induced in the system as well as substrate stretch (47). Thus, it is possible that the $Ca^{2+}{}_i$ response that the investigators observed was due to the pathway we describe here in response to oscillatory flow. Furthermore, the NO and PGE_2 response of loaded whole rat bones in an *in vivo* model has been shown to be eliminated by nifedipine (32). This is consistent with the view that oscillatory flow rather than steady flow is the cellular physical signal that regulates the adaption of bone to mechanical load *in vivo*.

Our data also suggest that the stretch activated (SA) membrane channel, blocked using gadolinium chloride, is not important for response to oscillatory fluid flow. This is in contrast to

data for steady flow where calcium responses were inhibited by blocking this channel (14,30). However, our finding that $GdCl_3$ did not influence steady-state OPN gene mRNA is consistent with the results of Chen et al. (14) that showed the effect of steady flow on cytoskeletal reorganization and COX-2 mRNA involved IP_3 mediated intracellular calcium release, but not extracellular calcium. One interpretation is that both oscillatory and steady flow activate an IP_3 cascade that is important in bone adaptation, however steady flow also stimulates an $GdCl_3$-sensitive calcium influx whereas oscillatory flow does not.

Our finding that thapsigargin completely blocked the calcium response to oscillatory flow demonstrated that the source of Ca^{2+} is release from intracellular stores. The next series of experiments were designed to further elucidate the mechanism of this release. The combination of the U73122 and the 2APB data strongly suggest that the IP_3 pathway is involved. We achieved a partial block of the calcium response using U73122. This may be because there are other pathways to the formation of IP_3 besides the PLC and PLA_2 pathways blocked by U73122. However the effect of U73122 is shown to be maximal at 10μM and we used only 4-5μM because we found that the concentration of solvent (DMSO) necessary to achieve the higher concentration of the drug induced cell toxicity. 2ABP, a novel IP_3 blocker that is specific to the IP_3 channel (41), resulted in a total block of the Ca^{2+} response. This finding is consistent with our previous observations using neomycin sulphate (54) and published results from other laboratories supporting the involvement of this second messenger in fluid flow responses in various cell types and flow regimes (13,14,29,30).

The role of ryanodine sensitive internal stores in mechanotransduction has received less attention, although they have been shown to be present in osteoblasts (55,56). Our finding that low concentration ryanodine inhibited the response of MC3T3-E1 cells to oscillatory flow confirms the presence of ryanodine sensitive calcium channels. In our experiments the opening of the ryanodine sensitive stores which would cause calcium to leave the stores before the flow was applied, in a similar way to thapsigargin, did have an inhibitory effect on the response,

though less than that of thapsigargin. However the blocking of the ryanodine sensitive channel with high concentration ryanodine had no significant effect on the calcium response. This suggests that ryanodine sensitive Ca^{2+} stores, which can also be mobilized by the IP_3 pathway (57), were partially depleted by the low concentration ryanodine, but that ryanodine sensitive channels were not affected by oscillatory fluid flow.

Interestingly, our finding that the source of the calcium response is IP_3 mediated release from intracellular stores seems to be contradicted by our finding that the L-type VOCC is also involved. If the VOCC is important to a calcium response mechanism one might expect to observe some residual calcium increase of extracellular origin, even in the presence of blockers of intracellular stored calcium. However, in our study both 2APB and thapsigargin totally abolished the calcium response to oscillatory fluid flow. Similar results were found in the Walker et al. substrate stretch study (31) in which thapsigargin inhibited the calcium response more than would be expected if only the residual calcium released after nifedipine treatment was from intracellular stores sensitive to thapsigargin. An explanation for these results may be that the IP_3 receptor on the endoplasmic reticulum (ER) has been shown to be co-regulated by cytosolic calcium concentration. Thus, the VOCC could potentate the fluid flow calcium response by regulating the local calcium concentration surrounding the ER IP_3 receptor, but at levels that are not detectable with our imaging system. This mechanism would require that the VOCC and ER IP_3 receptor are in close association. Such an arrangement has previously been described in muscle cells between the VOCC and ryanodine sensitive channels (58).

In the final phase of our investigation we related these intracellular signaling pathways to the regulation of gene expression. OPN has been implicated as an important factor in triggering bone remodeling caused by mechanical stress *in vivo* (21). Our OPN data are consistent with the *in vitro* results of Owan et al. (7). Steady-state OPN mRNA levels increased almost 4 fold within 24 hours after 2 hour oscillatory fluid flow. To elucidate the role of $Ca^{2+}{}_i$ in bone cell mechanotransduction and OPN gene regulation, thapsigargin was employed to empty $Ca^{2+}{}_i$ stores

which prevents Ca^{2+}_i from being available to the cells during the oscillatory flow period. Thapsigargin completely abolished the increase in steady-state OPN mRNA levels that occurred on application of fluid flow. This finding combined with OPN's role in mechanically mediated remodeling suggests a prominent role of cytosolic calcium mobilization in the adaptation of bone to mechanical loading.

While our results suggest that both Ca^{2+}_i and MAPK are involved in the mechanical stress induced OPN expression in bone cells via oscillatory flow, the relationships between Ca^{2+}_i and MAPK are still unclear. Our results show Ca^{2+}_i is required for OPN expression induced by oscillatory flow. However some investigators demonstrated that steady flow in chondrocytes activated ERK1/2 in a way which did not require Ca^{2+}_i, and Ca^{2+}_i alone was not sufficient for MAPK activation by steady flow (59). Therefore the role of Ca^{2+}_i in MAPK activation under oscillatory flow remains to be determined. Little is known about the signaling pathways between MAPK and target genes, although some investigations have shown that MAPK phosphatase-1 may act as a mediator to regulate target gene expression in vascular smooth muscle cells (27). Further investigation of the whole cascade of mechanotransduction in bone cells is necessary.

In summary, our study demonstrates that oscillatory fluid flow is a potent physiological stimulator, which induces Ca^{2+}_i release, and OPN gene expression via ERK1/2 and p38 activation, but not JNK. OPN gene expression required Ca^{2+}_i mobilization. Ca^{2+}_i is mobilized using primarily the IP_3 pathway, with the L-type VOCC membrane channel also playing a role. Our finding elucidates some important differences in the characteristics of the response of bone cells to oscillatory flow versus non-reversing steady/pulsatile flow. These different responses indicate that there are different mechanotransduction pathways in bone cells, depending on stimulus type, and selecting an appropriate mechanical stimulus is critical in understanding the role of mechanical loading in the regulation of bone cell metabolism *in vitro*.

ACKNOWLEDGEMENTS

The authors thank Dr. Deborah Grove for designing primers and completing the QRT RT-PCR protocols.

REFERENCES

1. Morey, E. R., and Baylink, D. J. (1978) *Science* **201**(4361), 1138-41
2. Sessions, N. D., Halloran, B. P., Bikle, D. D., Wronski, T. J., Cone, C. M., and Morey-Holton, E. (1989) *Am J Physiol* **257**(4 Pt 1), E606-10
3. Piekarski, K., and Munro, M. (1977) *Nature* **269**, 80-82
4. Weinbaum, S., Cowin, S. C., and Zeng, Y. A. (1994) *J Biomech* **27**, 339-360
5. Cowin, S. C., Weinbaum, S., and Zeng, Y. (1995) *J Biomech* **28**(11), 1281-1297
6. McLeod, K. J., Donahue, H. J., Levin, P. E., and Rubin, C. T. (1991) in *Electromagnetics in Biology and Medicine* (Brighton, C. T., and Pollack, S. R., eds), pp. 111-115, San Francisco Press, San Francisco
7. Owan, I., Burr, D. B., Turner, C. H., Qiu, J., Tu, Y., Onyia, J. E., and Duncan, R. L. (1997) *Am J Physiol Cell Physiol* **42**(3), C810-C815
8. Smalt, R., Mitchell, T., Howard, R. L., and Chambers, T. J. (1997) *Am J Physiol* **273**(Endocrinol. Metab. 36), E751-E758
9. You, J., Yellowley, C.E., Donahue, H.J., Zhang, Y., Chen, Q. and Jacobs, C. R. (2000) *J Biomech Eng* **122**(4), 387-93
10. Hung, C. T., Allen, F. D., Pollack, S. R., and Brighton, C. T. (1996) *J Biomech* **29**(11), 1403-1409
11. Knothe Tate, M. L., Niederer, P., and Knothe, U. (1998) *Bone* **22**(2), 107-117
12. Hung, C. T., Pollack, S. R., Reilly, T. M., and Brighton, C. T. (1995) *Clin Orthop* **313**, 256-69
13. Ajubi, N. E., Klein-Nulend, J., Alblas, M. J., Burger, E. H., and Nijweide, P. J. (1999) *Am J Physiol* **276**(1 Pt 1), E171-8
14. Chen, N. X., Ryder, K. D., Pavalko, F. M., Turner, C. H., Burr, D. B., Qiu, J., and Duncan, R. L. (2000) *Am J Physiol Cell Physiol* **278**(5), C989-97

15. Pavalko, F. M., Chen, N. X., Turner, C. H., Burr, D. B., Atkinson, S., Hsieh, Y. F., Qiu, J., and Duncan, R. L. (1998) *Am J Physiol* **275**(6 Pt 1), C1591-601

16. Jacobs, C. R., Yellowley, C. E., Davis, B. R., Zhou, Z., Cimbala, J. M., and Donahue, H. J. (1998) *J Biomech* **31**(11), 969-76

17. Seger, R., and Krebs, E. G. (1995) *Faseb J* **9**(9), 726-35

18. Kyriakis, J. M., Banerjee, P., Nikolakaki, E., Dai, T., Rubie, E. A., Ahmad, M. F., Avruch, J., and Woodgett, J. R. (1994) *Nature* **369**(6476), 156-60

19. Denhardt, D. T., and Guo, X. (1993) *Faseb J* **7**(15), 1475-82

20. Gerstenfeld, L. C., Uporova, T., Ashkar, S., Salih, E., Gotoh, Y., McKee, M. D., Nanci, A., and Glimcher, M. J. (1995) *Ann N Y Acad Sci* **760**, 67-82

21. Terai, K., Takano-Yamamoto, T., Ohba, Y., Hiura, K., Sugimoto, M., Sato, M., Kawahata, H., Inaguma, N., Kitamura, Y., and Nomura, S. (1999) *J Bone Miner Res* **14**(6), 839-49

22. Toma, C. D., Ashkar, S., Gray, M. L., Schaffer, J. L., and Gerstenfeld, L. C. (1997) *J Bone Miner Res* **12**(10), 1626-36

23. Harter, L. V., Hruska, K. A., and Duncan, R. L. (1995) *Endocrinology* **136**(2), 528-35

24. Kubota, T., Yamauchi, M., Onozaki, J., Sato, S., Suzuki, Y., and Sodek, J. (1993) *Arch Oral Biol* **38**(1), 23-30

25. Jo, H., Sipos, K., Go, Y. M., Law, R., Rong, J., and McDonald, J. M. (1997) *J Biol Chem* **272**(2), 1395-401

26. Yan, C., Takahashi, M., Okuda, M., Lee, J. D., and Berk, B. C. (1999) *J Biol Chem* **274**(1), 143-50

27. Li, C., Hu, Y., Mayr, M., and Xu, Q. (1999) *J Biol Chem* **274**(36), 25273-80

28. Liang, F., and Gardner, D. G. (1999) *J Clin Invest* **104**(11), 1603-12

29. Yellowley, C. E., Jacobs, C. R., and Donahue, H. J. (1999) *J Cell Physiol* **180**(3), 402-8

30. Hung, C. T., Allen, F. D., Pollack, S. R., and Brighton, C. T. (1996) *J Biomech* **29**(11), 1411-1417

31. Walker, L. M., Publicover, S. J., Preston, M. R., Said Ahmed, M. A., and El Haj, A. J. (2000) *J Cell Biochem* **79**(4), 648-661

32. Rawlinson, S. C., Pitsillides, A. A., and Lanyon, L. E. (1996) *Bone* **19**(6), 609-14

33. Zhen, X., Uryu, K., Wang, H. Y., and Friedman, E. (1998) *Mol Pharmacol* **54**(3), 453-8

34. Miyazaki, Y., Setoguchi, M., Yoshida, S., Higuchi, Y., Akizuki, S., and Yamamoto, S. (1990) *J Biol Chem* **265**(24), 14432-8

35. Thastrup, O., Cullen, P. J., Drobak, B. K., Hanley, M. R., and Dawson, A. P. (1990) *Proc Natl Acad Sci U S A* **87**(7), 2466-70

36. Hamill, O. P., and McBride, D. W., Jr. (1996) *Pharmacol Rev* **48**(2), 231-52

37. Ferrante, J., and Triggle, D. J. (1990) *Biochem Pharmacol* **39**(8), 1267-70

38. Meissner, G. (1986) *J Biol Chem* **261**(14), 6300-6

39. Hasselbach, W., and Migala, A. (1987) *FEBS Lett* **221**(1), 119-23

40. Bleasdale, J. E., Thakur, N. R., Gremban, R. S., Bundy, G. L., Fitzpatrick, F. A., Smith, R. J., and Bunting, S. (1990) *J Pharmacol Exp Ther* **255**(2), 756-68

41. Maruyama, T., Kanaji, T., Nakade, S., Kanno, T., and Mikoshiba, K. (1997) *J Biochem (Tokyo)* **122**(3), 498-505

42. Hamada, T., Liou, S. Y., Fukushima, T., Maruyama, T., Watanabe, S., Mikoshiba, K., and Ishida, N. (1999) *Neurosci Lett* **263**(2-3), 125-8

43. Jacobs, C. R., Yellowley, C. E., Nelson, D. V., and Donahue, H. J. (2000) *Comput Meth Biomech Biomed Eng* **3**, 31-40

44. Rodan, G. A., Bourret, L. A., Harvey, A., and Mensi, T. (1975) *Science* **189**, 467-469

45. Buckley, M. J., Banes, A. J., Levin, L. G., Sumpio, B. E., Sato, M., Jordan, R., Gilbert, J., Link, G. W., and Tran Son Tay, R. (1988) *Bone and Mineral* **4**, 225-236

46. Brighton, C. T., Strafford, B., Gross, S. B., Leatherwood, D. F., Williams, J. L., and Pollack, S. R. (1991) *J Bone Joint Surg* **73A,** 320-331

47. Brown, T. D. (2000) *J Biomech* **33**(1), 3-14

48. Geiger, R. V., Berk, B. C., Alexander, R. W., and Nerem, R. M. (1992) *Am J Physiol* **262**(6 Pt 1), C1411-7

49. Yellowley, C. E., Jacobs, C. R., Li, Z., Zhou, Z., and Donahue, H. J. (1997) *Am J Physiol Cell Physiol* **273**(1 Pt 1), C30-C36

50. Davis, R. J. (1993) *J Biol Chem* **268**(20), 14553-6

51. Johnson, G. L., and Vaillancourt, R. R. (1994) *Curr Opin Cell Biol* **6**(2), 230-8

52. Morooka, T., and Nishida, E. (1998) *J Biol Chem* **273**(38), 24285-8

53. Nebreda, A. R., and Porras, A. (2000) *Trends Biochem Sci* **25**(6), 257-60

54. Reilly, G. C., Yellowley, C. E., Donahue, H. J., and Jacobs, C. R. (2000) *J Bone Miner Res* **15**(Suppl 1), S508

55. McDonald, F., Somasundaram, B., McCann, T. J., Mason, W. T., and Meikle, M. C. (1996) *Arch Biochem Biophys* **326**(1), 31-38

56. Adebanjo, O. A., Biswas, G., Moonga, B. S., Anandatheerthavarada, H. K., Sun, L., Bevis, P. J., Sodam, B. R., Lai, F. A., Avadhani, N. G., and Zaidi, M. (2000) *Am J Physiol Renal Physiol* **278**(5), F784-91

57. Khodakhah, K., and Armstrong, C. M. (1997) *Biophys J* **73**(6), 3349-57

58. Weigl, L. G., Hohenegger, M., and Kress, H. G. (2000) *J Physiol* **525 Pt 2,** 461-9

59. Hung, C. T., Henshaw, D. R., Wang, C. C., Mauck, R. L., Raia, F., Palmer, G., Chao, P. H., Mow, V. C., Ratcliffe, A., and Valhmu, W. B. (2000) *J Biomech* **33**(1), 73-80

Figure Legends

Figure 1. (A) An example of the MC3T3-E1 cell $[Ca^{2+}]_i$ response traces obtained for oscillatory flow ($2N/m^2$, 1Hz). The arrow depicts the onset of flow and each line represents an individual cell response. (B) Fraction of MC3T3-E1 cells responding with an increase in $[Ca^{2+}]_i$ to oscillatory flow. 59.1±4.6% of cells increased $[Ca^{2+}]_i$ for flow period and 8.9±1.6% of cells increased $[Ca^{2+}]_i$ for no flow period. The data were obtained from 6 individual experiments and a total of 334 cells. *$p<0.001$ versus no flow control.

Figure 2. Time courses for p38, ERK1/2, and JNK activation during oscillatory flow ($2N/m^2$, 1Hz). At each time point the cells from two slides were combined to yield sufficient protein for the MAPK activity assay. Kinase activity was assayed by incubating lysates with [γ-^{32}P] ATP and MBP (for p38 MAPK or ERK1/2) or c-Jun GSK (for JNK). The reaction mix was subjected to SDS-PAGE and phosphorylation of substrates was determined by autoradiography.

Figure 3. The percent changes of cell osteopontin mRNA levels in response to oscillatory flow ($2N/m^2$, 1Hz) in the presence of different drugs compared with no flow control. Each bar represents the mean±SEM, and each experiment was repeated on 3 slides (n=3). *$p<0.05$ versus no flow control.

Figure 4. Effect of intracellular Ca^{2+} store modulators on the $Ca^{2+}{}_i$ response to oscillatory flow ($2N/m^2$, 1Hz) in MC3T3-E1 cells. (A): Mean percentage of cells showing a spontaneous Ca^{2+} transient in absence of flow (no-flow control), a response to an oscillatory flow (flow control), and the presence of 50nM thapsigargin, 10μM $GdCl_3$, 20μM nifedipine, 1μM ryanodine, 20μM

ryanodine, 100mM 2APB, 4-5μM U73343 and U73122 (No statistically significant difference was noticed between 4 and 5μM). Each bar represents the mean±SEM., and each experiment was repeated on 40, 40, 6, 6, 8, 10, 10, 7, 8 and 9 slides, respectively. (B): Mean increase in $[Ca^{2+}]_i$ in cells showing a spontaneous Ca^{2+} transient in a response to an oscillatory flow (flow control), and the presence of 50nM thapsigargin, 10μM $GdCl_3$, 20μM nifedipine, 1μM ryanodine, 20μM ryanodine, 4-5μM U73343 and U73122. Each bar represents the mean±SEM., and each experiment was repeated on 40, 6, 6, 8, 10, 10, 8 and 9 slides, respectively. *$p<0.05$ versus flow control. #$p<0.001$ versus flow control. **$p<0.01$ versus U73343.

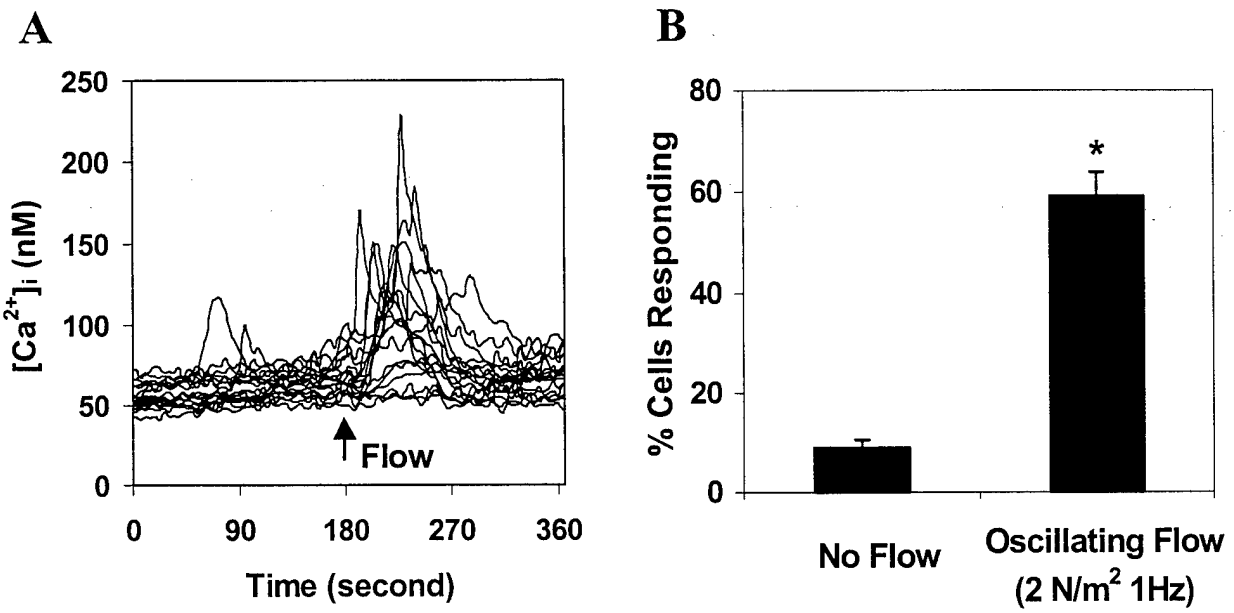

Figure 1 (You et al.)

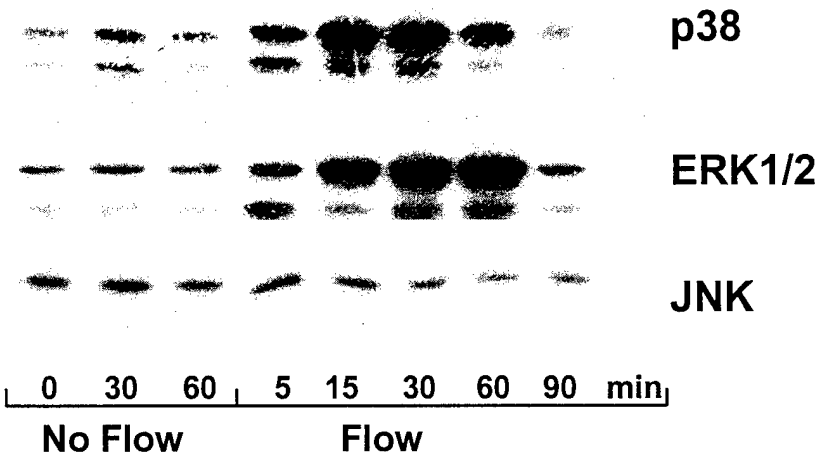

Figure 2 (You et al.)

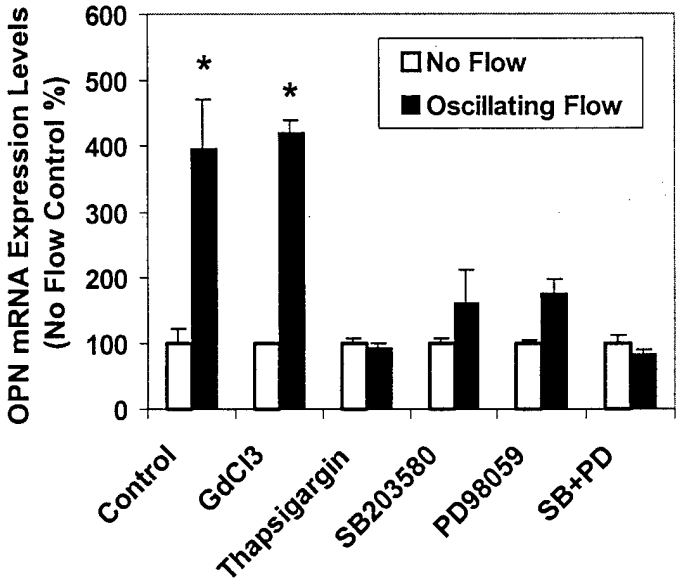

Figure 3 (You et al.)

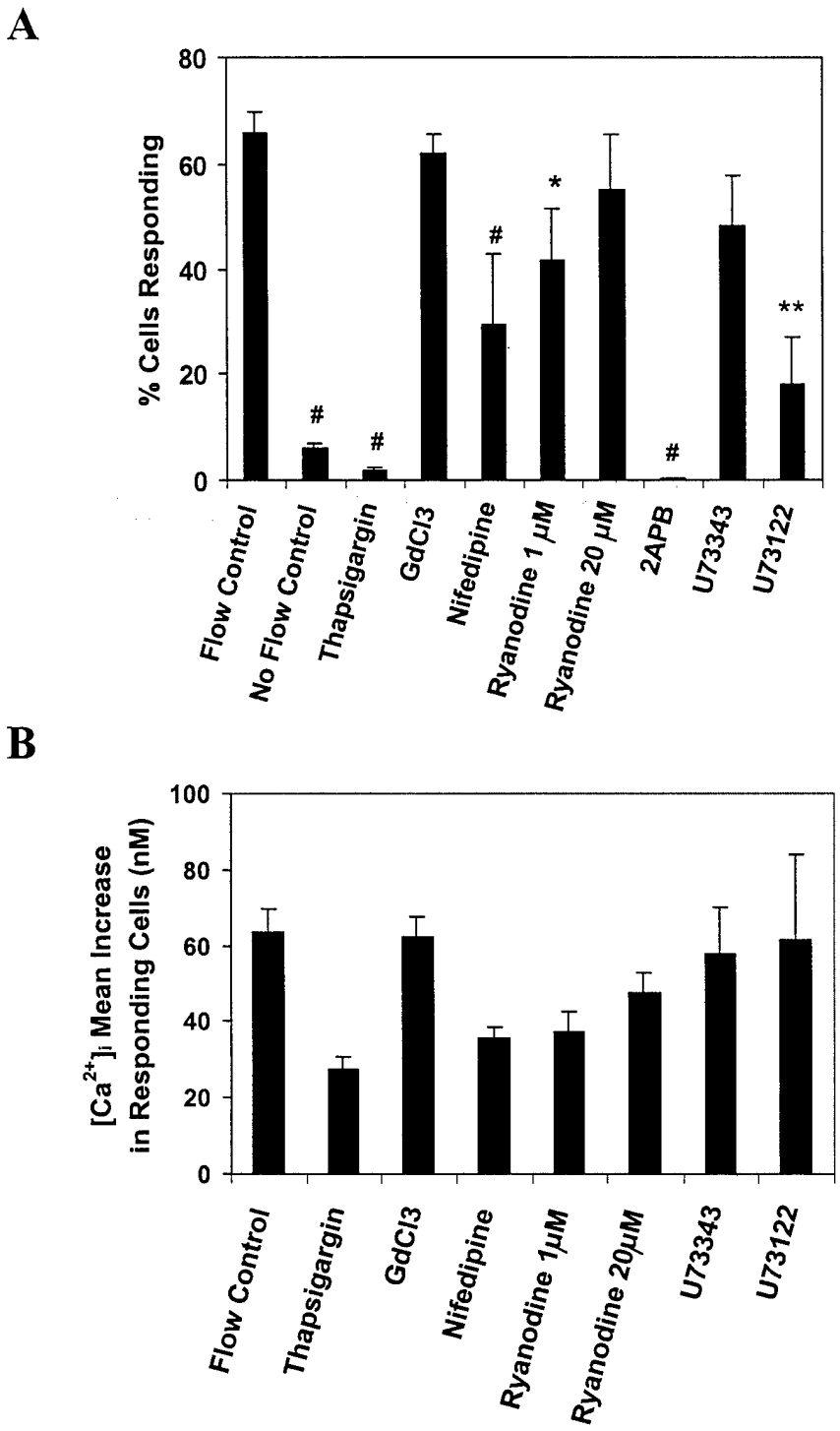

Figure 4 (You et al.)

Substrate Deformation Levels Associated With Routine Physical Activity Are Less Stimulatory to Bone Cells Relative to Loading-Induced Oscillatory Fluid Flow

J. You
e-mail: jyou@ortho.hmc.psu.edu

C. E. Yellowley

H. J. Donahue

Y. Zhang

Q. Chen

C. R. Jacobs

Musculoskeletal Research Laboratory,
Department of Orthopaedics and Rehabilitation,
The Pennsylvania State University
College of Medicine,
Hershey, PA 17033

Although it is well accepted that bone tissue metabolism is regulated by external mechanical loads, it remains unclear to what load-induced physical signals bone cells respond. In this study, a novel computer-controlled stretch device and parallel plate flow chamber were employed to investigate cytosolic calcium ($Ca^{2+}{}_i$) mobilization in response to a range of dynamic substrate strain levels (0.1–10 percent, 1 Hz) and oscillating fluid flow (2 N/m^2, 1 Hz). In addition, we quantified the effect of dynamic substrate strain and oscillating fluid flow on the expression of mRNA for the bone matrix protein osteopontin (OPN). Our data demonstrate that continuum strain levels observed for routine physical activities (<0.5 percent) do not induce $Ca^{2+}{}_i$ responses in osteoblastic cells in vitro. However, there was a significant increase in the number of responding cells at larger strain levels. Moreover, we found no change in osteopontin mRNA level in response to 0.5 percent strain at 1 Hz. In contrast, oscillating fluid flow predicted to occur in the lacunar–canalicular system due to routine physical activities (2 N/m^2, 1 Hz) caused significant increases in both $Ca^{2+}{}_i$ and OPN mRNA. These data suggest that, relative to fluid flow, substrate deformation may play less of a role in bone cell mechanotransduction associated with bone adaptation to routine loads. [S0148-0731(00)01204-8]

Introduction

It is well known that mechanical force is an important factor affecting bone adaption and formation. Removal of mechanical stimulation causes reduced bone matrix protein production, mineral content, and bone formation as well as an increase in bone resorption [1]. Conversely, increased mechanical loading can increase bone formation and decrease bone resorption [2]. Therefore, bone is capable of altering its external shape and internal structure to support the load bearing demands placed upon it efficiently. However, the mechanism by which bone cells sense and respond to their physical environment, including mechanical loading, is still poorly understood. This study is focused on the cellular level physical signals induced by external mechanical loading to which bone cells might be responding.

A number of potential physical signals have been investigated in terms of their ability to regulate bone cell metabolism with *in vitro* culture systems. However, the majority of these experiments have been criticized for either applying stimulus levels much in excess of those occurring in response to the routine bone loads or for employing mechanical stimulation systems that induce unintended physical signals. For example, bone cells are known to respond to electric fields; however, the levels of endogenously occurring electric fields have only a modest effect [3]. Another possibility is that bone cells directly sense the deformation of the substrate to which they are attached. Indeed, substrate deformation has been shown to influence DNA synthesis, second messenger production (cyclic AMP), release of paracrine factors (PGE_2), the activity of enzymes important to mineralization (alkaline phosphatase), and both collagenous and non-collagenous matrix protein synthesis [4–6]. However, the flexible membranes utilized as substrates in these studies exposed the cells to deformations of between 5-fold and 125-fold greater than observed to occur in bone during routine physical activity. For example, in humans during vigorous exercise, surface strains remain below 0.2 percent [7]. To apply smaller deformations, some investigators have utilized systems based on bending of rigid substrates such as glass slides [8–11]. Unfortunately this approach exposes the cells to significant fluid shear stress due to the lateral motion of the slide through the bathing media. This unintended fluid flow is complex and potentially turbulent in nature. Moreover, an appropriate control is problematic, since rocking or tilting of a control slide is unlikely to result in the same cellular fluid environment as the bending slide [9,11]. Owan et al. [10] were able to distinguish the effects of strain from the effects of fluid flow by varying slide thickness. They concluded that, with respect to osteopontin (OPN) expression, fluid flow was the predominant physical stimulus and that there was no response to strain levels below 8 percent. The approach taken in this study was to utilize a system designed to apply substrate deformation over a range from 0.1–10 percent without exposing the cells to fluid flow.

An alternative to the hypothesis that bone cells respond directly to deformation is that they sense loading-induced flow of fluid through the lacunar–canalicular network [12,13]. To date it has proven impossible to quantify lacunar–canalicular flow magnitudes. However, Weinbaum et al. [14] predicted that the wall shear stress levels experienced by bone cells *in vivo* range from 0.8–3 N/m^2 on the basis of a theoretical model validated with respect to the streaming potentials [13]. Smalt et al. [15] utilized a system capable of exposing bone cells to levels of substrate strain comparable to those experienced by bone cells *in vivo* during routine physical activities without induced fluid flow. They found no increase in NO or PGE_2 production in response to strain (0.05–

Contributed by the Bioengineering Division for publication in the JOURNAL OF BIOMECHANICAL ENGINEERING. Manuscript received by the Bioengineering Division July 21, 1999; revised manuscript received March 22, 2000. Associate Technical Editor: C. H. Turner.

0.5 percent). In contrast, exposure to fluid flow induced both PGE_2 and NO production in osteoblastic cells. However, these studies did not address the very early intracellular signaling event of intracellular calcium ($Ca^{2+}{}_i$) mobilization, which may be sensitive to substrate strain without affecting PGE_2 or NO production. Also, they did not employ a dynamic or oscillatory flow profile, which would be the predominant type of flow *in vivo* due to the dynamic nature of routine physical activities [16] and has been demonstrated to mobilize $Ca^{2+}{}_i$ *in vitro* [17].

$Ca^{2+}{}_i$ is an early response second messenger that plays a role in a number of metabolic pathways, and is typically observed to increase dramatically within seconds of stimulation. As a second messenger, $Ca^{2+}{}_i$ transduces extracellular changes (i.e., first messenger) to the cell interior and potentially to the genome, and is important in the regulation of cellular metabolism. $Ca^{2+}{}_i$ mobilization in response to steady fluid flow in bone cells has been studied [18], but not in response to substrate strain at levels known to occur during routine physical activities. We have taken an approach that allows us to distinguish the effects of dynamic substrate strain from those of fluid flow by applying precisely controlled, varied dynamic substrate strain levels, without induced fluid flow.

In addition to $Ca^{2+}{}_i$, we chose also to quantify mRNA levels of the osteopontin (OPN) gene in response to substrate deformation and fluid flow. OPN is characterized as one of the predominant noncollagenous proteins that are accumulated in the extracellular matrix of bone in a wide variety of vertebrates [19,20]. OPN is also believed to be an important factor associated with bone remodeling caused by mechanical stress *in vivo* [21]. In several recent studies expression levels of mRNA for OPN were shown to be modulated in response to mechanical stimulation of bone cells *in vitro* [6,22,23]. However, these data were obtained with applied strains in excess of those expected to occur during routine physical activities.

In this study we exposed bone cells to controlled levels of dynamic substrate strain ranging from 0.1–10 percent at 1 Hz in the absence of induced fluid flow and also to oscillating dynamic fluid flow expected to occur due to routine physical activities in the absence of substrate strain. In order to ensure that our findings are not an artifact of our cell culture model, we employed a variety of bone cell types including human osteoblastic cells (hFOB), primary cultures of rat osteoblasts (ROB), and osteocytic cells (MLO-Y4). In terms of biological outcomes, we quantified real-time changes in $Ca^{2+}{}_i$ and steady-state mRNA levels for the OPN gene. Our experimental design addresses several significant unstudied questions including: the dose response relationship between dynamic substrate strain and $Ca^{2+}{}_i$; whether $Ca^{2+}{}_i$ is affected by dynamic substrate strain levels expected to occur during routine physical activities; how this response compares with the response to levels of dynamic lacunar–canalicular fluid flow expected to occur during routine physical activities; and how these two physical signals independently affect OPN mRNA levels.

Materials and Methods

Cell Culture. Human fetal conditionally immortalized osteoblastic cells (hFOB 1.19) [24] were employed in this study. These cells were transfected with a temperature-sensitive promoter linked to the SV40 gene such that the gene is expressed at 37°C and expression is inhibited when the cells are cultured at 39.5°C. hFOB cells were grown in Dulbecco's modified Eagle medium (DMEM) with nutrient mixture F-12 (DMEM/F12, Gibco, Gaithersburg, MD) supplemented with 10 percent fetal bovine serum (FBS) and 1 percent penicillin and streptomycin at 37°C. Before experiments, hFOB cells were transferred into a 39.5°C incubator for 24 hours to express characteristics of mature osteoblasts [24]. To confirm that our dynamic substrate strain responses were not an artifact of the behavior of the cell line, we also utilized primary cultures of rat subperiosteal osteoblastic cells (ROB) and osteocytic (MLO-Y4) cells. ROB cells were isolated from long bones of four-month-old male Fischer-344 rats, as previously described [25]. We have demonstrated that cells isolated in this manner express characteristics of the osteoblast phenotype. ROB cells were cultured in DMEM containing 20 percent FBS and 1 percent penicillin and streptomycin. Osteocyte-like cells (MLO-Y4) [26] provided by Dr. Lynda Bonewald (University of Texas Health Science Center, San Antonio) were also tested for dynamic substrate strain responses. MLO-Y4 cells were cultured in alpha modified essential medium (αMEM) supplemented with 5 percent FBS, 5 percent calf serum (CS) and 1 percent penicillin and streptomycin. In the stretch experiments ROB and hFOB cells were grown on fibronectin-coated silicone membranes (Flexcell International, Hillsborough, NC) to enhance adhesion. MLO-Y4 cells were cultured on type I collagen (Flexcell International, Hillsborough, NC), which is required to maintain the osteocyte-like phenotype [26]. For the flow experiments, bone cells were cultured on quartz glass slides (76 mm×26 mm×1.6 mm) for calcium imaging and on normal glass slides (75 mm×38 mm×1.0 mm) for osteopontin studies.

Dynamic Substrate Stretch Device. Our dynamic substrate deformation apparatus consisted of a coated silicone membrane and a computer-controlled ZETA 6104 motor-driven micrometer (Parker Hannifin Corp., Rohner Park, CA). One end of the membrane was fixed to the microscope stage and the other end was connected to a micrometer (Fig. 1). The motor can be accurately positioned within 1 μm under computer control to apply the desired dynamic strain. Dynamic strains consisted of a triangle waveform ranging from zero to maximal tensile strain at 1 Hz. Strains in the substrate were verified by tracking optical markers to confirm that the substrate was accurately deformed. Cells were cultured on the precoated membranes within a plastic ring filled with medium (Tyrode's solution with 2 percent FBS) that minimized the fluid flow during dynamic stretch. The whole dynamic stretch device was placed on the stage of a Nikon Diaphot inverted microscope equipped for epifluorescence and computer image acquisition.

Fluid flow levels induced by our dynamic stretch apparatus were extremely low. For instance, 1 percent strain in our apparatus only creates 0.0001 N/m^2 average wall shear stress [27] and our data suggest that there is no $Ca^{2+}{}_i$ response for such low levels of shear stress. Likewise, 0.68 mm microscope slides were utilized in the flow experiments to eliminate substrate deformation.

Fluid Flow Device. A parallel plate flow chamber was used to apply fluid flow [17]. The design was modified from Frangos et al. [28] to accept the UV transparent quartz glass microscope slides required for fluorescent imaging. The flow rate was quantified with an ultrasonic flowmeter (Transonic Systems Inc., Ithaca, NY). Details of the chamber and the computer-controlled dynamic

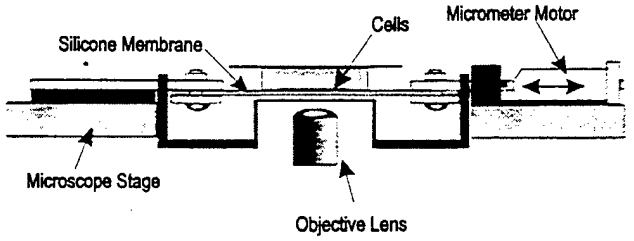

Fig. 1 Schematic of the substrate stretch device consisting of a silicone membrane and a computer motor-driven micrometer. One end of the membrane was fixed to the microscope stage and the other end was connected to the micrometer. Cells were cultured on the precoated membrane and a plastic ring filled with medium was placed on the membrane.

flow delivery system are given in Jacobs et al. [17]. For calcium studies, the rectangular fluid volume measured 38 mm×10 mm ×0.28 mm. A larger flow chamber with a rectangular fluid volume of 56 mm×24 mm×0.28 mm was employed for OPN studies to increase the mRNA yield.

Calcium Imaging. Intracellular calcium ion concentration ($[Ca^{2-}]_i$) was quantified with the fluorescent dye fura-2. Fura-2 exhibits a shift in absorption when bound to calcium such that emission intensity when illuminated with ultraviolet light at a wavelength of 340 nm increases with calcium concentration, and decreases with calcium concentration when illuminated at 380 nm.

Preconfluent (80 percent) cells were washed with Tyrode's solution at 37°C (39.5°C for hFOB), which contained 140 mM NaCl, 4 mM KCl, 1 mM $MgCl_2$, 2 mM $CaCl_2$, 5 mM N-2-hydroxyethylipiperazine-N-2-ethanesulphonic acid and 10 mM glucose, titrated to a final pH of 7.4 with 4 mM NaOH. Cells were then incubated with 1 μM fura-2-acetoxymethyl ester (Molecular Probes, Eugene, OR) solution for 30 min at 37°C (39.5°C for hFOB). The cells were then washed again with fresh Tyrode's solution prior to experiments.

Cell ensembles were illuminated at wavelengths of 340 and 380 nm in turn. Emitted light was passed through a 510 nm interference filter and detected with an ICCD camera (International LTD., Sterling, VA). Images were recorded at a rate of one every second and analyzed using image analysis software (Metafluor: Universal Imaging, West Chester, PA). Calibration ratios were obtained using fura-2 in buffered calcium standards supplied by the manufacturer (Molecular Probes, Inc., Eugene, OR). Basal $[Ca^{2+}]_i$ was sampled for 0.5 min followed by cyclic mechanical stretch. We first induced dynamic strains of 0.1 percent for 0.5 min followed by a 3 min rest period then 1 percent strain, rest, 5 percent, rest, 10 percent, and then rest (Fig. 2). The dynamic stretch was applied as a triangle wave at a frequency of 1 Hz. Also note that the corresponding strain rates were 0.2 percent/s, 2 percent/s, 10 percent/s, and 20 percent/s, respectively. $[Ca^{2+}]_i$ images were collected during the no-stretch rest period only. To negate any possible cumulative effect on the $[Ca^{2-}]_i$ responses of the different dynamic strains, we also applied the strain in order of decreasing magnitude (0.5 min no stretch period followed by a 3 min rest period then 10 percent strain, rest, 5 percent, rest, 1 percent, rest, 0.1 percent and then rest). For flow experiments, basal $[Ca^{2+}]_i$ was sampled for 0.5 min followed by fluid flow onset.

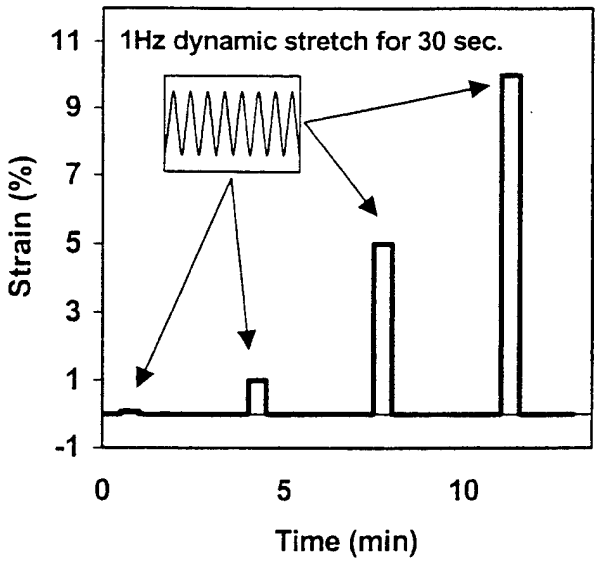

Fig. 2 Membrane stretch pattern. We first induced dynamic strains of 0.1 percent for 0.5 min followed by a 3 min rest period then 1 percent strain, rest, 5 percent, rest, 10 percent, and then rest. The order of strain levels was also reversed. The strain waveform was a triangle wave and the frequency for all strain experiments was 1 Hz.

Osteopontin mRNA Analysis. Quantitative real-time reverse transcription PCR (QRT RT-PCR) was employed to quantify steady-state osteopontin mRNA levels. This technique is based on the detection of a fluorescent signal produced by an OPN-specific oligonucleotide probe during PCR amplification. The RNeasy Mini Kit (Qiagen, Inc., Valencia, CA) was used to extract total RNA. Briefly, cells were washed with PBS, lysed, and homogenized using the QIAshredder mini column (Qiagen, Inc., Valencia, CA). After binding to the RNeasy column, total RNA was eluted with RNase-free water and collected. The osteopontin mRNA level was determined by using quantitative real time RT-PCR (Prism 7700 Sequence Detector, Applied Biosystems, Frost City, CA). The fluorogenic oligonucleotide probe for human osteopontin was 5'-CGC CGA CCA AGG AAA ACT CAC TAC CA-3' (Synthetic Genetics, San Diego, CA). The forward and reverse PCR primers were 5'-TTG CAG CCT TCT CAG CCA A-3', and 5'-CAA AAG CAA ATC ACT GCA ATT CTC-3', respectively [29]. Relative changes in the levels of OPN mRNA and 18S rRNA were quantified 72 hours after mechanical stimulation.

Data Analysis. We used a numerical procedure from mechanical analysis, known as Rainflow cycle counting, to identify calcium oscillations [17,30]. Briefly, this technique identifies complete cycles or oscillations in the time history data even when they are superimposed upon each other, and therefore can be used to distinguish and quantify $[Ca^{2+}]_i$ responses from background noise. We defined a response as an oscillation in $[Ca^{2+}]_i$ of 20 nm or greater. Base line $[Ca^{2+}]_i$ data were recorded for 0.5 min followed by application of desired dynamic substrate strain or fluid flow.

Data were expressed as mean ±SEM. To compare observations from different dynamic substrate strains, a two-sample Student's t-test was used in which sample variance was not assumed to be equal. To compare observations from more than two groups, a one-way analysis of variance was employed followed by a Student–Newman–Keuls multiple comparisons post-hoc test (Instat, GraphPad Software, Inc., San Diego, CA). $p<0.05$ was considered statistically significant.

Results

Ca^{2+}_i Responses to Different Substrate Strains. Typical cell Ca^{2+}_i responses are shown in Fig. 3. The fraction of hFOB

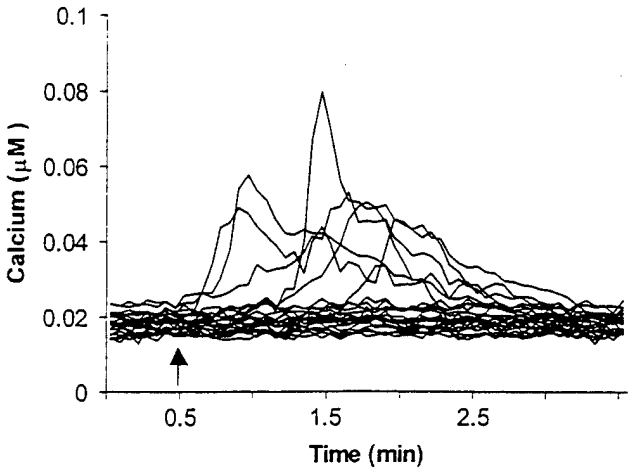

Fig. 3 An example of the hFOB cell $[Ca^{2+}]_i$ response traces obtained for oscillating flow (2 N/m², 1 Hz). Note that the arrow depicts the onset of flow.

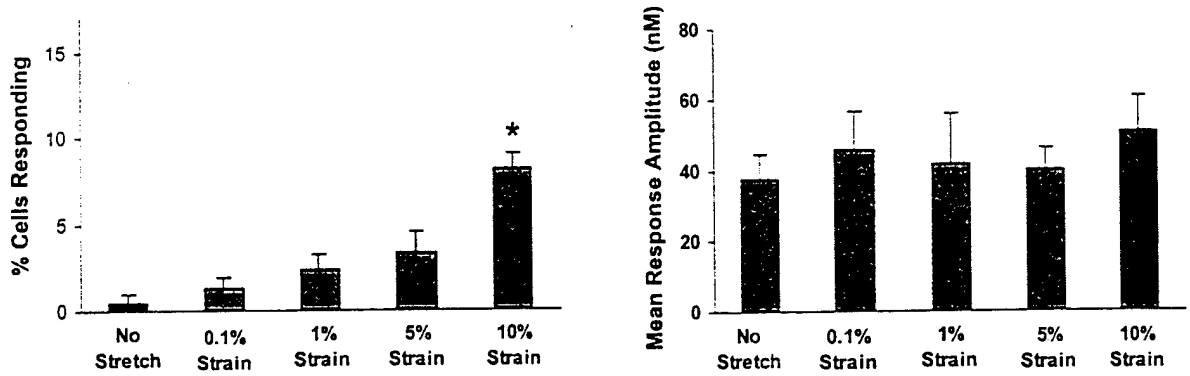

Fig. 4 Fraction of hFOB cells responding with an increase in $[Ca^{2+}]_i$ at different substrate strains and the mean response amplitude. 0.48±0.48 percent, 1.31±0.64 percent, 2.34±0.96 percent, 3.36±1.18 percent and 8.15±0.95 percent of hFOB cells responded for no stretch, 0.1, 1, 5, and 10 percent strain, respectively. Mean response amplitudes of hFOB cells were 37.53±6.83, 45.60±10.81, 41.68±14.00, 39.63±6.32, and 50.57±9.91 nM for no stretch, 0.1, 1, 5, and 10 percent strain, respectively. The data were obtained from six individual experiments and a total of 246 cells. (* represents statistically significant difference ($p<0.05$) from other four groups, no stretch, 0.1, 1, and 5 percent strain).

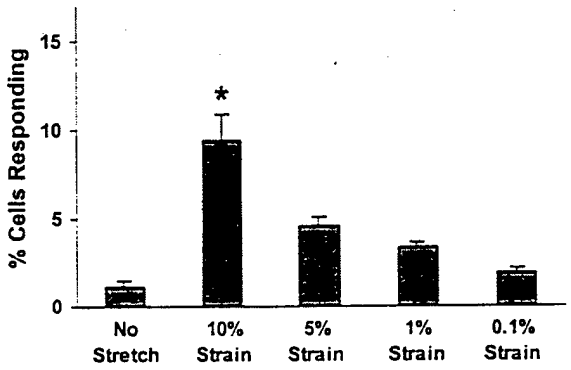

Fig. 5 Fraction of hFOB cells responding with an increase in $[Ca^{2+}]_i$ at the reversing ordering of application of the various substrate strains. 1.16±0.32, 9.40±1.46, 4.57±0.50, 3.40 ±0.22, and 1.90±0.29 percent of hFOB cells responded for no stretch, 10, 5, 1, and 0.1 percent strain, respectively. The data were obtained from four individual experiments and a total of 229 cells. (* represents statistically significant difference ($p<0.05$) from other four groups, no stretch, 5, 1, and 0.1 percent strain).

cells responding with an increase in $Ca^{2+}{}_i$ at different substrate strains is shown in Fig. 4. The data were obtained from six individual experiments (slides) and a total of 246 cells. The percentage of cells responding to substrate strain levels expected to occur during routine physical loading (0.1 percent, 1 Hz) was not statistically different from the percentage of cells exhibiting spontaneous $Ca^{2+}{}_i$ transients during the nonstretch control period (1.31 ±0.64 percent and 0.48±0.48 percent, respectively). When strains were increased to 1 percent and 5 percent, the percentage of cells responding increased to 2.34±0.96 percent and 3.36 ±1.18 percent, respectively. However, these changes were not significantly different from the nonstretch control period. At a strain of 10 percent, the percentage of cells responding increased to 8.15±0.95 percent, which was significantly greater than all the other strain levels ($p<0.05$). Mean response amplitudes are shown in Fig. 4. The amplitudes of 37.53±6.83 nM, 45.60 ±10.81 nM, 41.68±14.00 nM, 39.63±6.32 nM, and 50.57 ±9.91 nM ($p>0.05$) were not statistically different from one another. The fraction of hFOB cells responding with an increase in $Ca^{2+}{}_i$ to the reversed order of strain application is shown in Fig. 5. 10 percent dynamic strain still induced statistically significant $Ca^{2+}{}_i$ responses compared with all other cases. The results for

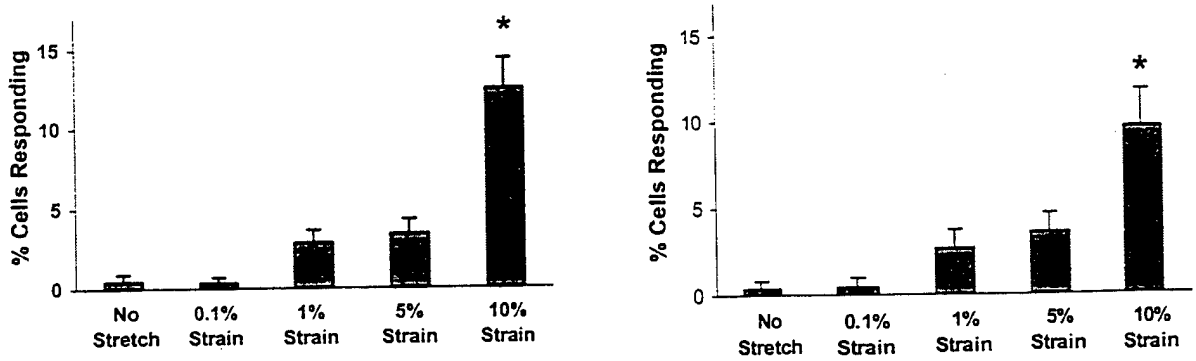

Fig. 6 Fraction of cells responding with an increase in $[Ca^{2+}]_i$ at different substrate strains for ROB cells (left) and MLO-Y4 cells (right). 0.45±0.45, 0.35±0.35, 2.85±0.79, 3.30±0.90, and 12.46±1.91 percent were the percentages of ROB cells responding for no stretch, 0.1, 1, 5, and 10 percent strain. Only the response for 10 percent strain was significantly different from those of four other cases. The results for ROB cells were from six individual experiments that contained total 293 cells. The percentages of responding MLO-Y4 cells were 0.39±0.39, 0.48±0.48, 2.72±1.04, 3.55±1.15, and 9.53±2.17 percent for no stretch, 0.1, 1, 5, and 10 percent strain. The response of 10 percent strain was significantly different from those for 0.1, 1, and 5 percent strain. Six individual experiments had total 227 MLO-Y4 cells. (* represents statistically significant difference ($p<0.05$) from other four groups, no stretch, 0.1, 1, and 5 percent strain).

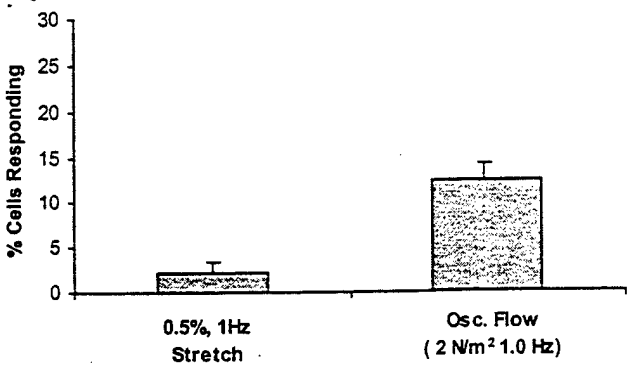

Fig. 7 Fraction of cells responding with an increase in $[Ca^{2+}]_i$ to dynamic substrate strain (0.5 percent, 1 Hz) and oscillatory flow (2 N/m², 1 Hz) for hFOB cells. The percentage numbers were 2.24±1.28 percent for dynamic strain and 12.30±1.88 percent for oscillating flow. The total cell numbers for strain and flow were 122 and 332, respectively.

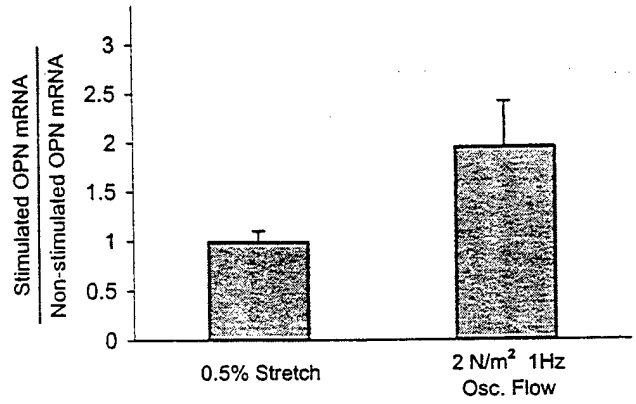

Fig. 8 The relative hFOB cell osteopontin mRNA level change in response to physical stimuli: substrate deformation 0.99 ±0.12 (n=3) and oscillating fluid flow 1.95±0.40 (n=2). The mRNA level was measured 72 hours after stimulation.

ROB and MLO-Y4 cells exposed to varying levels of substrate strain were similar to that obtained for hFOB cells (Fig. 6). As with the hFOB cells, a statistically significant response was found only for a 10 percent strain. The mean response amplitudes of ROB and MLO-Y4 cells were not significantly different for all cases (data not shown).

$Ca^{2+}{}_i$ Responses to Routine Substrate Strains and Oscillatory Fluid Flow. The levels of substrate strain and oscillatory fluid flow associated with routine physical activity were obtained from the literature [7,13]. The results for hFOB cells are given in Fig. 7. As in the previous experiments, the number of cells that responded to strains of 0.5 percent at 1 Hz was not significantly different from no-stretch control. In contrast, there was a significant ($p<0.05$) increase in the percentage of cells responding to oscillatory flow (2 N/m², 1 Hz).

Osteopontin mRNA Level. Osteopontin mRNA levels in hFOB were quantified in response to 0.5 percent substrate strain at 1 Hz and oscillating fluid flow at 1 Hz, resulting in a wall shear stress of 2 N/m² utilizing QRT RT-PCR. There was no statistically significant change in osteopontin mRNA level in response to 0.5 percent stretch (Fig. 8) compared to nonstretch controls. The relative change in hFOB osteopontin mRNA level was 0.99 ±0.12 (n=3). However, oscillating fluid flow increased the osteopontin mRNA level nearly 100 percent (1.95±0.40, n=2) relative to nonstretch controls.

Discussion

Whether mechanical adaptation of bone occurs as a direct response to strain, or indirectly as a response to strain-induced fluid flow remains a controversial subject. A number of studies of the biological effect of strains above 0.5 percent can be found in the literature [4–6,31]. However, there are few studies restricted to the effects of strain levels expected to occur due to routine mechanical loading (strain <0.5 percent [7,10,15]). In this study a novel, precisely controlled membrane stretch device was employed to assess the response of osteoblastic cells to varying mechanical strains (0.1–10 percent, 1 Hz) without inducing fluid flow. The effect of oscillatory fluid flow on bone cells was studied with a parallel plate flow chamber system [17] at levels expected to occur in the lacunar–canalicular system due to routine physical activity. These two methods give us the ability to separate the effects of substrate deformation from those of fluid flow. Focusing on physical signals that may occur due to routine physical activities is critical to fully understanding the mechanism of mechanotransduction in bone cells *in vivo*.

Our data demonstrate that continuum strain levels observed to occur in bone during routine physical activities do not induce $Ca^{2+}{}_i$ responses in human osteoblastic cells (hFOB), primary cultures of rat bone cells (ROB) or osteocytic cells (MLO-Y4) *in vitro*. There was no significant difference ($p>0.05$) in the percentage of cells responding in the no stretch period compared with 0.1 percent substrate strain at 1 Hz for all three cell types. Larger strains (1–5 percent) induced responses only in approximately 5 percent of total cells, which were still not significantly different from control ($p>0.05$). When the strain reached 10 percent, the number of cells exhibiting a $Ca^{2+}{}_i$ response increased significantly. The difference between 10 percent stretch and all other situations (no stretch, 0.1 percent, 1 percent or 5 percent stretch) was significant ($p<0.001$). The results of hFOB cells responding with an increase in $Ca^{2+}{}_i$ to the reversed order of application of strain application indicate that the $Ca^{2+}{}_i$ responses for each strain level were independent and not cumulative. We observed differences in $Ca^{2+}{}_i$ responsiveness, in terms of the fraction of responding cells, which were not paralleled by response amplitude. Thus, there was no relationship between $[Ca^{2+}]_i$ oscillation amplitude and the magnitude of substrate stretch. This suggests that the bone cell $Ca^{2+}{}_i$ response to substrate deformation is an all-or-none response and that bone cell sensitivity to loading intensity is expressed in terms of the number of responding cells rather than their $[Ca^{2+}]_i$ oscillation amplitude. This is consistent with observations of the $Ca^{2+}{}_i$ response of bovine aortic endothelial cells [32], articular chondrocytes [33] and bone cells [17,18] to fluid flow. Our data support the concept that there may be a threshold for bone cell response to substrate strain *in vitro*, and are in agreement with the conclusion of Owan et al. [10], that this threshold appears to be between 5 and 10 percent. Our results are also consistent with previous studies [4–6,31], which employed strain at or above 5 percent. However, *in vivo* data [7] have shown that continuum bone tissue strains remain less than 0.5 percent under routine conditions of physical activity. Indeed, tissue strains in excess of this level are associated with tissue failure. High strain magnitudes (5 percent and higher) can occur in pathologic conditions such as fracture. Thus bone cell mechanotransduction may involve two distinct pathways. The first pathway would play a role in bone tissue adaptation and homeostasis and would be mediated by loading-induced oscillating fluid flow as a cellular physical signal, but not substrate stretch. The second pathway would be activated in fracture healing and repair and involve direct cellular sensitivity to large substrate deformation.

In addition to substrate strain, mechanical loading of bone tis-

sue has been shown to increase fluid flow through the lacunar–canalicular spaces [34]. Therefore, in addition to examining the dose response of bone cell $[Ca^{2+}]_i$ to substrate strain, we also quantified the $[Ca^{2+}]_i$ and OPN mRNA responses to substrate strain relative to fluid flow regimes expected to occur due to typical physical activities. Lacunar–canalicular flow occurs due to two phenomena, arterial pressure that leads to steady flow, and mechanical loading that leads to oscillating flow. Loading-induced fluid flow is oscillatory due to the cyclic nature of the applied loads. When load is applied to bone, fluid flows from regions of relative high strain to regions of low relative strain, and reverses direction when the load is removed [35]. In this study, oscillating fluid flow resulting in a wall shear stress of 2 N/m^2 applied at 1 Hz induced $Ca^{2+}{}_i$ responses that were similar to those for 10 percent dynamic substrate strain at 1 Hz. Furthermore, dynamic strain at 0.5 percent and 1 Hz did not alter OPN mRNA level, but oscillating flow almost doubled the level of OPN mRNA. Furthermore, these results are consistent with the findings of Harter et al. [22] and Toma et al. [6] who found osteogenic changes in OPN expression only for strains in excess of 1 percent. Although the responsiveness of bone cells to steady flow has been reported to be greater than that to oscillatory flow [17], oscillatory flow is the predominant flow regime *in vivo* [16]. Moreover, relative to routine dynamic strain levels, our data suggest that routine levels of oscillating fluid flow may be more stimulatory to bone cells, possibly because fluid flow may result in more cellular deformation than substrate stretch.

This study has focused on determining the aspects of the physical environment of the cell involved in the response of bone tissue to routine mechanical loading. Two biological outcome variables were quantified, $Ca^{2+}{}_i$ mobilization and osteopontin mRNA level. $Ca^{2+}{}_i$, is a ubiquitous second messenger that controls a number of cellular responses [36–38], and, as such, may have an important role in the mechanotransduction mechanism for bone cells [17,18,39,40]. In addition, $Ca^{2+}{}_i$ mobilization is one of the earliest notable intracellular signals we can explore. Osteopontin (OPN) is one of the major noncollagenous proteins found in bone extracellular matrix and is considered to play an important role in bone formation, resorption and remodeling [21,41–43]. Thus, $[Ca^{2+}]_i$ and OPN expression have both been implicated in the literature to play important roles in the biochemistry of bone cell mechanotransduction. In our study they have been treated as two, possibly independent, biologic endpoints that span a range from relatively early to relatively late changes in bone cell metabolism. We do not, however, suggest that they are necessarily part of a single biochemical pathway.

Indeed, while our results suggest that oscillating fluid flow may be a more significant physical signal relative to substrate deformation in cellular sensing of routine physical activities, the biochemical mechanotransduction mechanism remains unclear. For example, both extracellular and intracellular Ca^{2+} sources are known to contribute to the $Ca^{2+}{}_i$ response to steady fluid flow in bone cells and chondrocytes [18,44]. It is possible that the Ca^{2+} sources contributing to $Ca^{2+}{}_i$ response we have observed for substrate deformation and oscillating fluid flow may be different. However, the significance of such an experiment is limited by our finding of a lack of a $Ca^{2+}{}_i$ response to continuum strain at levels observed to occur during routine physical activity. Identification of the source of $Ca^{2+}{}_i$ in the response to oscillating fluid flow as well as linking the $Ca^{2+}{}_i$ and OPN responses are important aims for future experiments, but not consistent with the focus of our current study, namely extracellular physical signals. Our results suggest that oscillating fluid flow is an appropriate physical signal for future investigations of the biochemical mechanotransduction pathway.

Some limitations should be acknowledged when interpreting our results. First, although accurate data are available concerning the continuum level of strain resulting from routine physical activities, no direct experimental quantification of lacunar–canalicular flow currently exists in the literature. We have based our applied flow regime on the best currently available scientific evidence. Specifically, our flow protocol is based on theoretical predictions that have been validated with respect to experimental measurements of flow-induced streaming potentials [13]. Also, due to the two different experimental apparatuses utilized in this study, the substrates upon which cells were cultured were different between dynamic substrate stretch and fluid flow experiments. In the hFOB and ROB stretch experiments the substrate was fibronectin coated silicone membranes versus uncoated quartz glass for the flow experiments. However, both published [17] and unpublished experiments in our laboratory have not found a significant effect on bone cell $[Ca^{2+}]_i$ sensitivity of a fibronectin coating versus uncoated quartz glass slides. All MLO-Y4 experiments were conducted with type I collagen coated substrates to maintain the osteocytic phenotype. Finally, the waveforms of the two devices were subtly different due to the technical capabilities of the two systems. A triangle wave was utilized in the strain experiments and a sine wave utilized in the flow experiments.

In summary, using our novel substrate stretch device and fluid flow chamber, we have been able to elucidate the effects of substrate deformation and fluid flow on bone cells independently. This study represents the first published results for the dose-response effect of dynamic substrate strains on cytosolic calcium mobilization and oscillatory fluid flow on OPN mRNA levels. Our data suggest that the continuum levels of dynamic substrate strain observed to occur due to routine physical activities do not increase $[Ca^{2+}]_i$ or OPN mRNA levels *in vitro*. However, a fluid flow regime predicted to occur due to routine physical loading increased both $[Ca^{2+}]_i$ and OPN mRNA levels. Therefore, relative to fluid flow, substrate deformation may play less of a role as a physical signal in bone cell mechanotransduction of routine loading.

Acknowledgments

The authors thank Dr. Deborah Grove for designing primers and completing the QRT RT-PCR protocols. This work was supported by the Whitaker Foundation, Arthritis Foundation, NIH RR11769, AG13087, AG00811 and AG17021, and The US Army Medical Research and Materiel Command award number DAMD 17-98-1-8509.

References

[1] Morey, E. R., and Baylink, D. J., 1978, "Inhibition of Bone Formation During Spaceflight," Science, **201**, pp. 1138–1141.
[2] Sessions, N. D., Halloran, B. P., Bikle, D. D., Wronski, T. J., Cone, C. M., and Morey-Holton, E. R., 1989, "Bone Response to Normal Weight Bearing After a Period of Skeletal Unloading," Am. J. Physiol., **257** (also: Endocinol. Metab., **20**), pp. E606–610.
[3] McLeod, K. J., Donahue, H. J., Levin, P. E., and Rubin, C. T., 1991, "Low-Frequency Sinusoidal Electric Fields Alter Calcium Fluctuations in Osteoblast-Like Cells," in: *Electromagnetics in Biology and Medicine*, Brighton, C. T., and Pollack, S. R., eds., San Francisco, San Francisco, pp. 111–115.
[4] Buckley, M. J., Banes, A. J., Levin, L. G., Sumpio, B. E., Sato, M., Jordan, R., Gilbert, J., Link, G. W., and Tran Son Tay, R., 1988, "Osteoblasts Increase Their Rate of Division and Align in Response to Cyclic, Mechanical Tension in Vitro," J. Bone Miner. Res., **4**, pp. 225–236.
[5] Rodan, G. A., Bourret, L. A., Harvey, A., and Mensi, T., 1975, "Cyclic AMP and Cyclic GMP: Mediators of the Mechanical Effects on Bone Remodeling," Science, **189**, No. 4201, pp. 467–469.
[6] Toma, C. D., Ashkar, S., Gray, M. L., Schaffer, J. L., and Gerstenfeld, L. C., 1997, "Signal Transduction of Mechanical Stimuli Is Dependent on Microfilament Integrity: Identification of Osteopontin as a Mechanically Induced Gene in Osteoblasts," J. Bone Miner. Res., **12**, pp. 1626–1636.
[7] Burr, D. B., Milgrom, C., Fyhrie, D., Forwood, M. R., Nyska, M., Finestone, A., Hoshaw, S., Saiag, E., and Simkin, A., 1996, "In Vivo Measurement of Human Tibial Strains During Vigorous Activity," Bone, **18**, pp. 405–410.
[8] Stanford, C. M., Stevens, J. W., and Brand, R. A., 1995, "Cellular Deformation Reversibly Depresses RT-PCR Detectable Levels of Bone-Related mRNA," J. Biomech., **28**, pp. 1419–1421.
[9] Zaman, G., Suswillo, R. F. L., Cheng, M. Z., Tavares, I. A., and Lanyon, L. E., 1997, "Early Responses to Dynamic Strain Change and Prostaglandins in Bone-Derived Cells in Culture," J. Bone Miner. Res., **12**, pp. 769–777.

[10] Owan, I., Burr, D. B., Turner, C. H., Qiu, J., Tu, Y., Onyia, J. E., and Duncan, R. L., 1997, "Mechanotransduction in Bone: Osteoblasts Are More Responsive to Fluid Forces Than Mechanical Strain," Am. J. Physiol., **273**, pp. C810–C815.
[11] Cheng, M. Z., Zaman, G., Rawlinson, S. C. F., Mohan, S., Baylink, D. J., and Lanyon, L. E., 1999, "Mechanical Strain Stimulates ROS Cell Proliferation Through IGF-II and Estrogen Through IGF-I," J. Bone Miner. Res., **14**, pp. 1742–1750.
[12] Kufahl, R. H., and Saha, S., 1990, "A Theoretical Model for Stress-Generated Fluid Flow in the Canaliculi–Lacunae Network in Bone Tissue," J. Biomech., **23**, No. 2, pp. 171–180.
[13] Cowin, S. C., Weinbaum, S., and Zeng, Y., 1995, "A Case for Bone Canaliculi as the Anatomical Site of Strain Generated Potentials," J. Biomech., **28**, pp. 1281–1297.
[14] Weinbaum, S., Cowin, S. C., and Zeng, Y. A., 1994, "A Model for Excitation of Osteocytes by Mechanical Loading Induced Bone Fluid Shear Stress," J. Biomech., **27**, pp. 339–360.
[15] Smalt, R., Mitchell, F. T., Howard, R. L., and Chambers, T. J., 1997, "Induction of NO and Prostaglandin E2 in Osteoblasts by Wall-Shear Stress but Not Mechanical Strain," Am. J. Physiol., **273**, No. 4, Pt. 1, pp. E751–E758.
[16] Zhang, D., Weinbaum, S., and Cowin, S. C., 1998, "Estimates of the Peak Pressure in Bone Pore Water," ASME J. Biomech. Eng., **120**, pp. 697–703.
[17] Jacobs, C. R., Yellowley, C. E., Davis, B. R., Zhou, Z., Cimbala, J. M., and Donahue, H. J., 1998, "Differential Effect of Steady Versus Oscillating Flow on Bone Cells," J. Biomech., **31**, pp. 969–976.
[18] Hung, C. T., Pollack, S. R., Reilly, T. M., and Brighton, C. T., 1995, "Real-Time Calcium Response of Cultured Bone Cells to Fluid Flow," Clin. Orthop., **313**, pp. 256–269.
[19] Denhardt, D. T., and Guo, X., 1993, "Osteopontin: a Protein With Diverse Functions," FASEB J., **17**, pp. 1476–1481.
[20] Gerstenfeld, L. C., Uporov, T., Ashka, S., Salih, E., Gerstenfeld, L. C., and Glimcher, M. J., 1995, "Regulation of Avian Osteopontin Pre- and Posttranslational Expression in Skeletal Tissue," Ann. NY Acad. Sci., **270**, pp. 67–82.
[21] Terai, K., Takano-Yamamoto, T., Ohba, Y., Hiura, K., Sugimoto, M., Sato, M., Kawahata, H., Inaguma, N., Kitamur, Y., and Nomur, S., 1999, "Role of Osteopontin in Bone Remodeling Caused by Mechanical Stress," J. Bone Miner. Res., **14**, pp. 839–849.
[22] Harter, L. V., Hruska, K. A., and Duncan, R. L., 1995, "Human Osteoblasts Like Cells Respond to Mechanical Strain With Increased Bone Matrix Protein Production Independent of Hormonal Regulation, " Endocrinology, **136**, pp. 528–535.
[23] Kubota, T. M., Yamauchi, M., Onozaki, S. S., Suzuki, Y., and Sodek, J., 1993, "Influence of an Intermittent Compressive Force on Matrix Expression by ROS 17/2.8 Cells With Selective Stimulation of Osteopontin," Arch. Oral Biol., **38**, pp. 23–30.
[24] Harris, S. A., Enger, R. J., Riggs, B. L., and Spelsberg, T. C., 1995, "Development and Characterization of a Conditionally Immortalized Human Fetal Osteoblastic Cell Line," J. Bone Miner. Res., **10**, No. 2, pp. 178–186.
[25] Donahue, H. J., Zhou, Z., Li, Z., and McCauley, L. K., 1997, "Age-Related Decreases in Stimulatory G Protein-Coupled Adenylate Cyclase Activity in Osteoblastic Cells," Am. J. Physiol., **273**, No. 4, Pt. 1, pp. E776–781.
[26] Kato, Y., Windle, J. J., Koop, B. A., Mundy, G. R., and Bonewald, L. F., 1997, "Establishment of an Osteocyte-Like Cell Line, MLO-Y4," J. Bone Miner. Res., **12**, pp. 2014–2023.
[27] White, F. M., 1994, *Fluid Mechanics*, 3rd ed., McGraw-Hill, New York.
[28] Frangos, J. A., Eskin, S. G., McIntire, L. V., and Ives, C. L., 1985, "Flow Effects on Prostacyclin Production by Cultured Human Endothelial Cells," Science, **227**, pp. 1477–1479.
[29] Crosby, A. H., Edwards, S. J., Murry, J. C., and Dixon, M. J., 1995, "Genomic Organization of the Human Osteopontin Gene; Exclusion of the Locus From a Causative Role in the Pathogenesis of Dentinogenesis Imperfecta Type II," Genomics, **27**, pp. 155–160.
[30] Jacobs, C. R., Yellowley, C. E., Nelson, D. V., and Donahue, H. J., 2000, "Analysis of Time-Varying Biological Data Using Rainflow Cycle Counting," Comput. Meth. Biomech. Biomed. Eng., **3**, pp. 31–40.
[31] Brighton, C. T., Strafford, B., Gross, S. B., Leatherwood, D. F., Williams, J. L., and Pollack, S. R., 1991, "The Proliferative and Synthetic Response of Isolated Calvarial Bone Cells of Rats to Cyclic Biaxial Mechanical Strain," J. Bone Jt. Surg., Am. Vol., **73**, No. 3, pp. 320–331.
[32] Geiger, R. V., Berk, B. C., Alexander, R. W., and Nerem, R. M., 1992, "Flow-Induced Calcium Transients in Single Endothelial Cells: Spatial and Temporal Analysis," Am. J. Physiol., **262**, No. 6, Pt. 1, pp. C1411–1417.
[33] Yellowley, C. E., Jacobs, C. R., Li, Z., Zhou, Z., and Donahue, H. J., 1997, "Effects of Fluid Flow on Intracellular Calcium in Bovine Articular Chondrocytes," Am. J. Physiol., **273**, No. 1, Pt. 1, pp. C30–C36.
[34] Knothe Tate, M. L., Knothe, U., and Neiderer, P., 1998, "Experimental Elucidation of Mechanical Load-Induced Fluid Flow and Its Potential Role in Bone Metabolism and Functional Adaptation," Am. J. Med. Sci., **316**, pp. 189–195.
[35] Weinbaum, S., Cowin, S. C., and Zeng, Y., 1991, "A Model for the Fluid Shear Stress Excitation of Membrane Ion Channels in Osteocytic Processes Due to Bone Strain," Vanderby, R., ed., *Advances in Bioengineering*, ASME BED-Vol. 20.
[36] Meldolesi, J., and Pozzan, T., 1987, "Pathways of Ca^{2+} Influx at the Plasma Membrane: Voltage-, Receptor-, and Second Messenger-Operated Channels," Exp. Cell Res., **171**, No. 2, pp. 271–283.
[37] Dolmetsch, R. E., Xu, K., and Lewis, R. S., 1998, "Calcium Oscillations Increase the Efficiency and Specificity of Gene Expression," Nature (London), **392**, No. 6679, pp. 933–936.
[38] Horne, J. H., 1999, "Regulatory and Spatial Aspects of Inositol Trisphosphate-Mediated Calcium Signals," Cell Biochem. Biophys., **30**, No. 2, pp. 267–286.
[39] Ajubi, N. E., Klein-Nulend, J., Nijweide, P. J., Vrijheid-Lammers, T., Alblas, M. J., and Burger, E. H., 1996, "Pulsating Fluid Flow Increases Prostaglandin Production by Cultured Chicken Osteocytes—a Cytoskeleton-Dependent Process," Biochem. Biophys. Res. Commun., **225**, No. 1, pp. 62–68.
[40] Ajubi, N. E., Klein-Nulend, J., Alblas, M. J., Burger, E. H., and Nijweide, P. J., 1999, "Signal Transduction Pathways Involved in Fluid Flow-Induced PGE2 Production by Cultured Osteocytes," Am. J. Physiol., **276**, No. 1, Pt. 1, pp. E171–178.
[41] Weinreb, M., Shinar, D., and Rodan, G. A., 1990, "Different Pattern of Alkaline Phosphatase, Osteopontin, and Osteocalcin Expression in Developing Rat Bone Visualized by In Situ Hybridization," J. Bone Miner. Res., **5**, pp. 831–842.
[42] Merry, K., Dodds, R., Littlewood, A., and Gowen, M., 1993, "Expression of Osteopontin mRNA by Osteoclasts and Osteoblasts in Modeling Adult Human Bone," J. Cell. Sci., **104**, pp. 1013–1020.
[43] McKee, M. D., Farach-Carson, M. C., Butler, W. T., Hauschka, P. V., and Nanci, A., 1993, "Ultrastructural Immunolocalization of Noncollagenous (Osteopontin and Osteocalcin) and Plasma (Albumin and α_2 HS-Glycoprotein) Proteins in Rat Bone," J. Bone Miner. Res., **8**, pp. 485–496.
[44] Yellowley, C. E., Jacobs, C. R, and Donahue, H. J., 1999, "Mechanisms Contributing to Flow Induced $Ca^{2-}{}_{i}$ Mobilization in Articular Chondrocytes," J. Cell Physiol., **180**, pp. 402–408.

JOURNAL OF BONE AND MINERAL RESEARCH
Volume 15, Number 2, 2000

Functional Gap Junctions Between Osteocytic and Osteoblastic Cells*

CLARE E. YELLOWLEY, ZHONGYONG LI, ZHIYI ZHOU, CHRISTOPHER R. JACOBS, and HENRY J. DONAHUE

ABSTRACT

Morphological evidence shows that osteocytes, bone cells that exist enclosed within bone matrix, are connected to one another and to surface osteoblasts via gap junctions; however, it is unknown whether these gap junctions are functional. Using a newly established murine osteocytic cell line MLO-Y4, we have examined functional gap junctional intercellular communication (GJIC) between osteocytic cells and between osteocytic and osteoblastic cells. In our hands, MLO-Y4 cells express phenotypic characteristics of osteocytic cells including a stellate morphology, low alkaline phosphatase activity, and increased osteocalcin messenger RNA (mRNA) compared with osteoblastic cells. Northern and Western blot analysis revealed that MLO-Y4 cells express abundant connexin 43 (Cx43) mRNA and protein, respectively. Lucifer yellow dye transferred from injected to adjacent cells suggesting that osteocytic cells were functionally coupled via gap junctions. Functional GJIC between osteocytic and osteoblastic (MC3T3-E1) cells was determined by monitoring the passage of calcein dye between the two cell types using a double labeling technique. The ability of bone cells to communicate a mechanical signal was assessed by mechanically deforming the cell membrane of single MLO-Y4 cells, cocultured with MC3T3-E1 cells. Deformation induced calcium signals in MLO-Y4 cells and those elicited in neighboring MC3T3-E1 cells were monitored with the calcium sensitive dye Fura-2. Our results suggest that osteocytic MLO-Y4 cells express functional gap junctions most likely composed of Cx43. Furthermore, osteocytic and osteoblastic cells are functionally coupled to one another via gap junctions as shown by the ability of calcein to pass between cells and the ability of cells to communicate a mechanically induced calcium response. (J Bone Miner Res 2000;15:209–217)

Key words: calcein, connexin 43, mechanotransduction, cell-cell communication, bone

INTRODUCTION

DOTY PROVIDED THE first morphological evidence for the existence of gap junctions between bone cells in vivo.[1] This observation had significant implications in the field of bone cell biology, because gap junctions are known to be involved in intercellular communication. Gap junctions are membrane spanning channels, which facilitate intercellular communication by allowing passage of small molecules (<1 kDa), such as calcium, inositol phosphates, and cyclic nucleotides, from cell to cell. They also provide a means by which cells can be electrically coupled. It has been recognized for some time that this network of interconnecting bone cells might play a role in coordinating cellular activity in bone.

Using theoretical and experimental approaches, several functions for gap junctions in bone have been proposed. These include, for example, a role for gap junctional intercellular communication (GJIC) in the transmission of

*Presented in part at the 43rd Annual Meeting of the Biophysical Society, Baltimore 1999 and the 38th Annual Meeting of the American Society of Cell Biology 1998.

Musculoskeletal Research Laboratory, Departments of Orthopaedics and Rehabilitation and Cellular and Molecular Physiology, The Pennsylvania State University College of Medicine, Hershey, Pennsylvania, U.S.A.

mechanical and chemical (hormonal) signals from one area of bone to another and the ability of cellular networks to initiate a coordinated response to external stimuli. A role for GJIC in hormonal responsiveness was suggested by experiments that showed that osteoblastic cells, rendered gap junction deficient by transfection with antisense to connexin 43 (Cx43), were dramatically less responsive to parathyroid hormone.[2] In addition, it has been shown that calcium signals induced by direct membrane deformation are propagated via gap junctions to neighboring cells.[3,4] These data suggest that GJIC is critical to the mechanism by which external signals, both chemical (hormonal) and mechanical, are transduced and integrated by bone cell networks.

To date, experimental work has focused primarily on the nature and function of gap junctional coupling between adjacent osteoblastic cells. Osteoblasts are found on areas of growing or remodeling bone, where they are responsible for matrix synthesis and mineralization.[5] As a result of matrix deposition, osteoblasts become embedded in the matrix, cease matrix synthesis, and become osteocytes. Morphometric studies suggest that osteocytes retain contact with neighboring osteocytes and ultimately surface osteoblasts, via slender cytoplasmic processes, which contain gap junctions. Osteocytes, from their position deep within the bone matrix are ideally situated to detect mechanical loading and transduce it into an appropriate remodeling response. Additionally, gap junctions might enable osteocytes to act in a coordinated manner passing information between themselves and surface osteoblasts. However, there is relatively little known about the structure and function of gap junctions between osteocytes, attributable to, in part, the difficulty associated with isolating and culturing these cells. Indeed, it is unknown whether osteocytes express functional gap junctions. Early attempts to demonstrate functional bone cell GJIC in vivo were equivocal and did not clearly show osteocytic GJIC.[6]

To overcome the difficulties associated with isolating and culturing large numbers of osteocytes, Kato et al. have established an osteocytic cell line MLO-Y4, which is derived from murine long bone.[7] This cell line was developed from transgenic mice in which the SV40 large T-antigen oncogene was expressed under the control of the osteocalcin promoter, which is abundantly expressed in osteocytes. Cells were isolated, and the cell line MLO-Y4 was cloned from a single colony, which was selected based on expressing the characteristic osteocyte dendritic morphology. The successful establishment of an osteocytic cell line allows us to examine directly the hypothesis that osteocytes express functional gap junctions and that they communicate with osteoblasts via gap junctions. We found that murine osteocytic MLO-Y4 cells not only express functional gap junctions, but they also are coupled to murine osteoblastic MC3T3-E1 cells via gap junctions.

METHODS

Cell culture

The immortalized mouse osteocytic cell line MLO-Y4 was kindly provided by Dr. Lynda Bonewald (University of Texas Health Science Center, San Antonio, TX). Cells were cultured on collagen-coated dishes (rat tail collagen type I, 0.15 mg/ml, Collaborative Biomedical Products, MA, U.S.A.) and maintained in α modified essential medium (α-MEM) supplemented with 5% fetal bovine serum (FBS), 5% calf serum (CS), and 1% penicillin and streptomycin, in a humidified 95% air 5% CO_2 atmosphere at 37°C, as described.[7] MC3T3-E1 mouse osteoblastic cells were cultured in α-MEM supplemented with 10% FBS and 1% penicillin and streptomycin, conditions under which these cells are not fully differentiated. However, MC3T3-E1 cells used for quantification of alkaline phosphatase activity were grown in differentiation media, α-MEM with 10% charcoal stripped FBS, 10^{-8} M 1,25-dihydroxyvitamin D_3 [$1,25(OH)_2D_3$], 50 μg/ml ascorbic acid, and $10^{-}8$ M menadione. For dye transfer and calcium signal propagation experiments, cells were plated on 25-mm round coverslips (no. 1) coated with collagen type I and grown to 90–100% confluence (approximately 48–72 h). Rat osteoblastic ROS 17/2.8 cells were cultured in Ham's F12 supplemented with 10% FBS, 1% Na pyruvate, and 1% penicillin and streptomycin while rat osteoblastic UMR106 cells were cultured in MEM supplemented with 10% FBS, 1% nonessential amino acids, 2% HEPES, and 1% penicillin and streptomycin.

RNA isolation and Northern blot analysis

Cells were plated at 2×10^4 cells/cm^2 in 100-mm-diameter dishes, cultured to confluence (approximately 48–72h) and total RNA was isolated as previously described.[8] Briefly, 20 μg of total RNA, as determined by absorption at 260 nm, was subjected to electrophoresis on a 1% agarose-formaldehyde gel. The gel was capillary-blotted with 0.1 M sodium phosphate onto membranes (Gene Screen Hybridization Transfer Membrane, Du Pont New Research Products, Boston, MA, USA) and prehybridized for 15 minutes at 55°C in 1% bovine serum albumin (BSA), 0.35 M sodium phosphate, 7% sodium dodecyl sulfate (SDS), and 30% (vol/vol) deionized formamide and then hybridized overnight in the same solution with [α-^{32}P]deoxycytosine triphosphate ([α-^{32}P]dCTP)–labeled probes for the entire 1.3-kilobase (kb) coding region of Cx43 complementary DNA (cDNA), the entire 1.2-kb coding region of Cx45 cDNA, a 0.52-kb *Eco*RI fragment of rat osteocalcin cDNA, and 18S ribosomal RNA (rRNA).[8–10] The blots were washed once in 150 mM sodium phosphate and 0.1% SDS at room temperature and two more times at 55°C. For photographic representation, the membranes were exposed to Kodak X-OMAT AR film for various time periods.

Detection of Cx43 protein

Cells were plated at 2×10^4 cells/cm^2 in 100-mm-diameter culture dishes, grown to confluence (approximately 48–72 h) and the crude membrane protein fraction was isolated from cells and subjected to Western blot analysis as previously described.[8] Before electrophoresis, protein concentration was quantified by the method of Bradford.[11] Equivalent amounts of protein (10 μg) from each cell type were loaded onto 12% SDS-polyacrylamide gels, resolved

by electrophoresis and transferred to nitrocellulose membranes that were blocked by Blotto (10% nonfat milk, 10 mM Tris-HCl 8.0, 150 mM NaCl, and 0.05% Tween-20) at pH 8.0. The membranes then were incubated for 3 h at room temperature with antibodies directed against amino acids 252–270 of Cx43 diluted 1:1000 in Blotto. The membranes were washed three times and incubated for 1 h with goat anti-mouse immunoglobulin G (IgG) linked to horseradish peroxidase (Jackson ImmunoResearch Laboratories, Inc., Avondale, PA, U.S.A.) diluted 1:5000. After three additional washes with phosphate buffered saline (PBS) the membranes were soaked in enhanced chemiluminescence (ECL) detection reagents (Amersham Corp., Amersham, U.K.). The sheet then was air-dried and exposed to X-ray film.

Quantification of alkaline phosphatase activity

MLO-Y4 and MC3T3-E1 cells were plated at 4×10^4 cells/cm^2 in 24-well plates and cultured 12 days in α-MEM media with 10% charcoal stripped FBS, 10^{-9} M $1,25(OH)_2D_3$, 50 μg/ml ascorbic acid, and 10^{-8} M menadione. On day 3, 6, 9, and 12 media was removed and cellular alkaline phosphatase activity was determined by the conversion of *p*-nitrophenyl phosphate to *p*-nitrophenol as previously described.[12] Briefly, cells were washed twice with PBS and incubated for 30 minutes in 0.5 ml of 0.75 M 2-amino-2-methyl-1-propanol, pH 10.3, containing 2 mg/ml *p*-nitrophenol phosphate substrate. The reaction solution was mixed with an equal volume of 50 mM NaOH and then diluted 1:40 with 20 mM NaOH. Absorption was measured at 410 nm and conversion to enzyme activity was made using a *p*-nitrophenol standard absorption curve. Data were normalized to protein levels as determined by the Bradford method.[11] Enzyme activity was described in terms of Sigma units per milligram protein, where 1 U will hydrolyze 1.0 μM of *p*-nitrophenyl phosphate per minute at pH 10.4 and 37°C.

Immunostaining

MLO-Y4 cells were cultured on chamber slides (Nunc) until confluent (approximately 48–72 h). Cells were washed twice with 0.1 M PBS, fixed with 4% paraformaldehyde in 0.3% Triton X-100 for 15 minutes at room temperature and then washed twice with PBS. Then cells were incubated overnight at 4°C with a 1:150 dilution of antibody directed to amino acids 252–270 of Cx43. The cells then were washed three times more with PBS and incubated at room temperature for 45 minutes with a 1:200 dilution of rhodamine goat anti-mouse IgG in 1% BSA. Cells were again washed three times with PBS and mounted with FluorSave (Calbiochem Corp., La Jolla, CA, U.S.A.). PBS without antibody was used as a negative control. Fluorescent micrographs were obtained using a Nikon epifluorescence microscope.

Lucifer yellow dye transfer

Intercellular transfer of lucifer yellow, a fluorescent dye that can pass easily through gap junctions, was used to assess gap junctional coupling in MLO-Y4 cells.[2,13] MLO-Y4 cells grown to confluence (approximately 48–72 h) on collagen-coated coverslips, were washed with α-MEM without FBS at 37°C and transferred to an inverted fluorescence microscope. Individual cells were impaled with glass micropipettes that had been backfilled with 10% lucifer yellow dye dissolved in 1 M $LiCl_2$ solution. Cells were impaled for 2 minutes, the pipette was removed, and the number of neighboring cells to which the dye had spread were counted after an additional 3 minutes. The dye was excited at 450–490 nm and emitted light was visualized at 515 nm. 18α-Glycyrrhetinic acid (GA), which blocks gap junctional communication, was used to assess the role of GJIC in dye transfer. MLO-Y4 cells were incubated in 30 μM GA for 10 minutes at 37°C before injection. GA also was present in the media during dye injection.

Calcein dye transfer

Gap junctional coupling between MC3T3-E1 and MLO-Y4 cells was assessed by a double fluorescent labeling technique.[14] Cells were labeled simultaneously with 10 μM calcein acetoxymethyl ester and 10 μM 1,1′-dioctadecyl-3,3,3′,3′-tetramethylindocarbocyanine perchlorate (DiI) (Molecular Probes, Inc., Eugene, OR, U.S.A.). Although calcein is able to permeate gap junctions, DiI is membrane bound. Labeled cells were then trypsinized, centrifuged at 200*g* for 5 minutes, resuspended in the appropriate growth medium, and counted. Labeled cells were then dropped (parachuted) onto confluent plates of unlabeled cells at a ratio of 1:500 labeled-to-unlabeled cells. After gap junctions are established between cells in the monolayer and the labeled parachuted cells, calcein transfers through these channels from labeled-to-unlabeled cells, which then fluoresce green. DiI, which fluoresces red and does not transfer from cell to cell, thus can be used to visualize the original labeled cell. Forty-five minutes after parachuting, cells were visualized using both fluorescein (excitation, 450–490 nm; emission, 520) and rhodamine (excitation, 546/10; emission, 590) filters to locate calcein and DiI-loaded cells. The number of neighboring cells that calcein had transferred to from one double labeled cell was counted. In some experiments GA was used to assess the role of gap junctions in calcein transfer. Unlabeled cells were treated with 75 μM GA in complete media for 10 minutes before addition of labeled cells. We used 75 μM, because in the presence of serum it is necessary to increase the concentration of GA to achieve similar levels of inhibition of cell-to-cell communication.[15] As a vehicle control for GA, in some experiments, unlabeled cells were treated with 0.17% dimethylsulfoxide (DMSO).

Calcium signal propagation

Confluent MLO-Y4 cells were labeled with DiI, trypsinized, centrifuged at 200*g* for 5 minutes, resuspended in the appropriate growth medium, and mixed with MC3T3-E1 cells at a concentration of 1:500, MLO-Y4 to MC3T3-E1. Cells were then plated onto collagen-coated glass coverslips at a sufficient concentration to form a confluent monolayer

and maintained overnight in a humidified 95% air 5% CO_2 atmosphere at 37°C. Cells were washed with Tyrodes solution at 37°C, which contained (in mM) 140 NaCl, 4 KCl, 1 $MgCl_2$, 2 $CaCl_2$, 5 *N*-2-hydroxyethylpiperazine-*N'*-2-ethanesulphonic acid, and 10 glucose, and titrated to a final pH of 7.4 with 4 mM NaOH. Cells were then incubated with 1 μM fura-2-acetoxymethyl ester (Molecular Probes, Inc., Eugene, OR, U.S.A.) solution for 30 minutes at 37°C. The cells were washed again with fresh Tyrodes solution at 37°C, and the slide was transferred to an epifluorescence microscope. Individual MLO-Y4 cells were located using a rhodamine filter as described above. Membranes of single MLO-Y4 cells were deformed by gently pressing a glass patch pipette fashioned from unfilamented borosilicate glass (Corning 7052, A.M. Systems) against the cell membrane. Calcium responses in the deformed cell and its neighbors were detected as previously described.[16,17] Briefly, a Metafluor imaging system (Universal Imaging, West Chester, PA, U.S.A.) was used to sample and record the emitted light from the cells in the field of view once every 2.5 s, and Metafluor imaging software was used to subtract the background fluorescence from each image and to outline and calculate the 340:380 ratio for each cell in the field of view, which directly reflects $[Ca^{2+}]_i$. A calibration curve was constructed by acquiring 340:380 values (background subtracted) for a series of solutions of known free Ca^{2+} concentration (0–39.8 μM, Molecular Probes, Inc., Eugene, OR, U.S.A.) and 1 μM Fura-2 pentapotassium salt (Molecular Probes, Inc., Eugene, OR, U.S.A.). This calibration curve was used to convert ratio values from individual cells into $[Ca^{2+}]_i$. To identify Ca^{2+} oscillations, we used an adapted numerical procedure from mechanical analysis, known as rainflow cycle counting, previously used successfully to identify oscillations in $[Ca^{2+}]_i$ in bone cells.[18] This technique identifies complete cycles or oscillations in the time history data even when they are superimposed on each other and therefore can be used to distinguish and quantify $[Ca^{2+}]_i$ responses from background signal noise. We defined a response as an oscillation in $[Ca^{2+}]_i$ of 10 nM or greater.

Data analysis

Data are expressed as mean ± SEM. To compare observations from different groups with unequal sample size, a two-sample Students *t* est was used in which sample variance was not assumed to be equal. To compare observations from more than two groups, a one-way analysis of variance was used followed by a Student–Newman–Keuls multiple comparisons post hoc test (Instat, GraphPad Software, Inc.). The value of $p < 0.05$ was considered statistically significant.

RESULTS

Characterization of the osteocytic phenotype of MLO-Y4 cells

Phenotypic characteristics of osteocytic MLO-Y4 cells, reported in the original publication describing the establishment of this cell line, include a stellate morphology, decreased alkaline phosphatase activity and increased osteocalcin relative to osteoblastic cell lines.[7] In our hands MLO-Y4 cells also display a morphology similar to that described.[7] As shown in Fig. 1, a majority of MLO-Y4 cells exhibit a stellate morphology with several dendritic-like processes extending from the cell body. These cells also display osteocalcin messenger RNA (mRNA) to a greater degree than osteoblastic MC3T3-E1 and UMR106 cells but somewhat less than ROS 17/2.8 cells (Fig. 2). However, alkaline phosphatase activity was decreased in MLO-Y4 relative to MC3T3-E1 (Fig. 3). Alkaline phosphatase activity increased with time in culture in MC3T3-E1 in the presence of $1,25(OH)_2D_3$, such that activity levels on day 12 were over 30-fold greater than on day 3. However, there was no significant increase in alkaline phosphatase activity in MLO-Y4 and by day 12 the activity in MLO-Y4 was less than 5% that of MC3T3-E1.

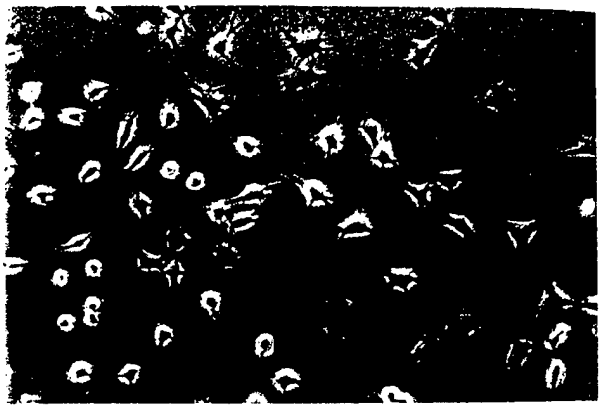

FIG. 1. Phase contrast photomicrograph of osteocytic MLO-Y4 cells. Note stellate morphology with extensive dendritic-like processes. Magnification was ×20.

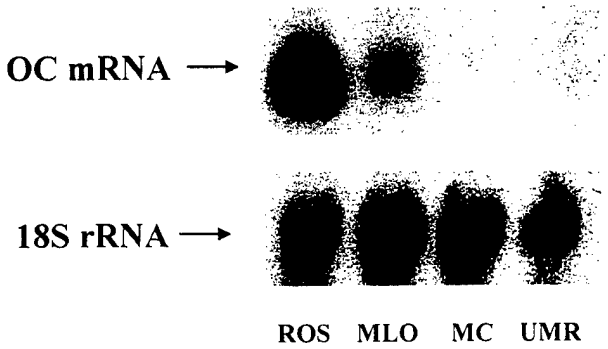

FIG. 2. Northern blot analysis of osteocalcin (OC) mRNA and 18S rRNA in osteocytic MLO-Y4 (MLO) and osteoblastic cells, ROS 17/2.8 (ROS), MC3T3-E1 (MC) and UMR106 (UMR). Twenty micrograms of total RNA was subjected to Northern blot analysis using either a 520 base pair (bp) rat osteocalcin radiolabeled probe or an 18S rRNA radiolabeled probe. Three separate experiments resulted in similar results.

Cx43 expression in osteocyte-like MLO-Y4 cells

Northern and Western blot analysis for Cx43 mRNA and protein, respectively, were performed on MLO-Y4 cells and

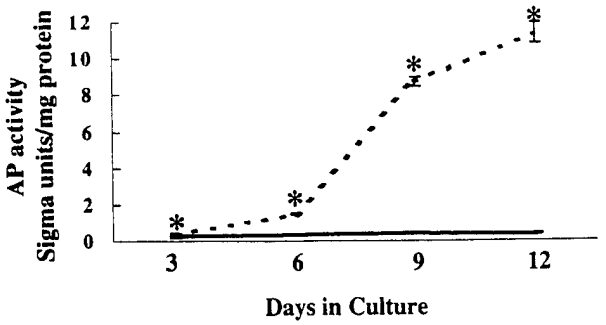

FIG. 3. Alkaline phosphatase activity in osteocytic MLO-Y4 cells and osteoblastic MC3T3-E1 cells. Cells were cultured for 12 days as described in text. Although alkaline phosphatase activity increased dramatically with time in culture in MC3T3-E1 cells (dashed line), it remained at relatively low levels throughout the culture period in MLO-Y4 cells (solid line). *Significantly different from MLO-Y4 cells, $p < 0.05$, $n = 4$.

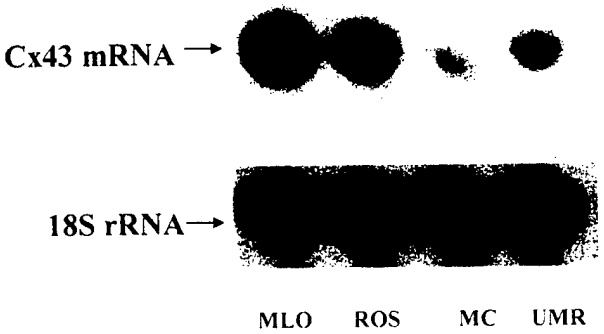

FIG. 4. Northern blot analysis of Cx43 mRNA and 18S/rRNA expression in osteocytic MLO-Y4 (MLO) and osteoblastic cells ROS 17/2.8 (ROS), MC3T3-E1 (MC), and UMR106 (UMR). Twenty micrograms of total RNA was subjected to Northern blot analysis using either an 890-bp rat Cx43 cDNA radiolabeled probe or an 18S cDNA radiolabeled probe. Three separate experiments resulted in similar results.

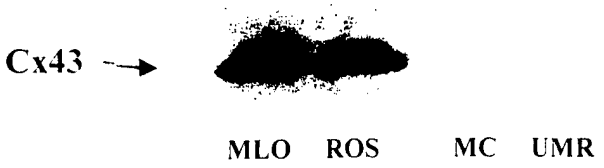

FIG. 5. Western blot analysis of Cx43 protein in osteocytic MLO-Y4 (MLO) and osteoblastic cells ROS 17/2.8 (ROS), MC3T3-E1 (MC), and UMR106 (UMR). Equivalent amounts of total cell extract enriched for membrane proteins were separated by SDS-polyacrylamide gel electrophoresis, transferred to nitrocellulose, and analyzed using a polyclonal antibody to rat Cx43. Three separate experiments resulted in similar results.

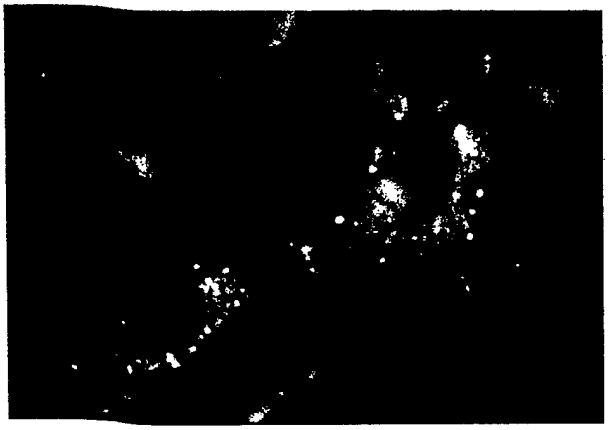

FIG. 6. Photomicrograph of Cx43 immunoreactivity in osteocytic MLO-Y4 cells. Cells plated at 50,000 cells/cm^3 and grown for 48 h were fixed, permeabilized, and incubated with a polyclonal antibody to rat Cx43. A fluorescein conjugated secondary antibody was used for visualization under a broadband ultraviolet light. These experiments were performed four times.

osteoblastic ROS 17/2.8, MC3T3-E1, and UMR106 cells (Figs. 4 and 5). MLO-Y4 cells expressed a greater abundance of Cx43 mRNA and protein relative to either MC3T3-E1 or UMR106 cells. However, Cx43 abundance was similar to that of ROS 17/2.8. Indirect immunostaining of MLO-Y4 cells revealed diffuse distribution of Cx43 immunoreactivity at the interface of adjoining cells and diffuse staining throughout the cytoplasm (Fig. 6). MLO-Y4 cells did not express appreciable Cx45 (data not shown).

Gap junctional coupling in osteocytic MLO-Y4 cells

Lucifer yellow dye transfer was used to assess the degree of functional gap junctional coupling between osteocytic cells (Fig. 7). After 5 minutes, lucifer yellow dye spread from the injected cell to 7.4 ± 0.9 of its neighbors. GA, the gap junctional uncoupler, was applied at a concentration of 30 μM, which decreased the number of dye-loaded neighboring cells to 0.7 ± 0.1.

Gap junctional coupling between osteocytic (MLO-Y4) and osteoblastic (MC3T3-E1) cells

Both MLO-Y4 and MC3T3-E1 were able to form functional gap junctions, as determined by calcein dye transfer, within 45 minutes of cell parachuting (Fig. 8). MC3T3-E1 cells transferred calcein to an average of 33.8 ± 2.0 MLO-Y4 cells, whereas MLO-Y4 cells transferred dye to an average of 6.6 ± 0.4 MC3T3-E1 cells (Fig. 9). Forty-five percent of MLO-Y4 cells and 21% of MC3T3-E1 cells were rounded, tenuously attached to the underlying monolayer, and unable to form gap junctions. Seventy-five micromolar GA blocked all calcein dye transfer from MLO-Y4 to MC3T3-E1 cells in monolayer ($n = 43$), while reducing calcein spread from MC3T3-E1 cells to MLO-Y4 to only

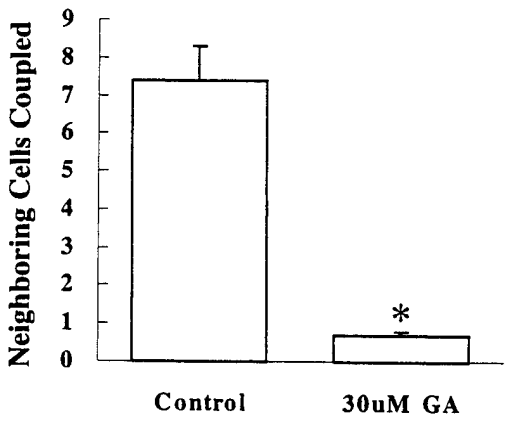

FIG. 7. Gap junctional coupling in osteocytic cells. Functional coupling was assessed in MLO-Y4 cells by lucifer yellow dye injection. Each bar represents the mean ± SEM number of adjacent cells that take up dye within 5 minutes in the presence or absence of GA. Thirty-one injections were performed under control conditions and 26 in the present of 30 μM GA. *Represents a statistically significant difference from control, $p < 0.05$.

5.3 ± 0.6 cells (Fig. 9). The 0.16% DMSO, added as a vehicle control for GA, had no effect on calcein dye transfer. In the presence of DMSO, MLO-Y4 cells transferred dye to 6.75 ± 0.6 MC3T3-E1 cells and MC3T3-E1 cells transferred dye to 32.96 ± 2.4 MLO-Y4 cells (Fig. 9).

Calcium signal propagation

Mechanical deformation of a single osteocytic MLO-Y4 cell induced a transient increase in internal $[Ca^{2+}]_i$, which was propagated rapidly to 4.6 ± 0.5 neighboring MC3T3-E1 cells (Fig. 10). In the presence of 30 μM GA, a Ca^{2+} response was observed in only 0.5 ± 0.5 neighboring MC3T3-E1 cells. Deformation of MLO-Y4 cells induced a mean Ca^{2+} response amplitude of 0.077 μM ± 0.012 μM, which was not significantly different in the presence of GA, 0.048 μM ± 0.011 μM. The mean Ca_i^{2+} response amplitude in neighboring MC3T3 cells was 0.033 μM ± 0.04 μM.

DISCUSSION

The existence of gap junctions between osteocytic processes in bone canaliculi has been confirmed with a number of techniques. Shapiro provided transmission electron micrographs, which showed clearly the complexity and extent of gap junctions between osteocytic processes in intact rat and mouse long bone.[19] Cx43, a specific gap junction protein first identified in the heart, which is the most predominant connexin found in osteoblastic cells, was visualized at osteocytic gap junctions by immunolabeling in intact rat calvarial bone.[13,20,21] Subsequently, the reverse transcriptase polymerization chain reaction has been used to show Cx43 mRNA expression in osteocytes from rat cortical bone in vivo and in situ hybridization and immunohistochemistry has identified Cx43 mRNA and protein, respectively, in osteocytes within rat mandibular bone.[22,23] However, because of their position deep within the mineralized bone matrix, it has been difficult to study the functionality of gap junctions between osteocytes. This has been partially overcome by the establishment of an osteocytic cell line MLO-Y4.[7]

In our hands, MLO-Y4 express phenotypic characteristics of osteocytic cells[7] including a stellate morphology, low alkaline phosphate activity, and increased osteocalcin and Cx43 mRNA. It should be noted that although steady state osteocalcin mRNA levels were greater in osteocytic MLO-Y4 than osteoblastic MC3T3-E1 and UMR106, they were lower than in osteoblastic ROS 17/2.8 cells. Kato et al. did not examine osteocalcin synthesis in MLO-Y4 relative to ROS 17/2.8 so it is not possible to state whether our results are consistent with their results in this regard. However, where comparisons are possible, our data are very similar to Kato et al., suggesting that the osteocytic phenotype of MLO-Y4 is quite stable.

Although other studies have shown that osteocytic cells express abundant Cx43, they have not examined gap junction function. It is critical that this be shown if one wishes to examine the role of gap junctional coupling in osteocytic function. Using the recently established osteocytic cell line MLO-Y4, this study provides the first functional data regarding gap junctions between osteocytic cells. Using lucifer yellow dye transfer we showed that MLO-Y4 cells are well coupled to one another via gap junctions. We also found that MLO-Y4 expresses large quantities of Cx43 protein and mRNA. Our immunostaining suggests that although osteocytes synthesize abundant Cx43 protein, a large proportion of this is localized in the cytoplasm. Another key question is whether osteocytes are functionally coupled to osteoblasts.

Again, because of their position within the mineralized matrix, there has been no functional data regarding the ability of osteocytes to communicate with osteoblasts via gap junctions. Doty first visualized gap junctions between osteocytes and osteoblasts, and more recently, Shapiro has described the variation in form and extent of these junctions.[1,19] Cx43 also has been shown to localize at junctions between osteocytes and osteoblasts by immunolabeling.[21] Using a double dye–labeling parachute technique we have been able to show that osteoblastic and osteocytic cells also are functionally coupled.

Our data suggest that within 45 minutes, osteocytic and osteoblastic cells were able to form functional gap junctional channels as assessed by calcein dye transfer. Dye transferred to fewer osteoblastic MC3T3-E1 cells from osteocytic MLO-Y4 cells than vice versa, which may reflect poor coupling between MC3T3-E1 cells. This is because once gap junctions have been established and dye transferred between the parachuted cell and the cells on which it lands, the degree of subsequent dye spread is dependent on the coupling between cells in the monolayer. The reason for poor coupling between MC3T3-E1 cells might possibly be the result of the fact that these cells were not fully differentiated. Recently, we have shown, using human fetal osteoblastic cells (hFOB), that cell-to-cell communication is highly dependent on cell differentiation state.[24] However,

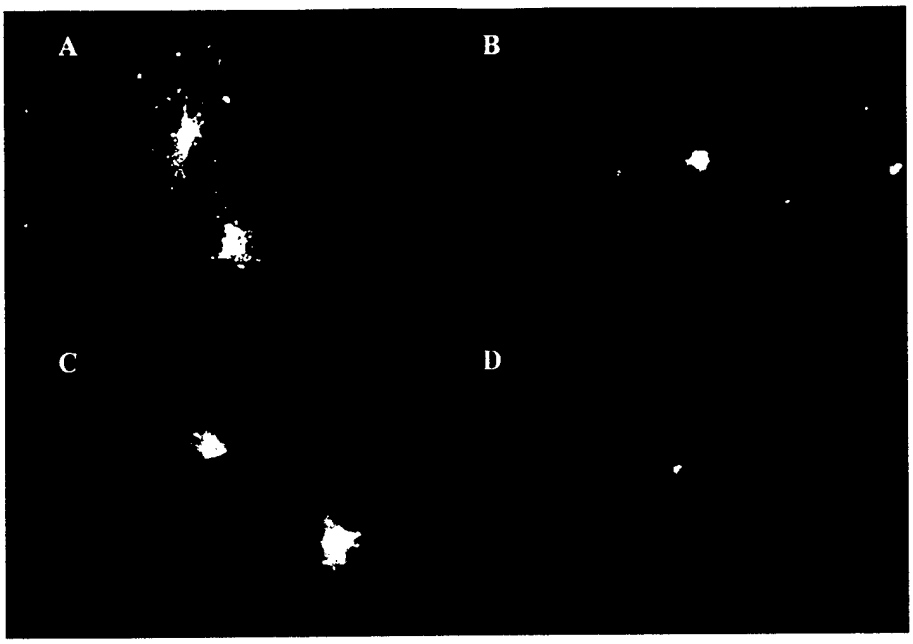

FIG. 8. Gap junctional communication between osteocytic (MLO-Y4) cells and osteoblastic (MC3T3-E1) cells. Calcein- and DiI-labeled MC3T3-E1 cells were parachuted onto an 80–100% confluent layer of MLO-Y4 cells in the (A) absence or (C) presence of 75 μM GA. MLO-Y4 cells also were labeled and parachuted onto MC3T3-E1 cells in the (B) absence and (D) presence of GA. Photomicrographs of the cells were double-exposed with fluorescein and rhodamine filter sets. Double-labeled cells appear yellow/white; those cells that received calcein alone via gap junctional diffusion appear green. Each experiment was performed on at least 27 cells.

despite the low abundance of Cx43 mRNA and protein in MC3T3-E1 cells we still saw significant osteocyte-osteoblast coupling. Interestingly, the number of MLO-Y4 cells coupled, as assessed by lucifer yellow dye transfer, was significantly less than the number coupled using calcein as a dye tracer. Other studies have shown that lucifer yellow can fail to transfer between cells that are shown to be coupled by other tracers, such as biocytin and carboxyfluorescein.[25] It has been suggested that sulfate-containing compounds such as lucifer yellow may interfere with dye coupling in some cell types, by direct or indirect modulation of gap junctional channels.[25] This may explain why in some cell types coupling as assessed by lucifer yellow dye transfer was less than that assessed by calcein transfer and furthermore it suggests that calcein, which does not contain sulfate groups, may be a superior tracer for analysis of gap junctional coupling.

The parachute technique has been used by Ziambaras et al. who used it to assess the effect of cyclic stretch on gap junctional communication between osteoblastic cells.[26] However, in these experiments the cells were loaded with calcein only and "donor" cells were identified as those cells that were brightest and were in an elevated focal plane to the "acceptor" cells. In our experiments we further refined this method by colabeling cells with DiI, as described by Goldberg et al.[14] DiI, which fluoresces red and does not transfer from cell to cell, allowed us to identify easily the original dye-loaded cells.

The existence of gap junctions between adjacent osteocytic cells, adjacent osteoblastic cells, and between osteo-

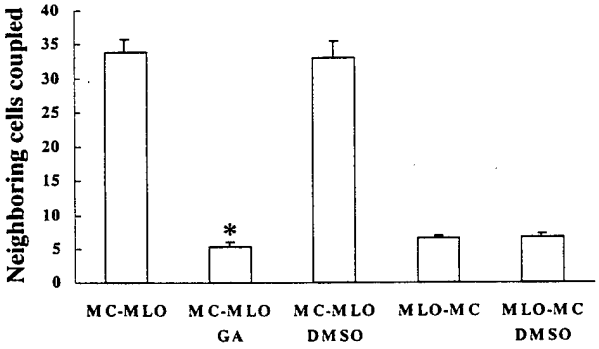

FIG. 9. Quantification of gap junctional coupling between osteocytic and osteoblastic cells. Functional coupling was assessed between MLO-Y4 (MLO) and MC3T3-E1 (MC) cells by calcein dye transfer from a parachuted, labeled cell. Each bar represents the mean ± SEM number of adjacent cells that take up dye within 5 minutes in the presence or absence of 75 μM GA. Experiments also were performed in the presence of DMSO as a vehicle control for GA. MC3T3-E1 cells were parachuted onto MLO-Y4 cells under normal conditions (MC-MLO, $n = 27$) and in the presence of GA (MC-MLO GA, $n = 36$) or DMSO (MC-MLO DMSO, $n = 25$). MLO-Y4 cells were parachuted onto MC3T3-E1 cells under normal conditions (MLO-MC, $n = 69$) and in the presence of DMSO (MLO-MC DMSO, $n = 24$). GA blocked all dye transfer and is therefore not graphed ($n = 43$). *Represents a statistically significant difference from MC-MLO, $p < 0.05$.

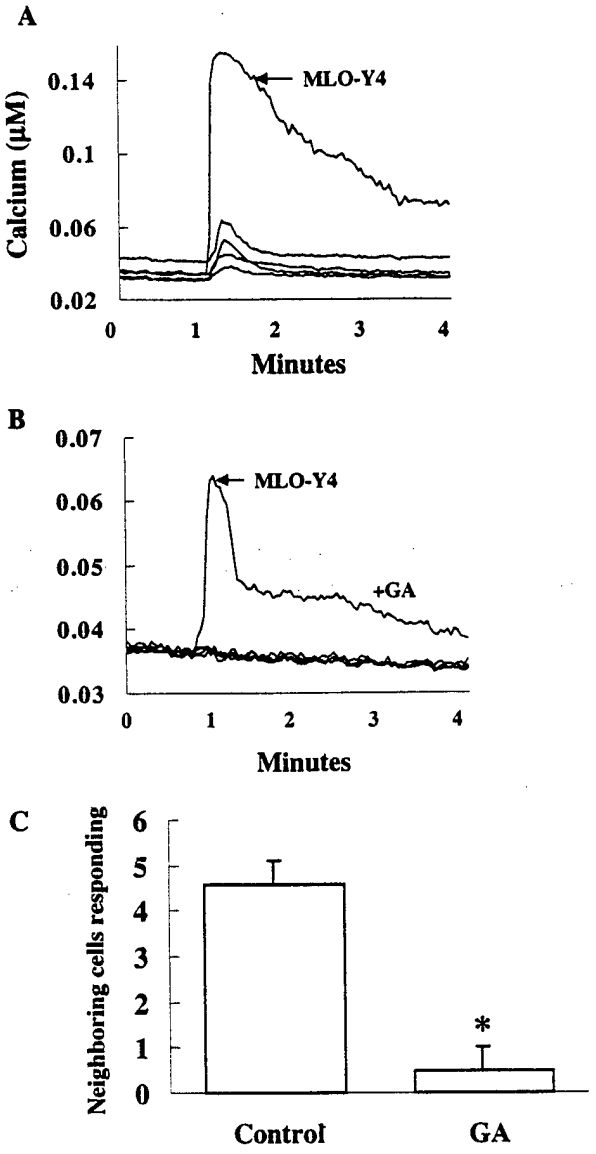

FIG. 10. Calcium signal propagation between bone cells. (A) Deformation of a single MLO-Y4 cell (arrow) elicits an intracellular calcium transient, which is propagated to neighboring MC3T3-E1 cells. (B) The presence of 30 μM GA in the media inhibits calcium signal propagation to neighboring MC3T3-E1 cells. (C) Mean number of neighboring MC3T3-E1 cells showing a Ca_i^{2+} transient elicited in response to deformation of a single MLO-Y4 cell in the presence ($n = 4$) and absence ($n = 9$) of 30 μM GA. Each bar represents the mean ± SEM. *Represents a statistically significant difference from control, $p < 0.05$.

cytic and osteoblastic cells suggests that within bone there is an extensive and functional interconnected network of cells. As such, this network would provide an ideal signal integration and amplification mechanism in bone. It is possible that gap junctions will facilitate the transmission of extracellular signals, such as hormones, from cells adjacent to blood vessels to those buried deeper in less vascular cortical areas. It is also possible that signals induced by locally secreted stimulatory factors, such as cytokines and prostaglandins, will be propagated through the network. In addition, it has been recognized for some time that osteocytes are situated ideally within the bone matrix to detect and respond to mechanical signals.[27] Indeed, it has been shown that mechanical loading does stimulate an early response in osteocytes.[28] Therefore, it is possible, that this osteocytic network will provide the necessary mechanism by which mechanical information is relayed through the matrix to osteoblastic cells on the surface that are more intimately involved in the early stages of the bone remodeling cycle. This notion is supported by our results showing that osteocytic cells in vitro could communicate mechanical signals to osteoblasts via changes in intracellular calcium. Although mechanical loading does cause strain in the matrix, there is increasing evidence to suggest that the cells might actually be responding to mechanically induced fluid flow through the canaliculi.[29,30] Because fluid flow would promote chemotransport of nutrients to and from the cell, as well as directly deforming the cell membrane, it will be important to assess the ability of osteocytes to transduce and communicate not only mechanical signals, but also chemical signals.

An important consideration in interpreting these results is that the cells are outside of their natural three-dimensional environment, which may affect cell-to-cell communication. Considering these issues, our data do not prove that osteoblasts and osteocytes functionally communicate in vivo; however, it shows that they have the potential to do so.

In summary we have shown that osteocytic cells in vitro express functional gap junctions most likely composed of Cx43. Furthermore, osteocytic cells and osteoblastic cells are functionally coupled to one another via gap junctions as shown by the ability of calcein dye to pass between cells. These data support the possibility that a functional network of interconnecting cells exists in vivo, which may provide bone with a powerful regulatory mechanism, whereby signals could be integrated and amplified, and cells could respond in a coordinated manner to extracellular signals.

ACKNOWLEDGMENTS

This work was supported by grant AG-13087 from the National Institutes on Aging (H.J.D.), grant 1F32 AR08514–01 from the National Institute of Arthritis and Musculoskeletal and Skin Diseases (C.E.Y.), the Whitaker foundation, and the U.S. Army Medical Research Acquisition Activity grant DAMD17–98–1-85oq (C.R.J.).

REFERENCES

1. Doty SB 1981 Morphological evidence of gap junctions between bone cells. Calcif Tissue Int **33**:509–12.
2. Vander Molen MA, Rubin CT, McLeod KJ, McCauley LK, Donahue HJ 1996 Gap junctional intercellular communication contributes to hormonal responsiveness in osteoblastic networks. J Biol Chem **271**:12165–12171.

3. Xia SL, Ferrier J 1992 Propagation of a calcium pulse between osteoblastic cells. Biochem Biophys Res Commun **186:**1212–1219.
4. Jorgensen NR, Geist ST, Civitelli R, Steinberg TH 1997 ATP- and gap junction-dependent intercellular calcium signaling in osteoblastic cells. J Cell Biol **139:**497–506.
5. Rodan GA, Rodan SB 1983 Expression of the osteoblastic phenotype. In: Peck WA (ed.) Bone and Mineral Research, Annual 2. Elsevier Science Publishers, New York, NY, U.S.A., pp. 244–285.
6. Jeansonne BG, Feagin FF, McMinn RW, Shoemaker RL, Rehm WS 1979 Cell-to-cell communication of osteoblasts. J Dent Res **58:**1415–1423.
7. Kato Y, Windle JJ, Koop BA, Mundy GR, Bonewald LF 1997 Establishment of an osteocyte-like cell line, MLO-Y4. J Bone Miner Res **12:**2014–2023.
8. Li Z, Zhou Z, Daniel EE 1993 Expression of gap junction connexin 43 and connexin 43 mRNA in different regional tissues of intestine in dog. Am J Physiol **265:**G911–G916.
9. Kanter HL, Saffitz JE, Beyer EC 1992 Cardiac myocytes express multiple gap junction proteins. Circ Res **70:**438–444.
10. Weinreb M, Shinar D, Rodan GA 1990 Different pattern of alkaline phosphatase, osteopontin, and osteocalcin expression in developing rat bone visualized by in situ hybridization. J Bone Miner Res **5:**831–842.
11. Bradford MM 1976 A rapid and sensitive method for the quantitation of microgram quantities of protein utilizing the principle of protein-dye binding. Anal Biochem **72:**248–254 .
12. McLeod KJ, Donahue HJ, Levin PE, Fontaine MA, Rubin CT 1993 Electric fields modulate bone cell function in a density-dependent manner. J Bone Miner Res **8:**977–984.
13. Donahue HJ, McLeod KJ, Rubin CT, Andersen J, Grine EA, Hertzberg EL, Brink PR 1995 Cell-to-cell communication in osteoblastic networks: Cell line-dependent hormonal regulation of gap junction function. J Bone Miner Res **10:**881–889.
14. Goldberg GS, Bechberger JF, Naus CC 1995 A pre-loading method of evaluating gap junctional communication by fluorescent dye transfer [published erratum appears in Biotechniques 1995 Aug;19(2):212]. Biotechniques **18:**490–497.
15. Davidson JS, Baumgarten IM, Harley EH 1986 Reversible inhibition of intercellular junctional communication by glycyrrhetinic acid. Biochem Biophys Res Commun **134:**29–36.
16. Lee YC, Yellowley CE, Li Z, Donahue HJ, Rannels DE 1997 Expression of functional gap junctions in cultured pulmonary alveolar epithelial cells. Am J Physiol **272:**L1105–L1114.
17. Yellowley CE, Jacobs CR, Li Z, Zhou Z, Donahue HJ 1997 Effects of fluid flow on intracellular calcium in bovine articular chondrocytes. Am J Physiol Cell Physiol **273:**C30–C36.
18. Jacobs CR, Yellowley CE, Nelson DV, Donahue HJ 1999 A novel application of rainflow counting to time-varying biophysical data. Comput Methods Biomech Biomed Eng **2:**1–10.
19. Shapiro F 1997 Variable conformation of GAP junctions linking bone cells: A transmission electron microscopic study of linear, stacked linear, curvilinear, oval, and annular junctions. Calcif Tissue Int **61:**285–293.
20. Civitelli R, Beyer EC, Warlow PM, Robertson AJ, Geist ST, Steinberg TH 1993 Connexin43 mediates direct intercellular communication in human osteoblastic cell networks. J Clin Invest **91:**1888–1896.
21. Jones SJ, Gray C, Sakamaki H, Arora M, Boyde A, Gourdie R, Green C 1993 The incidence and size of gap junctions between the bone cells in rat calvaria. Anat Embryol **187:**343–352.
22. Mason DJ, Hillam RA, Skerry TM 1996 Constitutive in vivo mRNA expression by osteocytes of beta-actin, osteocalcin, connexin-43, IGF-I, c-fos and c-jun, but not TNF-alpha nor tartrate-resistant acid phosphatase. J Bone Miner Res **11:**350–357.
23. Su M, Borke JL, Donahue HJ, Warshawsky NM, Russell CM 1997 Expression of connexin 43 in rat mandibular bone and PDL cells during experimental tooth movement. J Dent Res **76:**1357–1366.
24. Donahue HJ, Li Z, Zhou Z, Yellowley CE 2000 Differentiation of human fetal osteoblastic cells is partially dependent on gap junctional intercellular communication. Am J Physiol (Cell) **278**(2):C315–C322.
25. Little TL, Xia J, Duling BR 1995 Dye tracers define differential endothelial and smooth muscle coupling patterns within the arteriolar wall. Circ Res **76:**498–504.
26. Ziambaras K, Lecanda F, Steinberg TH, Civitelli R 1998 Cyclic stretch enhances gap junctional communication between osteoblastic cells. J Bone Miner Res **13:**218–228.
27. Duncan RL, Turner CH 1995 Mechanotransduction and the functional response of bone to mechanical strain [Review]. Calcif Tissue Int **57:**344–358.
28. Skerry TM, Bitensky L, Chayen J, Lanyon LE 1989 Early strain-related changes in enzyme activity in osteocytes following bone loading in vivo. J Bone Miner Res **4:**783–788.
29. Owan I, Burr DB, Turner CH, Qiu J, Tu Y, Onyia JE, Duncan RL 1997 Mechanotransduction in bone: Osteoblasts are more responsive to fluid forces than mechanical strain. Am J Physiol Cell Physiol **42:**C810–C815.
30. Jacobs CR, Yellowley CE, Davis BR, Zhou Z, Donahue HJ 1998 Differential effect of steady versus oscillating flow on bone cells. J Biomech **31:**969–976.

Address reprint requests to:
Clare Yellowley
Musculoskeletal Research Laboratory
Department of Orthopaedics and Rehabilitation
Pennsylvania State College of Medicine
The Milton S. Hershey Medical Center
Hershey, PA, 17033, U.S.A.

Received in original form April 7, 1999; in revised form August 20, 1999; accepted September 27, 1999.

JOURNAL OF CELLULAR PHYSIOLOGY 180:402–408 (1999)

Mechanisms Contributing to Fluid-Flow-Induced Ca^{2+} Mobilization in Articular Chondrocytes

CLARE E. YELLOWLEY,* CHRISTOPHER R. JACOBS, AND HENRY J. DONAHUE

Musculoskeletal Research Laboratory, Departments of Orthopaedics and Rehabilitation and Cellular and Molecular Physiology, The Pennsylvania State University College of Medicine, Hershey, Pennsylvania

We previously showed that fluid flow, which chondrocytes experience in vivo and which results in a variety of morphological and metabolic changes in cultured articular chondrocytes, can also stimulate a rise in intracellular calcium concentration ($[Ca^{2+}]_i$). However, the mechanism by which Ca^{2+} is mobilized in response to flow is unclear. In this study, we investigated the roles of intracellular Ca^{2+} stores, G-proteins, and extracellular ATP in the flow-induced Ca^{2+} response in bovine articular chondrocytes (BAC). Cells loaded with the Ca^{2+} sensitive dye Fura-2 were exposed to steady flow at 34 ml/min (37 dynes/cm^2) in a parallel plate flow chamber. Whereas ryanodine and caffeine had no effect, both neomycin and thapsigargin significantly decreased the $Ca^{2+}{}_i$ response to flow, suggesting a role for Ca^{2+} store release, possibly through an inositol 1,4,5-trisphosphate (IP_3)-dependent mechanism. Twenty-four-hour treatment with pertussis toxin also significantly decreased the response, suggesting that the mechanism may be G-protein regulated. In addition, ATP release by chondrocytes does not appear to mediate the flow-induced Ca^{2+} response because suramin, a P2 purinergic blocker, had no effect. These results suggest that BAC respond rapidly to changes in their mechanical environment, such as increased fluid flow, by a mechanism that involves IP_3 stimulated $Ca^{2+}{}_i$ release and G-protein activation. J. Cell. Physiol. 180:402–408, 1999. © 1999 Wiley-Liss, Inc.

Mechanical loading resulting from normal joint motion has a profound influence on cartilage matrix. For instance, changes in mechanical loading that occur in vivo as a result of limb immobilization or exercise result in changes in the composition of the cartilage matrix and thus alter its biomechanical properties (Caterson and Lowther, 1978; Behrens et al., 1989; Jurvelin et al., 1989). It has been proposed that chondrocytes embedded within the matrix are ideally situated to detect and transduce mechanical signals and alter the composition of the matrix accordingly. However, the exact nature of the physical stimulus that chondrocytes are responsive to is unclear because the mechanical environment they experience during mechanical loading is complex.

Recently, fluid flow has been used in a number of studies as a physiologically relevant stimulus for chondrocytes (Smith et al., 1995; Mohtai et al., 1996; Yellowley et al., 1997). Fluid flow can be applied in a reliable and reproducible manner by using a parallel plate flow chamber (Frangos et al., 1988) and imposes not only shear stress but also direct mechanical strain and electrokinetic effects, all of which chondrocytes experience in vivo (Mow et al., 1994). The emerging data suggest that chondrocytes are extremely sensitive to fluid flow. Fluid-induced shear stress applied to both human and bovine articular chondrocytes (BAC) for 24–72 h induced morphological and metabolic changes including elongation, reorientation, and changes in proteoglycan synthesis and size (Smith et al., 1995; Mohtai et al., 1996).

The mechanism by which fluid flow signals are perceived and then transduced into a functional response by chondrocytes is unknown. We previously showed that fluid flow causes mobilization of intracellular calcium ($Ca^{2+}{}_i$) in BAC (Yellowley et al., 1997), similar to that seen in other cells such as endothelial and bone cells (Geiger et al., 1992; Helmlinger et al., 1995; Hung et al., 1995) in response to flow. Thus, $Ca^{2+}{}_i$ appears to

Contract grant sponsor: NIH; Contract grant numbers: 1 F32 AR 08514-01, RR 11769, and AG 15107; Contract grant sponsor: Whitaker Foundation; Contract grant sponsor: U.S. Department of Defense.

Portions of this work were presented at the 44th annual meeting of the Orthopaedic Research Society, 16–19 March 1998 and the Biomedical Engineering Society, 2–5 October 1997.

*Correspondence to: Clare Yellowley, Musculoskeletal Research Laboratory, Department of Orthopaedics and Rehabilitation, Pennsylvania State College of Medicine, The Milton S. Hershey Medical Center, Hershey, PA 17033. E-mail: cyellowl@ortho.hmc.psu.edu

Received 11 September 1998; Accepted 10 March 1999

be an important second messenger in biophysical signal transduction in chondrocytes. However, the mechanism by which $Ca^{2+}{}_i$ is mobilized in response to fluid flow is unclear.

Although the mechanism by which flow mobilizes $Ca^{2+}{}_i$ is unclear, a role for G-proteins in BAC mechanotransduction has been suggested by studies demonstrating that fluid-flow-induced glycosaminoglycan synthesis in BAC and prostaglandin E_2 production in osteoblasts are inhibited by the G-protein inhibitors pertussis toxin (PTX) and guanosine 5′-O-C2-Thiodiphosphate (GDPβS) (Das et al., 1997; Reich et al., 1997). It is not known, however, at which step in the mechanotransduction pathway G-proteins are involved. To address this issue further, we examined whether G-proteins are involved in stimulating the $Ca^{2+}{}_i$ response to flow in BAC.

In addition to G-proteins, ATP, acting as an autocrine and paracrine agent, has also been implicated in fluid-flow-induced $Ca^{2+}{}_i$ mobilization. For instance, in endothelial cells, the concentration of ATP at the cell surface increases with increased fluid-flow-induced shear stress (Milner et al., 1990) and addition of ATP to the perfusate augments the $Ca^{2+}{}_i$ response to flow (Ando et al., 1991). This suggests that a $Ca^{2+}{}_i$ response to fluid flow in vivo may include both biophysical and biochemical components. Because ATP has been shown to stimulate $Ca^{2+}{}_i$ transients in BAC (D'Andrea and Vittur, 1996), it may also act as an autocrine and paracrine agonist in fluid flow–induced $Ca^{2+}{}_i$ mobilization. Therefore, we also investigated the role of ATP in fluid-flow-induced $Ca^{2+}{}_i$ mobilization in BAC.

METHODS

Chondrocyte isolation and culture

BAC were isolated as previously described (Yellowley et al., 1997). Briefly, slices of articular cartilage were dissected from bovine hock joints, diced, and digested for 2–4 h in a mixture of 0.15 mg/ml deoxyribonuclease, 2 mg/ml collagenase, and 0.1 mg/ml hyaluronidase at 37°C. The supernatent was removed, filtered through a 120- μM Nytex filter (Tetko, Briarcliff Manor, NY), and centrifuged at 200*g* for 5 min. The resulting cell pellet was washed three times in Hank's balanced salt solution and resuspended in RPMI 1640 medium supplemented with 20% fetal bovine serum and 1% penicillin and streptomycin (all Gibco BRL, Grand Island, NY). The cells were plated in 25-cm^2 culture flasks (Corning Glass Works, Corning, NY) and grown to confluency (10–14 days). The cells were subcultured with a 0.25% sterile trypsin solution and plated onto 24- × 60-mm, 1.6-mm-thick quartz slides (Friedrich and Dimmock, Inc., Millville, NJ) for the flow experiments. Only passage 1 cells were used for the flow experiments. Fifteen separate chondrocyte isolations were used during the flow experiments. We previously showed that chondrocytes isolated in this manner express characteristics of the chondrocyte phenotype, including a chondrocytic morphology and expression of type II collagen as detected by indirect immunofluorescence (Yellowley et al., 1997).

Fluid flow

A quartz slide with attached chondrocytes formed the bottom plate of the parallel plate flow chamber and a machine milled polycarbonate plate formed the top, as previously described (Yellowley et al., 1997). We generated fluid flow at 34 ml/min with a Harvard syringe pump (Harvard Apparatus, Natick, MA) that induced a shear stress of 37 dynes/cm^2. We chose a fluid flow rate of 34 ml/min because we previously showed that this produces a $Ca^{2+}{}_i$ response in more than 70% of BAC in a field of view (Yellowley et al., 1997).

Ca^{2+} imaging

Preconfluent cells were washed with Tyrode's solution at 37°C, which contained (in mM) 140 NaCl, 4 KCl, 1 $MgCl_2$, 2 $CaCl_2$, 5 N-2-hydroxyethylpiperazine-N′-2-ethanesulphonic acid, and 10 glucose, and titrated to a final pH of 7.4 with 4 mM NaOH. Cells were then incubated with 1 μM fura-2-acetoxymethyl ester (fura-2; Molecular Probes, Eugene, OR) solution for 30 min at 37°C. The cells were then washed with fresh Tyrode's solution at 37°C, and the slide was mounted on a parallel plate flow chamber. The chamber was placed on an inverted fluorescence microscope (Nikon Diaphot 300) and left undisturbed for 30 min. The cells were illuminated as previously described (Yellowley et al., 1997). A Metafluor imaging system (Universal Imaging, West Chester, PA) was used to sample and record the emitted light from the cells in the field of view once every 2.5 sec, and Metafluor imaging software was used to subtract the background fluorescence from each image and to outline and calculate the 340:380 ratio for each cell in the field of view, which directly reflects $[Ca^{2+}]_i$. A calibration curve was constructed by acquiring 340:380 values (background subtracted) for a series of solutions of known free Ca^{2+} concentration (0–39.8 μM; Molecular Probes) and 1 μM fura-2 pentapotassium salt (Molecular Probes). This calibration curve was used to convert ratio values from individual cells into $[Ca^{2+}]_i$.

Pharmacological agents

Different pharmacological agents were used to assess the contribution of intracellular stores to the fluid-flow-induced $Ca^{2+}{}_i$ response in BAC. Agents included (1) thapsigargin (50 nM), which inhibits the ATP-dependent Ca^{2+} pump of intracellular stores and causes Ca^{2+} discharge (Thastrup et al., 1990); (2) caffeine (10 mM), which enhances the activity of the ryanodine receptor on intracellular Ca^{2+} stores and potentiates Ca^{2+} release (Tsien and Tsien, 1990; Zacchetti et al., 1991); (3) ryanodine, which at high concentration (>10 μM) blocks Ca^{2+} release from intracellular calcium stores and at low concentration (<10 μM) activates Ca^{2+} release by its action on the ryanodine-sensitive Ca^{2+} release channel (Fill and Coronado, 1988; Tsien and Tsien, 1990); and (4) neomycin (10 mM), which blocks the hydrolysis of phosphatidylinositol 4,5-bisphosphate (PIP_2) to inositol 1,4,5-trisphosphate (IP_3) and diacylglycerol (DAG) and thus Ca^{2+} release from IP_3-sensitive stores by its action on phospholipase C (PLC). Thapsigargin or caffeine were perfused over the cells in the flow chamber for 2 min at a flow rate of 1 ml/min (which did not elicit calcium responses in BAC) followed by a period of no flow for 2 min. Fluid flow was then applied at 34 ml/min for 3 min. Neomycin was applied to the cells for 30 min prior to fluid flow. Ryanodine was applied at both 1 μM and 20 μM to

cells for 30 min prior to fluid flow. All of these drugs were also present at their respective concentrations in the fluid flowing past the cells. PTX (Calbiochem, San Diego, CA) was used to assess the role of G-proteins in the Ca^{2+} response to fluid flow in BAC. Cells were exposed to 0.5 μg/ml PTX in media for 24 h prior to exposure to fluid flow.

Suramin was used to assess the contribution of ATP to the fluid-flow-induced $Ca^{2+}{}_i$ response in BAC. Suramin (100 μM), which is a P2 purinergic blocker, was applied to the cells for 30 min prior to fluid flow or ATP challenge.

Data analysis

To identify Ca^{2+} transients, we used an adapted numerical procedure from mechanical fatigue analysis, known as Rainflow Cycle Counting (Downing and Socie, 1982). This simple algorithm reliably and automatically identifies and determines the amplitudes of spikes and transients in time history data even when superimposed over each other or in the presence of background noise that otherwise might make amplitude determination challenging. We previously used this algorithm to identify transients in $[Ca^{2+}]_i$ in bone cells (Jacobs et al., 1998).

We defined a response as a transient in $[Ca^{2+}]_i$ of 20 nM or greater. Data were collected for 1 min at the start of each experiment in the absence of flow and then for a period of 3 min in the presence of flow at 34 ml/min. Data are expressed as mean ± S.E.M. To compare observations from different groups with unequal sample size, a two-sample Student's *t*-test was used in which sample variance was not assumed to be equal. To compare observations from more than two groups, a one-way analysis of variance was used followed by a Student-Newman-Keuls multiple comparisons post hoc test (Instat, GraphPad Software Inc., San Diego, CA). $P < 0.05$ was considered statistically significant.

RESULTS

Role of intracellular calcium stores in the cellular response to fluid flow

We previously demonstrated that fluid flow induces $[Ca^{2+}]_i$ transients in BAC (Yellowley et al., 1997). The following experiments were performed to assess the contribution of release of Ca^{2+} from intracellular stores to the fluid-flow-induced intracellular Ca^{2+} response in BAC. Figure 1 shows the effect of different pharmacological blockers on the $Ca^{2+}{}_i$ response to a steady flow rate of 34 ml/min; 6.7 ± 1.2% of cells mounted on the flow chamber but subjected to no flow for 3 min (no-flow control) showed spontaneous, transient increases in $[Ca^{2+}]_i$; 51.4 ± 5.6% of cells showed a $Ca^{2+}{}_i$ response to a flow rate of 34 ml/min in the absence of blockers (flow control). In the presence of 50 nM thapsigargin and 10 mM neomycin, the percentage of cells responding to a flow rate of 34 ml/min was significantly decreased relative to the flow control, to 8.0 ± 2.8% and 6.4 ± 4.0%, respectively. In the presence of ryanodine, 1 μM and 20 μM, and 10 mM caffeine, the percentage of cells responding was 34.1 ± 2.6%, 56.9 ± 6.1%, and 44.7 ± 2.6%, respectively, none of which were significantly different from the flow control. Figure 1B shows the mean intracellular Ca^{2+} amplitude of those cells responding during fluid flow in the presence and absence

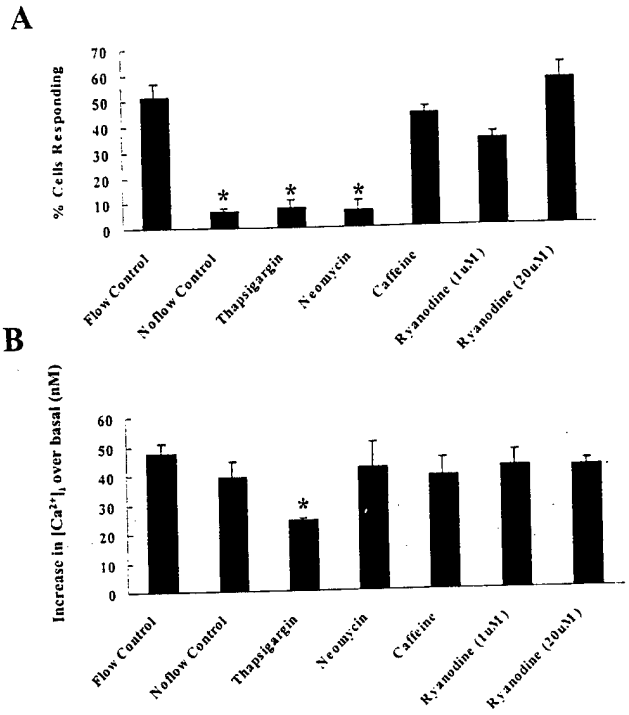

Fig. 1. Effect of intracellular Ca^{2+} store modulators on the $Ca^{2+}{}_i$ response to flow in bovine articular chondrocytes. **A:** Mean percentage of cells showing a spontaneous Ca^{2+} transient in the absence of flow (no-flow control), a response to a flow rate of 34 ml/min in normal saline (flow control), and the presence of 50 nM thapsigargin, 10 mM neomycin, 10 mM caffeine, 1 μM and 20 μM ryanodine. Each bar represents the mean ± S.E.M., and each experiment was repeated on 9, 12, 4, 4, 4, 3 and 3 plates, respectively. **B:** Mean increase in $[Ca^{2+}]_i$ in cells showing spontaneous transients (no-flow control) and response during fluid flow (34 ml/min) in normal saline (flow control) and in the presence of thapsigargin, neomycin, caffeine, and ryanodine. Each bar represents the mean ± S.E.M., and each experiment was repeated on 9, 12, 4, 4, 4, 3, and 3 plates, respectively. $^*P < 0.05$ versus flow control.

of intracellular store blockers. There was no significant difference between experimental groups with respect to mean intracellular Ca^{2+} response amplitudes, with the exception of thapsigargin, which reduced the mean amplitude to 24.1 ± 0.8 nM compared with the flow control, 47.69 ± 3.3 nM. It should be noted that the $[Ca^{2+}]_i$ amplitudes recorded in the presence of thapsigargin or neomycin reflect the amplitudes of spontaneous increases in $[Ca^{2+}]_i$ because, in the presence of these two agents, flow did not increase the percentage of cells responding over no-flow controls.

Role of G-proteins in the cellular response to fluid flow

Experiments were performed to assess the role of G-proteins in the fluid-flow-induced intracellular Ca^{2+} response in BAC. Cells were exposed to 0.5 μg PTX for 24 h prior to fluid flow. Exposure to PTX significantly decreased the percentage of cells responding to fluid flow from 67.47 ± 8.39% to 29.20 ± 8.54% (Fig. 2A). PTX exposure also decreased the mean increase in $[Ca^{2+}]_i$ in those cells responding during fluid flow, from 55.01 ± 4.27 nM to 37.72 ± 2.83 nM (Fig. 2B).

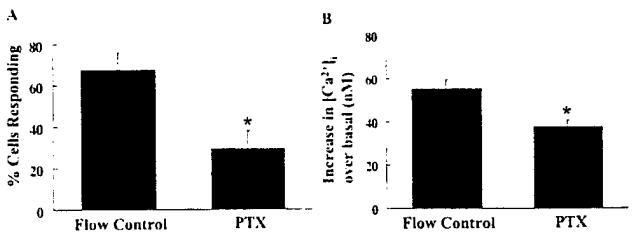

Fig. 2. **A:** Effects of pertussis toxin (PTX) on the $Ca^{2+}{}_i$ response to fluid flow in bovine articular chondrocytes. Mean percentage of cells showing a $Ca^{2+}{}_i$ response to a flow rate of 34 ml/min with and without prior exposure to 0.5 μg PTX for 24 h. Each bar represents the mean ± S.E.M., and each experiment was repeated on at least four separate slides. **B:** Mean increase in $[Ca^{2+}]_i$ in cells responding during fluid flow (34 ml/min) with and without prior exposure to 0.5 μg PTX for 24 h. Each bar represents the mean ± S.E.M., and each experiment was repeated on at least four separate slides. $^*P < 0.05$ versus flow control.

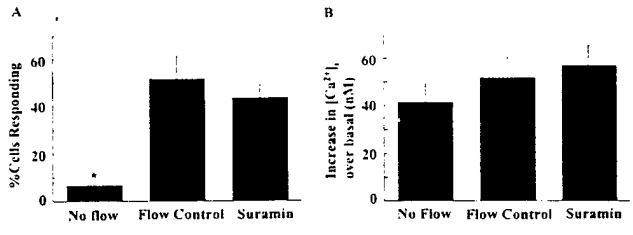

Fig. 3. **A:** Effects of suramin on the $Ca^{2+}{}_i$ response to fluid flow. Mean% of cells showing a spontaneous Ca^{2+} transient in the absence of flow (no-flow), a response to a flow rate of 34 ml/min in normal saline (flow control), and the $Ca^{2+}{}_i$ response to a flow rate of 34 ml/min with prior exposure to 100 μM suramin for 30 min. Each bar represents the mean ± S.E.M., and each experiment was repeated on at least three separate slides. **B:** Mean increase in $[Ca^{2+}]_i$ in cells showing spontaneous transients (no-flow) and response during fluid flow (34 ml/min) with and without prior exposure to 100 μM suramin for 30 min. Each bar represents the mean ± S.E.M., and each experiment was repeated on at least three separate slides. $^*P < 0.05$ versus flow control.

Role of ATP in the cellular response to fluid flow

Experiments were performed to assess the contribution of ATP to the fluid-flow-induced intracellular Ca^{2+} response. Figure 3 shows the effect of exposing cells to 100 μM suramin, a P2 purinergic blocker, for 30 min prior to fluid flow. In the presence of suramin, 43.45 ± 5.61% of cells exhibited a $Ca^{2+}{}_i$ response that was not significantly different from that of the control, 51.67 ± 9.61%; 6.60 ± 1.09% of cells showed spontaneous $[Ca^{2+}]_i$ transients in the absence of fluid flow (Fig. 3A). The mean increase in $[Ca^{2+}]_i$ in cells responding during fluid flow in the presence of suramin was 56.95 ± 8.73 nM, which was not significantly different from that of either the control, 51.85 ± 8.45 nM, or spontaneous, 41.39 ± 7.89 nM, calcium transients (Fig. 3B).

Experiments were performed to determine whether suramin was acting as an effective P2 purinergic blocker in BAC. BAC were grown on 1.25-cm-diameter glass coverslips and mounted in an open experimental bath. Figure 4A shows the effect of introducing Na-ATP to a final concentration of 100 μM to the experimental bath; 99.44 ± 0.27% of cells responded to an ATP challenge, with a mean $[Ca^{2+}]_i$ response amplitude of 323.54 ± 62.88 nM (Fig. 4C,D). Exposure of cells to 100 μM suramin for 30 min prior to ATP challenge (Fig. 4B) significantly decreased the percentage of cells responding to 4.98 ± 2.48% and the mean amplitude of responding cells to 42.52 ± 2.57 nM (Fig. 4C,D).

DISCUSSION

As expected, our experiments showed that fluid flow increases $[Ca^{2+}]_i$ in BAC. The mean $[Ca^{2+}]_i$ response amplitude to fluid flow was less than that seen in endothelial cells (Geiger et al., 1992) but similar to the responses of other cells of the musculoskeletal system such as osteoblasts (Hung et al., 1995). We also found that the $Ca^{2+}{}_i$ response to fluid flow was modest when compared with the $Ca^{2+}{}_i$ response to ATP challenge. However, this most likely reflects the magnitude of the applied stimulus because the $Ca^{2+}{}_i$ response amplitude to ATP in chondrocytes has been show to be concentration dependent (Kaplan et al., 1996; Koolpe and Benton, 1997). Similarly, rabbit chondrocytes poked with a micropipette, which subjects cells to a significantly different type of mechanical stimulus, especially in terms of magnitude of the stimulus, results in $[Ca^{2-}]_i$ responses of almost 2,000 nM (Grandolfo et al., 1998).

Many extracellular signals stimulate increases in $[Ca^{2+}]_i$, which are produced by an influx of Ca^{2+} across the cell membrane, release of Ca^{2+} from intracellular stores, or a combination of the two. Data from previous experiments strongly suggest that influx of extracellular Ca^{2+} plays a significant role in generating the intracellular Ca^{2+} response to fluid flow in BAC (Yellowley et al., 1997). However, the role of intracellular stores, in particular the involvement of IP_3, and ryanodine-sensitive stores is less clear.

Thapsigargin, which inhibits the ATP-dependent Ca^{2+} pump on intracellular stores and causes Ca^{2+} discharge, decreased the percentage of cells responding to flow, to levels similar to those of the no-flow controls. This suggests that Ca^{2+} mobilization from internal stores is required for the $Ca^{2+}{}_i$ response to flow in BAC. During a period of no flow, BAC displayed spontaneous and transient increases in $[Ca^{2+}]_i$. The percentage of cells displaying increases in $[Ca^{2+}]_i$ during fluid flow in the presence of neomycin or thapsigargin was not significantly different from that of the no-flow controls. This suggests that these increases in $[Ca^{2-}]_i$ were spontaneous and that the occurrence of spontaneous transients was not affected by neomycin or thapsigargin. However, thapsigargin did decrease the amplitude of the spontaneous transients. The finding that neither neomycin nor thapsigargin affected the occurrence of spontaneous transients but decreased the occurrence of flow-induced transients suggests that spontaneous $[Ca^{2+}]_i$ transients may occur through mechanisms different from those of flow-induced $[Ca^{2+}]_i$ transients.

Although our thapsigargin data suggest a role for intracellular store Ca^{2+} release in response to flow, they provide no information concerning the type of store involved. However, data from the present experiments involving the application of neomycin, which disrupts the inositol phospholipid pathway, suggest that IP_3 generation and subsequent mobilization of Ca^{2+} are required for the Ca^{2+} response to flow in BAC. However, neither ryanodine nor caffeine affected the

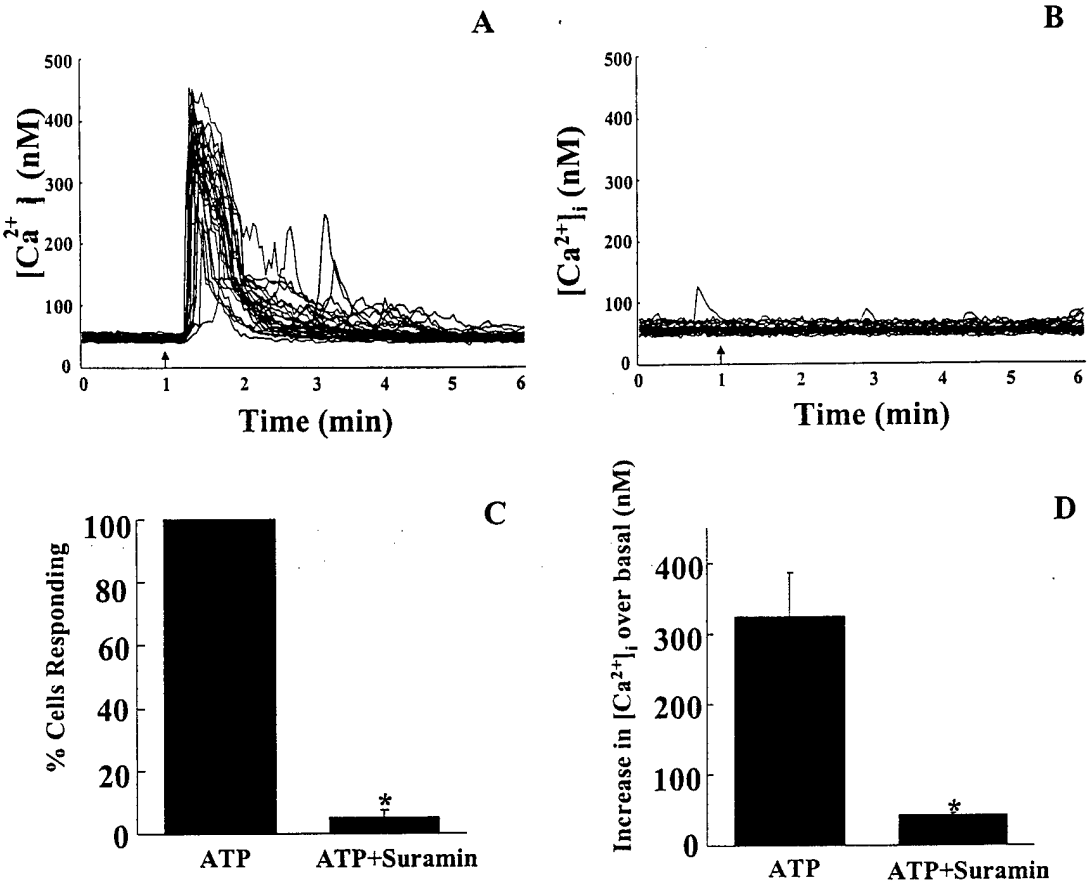

Fig. 4. **A:** Effect of 100 μM ATP applied externally on $[Ca^{2+}]_i$ in bovine articular chondrocytes (BAC). Each line represents the intracellular Ca^{2+} signal from a single cell. The arrow indicates the time of application of ATP. **B:** Effect of a 30-min exposure to 100 μM suramin on the $[Ca^{2+}]_i$ response to 100 μM ATP applied externally in BAC. The arrow indicates the time of application of ATP. **C:** Mean percentage of cells showing a $[Ca^{2+}]_i$ response to 100 μM ATP applied externally with and without prior exposure to 100 μM suramin. Each bar represents the mean ± S.E.M., and each experiment was repeated on at least three separate slides. **D:** Mean increase in $[Ca^{2+}]_i$ in cells responding to 100 μM ATP applied externally with and without prior exposure to 100 μM suramin. Each bar represents the mean ± S.E.M., and each experiment was repeated on at least three separate slides. *$P < 0.05$ versus control (ATP).

flow response, suggesting that ryanodine-sensitive Ca^{2+} store release was not involved. Although neomycin has been shown to have other cellular effects (e.g., in certain cells types, it blocks voltage-sensitive Ca^{2+} channels), our results are similar to those reported for both bone and endothelial cells. For instance, an increase in IP_3 levels in response to fluid flow has been demonstrated in rat calvarial osteoblasts (Reich and Frangos, 1991) and human and bovine endothelial cells (Nollert et al., 1990; Bhagyalakshmi et al., 1992; Prasad et al., 1993). In addition, neomycin has been shown to block the shear-stress-induced $[Ca^{2+}]_i$ response in rat calvarial osteoblasts (Hung et al., 1996). Taken together, although our data suggest that the fluid-flow-induced Ca^{2+} response involves both Ca^{2+} influx through membrane ion channels and intracellular Ca^{2+} release, the exact sequence of these events remains to be elucidated.

G-proteins are heterotrimeric GTP binding and hydrolyzing proteins that link a variety of cell-surface receptors to effector proteins such as membrane ion channels at the plasma membrane. In a variety of cell types, PLC, which catalyzes the hydrolysis of PIP_2 to produce IP_3, thus stimulating the release of Ca^{2+} from intracellular stores (Berridge, 1993), can also be activated by G-protein-linked receptors. PTX has been shown to block predominately the Gi/o family of G-proteins (Hepler and Gilman, 1992). In the present study, PTX significantly decreased the percentage of cells responding to fluid. Furthermore, fluid-flow-stimulated glycosaminoglycan synthesis, which may involve $Ca^{2+}{}_i$ mobilization, has also been shown to be sensitive to PTX in BAC (Das et al., 1997). Taken together, these data suggest that G-proteins of the Gi/o family are involved in the $Ca^{2+}{}_i$ response pathway. However, potential roles for Gs, Gq/G11, or the G12/13 families of G-proteins cannot be excluded.

Although the present experiments show that BAC are clearly responsive to fluid flow, the exact nature of the stimulus is unknown. For example, the cells may be responding to a purely mechanical signal, electrokinetic effects, a chemical factor present in the media, or even a combination of these three signals. Chemotransport effects, induced by fluid flow through the cartilage matrix replenishing the fluid environment around the chondrocytes, may be an important factor in the sensi-

tivity of chondrocytes to the flow environment. For example, the $Ca^{2+}{}_i$ response to flow in BAC has been shown to be augmented by addition of 2% fetal bovine serum to the perfusate (Hung et al., 1997). In addition, we have presented data consistent with the hypothesis that, in bone cells, the Ca^{2+} response to fluid flow is dependent on chemotransport effects (Jacobs et al., 1998). The agents involved in chemotransport are not known. However, in endothelial cells, it has been proposed that chemotransport of ATP released by the cells themselves mediates the $Ca^{2+}{}_i$ response to flow. For example, the ATP/ADPase, apyrase, which would be expected to break down extracellular ATP, inhibited a fluid-shear-induced $Ca^{2+}{}_i$ response in endothelial cells (Grierson and Meldolesi, 1995). Therefore, we postulated that chemotransport of ATP may be contributing to flow-induced $Ca^{2+}{}_i$ mobilization in BAC. However, suramin, a P2 purinergic blocker, had no effect on the $Ca^{2+}{}_i$ response to flow in BAC, suggesting that the response is not mediated by release of ATP by the cells. Although suramin can have a variety of effects on cells including inhibition of various types of ATPases, GTPase, DNA and RNA polymerases, reverse transcriptase, and inhibition of binding of certain growth factors to their receptors, we chose it for its reported ability to antagonize P_2-purinoceptor responses (Hoyle et al., 1990). Our data showed that it completely inhibited an ATP-induced $[Ca^{2+}]_i$ transient in BAC, suggesting that it was acting as an effective P_2-purinergic blocker in these experiments. The P_2 family of receptors was originally divided into two subtypes, P_{2X} and P_{2Y}, based on receptor affinity for a variety of ATP analogues (Burnstock and Kennedy, 1985). More recent evidence suggests the existence of a receptor that responds to ATP or UTP, named P_{2U} (Conigrave and Jiang, 1995). Although we have focused on the role of ATP in these studies, it is possible that our data using suramin also rule out a role for ATP analogues and UTP in the $Ca^{2+}{}_i$ response to fluid flow in BAC. Our results suggest that chemotransport of ATP is not involved in flow-induced $Ca^{2+}{}_i$ mobilization in BAC. However, we cannot exclude the possibility that chemotransport of other agents is involved.

In summary, our data suggest that the fluid-flow-induced $Ca^{2+}{}_i$ response in BAC involves both influx of external Ca^{2+} and release of internal Ca^{2+} from IP_3-sensitive stores and that the mechanism is G-protein activated. In addition, ATP release by chondrocytes does not appear to mediate the flow-induced $Ca^{2+}{}_i$ response.

ACKNOWLEDGMENTS

We thank Emmanuel Paul for technical assistance. This study was supported by grants from the NIH (RR 11769 to C.R.J., AG 15107 to H.J.D., 1 F32 AR 08514-01 to C.E.Y.), the Whitaker Foundation (C.R.J.), and the U.S. Army (C.R.J.).

LITERATURE CITED

Ando J, Ohtsuka A, Korenaga R, Kamiya A. 1991. Effect of extracellular ATP level on flow-induced Ca++ response in cultured vascular endothelial cells. Biochem Biophys Res Commun 179:1192–1199.

Behrens F, Kraft EL, Oegema TR Jr. 1989. Biochemical changes in articular cartilage after joint immobilization by casting or external fixation [Erratum. J Orthop Res 1990;8:627]. J Orthop Res 7:335–343.

Berridge MJ. 1993. Inositol trisphosphate and calcium signalling. Nature 361:315–325.

Bhagyalakshmi A, Berthiaume F, Reich KM, Frangos JA. 1992. Fluid shear stress stimulates membrane phospholipid metabolism in cultured human endothelial cells. J Vasc Res 29:443–449.

Burnstock G, Kennedy C. 1985. Is there a basis for distinguishing two types of P2-purinoceptor? Gen Pharmacol 16:433–440.

Caterson B, Lowther DA. 1978. Changes in the metabolism of the proteoglycans from sheep articular cartilage in response to mechanical stress. Biochim Biophys Acta 540:412–422.

Conigrave AD, Jiang L. 1995. Review: Ca(2+)-mobilizing receptors for ATP and UTP. Cell Calcium 17:111–119.

D'Andrea P, Vittur F. 1996. Ca^{2+} oscillations and intercellular Ca^{2+} waves in ATP-stimulated articular chondrocytes. J Bone Miner Res 11:946–954.

Das P, Schurman DJ, Smith RL. 1997. Nitric oxide and G proteins mediate the response of bovine articular chondrocytes to fluid-induced shear. J Orthop Res 15:87–93.

Downing SD, Socie DF. 1982. Simple rainflow counting algorithms. Int J Fatigue 4:31–40.

Fill M, Coronado R. 1988. Ryanodine receptor channel of sarcoplasmic reticulum. Trends Neurosci 11:453–457.

Frangos JA, McIntire LV, Eskin SG. 1988. Shear stress induced stimulation of mammalian cell metabolism. Biotechnol Bioeng 32: 1053–1060.

Geiger RV, Berk BC, Alexander RW, Nerem RM. 1992. Flow-induced calcium transients in single endothelial cells: spatial and temporal analysis. Am J Physiol 262(6 Pt 1):C1411–C1417.

Grandolfo M, Calabrese A, D'Andrea P. 1998. Mechanism of mechanically induced intercellular calcium waves in rabbit articular chondrocytes and in HIG-82 synovial cells. J Bone Miner Res 13:443–453.

Grierson JP, Meldolesi J. 1995. Shear stress-induced [Ca^{2+}]i transients and oscillations in mouse fibroblasts are mediated by endogenously released ATP. J Biol Chem 270:4451–4456.

Helmlinger G, Berk BC, Nerem RM. 1995. Calcium responses of endothelial cell monolayers subjected to pulsatile and steady laminar flow differ. Am J Physiol 269(2 Pt 1):C367–C375.

Hepler JR, Gilman AG. 1992. G proteins. Trends Biochem Sci 17:383–387.

Hoyle CH, Knight GE, Burnstock G. 1990. Suramin antagonizes responses to P2-purinoceptor agonists and purinergic nerve stimulation in the guinea-pig urinary bladder and taenia coli. Br J Pharmacol 99:617–621.

Hung CT, Pollack SR, Reilly TM, Brighton CT. 1995. Real-time calcium response of cultured bone cells to fluid flow. Clin Orthop 313:256–269.

Hung CT, Allen FD, Pollack SR, Brighton CT. 1996. Intracellular Ca^{2+} stores and extracellular Ca^{2+} are required in the real-time Ca^{2+} response of bone cells experiencing fluid flow. J Biomech 29:1411–1417.

Hung CT, Valhmu WB, Ratcliffe A, Mow VC, Allen FD. 1997. Articular chondrocyte calcium response to transient fluid-induced shear stress. Bioengineering Conference, ASME. June 11–15, Sun River, OR.

Jacobs CR, Yellowley CE, Davis BR, Zhou Z, Donahue HJ. 1998. Differential effect of steady versus oscillating flow on bone cells. J Biomech 31(11):969–976.

Jurvelin J, Kiviranta I, Saamanen AM, Tammi M, Helminen HJ. 1989. Partial restoration of immobilization-induced softening of canine articular cartilage after remobilization of the knee (stifle) joint. J Orthop Res 7:352–358.

Kaplan AD, Kilkenny DM, Hill DJ, Dixon SJ. 1996. Extracellular nucleotides act through P2U purinoceptors to elevate [Ca^{2+}]i and enhance basic fibroblast growth factor-induced proliferation in sheep chondrocytes. Endocrinology 137:4757–4766.

Koolpe M, Benton HP. 1997. Calcium-mobilizing purine receptors on the surface of mammalian articular chondrocytes. J Orthop Res 15:204–212.

Milner P, Bodin P, Loesch A, Burnstock G. 1990. Rapid release of endothelin and ATP from isolated aortic endothelial cells exposed to increased flow. Biochem Biophys Res Commun 170:649–656.

Mohtai M, Gupta MK, Donlon B, Ellison B, Cooke J, Gibbons G, Schurman DJ, Smith RL. 1996. Expression of interleukin-6 in osteoarthritic chondrocytes and effects of fluid-induced shear on this expression in normal human chondrocytes in vitro. J Orthop Res 14:67–73.

Mow VC, Bachrach NM, Setton LA, Guilak F. 1994. Stress, strain pressure and flow fields in articular cartilage and chondrocytes. In:

Mow VC, Guilak F, Tran-Son-Tay R, Hochmuth RM. Cell mechanics and cellular engineering. New York: Springer-Verlag. p 345–379.
Nollert MU, Eskin SG, McIntire LV. 1990. Shear stress increases inositol trisphosphate levels in human endothelial cells. Biochem Biophys Res Commun 170:281–287.
Prasad AR, Logan SA, Nerem RM, Schwartz CJ, Sprague EA. 1993. Flow-related responses of intracellular inositol phosphate levels in cultured aortic endothelial cells. Circ Res 72:827–836.
Reich KM, Frangos JA. 1991. Effect of flow on prostaglandin E2 and inositol trisphosphate levels in osteoblasts. Am J Physiol Cell Physiol 261:C428–C432.
Reich KM, McAllister TN, Gudi S, Frangos JA. 1997. Activation of G proteins mediates flow-induced prostaglandin E2 production in osteoblasts. Endocrinology 138:1014–1018.
Smith RL, Donlon BS, Gupta MK, Mohtai M, Das P, Carter DR, Cooke J, Gibbons G, Hutchinson N, Schurman DJ. 1995. Effects of fluid-induced shear on articular chondrocyte morphology and metabolism in vitro. J Orthop Res 13:824–831.
Thastrup O, Cullen PJ, Drobak BK, Hanley MR, Dawson AP. 1990. Thapsigargin, a tumor promoter, discharges intracellular Ca^{2+} stores by specific inhibition of the endoplasmic reticulum Ca2(+)-ATPase. Proc Natl Acad Sci USA 87:2466–2470.
Tsien RW, Tsien RY. 1990. Calcium channels, stores, and oscillations. Annu Rev Cell Biol 6:715–760.
Yellowley CE, Jacobs CR, Li Z, Zhou Z, Donahue HJ. 1997. Effects of fluid flow on intracellular calcium in bovine articular chondrocytes. Am J Physiol Cell Physiol 273(1 Pt 1):C30–C36.
Zacchetti D, Clementi E, Fasolato C, Lorenzon P, Zottini M, Grohovaz F, Fumagalli G, Pozzan T, Meldolesi J. 1991. Intracellular Ca^{2+} pools in PC12 cells. A unique, rapidly exchanging pool is sensitive to both inositol 1, 4, 5-trisphosphate and caffeine-ryanodine. J Biol Chem 266:20152–20158.

Saunders, Marnie M (1)
Hershey Medical Center
Hershey, PA, 17033
(717) 531-6697 / Fax: (717) 531-7583 /
msaunder@ortho.hmc.psu.edu

Preferences and Keywords
Please consider for the NIRAs
Bone Mechanics;Bone Growth/Remodeling

ABSTRACT NO. _____
PAPER NO. _____
Check One: _ Clinical _ Biology _ Engineering
Disclosure

OSCILLATORY FLUID FLOW-INDUCED PROSTAGLANDIN E2 PRODUCTION IS DEPENDENT UPON GAP JUNCTIONAL INTERCELLULAR COMMUNICATION IN OSTEOBLASTIC MC3T3-E1 CELLS

+*Saunders, M M; *You, J; **Trosko, J; ***Yamasaki, H; *Donahue, H J; *Jacobs, C R
+*Musculoskeletal Research Laboratory, Department of Orthopaedics and Rehabilitation, Pennsylvania State University College of Medicine. Hershey Medical Center, Hershey, PA, 17033, (717) 531-6697, Fax: (717) 531-7583, msaunder@ortho.hmc.psu.edu

Introduction: Gap junctions are protein channels that physically link neighboring cells and allow the passage of small molecules and ions (<1kDa) by rapid diffusion, a process known as gap junctional intercellular communication (GJIC). Although gap junctions have been identified in bone, their function is unclear. It has been suggested that they may be involved in differentiation and extracellular signal responsiveness (1). In the latter scenario, it is possible that gap junctions sensitize cells and enable cell ensembles to respond to physical stimuli with a more robust response than that attained if the cells are not coupled. To investigate this, we subjected osteoblastic cells to physiologic levels of oscillatory fluid flow and quantified prostaglandin E_2 (PGE_2) production and intracellular calcium concentration ($[Ca^{2+}]_i$). To correlate these findings with the role of GJIC, we utilized osteoblastic MC3T3-E1 (MC) cells; MC cells expressing a dominant negative Cx43 (DN-8), the predominant gap junction protein in bone, and control transfectants (DN-VC).

Methods: Cultures: MC cells were maintained in MEM-α supplemented with 10% fetal bovine serum (FBS) and 1% penicillin/streptomycin. DN-VC and DN-8 cells were maintained in neomycin-supplemented MC media. Cell lines were maintained in culture for 24, 48 or 96hrs at 37°C and 5% CO_2. GJIC Quantification: Donor cells labeled for 30mins with 10M calcein AM and DiI were trypsinized, centrifuged, resuspended in media and dropped onto confluent monolayers of unlabeled acceptor cells for 90mins. If GJIC occurs, the calcein, which is gap junction permeant, transfers to neighboring cells which then fluoresce green while the DiI remains on the donor cell and is used as an identification marker. GJIC was quantified with fluorescent microscopy in the three cell lines at 24, 48 and 96hrs. PGE_2 Quantification: Plated cells were inverted on the parallel plate flow chamber and subjected to oscillatory fluid flow at 1Hz and a shear stress of 20 dyne/cm^2 for 1hr (2). Following flow, plates of cells were incubated in 10mL of fresh media for 1hr. The media was then collected and assayed. PGE_2 was normalized to total protein and quantified in the cell lines at 48 and 96hrs. $[Ca^{2+}]_i$ Imaging: Plated cells loaded with 10μM fura2-AM were inverted on a parallel plate flow chamber and subjected to oscillatory fluid flow at 1Hz and a shear stress of 20dyne/cm^2 for 3mins preceded by a 3min no flow baseline. Using fluorescent microscopy, images were captured with acquisition and analysis software and converted into ratios quantifying $[Ca^{2+}]_i$ in the three cell lines at 96hrs.

Results: GJIC Assays: GJIC was quantified at 24, 48 and 96hrs (Table 1). GJIC in MC and DN-VC cells was not dependent upon time in culture up to 96hrs and did not differ statistically from themselves or each other at the various timepoints. DN-8 cells at 96hrs exhibited a significant decrease in coupling in comparison to the MC and DN-VC cells ($p<0.001$), as well as in comparison to itself at 24 and 48hrs ($p<0.001$). The difference between 24 and 48hrs in the DN-8 cells was also significant ($p<0.05$).

	MC3T3-E1	DN-VC	DN-8
24 HRS	10.32 ± .46	10.69 ± .45	11.10 ± .42
48 HRS	10.08 ± .48	9.98 ± .62	9.85 ± .37
96 HRS	9.68 ± .60	9.78 ± .53	1.96 ± .53

Table 1. Results of GJIC assays at 96hrs. The numbers represent the number of neighboring cells (maximum of fifteen) in monolayer fluorescing green via GJIC. Cell counts are shown as mean±SEM with each number representative of at least 60 cells.

PGE_2 Assays: At 96hrs, oscillatory fluid flow induced a significant increase in PGE_2 production in both the MC ($p<0.0004$) and DN-VC ($p<0.0001$) cells (Figure 1). For the DN-8 cell line at 96hrs when these cells displayed reduced coupling, oscillatory fluid flow did not induce a PGE_2 response; however, basal levels of PGE_2 were elevated. Importantly, at 48hrs when these cells displayed GJIC equivalent to the other cell lines examined, DN-8 cells exhibited a significant increase in PGE_2 production ($p<0.0421$) which was not statistically different from the other lines at this timepoint (data not shown). $[Ca^{2+}]_i$ Imaging: Exposure to oscillatory fluid flow resulted in a significant increase in the percentage of cells displaying an increase in $[Ca^{2+}]_i$ in all cell lines examined (Figure 2). However, the percentage of cells responding to oscillatory fluid flow was similar in all three cell lines despite differences in GJIC.

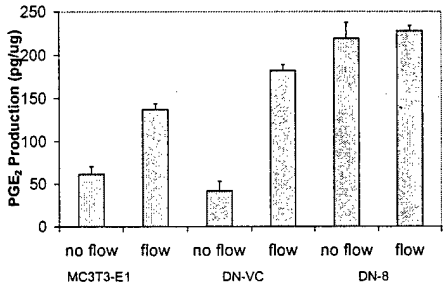

Figure 1. Results of PGE_2 quantification at 96hrs. The numbers represent oscillatory fluid flow-induced PGE_2 production normalized to total protein. The responses are shown as mean±SEM with each number representative of at least ten experiments.

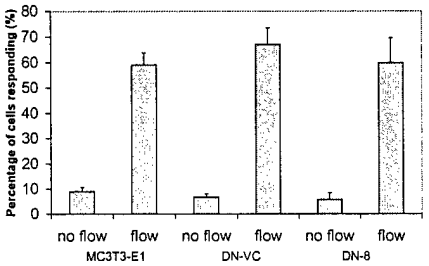

Figure 2. Results of $[Ca^{2+}]_i$ imaging at 96hrs. The numbers represent the percentage of cells responding to oscillatory fluid flow with an increase in $[Ca^{2+}]_i$. The responses are shown as mean±SEM with each number representative of at least six experiments.

Discussion: DN-8 cells displayed an 82.3% decrease in GJIC from 24 to 96hrs in culture demonstrating the power of this novel cell line. Osteoblastic cells with abundant GJIC (MC and DN-VC) displayed a robust $[Ca^{2+}]_i$ and PGE_2 response to fluid flow as did DN-8 cells at 48hrs when they also displayed abundant GJIC. However, at 96hrs when DN-8 cells displayed decreased GJIC, their PGE_2 response to oscillatory fluid flow was also decreased whereas the cytosolic Ca^{2+} response was intact. Thus, our results suggest that gap junctions contribute to the PGE_2 but not the Ca^{2+} response to oscillatory fluid flow. These findings implicate gap junctions in bone cell ensemble responsiveness to oscillatory fluid flow and suggest that gap junctions and GJIC play a pivotal role in mechanotransduction mechanisms in bone.

References: (1)Donahue HJ, 2000 Bone (2)Jacobs CR, 1998 J Biomechanics.
Acknowledgments: Zhiyi Zhou, MD for cell culture maintenance. This work was supported by Army grant DAMD17-98-1-8509, NIH AG15107, AR45989 and the Whitaker Foundation.
**Michigan State University, Department of Pediatrics and Human Development, College of Human Development, East Lansing, MI 48824.
***Kwansei Gakuin University, Uegahava, Nishinomiya, Japan.

Donahue, Seth W. (1)
P.O. Box 850
500 University Dr.
Hershey, PA 17033-0850
717-531-4819 / Fax: 717-531-7583 /
sdonahue@ortho.hmc.psu.edu

Preferences and Keywords
Please consider for the NIRAs
Bone Mechanics;Mechanotransduction;Bone Cell;Bone Adaptation;Osteoporosis

ABSTRACT NO. _____
PAPER NO. _____
Check One: _ Clinical _ Biology _ Engineering
Disclosure
(A-NIH RO1AR45989, U. S. Army DAMD17-98-1-8509) (A-NIH R01AG13087)

MECHANOSENSITIVITY OF RAT OSTEOBLASTIC CELLS IS A FUNCTION OF AGE, LOADING FREQUENCY, AND SHEAR STRESS

+*Donahue, S W.; *Jacobs, C R. (A-NIH RO1AR45989, U. S. Army DAMD17-98-1-8509); *Donahue, H J. (A-NIH R01AG13087)
+*Musculoskeletal Research Laboratory, Dept. of Orthopaedics and Rehabilitation, Pennsylvania State University, Hershey, Pennsylvania. P.O. Box 850, 500 University Dr. , Hershey, PA 17033-0850, 717-531-4819, Fax: 717-531-7583, sdonahue@ortho.hmc.psu.edu

Introduction

Mechanical loading influences bone cell metabolism and bone structure. For example, four-point bending increases bone formation in rat long bones.[1] It has been demonstrated that this adaptation is dependent on the frequency and magnitude of loading,[2] and that the capacity for adaptation to mechanical loading declines with age.[3] The mechanotransduction signaling pathways which mediate bone adaptation to mechanical loading, and how they change with age, are unknown. However, several studies have demonstrated that mechanical signals induce cytosolic calcium oscillations in bone cells.[4] Therefore, we hypothesized that calcium oscillations in osteoblastic cells isolated from rat long bones would be dependent on loading frequency, shear stress, and the age of the rat from which the cells were isolated.

Methods

Bone Cells Subperiosteal osteoblastic cells were isolated from the humeri, tibiae, and femora of young (4 mos., n = 7), mature (12 mos., n = 6), and old (24 mos., n = 7) male Fisher 344 rats. All soft tissues were stripped from the bones and cells were isolated by sequential collagenase digestions at 37°C. Cells from the second digestion were collected by centrifugation and grown to confluency in DMEM, 20% FBS, and 1% penicillin/streptomycin. Cells isolated by this technique display osteoblastic characteristics.[5] Cells were plated on quartz microscope slides at concentrations that reached 70% confluency on the day of experimentation. Cells were incubated at 37°C with 10 µL (µM) Fura-2 AM for 30 minutes prior to mechanical stimulation.

Fluid Flow System The slides were mounted in a parallel plate flow chamber. A materials testing machine was used to pump a syringe, in series with rigid wall tubing and a flow meter, to drive oscillating fluid flow through the chamber. The flow media consisted of DMEM and 2% FBS. Cells were exposed to 3 minutes of oscillating fluid flow that produced shear stresses of 1 or 2 Pa at frequencies of 0.2, 1, or 2 Hz. Six slides of cells from each rat were randomly assigned to one of the six shear stress/frequency combinations.

Calcium Imaging The flow chamber was mounted on the stage of a fluorescent microscope. Images of the fluorescence intensity were collected for a 3-minute no flow period and 3 minutes of oscillating flow. Image analysis software (Metaflour, West Chester, PA) was used to determine real-time intracellular calcium concentrations ($[Ca^{2+}]_i$) using ratiometric dye methodology. $[Ca^{2+}]_i$ was determined for 25-35 individual cells for each slide.

Statistics A factorial ANOVA was used to assess the influence of age, loading frequency, and shear stress on the percentage of cells responding to fluid flow with a calcium oscillation greater than 50 nM.

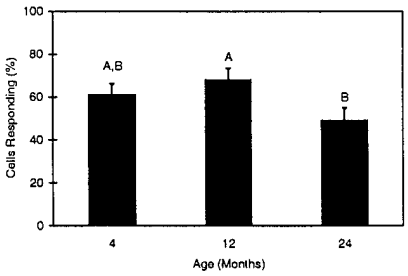

Figure 1: Influence of age on the % of cells responding to oscillating fluid flow. Means with standard error bars (n = 42 for 4 and 24 mos., n = 36 for 12 mos.). Groups with the same letter are not significantly different (p < 0.05).

Results

Resting $[Ca^{2+}]_i$ were 20-50 nM. Spontaneous calcium oscillations ocurred in cells from young (9%), mature (8%), and old (2%) rats during the no flow period. Significantly ($p < 0.0001$) more cells displayed calcium oscillations during fluid flow. Age ($p = 0.043$), loading frequency ($p = 0.0001$), and shear stress ($p = 0.038$) significantly influenced the number of cells responding to fluid flow. Mature cells were more responsive than old cells (Figure 1). Cells were more responsive to 0.2 Hz than to 1 or 2 Hz (Figure 2). Cells were more responsive to 2 Pa than 1 Pa (Figure 3).

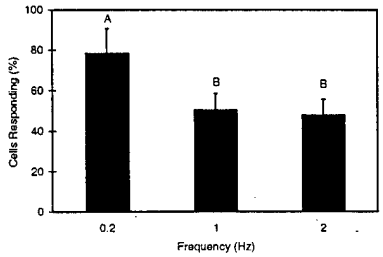

Figure 2: Influence of loading frequency on the % of cells responding to oscillating fluid flow. Means with standard error bars (n = 40 slides for each group). Groups with the same letter are not significantly different (p < 0.05).

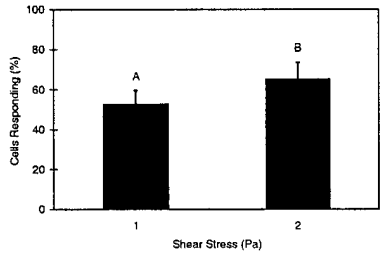

Figure 3: Influence of shear stress on the % of cells responding to oscillating fluid flow. Means with standard error bars (n = 60 slides for each group). Groups with the same letter are not significantly different (p < 0.05).

Discussion

Bones adapt to mechanical loading in a frequency and magnitude dependent fashion. However, their ability to adapt is compromised with age. We found that calcium signaling in an ensemble of osteoblastic cells was dependent on the frequency and magnitude of fluid flow induced shear stress. This suggests that intracellular calcium signaling is an important component of mechanotransduction in bone. The magnitude and frequency of mechanical loading may be encoded in the calcium signaling response, which may influence down stream signaling events. We also showed that the mechanosensitivity of an ensemble of bone cells declines in old age. Bone adaptation to increased mechanical loading is likely to be mediated by a complex molecular signaling cascade, which ultimately leads to gene expression, matrix production, and new bone formation. $[Ca^{2+}]_i$ oscillations are believed to be an important and early response to mechanical loading. $[Ca^{2+}]_i$ oscillations are required for fluid flow induced upregulation of osteopntin mRNA expression in MC3T3 osteoblastic cells.[6] The decreased mechanoresponsiveness of bone cells from old rats may partially explain why adaptation to mechanical loading is impaired in old rats. Understanding mechanotransduction pathways in bone cells, and how they are influenced by age and mechanical loading parameters, may help elucidate the etiologies of senile and disuse osteopenias.

References

1. Turner, C. H. et al. *J. Bone Miner Res* 9:87-97; 1994. **2.** Turner, C. H., and Forwood, M. R.. In: A. Odgard and H. Weinans. Eds. *Bone Structure and Remodeling*; 65-77,1995. **3.** Turner, C. H. et al. *J. Bone Miner Res* 10:1544-9; 1995. **4.** Jacobs, C. R. et al. *J Biomech* 31:969-976, 1998. **5.** Donahue, H. J. et al. *J Bone & Mineral Research* 10:81-9, 1995. **6.** You, J. et al. *Trans Ortho Res Soc* 46: 291, 2000.

OSCILLATORY FLOW-INDUCED PROSTAGLANDIN E2 RELEASE INVOLVES PROTEIN KINASE A AND CYCLOOXYGENASE-2 IN MC3T3-E1 OSTEOBLASTS

J. You, M.M. Saunders, C.E. Yellowley, H.J. Donahue, and C.R. Jacobs

Musculoskeletal Research Laboratory, Department of Orthopaedics and Rehabilitation
The Pennsylvania State University College of Medicine, Hershey, PA 17033, U.S.A.

External mechanical loading of bone results in a variety of biophysical signals that may affect cellular metabolism and gene expression. Recently one of these physical signals, lacunar-canalicular fluid flow, has been shown to induce a variety of physiological responses linked to bone maintenance, including increased paracrine factor release and gene transcription *in vitro*. For instance, prostaglandin E_2 (PGE_2), an anabolic agent *in vivo* that stimulates bone formation, was induced by steady and pulsating fluid flow in bone cells via a mechanism involving intracellular calcium ($[Ca^{2+}]_i$) signaling. However, the mechanotransduction pathways of flow-induced PGE_2 production in bone cells is still unclear, in particular for oscillatory flow, which occurs physiologically. Moreover the roles of $[Ca^{2+}]_i$ and cyclooxygenase-2 (Cox-2), an important enzyme for PGE_2 production, in flow-induced PGE_2 production are uncertain. Therefore, the goals of this study were to investigate the effects of oscillatory flow on the synthesis of PGE_2 and Cox-2 mRNA level, and to elucidate the oscillatory flow-induced PGE_2 signal pathways in bone cells. We employed a parallel plate flow chamber and a servopneumatic loading frame to apply the desired sinusoidally oscillating flow. $[Ca^{2+}]_i$ was monitored for 3 minutes after onset of flow. PGE_2 and Cox-2 mRNA level were measured after one hour oscillatory flow and a one hour post-incubation period. Our results show that oscillating flow induced an increase in $[Ca^{2+}]_i$ in 59% of cells which was significantly different from no flow period (9%), and doubled the production of PGE_2, while elevating Cox-2 mRNA levels by 410% compared with the no flow period. Suramin, an anti-neoplastic agent that uncouples G-proteins from receptors, totally abolished both the flow-induced $[Ca^{2+}]_i$ and PGE_2 production, suggesting a role for G-protein coupled membrane receptors in the mechanotransduction pathway. Protein kinase A inhibitor 14-22 Amide, a highly specific inhibitor of cAMP-dependent protein kinase, had effects on both PGE_2 production and Cox-2 mRNA levels, inhibiting about 84% of the flow induced PGE_2 production and lowering flow-induced Cox-2 mRNA levels by 73%. These results suggested a signal transduction pathway involving cAMP and indicated that protein kinase A may exert effects on PGE_2 production at the expression level. The Cox-2 enzyme inhibitor NS-398 blocked the flow-induced PGE_2 response and lowered the base level of PGE_2 production by about 502%, suggesting Cox-2 is critical for oscillatory flow-induced PGE_2 production. In contrast, thapsigargin, an inhibitor of the ATP-dependent Ca^{2+} pump of intracellular stores which causes Ca^{2+} discharge, completely blocked the intracellular calcium in response to oscillating flow, but only had moderate effects on both PGE_2 production and Cox-2 mRNA levels, suggesting a partial requirement for intracellular calcium release or possibly the existence of a non-calcium dependent PGE_2 stimulatory pathway. In summary, oscillating flow increased $[Ca^{2+}]_i$ and Cox-2 dependent PGE_2 production in osteoblastic cells. Furthermore, our data indicate that the PGE_2 release involves cAMP and protein kinase A, and may be influenced by $[Ca^{2+}]_i$. Finally our data also suggest that activation of G-protein coupled membrane receptors may be the common first step in the mechanotransduction pathway.

ACKNOWLEDGMENTS

This work was supported by NIH AR45989, AG13087, the Whitaker Foundation, and The US Army Medical Research and Materiel Command award number DAMD 17-98-1-8509.

ANALYSIS OF THE GLYCOCALYX OF TWO BONE CELLS TYPES, IN VITRO, IN ORDER TO INVESTIGATE FLUID FLOW EFFECTS

Gwendolen C. Reilly, Clare E. Yellowley, Henry J. Donahue and Christopher R. Jacobs

Musculoskeletal Research Laboratory, Penn State College of Medicine, Hershey, Pennsylvania 17033, USA.

Bone adapts to mechanical loading and the likely candidates for transduction of a mechanical signal into a cellular response are bone cells, particularly osteocytes. Experiments have shown that physiological strains do not induce responses in bone cells when applied directly. However fluid flow, which would be induced by loading *in vivo*, does produce responses such as intracellular calcium signals when applied to bone cells *in vitro* (You et al. 2000. J. Biomechanical engineering, In Press). The theoretical shear stresses assumed to be experienced by osteocytes *in vivo* have been calculated assuming the bone cells have a proteoglycan rich cell coat (glycocalyx). However, there is no evidence that there is a glycocalyx around bone cells cultured *in vitro* or around osteocytes *in vivo*, though there is some evidence that proteoglycans are present in the space between the osteocyte membrane and the bone matrix. Our long term goal is to investigate the role of the glycocalyx in the response of bone cells *in vitro* to fluid flow. Therefore, the purpose of this study was to characterize the glycocalyx of cultured bone cells using lectin binding and alcian blue staining experiments. The osteoblastic cell line MC3T3-E1 and the osteocytic cell line MLO-Y4 (kindly supplied by Dr. L. Bonewald, University of Texas Health Science Center) were cultured on slides and fixed in 3.7% formaldehyde, once they had grown to about 80% confluence. The binding ability of three fluorescently labeled lectins was investigated : 1) Concanavalin agglutinin (ConA), which binds to Glucose and Mannose, found in hyaluronic acid 2) Vicia Villosa agglutinin (VVA) which binds to N-acetyl-D-galactosamine (GalNac), found in chondroitin sulphate and 3) Wheat Germ agglutinin (WGA) which binds to N-acetyl-D-glucosamine (GlcNac) and N-acaetyl neraminic acid (NeuNac) found in hyaluronic acid and heparin sulphate. Either 50 μg/ml of lectin alone or lectin which had been incubated for 2 hrs with an inhibiting sugar (Glucose, GalNac and GlcNac respectively) was applied to the cells for 1 hr. Alcian blue was dissolved in sodium acetate buffer with two different concentrations of magnesium chloride. At low concentrations of $MgCl_2$ alcian blue should stain all proteoglycans (due to their weak negative charge), but at high concentrations (>0.2M) it stains only highly negatively charged proteoglycans such as the sulphated proteoglycans. Alcian blue was applied to the slides overnight. MC3T3-E1 cells and MLO-Y4 cells exhibited the same staining patterns, indicating that osteoblasts and osteocytes may synthesis a similar type of glycocalyx. Lectin binding was greatest with ConA and weakest with VVA all binding was reduced by the addition of the inhibiting sugar, greatest inhibition was seen with WGA. Alcian Blue stained very well at the low concentration of $MgCl_2$, but not at all at the high concentration. Taken together these results show that bone cells have a glycocalyx rich in Glucose and GlcNac, probably containing hyaluronic acid and with little if any sulphated proteoglycans present. Although this contradicts data showing sulphated proteoglycans around osteocytes in bone, it agrees with the hypothesized model of an endothelial-like glycocalyx consisting of long hyaluronic acid chains. This information can be used to manipulate the bone cell glycocalyx for fluid flow studies in order to better understand the role of fluid flow in bone cell mechanotransduction. This work was supported by NIH grants AR45989 and AG13087, US Army Medical Research and Material Command award no.DAMD17-98-1-8509 and the Whitaker Foundation

FIGURES: 1: Light microscope image of staining of the glycocalyx of MLO-Y4 cells with alcian blue at 0.1M $MgCl_2$ (A) and the absence of staining at 0.5 M $MgCl_2$ (B). **2**: Fluorescent microscope image of MC3T3-E1 cells after application of FITC labeled ConA lectin (A) and the reduced binding when the inhibiting sugar was present (B) (field of view 1mm wide).

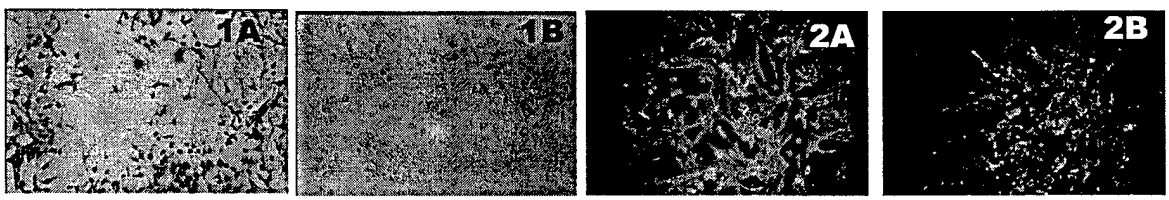

You, Jun (1)
Mail Code H089
P.O. Box 850
Hershey, PA 17033
717-531-4819 / Fax: 717-531-7583 /
jyou@ortho.hmc.psu.edu

Preferences and Keywords
Please consider for the NIRAs
Bone Growth/Remodeling;Prostaglandin E2;Cyclooxygenase-2;Mechanotransduction;Oscillatory Fluid Flow

ABSTRACT NO. _____
PAPER NO. _____
Check One: _ Clinical _ Biology _ Engineering
Disclosure
(A-NIH) (A-NIH) (A-NIH USArmy Whitaker)

OSCILLATORY FLOW STIMULATES PROSTAGLANDIN E2 RELEASE VIA PROTEIN KINASE A IN MC3T3-E1 OSTEOBLASTS INVOLVING CYCLOOXYGENASE-2

+*You, J; *Saunders, M M; *Yellowley, C E (A-NIH); *Donahue, H J (A-NIH); *Jacobs, C R (A-NIH USArmy Whitaker)
+*Musculoskeletal Research Laboratory , Dept. of Orthopaedics and Rehabilitation, Penn State University, Hershey, Pennsylvania. Mail Code H089, P.O. Box 850, Hershey, PA 17033, 717-531-4819, Fax: 717-531-7583, jyou@ortho.hmc.psu.edu

INTRODUCTION

Recently lacunar-canalicular fluid flow has been shown to induce a variety of physiological responses linked to bone maintenance, including increased paracrine factor release and gene transcription *in vitro* (1). For instance, prostaglandin E_2 (PGE_2), an anabolic agent *in vivo* that stimulates bone formation, was induced by steady and pulsating (2) fluid flow in bone cells via a mechanism involving intracellular calcium signaling. However, the mechanotransduction pathways of flow-induced PGE_2 production in bone cells is still unclear, in particular for oscillatory flow, which occurs physiologically. Moreover the role of cyclooxygenase-2 (Cox-2), an important enzyme for PGE_2 production, in flow-induced PGE_2 production is uncertain. Therefore, the first goal of this study was to investigate the effects of oscillatory flow on the synthesis of PGE_2 and Cox-2 mRNA level. The second goal of the study was to elucidate the oscillatory flow-induced PGE_2 signal pathways in bone cells.

METHODS

Cell culture and fluid flow chamber: The mouse osteoblastic cell line MC3T3-E1 was cultured in α-MEM containing 10% FBS and maintained in 5% CO_2 at 37°C. The fluid flow chamber employed in this study is a parallel plate design. A flow delivery device generated 1Hz sinusoidally oscillating flow (peak shear stress $2N/m^2$) (3). Medium PGE_2 measurement: Confluent cells cultured for 2 days on glass slides were exposed to oscillatory fluid flow (α-MEM, 2% FBS) for 1 hour in the flow chamber, then incubated for one hour in 10 ml fresh medium (α-MEM, 2% FBS). PGE_2 was then quantified using a nonradioactive enzyme immunoassay system (Amersham). PGE_2 levels were normalized to total protein. Cox-2 mRNA Analysis: Quantitative real-time RT-PCR was employed to quantify changes in steady-state Cox-2 mRNA levels. Cox-2 mRNA levels were measured after one hour oscillatory flow and one hour post-incubation. Pharmacological agents: The effects of fluid flow on PGE_2 production and Cox-2 mRNA levels were examined in the presence of the following pharmacological agents. Suramin (Sura.) is an anti-neoplastic agent that uncouples G-proteins from receptors presumably by blocking the interaction with intracellular receptor domains. Thapsigargin (Thap.) inhibits the ATP-dependent Ca^{2+} pump of intracellular stores and causes Ca^{2+} discharge. Protein Kinase A Inhibitor 14-22 Amide (PKAI) is a highly specific inhibitor of cAMP-dependent protein kinase (PKA). NS-398 (NS) is a selective inhibitor of Cox-2. Cells were exposed to these agents before (45 min), during and after the flow period.

RESULTS

Oscillating flow doubled the production of PGE_2, while elevating Cox-2 mRNA levels by 410% for the control case (no pharmacological agent present, figure 1). Suramin (100μM) totally abolished the flow-induced PGE_2 production. Protein kinase A inhibitor 14-22 Amide (1μM) had effects on both PGE_2 production and Cox-2 mRNA levels, inhibiting about 84% of the flow induced PGE_2 production and lowering flow-induced Cox-2 mRNA levels by 73%. The Cox-2 enzyme inhibitor NS-398 (20μM) blocked the flow-induced PGE_2 response and lowered the base level of PGE_2 production by about 502%. In contrast, thapsigargin (50nM) had only moderate effects on both PGE_2 production and Cox-2 mRNA levels, inhibiting by 26% and 29% respectively.

DISCUSSION

We have shown that oscillating flow increased PGE_2 production and Cox-2 mRNA levels in MC3T3-E1 osteoblastic cells. The NS-398 data suggest that Cox-2 is critical for oscillatory flow-induced PGE_2 production. Suramin completely abolished flow-induced PGE_2 production, suggesting a role for G-protein coupled membrane receptors in the mechanotransduction pathway. PKAI substantially inhibited PGE_2 production in response to oscillatory flow, suggesting a signal transduction pathway involving cAMP. PKAI also decreased Cox-2 mRNA levels indicating that protein kinase A may exert effects on PGE_2 production at the expression level. Previously, we have shown that thapsigargin completely blocks the intracellular calcium in response to oscillating flow (1). Thapsigargin moderately inhibited flow-induced PGE_2 production suggesting a partial requirement for intracellular calcium release or possibly the existence of a non-calcium dependent PGE_2 stimulatory pathway.

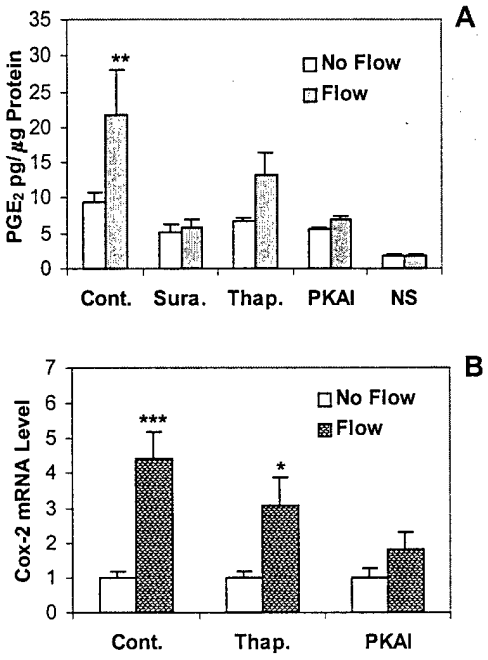

*Figure 1. The effects of different pharmacological agents on PGE_2 production (A) and Cox-2 mRNA levels (B) in response to oscillating flow. Control was no pharmacological agent present. All results represent the mean ± stand error of at least three independent experiments. A one-way ANOVA was used to examine differences between no flow and flow. *$p<0.05$, **$p<0.01$, ***$p<0.001$.*

In summary, oscillating flow induced Cox-2 dependent PGE_2 production in osteoblastic cells. Furthermore, our data indicate that the PGE_2 release involves cAMP and protein kinase A, and may be influenced by intracellular calcium. Finally our data also suggest that activation of G-protein coupled membrane receptors may be the common first step in the mechanotransduction pathway.

REFERENCES

1). You et al. (2000) Trans ORS 46:293; 2). Ajubi et al. (1999) *Am J Physiol* 276:E171-E178; 3). Jacobs et al. (1998) *J Biomech* 31:969-976.

ACKNOWLEDGMENTS

We thank Drs. Y. Zhang and Q. Chen for their assistance. This work was supported by NIH AR45989, AG13087, the Whitaker Foundation, and The US Army Medical Research and Materiel Command award number DAMD 17-98-1-8509.

Reilly, Gwendolen C (1)
Musculoskeletal Research Laboratory,
Department of Orthopaedics and Rehabilitation
MC H089, Penn State College of Medicine, 500 University Drive, Hershey, PA 17033
717 531 6697 / Fax: 717 531 7583 /
greilly@ortho.hmc.psu.edu

Preferences and Keywords
Please consider for the NIRAs
Bone Mechanics;cell culture;signal transduction;shear stress;mechanotransduction

ABSTRACT NO. _____
PAPER NO. _____
Check One: _ Clinical _ Biology _ Engineering
Disclosure
(A-NIH) (A-NIH) (A-NIH, US Army, Whitaker)

THE SOURCE OF THE INTRACELLULAR CALCIUM INCREASE IN THE RESPONSE OF BONE CELLS TO OSCILLATING FLUID FLOW

+*Reilly, G C; *You, J; *Yellowley, C E (A-NIH); *Donahue, H J (A-NIH); *Jacobs, C R (A-NIH, US Army, Whitaker)
+*Penn State College of Medicine, Hershey, Pennsylvania. Musculoskeletal Research Laboratory, Department of Orthopaedics and Rehabilitation MC H089, Penn State College of Medicine, 500 University Drive, Hershey, PA 17033, 717 531 6697, Fax: 717 531 7583, greilly@ortho.hmc.psu.edu

INTRODUCTION:

Fluid flow in bone is a likely candidate for the mechanical signal with which osteocytes *in vivo* detect load. It is known that bone cells will respond to fluid flow with a variety of signalling and metabolic events (1,2,3,4). One of the first responses to occur in bone cells studied *in vitro* is a rapid increase in intracellular calcium (Ca^{2+}), which is essential for further downstream events (4). The purpose of this study was to define the source of this Ca^{2+} signal, in terms of the membrane and intracellular channels and pathways involved. Since the cellular response may be sensitive to the type of flow stimulus, we studied the response to ocillating fluid flow, which best approximates habitual load induced fluid flow that occurs *in vivo*.

METHODS:

MC3T3-E1 cells (mouse calvarial osteoblast-like cells) were plated onto quartz slides and grown for 2 days until they reached about 80% confluency in α MEM supplemented with 10% FBS and 2% penicillin and streptomycin. Prior to mounting in the flow chamber cells were incubated with 10 μM Fura2-AM which is an indicator of Ca^{2+} concentration ($[Ca^{2+}]$), for 45 minutes. The slides were mounted in a parallel plate flow chamber as previously described (3). Cells were placed in the chamber in flow media (α MEM with 2% FBS plus additions as described in table 1) for 30 minutes prior to flow. A variety of drugs that are known to block specific Ca^{2+} channels or signaling pathways were added to the flow media as shown in table 1. For analysis, vehicle (ethanol added) controls were combined with media only controls, as no significant effect of vehicle was noted (Student's t-test). The flow regime applied was 1 Hz oscillating flow using a sinusoidal waveform at 18 mls/min, which gives 2 Pa peak shear stress. Images of a selected field of view were collected every 3 seconds for 3 minutes without flow and for 3 minutes during flow. Image acquisition and analysis software (Metafluor, Universal imaging, West Chester, PA) was used to capture and convert fluorescent signals into real time $[Ca^{2+}]$ values. A cell was considered to show an increase in $[Ca^{2+}]$ when a $[Ca^{2+}]$ change was over 2 x the baseline, where baseline was the mean of the $[Ca^{2+}]$ fluctuations seen in the no flow controls. Baseline was recalculated each day as significant variation between days was noted (all experiments were performed over at least two days with two different passages of cells). The fraction of cells exhibiting a $[Ca^{2+}]$ increase was calculated for each slide. The number of cells exhibiting an increase after the initiation of flow was normalized by subtracting the number of cells exhibiting an increase before flow and dividing by the total number of cells. A two way ANOVA was used to examine differences between control and treated in the normalized percentage of cells responding to flow with the other factor being the day on which the experiment was performed.

Table 1: Drugs, the concentrations at which they were used, their expected effect on Ca^{2+} pathways and the type of control treatment used. The numbers of slides (S) and cells (C) used for each experiment are shown (treated top and control bottom).

Drug	Conc.	Expected action	Controls	N (S)	N (C)
Nifedipine	20 μM	Blocks membrane L-type voltage channels	Media only or with 1% ethanol	8 8	340 418
Neomycin	10 mM	Inhibits IP_3 pathway and L-type voltage channels	Media only	8 7	277 254
U 73122	5 μM	Inhibits formation of IP_3	Inert isoform drug, U73343	9 8	781 794
Ryanodine	1 μM	Holds open ryanodine sensitive channels	Media only or with 1% ethanol	10 12	258 504
Ryanodine	20 μM	Blocks ryanodine sensitive channels	Media only or with 1% ethanol	10 10	258 415

RESULTS:

Figure 1: The mean (with standard error bars) of the Ca^{2+} response to oscillating fluid flow expressed as % increase compared to the no-flow situation. Numbers of slides and cells as in table 1. *p < 0.05, **p<0.01, ***p<0.005, for two way ANOVA on treated compared with controls for each experiment.

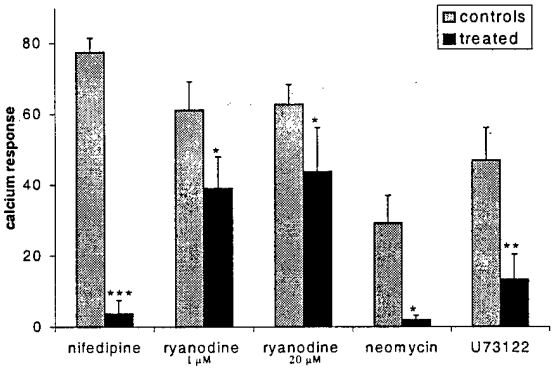

All the drugs used had some effect on the $[Ca^{2+}]$ increase. Nifedipine reduced the number of cells exhibiting an increase to near no-flow levels indicating that a response does not occur when the L-type voltage channel is blocked. Ryanodine, at levels in which the channel would remain open and Ca^{2+} could be lost from the internal store, and at levels which should block the channel, reduced the number of cells showing a $[Ca^{2+}]$ increase. U73122 which inhibits the production of IP_3 by its action on Phospholipase C (PLC) and therefore Ca^{2+} release from IP_3 sensitive stores, greatly reduced the number of cells responding compared to the control (the isoform drug U73343 which binds to PLC but does not inhibit its activity). Neomycin also inhibits the PLC/ IP_3 pathway, and has some inhibitory effect on the L-type voltage channel. Neomycin reduced the Ca^{2+} response to close to no-flow levels.

DISCUSSION:

These data suggest that the L-type voltage sensitive Ca^{2+} channel is involved in the intracellular Ca^{2+} response of MC3T3 cells to oscillating fluid flow. This is interesting in the light of previous data from our laboratory showing that the stretch activated membrane channel is not involved (4). In contrast the L-type channel was not necessary for a Ca^{2+} response to steady flow in primary rat calvarial cells (2). The reduction in Ca^{2+} response when the IP_3 pathway is blocked has also been shown to occur in steady flow (1, 2) and supports a hypothesis that the internal IP_3 sensitive stores are one of the sources of Ca^{2+} in the response to fluid-flow by bone cells. Ryanodine sensitive channels have not previously been shown to be involved in bone cell fluid flow responses. The partial reduction in Ca^{2+} response with ryanodine treatment indicates that ryanodine sensitive stores may also be a source of intracellular Ca^{2+}. In summary: we have shown that that the increase in intracellular $[Ca^{2+}]$ seen in MC3T3-E1 osteoblast-like cells after stimulation with oscillating fluid flow is due to extracellular Ca^{2+} entering through L-type voltage sensitive Ca^{2+} channels and Ca^{2+} release from internal stores, primarily the IP_3 sensitive store.

Reilly, Gwendolen C (1)
Musculoskeletal Research Laboratory, Dept. of Orthopaedics and Rehabilitation, MC H089, Penn State College of Medicine, 500 University Drive, Hershey, PA 17033
717 531 6697 / Fax: 717 531 7583 /
greilly@ortho.hmc.psu.edu

Preferences and Keywords
Please consider for the NIRAs
Bone Mechanics;proteoglycans;cell mechanics;shear stress;mechanotransduction

ABSTRACT NO. _____
PAPER NO. _____
Check One: _ Clinical _ Biology _ Engineering
Disclosure
(A-NIH) (A-NIH) (A-NIH, US army, Whitaker)

MANIPULATION OF THE BONE CELL GLYCOCALYX REDUCES CALCIUM RESPONSES TO FLUID FLOW

+*Reilly, G C; *Yellowley, C E (A-NIH); *Donahue, H J (A-NIH); *Jacobs, C R (A-NIH, US army, Whitaker)
+*Penn State College of Medicine, Hershey, Pennsylvania. Musculoskeletal Research Laboratory, Dept. of Orthopaedics and Rehabilitation, MC H089, Penn State College of Medicine, 500 University Drive, Hershey, PA 17033, 717 531 6697, Fax: 717 531 7583, greilly@ortho.hmc.psu.edu

INTRODUCTION:

It has been hypothesized that bone cells *in vivo* have a glycocalyx (cell coat) composed of hyaluronic acid chains and other proteoglycans and that this glycocalyx causes fluid flow induced shear stresses around bone cells in the range of 6-30 Pa (6). This value corresponds to the fluid shear stresses at which signaling and endocrine responses are observed in *in vitro* bone cell cultures (1, 3). An initial, rapid response to fluid flow is an increase in intracellular calcium (Ca^{2+}), which is important for further downstream responses (7). There is some evidence that there are proteoglycans present in the space between osteocytes and the bone matrix (5), but as of yet no evidence specifically for a glycocalyx, or its composition has been shown. We used alcian blue staining to characterize the glycocalyx of cultured MC 3T3-E1 osteoblast-like cells. We also examined whether an enzyme which specifically breaks down hyaluronic acid would affect the calcium response of these cells to oscillating fluid flow.

METHODS:

Characterization of the glycocalyx:

MC3T3-E1 cells (mouse calvarial osteoblast-like cells) were plated onto quartz slides and grown for 2 days until they reached about 80% confluence in α MEM supplemented with 10% FBS and 2% penicillin and streptomycin. These cells were chosen because they have been widely used in this lab and others to examine bone cells responses to fluid flow. Cells were stained in alcian blue using the critical electrolyte concentration method (4). Cells were fixed in 3.7% formaldehyde in PBS and stained in 0.2% alcian blue in .025 M sodium acetate buffer with either 0.1 M or 0.5M Magnesium chloride. In a low molarity solution of electrolyte (<0.2 M $MgCl_2$) all negatively charged proteoglycans are expected to be labeled, including hyaluronic acid, whereas at high concentrations (>0.2M $MgCl_2$) only highly negatively charged groups such as the sulphated proteoglycans will be labeled.

Calcium response to fluid flow:

MC3T3-E1 cells grown in the same way as for glycocalyx characterization were treated with either 46 U/ml of the enzyme hyaluronate lyase (hyaluronidase) from *streptomyces hyaluronlyticus* dissolved in PBS (pH 6.8) or with PBS only. 6mls of PBS or PBS plus enzyme was added to the slides in a petri dish and the dish was agitated in a water bath at 37°C for 30 mins. After enzyme or control treatment cells were rinsed in α MEM and incubated with 10 μM Fura 2AM, an intracellular calcium concentration indicator, for 45 minutes. The slides were mounted in a parallel plate flow chamber (3). Cells were placed in the chamber in flow media (α MEM plus 2% FBS) for 30 minutes prior to flow. The flow regime induced was 1 Hz oscillating flow using a sinusoidal waveform at 18 mls/min, which gives 20 Pa peak shear stress. Images of a selected field of view were collected every 3 seconds for 3 minutes without flow and for 3 minutes during flow. Image acquisition and analysis software (Metafluor, Universal imaging, West Chester, PA) was used to capture and convert fluorescent signals into real time calcium values. A calcium increase was considered to be a change over 2 times the baseline where baseline was the mean of the calcium changes seen in the no flow controls. A cell exhibiting such an increase was considered to be a 'responding cell'. 6 slides were examined for each group, 328 control cells and 356 enzyme treated cells with the experiments being run over 2 days.

RESULTS:

Figures 1a and 1b show MC3T3-E1 cells stained in alcian blue at the two concentrations of $MgCl_2$. The cells stain very well at the low concentration and barely at all at the higher concentration. The enzyme treated cells respond less well to oscillating fluid flow compared to controls (Figure 2). In the no flow case 9.8% of controls exhibit calcium increases compared to 5.8% of hyaluronidase treated cells. During the oscillating fluid flow period 41.2% of controls exhibit an increase compared to 27% of treated cells. A z statistic for proportions was used to compare the proportion of cells responding to fluid flow between the two groups (2) $p<0.01$.

Figure 1: MC3T3 cells stained in alcian blue at 0.1M $MgCl_2$ (A) and 0.5M $MgCl_2$ (B). Note that the cells in A are more darkly stained than in B indicating the presence of negatively charged carboxylated proteoglycans but not more highly negatively charged sulphated proteoglycans. (Field of view 1mm wide).

Figure 2: Fraction of cells exhibiting a calcium increase over 2 × baseline, during the no-flow and flow periods for the control and enzyme treated groups (error bars are standard errors of proportion), * $p<0.01$.

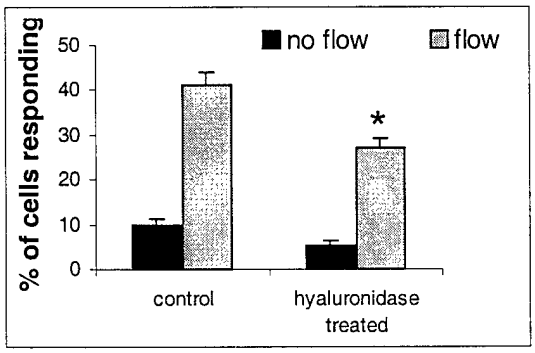

DISCUSSION:

We have shown that cultured osteoblast-like cells have a coating that stains well in alcian blue at low electrolyte concentration but not at high concentrations, this strongly suggests that bone cells have a glycocalyx rich in carboxylated proteoglycans one of which may be hyaluronic acid. We proceeded to manipulate the glycocalyx using an enzyme which would break down hyaluronic acid and found that the number of cells responding to oscillating fluid flow with an increase in intracellular calcium was reduced. This is the is the first piece of experimental evidence that supports the hypothesis that a hyaluronic acid rich cell glycocalyx is present around bone cells and that it contributes to bone cell mechanotransduction.

T7.42

Increased Adherence of Flowing Monocytes to Cultured Endothelial Cells After Hypoxia/Reoxygenation: Involvement of Rac-1, ROS and VCAM-1

Chi Kin Domingos Ng, Kaikobad Irani, *B. Rita Alevriadou*
Johns Hopkins University, School of Medicine, BME Dept., Baltimore, MD

Previous studies have shown that neutrophil adhesion to endothelial cells (ECs) exposed to hypoxia followed by reoxygenation (H/R) is greatly enhanced, due to production of reactive oxygen species (ROS), activation of nuclear factor (NF)-kB and upregulation of EC adhesion molecules. We examined the adhesion of monocytic U937 cells under flow conditions (1 dyne/cm2) to cultured HUVECs subjected to H/R (1h hypoxia/13h reoxygenation). Video microscopy and a parallel-plate flow system were used to measure monocyte-EC adhesive interactions (tethering, rolling, stable adhesion). The number of total interactions was significantly greater (2.5-fold) after H/R, compared to normoxic controls. Either EC pretreatment with the antioxidant pyrrolidine dithiocarbamate (PDTC), a selective NF-kB inhibitor, or adenoviral-mediated gene transfer of a dominant negative Rac-1 gene product (Ad.Rac1N17) significantly decreased the H/R-induced cell rolling and stable adhesion. Since VCAM-1 is a major EC receptor for monocyte adhesion, we examined VCAM-1 expression by whole cell ELISA. While H/R significantly upregulated VCAM-1, both PDTC and Ad.Rac1N17 effectively inhibited VCAM-1 expression. In summary: (a) H/Rtreated ECs can support all stages of adhesion of flowing monocytes; (b) Rac-1 activation and production of ROS are crucial in regulating VCAM-1 expression and, hence, monocyte adhesion to ECs.

T7.43

The Role of VLA-4/VCAM-1 in Sickle Red Blood Cell-Endothelium Interactions

Eileen Finnegan, Gilda Barabino
Northeastern University, Chemical Engineering, Boston, MA

Vaso-occlusive crises in sickle cell disease may be initiated by a number of adhesive interactions between sickle erythrocytes (SS RBC) and the microvascular endothelium of post-capillary venules. We are currently examining the integrin a4b1, also known as very late activation antigen-4 (VLA-4), which is expressed on a subpopulation of sickle erythrocytes. VLA4 forms a ligand pair with vascular cell adhesion molecule-1 (VCAM-1), which is present on activated endothelial cells and is upregulated by the inflammatory cytokine, tumor necrosis factor (TNF-a). VLA-4 interactions with VCAM-1 may be important targets for therapeutic intervention in sickle cell disease.

We have found that a multidisciplinary approach involving complementary in vitro and ex vivo experimental systems is effective in providing a more complete understanding of factors contributing to sickle vaso-occlusion. Using a parallel plate flow adhesion assay, we investigated SSRBC adhesion under venous shear conditions (1 dyne/cm2) to four cultured endothelial cell lines: murine microvasculature (brain and lung) and human dermal microvasculature (MDEC) and human large vessel (HUVEC). Using a novel intravital microscopy technique, we examined SS RBC adhesion within the microcirculation of skull bone marrow of normal and transgenic sickle cell mice under physiologic flow. Results from these investigations demonstrating sickle cell-endothelial interactions mediated by the adhesive receptor combination VLA-4/VCAM-1 will be presented.

T7.44

Control of the Shape of a Neointima-Like Structure by Blood Shear Stress

Shu Liu,
Northwestern University, Evanston, IL

Fluid mechanical factors are thought to influence vascular morphogenesis. Here the author shows how blood shear stress regulates the shape of a neointima-like tissue around a polymer micro-cylinder implanted in the rat vena cava through the vessel center with its axis perpendicular to blood flow. In such a model, the micro-cylinder is exposed to a laminar flow with a known shear stress field in the leading region and a vortex flow in the trailing region. At 1, 5, 10, 20, and 30 days after implantation, it was found that the micro-cylinder was encapsulated by a neointima-like structure with a streamlined body profile. The highest growth rate of the neointimalike tissue was found at the leading and trailing stagnation points of the micro-cylinder. Blood shear stress in the leading laminar flow region was inversely correlated with the rate of neointimal growth, the rate of cell proliferation, and the rate of smooth muscle cell (SMC) actin filament formation. These rates were significantly higher in the trailing vortex flow region than those in the leading laminar flow region. An elimination of blood flow led to a rapid formation of an irregular thrombus-like structure around the micro-cylinder, followed by vessel occlusion within 1 day after surgery. These results suggest that blood shear stress regulates the shape of the neointima-like structure. The formation of a streamlined neointimal structure is possibly to reduce drag due to vortex blood flow.

T7.45

Prostaglandin E_2 (PGE_2) Response in MC3T3-E1 Osteoblastic Cells is Dependent Upon Gap Junction Coupling

Marnie Saunders[1], Jun You[1], James Trosko[2], Hiroshi Yamasaki[3], Henry Donahue[1], Christopher Jacobs[1]
[1]Pennsylvania State University, College of Medicine, Orthopaedics and Rehabilitaiton, Hershey, PA, [2]Michigan State University, Pediatrics/Human Development Department, College of Human Medicine, East Lansing, Michigan, [3]Kwansei Gakuin University, Uegahava, Nishinomiya, Japan

Fluid flow has been demonstrated to be a potent stimulator of bone cell activity in vitro suggesting a mechanotransduction role. Although the specific manner in which the biophysical signal is transduced is unknown, it is possible that gap junctions play a pivotal role. Gap junctions, which physically link neighboring cells, may allow cells to respond in concert to a stimuli thereby amplifying the ensemble response. We exposed osteoblastic cells to oscillatory fluid flow and quantified PGE_2 production; in simultaneous experiments, gap junction coupling (GJC) was quantified. Osteoblastic MC3T3-E1 cells and a MC3T3-E1 cell line transfected with a dominant/negative Cx43 exhibiting reduced GJC (DN-8) were utilized. Cells were subjected to fluid flow for 1hour at 20dyne/cm^2 utilizing a sinusoidal waveform at 1Hz. Following fluid flow, media was collected for PGE_2 quantification and normalized to protein. GJC was quantified using fluorescent dye transfer. We found that the DN-8 cell line, exhibiting a 75% reduction in coupling, showed no response to fluid flow in contrast to the MC3T3-E1 which exhibited extensive coupling and a 115% increase in PGE_2 Results were statistically significant and demonstrate that GJC in osteoblastic cell lines is a strong regulator of PGE_2 production in response to oscillatory fluid flow.

7.2.3 Vascular Cell–Cell Adhesive Interactions

T7.46

Neutrophil Morphological Regulation of Selectin Binding in Shear Flow

Eric Park, McRae Smith, Michael Lawrence
University of Virginia, Biomedical Engineering, Charlottesville, VA

It is known that the kinetics of the receptor-ligand bond perform an important role in regulating cell adhesion for various physiological phenomena. We have developed a cell-free system that excludes the involvement of cellular properties (i.e. cell deformability and microvillus stretching) in the regulation of selectin bond lifetimes. PSGL-1 coated polystyrene microspheres were perfused over a P-selectin substrate in a parallel-plate flow chamber (100 sites/μm2; 0.1-1 dyn/cm2 wall shear stress). Analysis of the P-selectin/PSGL-1 interactions showed that the kinetics of the bead dissociation were similar in magnitude to those of neutrophil interactions on P-selectin at 25 sites/μm2 or less. Differences that existed between the microbead and neutrophil estimates of P-selectin dissociation constants varied with force, and may be due to the existence on the neutrophil of an elastic microvillus. Microvilli of neutrophils adhering at a wall shear stress of 0.6 dyn/cm2 (force/bond (Fb)=72 pN) are estimated to be approximately 0.3 ìm and increased to 1.58 μm at 2 dyn/cm2. A viscoelastic model was employed to evaluate the microvillus mechanical properties. We conclude that microvillus extension plays a significant role in maintaining the adhesive interactions between neutrophils and endothelial cells. Work supported by NIH HL54614 and AHA 9940026N.

T7.47

Leukocyte Rolling and Deformation on P-selectin in Whole Blood

David Schmidtke, Scott Diamond L.
University of Pennsylvania, Chemical Engineering, Philadelphia, PA

Leukocyte adhesion to the vessel wall is a key step in the processes of inflammation and thrombosis. The initial adhesion and subsequent rolling is mediated by the selectins. Due to poor penetration of light in whole blood, conventional in vitro flow assays have studied the initial adhesive events with isolated leukocytes suspended in saline. Thus ignoring the presence and influence of red blood cells (RBCs) on the fluid viscosity and spatial distribution of cells, both of which will influence the adhesion process. In part, this is the cause of known discrepancies between in vitro and in vivo studies. In contrast, in vitro assays involving fluorescently labeled cells in whole blood suffer from poor resolution of the cell surface. To overcome these difficulties we have used a microslide flow chamber which allowed us to do dual oil-immersion differential interference contrast (DIC) microscopy of leukocyte adhesion to P-selectin in whole blood. Using this technique we examined the effect of RBCs on leukocyte adhesion, rolling, and deformation. This data helps resolve the differences between in vitro vs in vivo studies.

Appendix 14

T7.48

IL-8 Dose and ICAM-1 Site Density Determine the Dynamics of Neutrophil Adhesion Under Fluid Shear

Aaron Lum, Scott Simon
University of California, Davis, Biomedical Engineering, College of Engineering, Davis, CA

Neutrophil (PMN) emigration at regions of inflammation involves chemotactic activation that leads to adhesion via β2-integrins binding to endothelial expressed ICAM-1. Interleukin-8 (IL-8) binds to its receptor with Kd ~1 nM and activates this adhesion process. Flow cytometry was used to measure the kinetics of neutrophil adhesion to fluorescent latex microspheres (1μm) derivitized with recombinant ICAM-1-Ig. We examined the relationship between the dose of IL-8 stimulation and the rate and extent of bead capture under fluid shear. Onset of adhesion was detected at 50 pM of IL8, as few as 10 IL-8 receptors/PMN. A boost in the capture rate peaked within seconds of addition of IL-8, and plateaued by ~5 minutes. Optimal adhesion to ICAM-1 required expression of both LFA-1 and Mac-1, subunits of β2-integrin. However, LFA-1 alone supported the boost in microsphere capture. An ICAM-1 site density of ~300/μm^2 supported optimal bead capture, which decreased by 50% at ~60/μm^2 ICAM-1 . The rate and extent of bead capture appeared to decrease nonlinearly with the site density of ICAM-1. LFA-1 is essential for capture of ICAM-1, whereas Mac-1 is involved in stabilizing adhesion.

T7.49

Platelet Glycoprotein Ibalpha: A Multifunctional Receptor for Tethering Under Flow Conditions

Larry McIntire[1], Alcia Schade[1], Jing-Fei Dong[2], Jose Lopez[2]
[1]Rice University, Institute of Biosciences and Bioengineering, Houston, TX, [2]Baylor College of Medicine, Department of Medicine, Houston, TX

Platelet Glycoprotein Ibalpha, part of the GP Ib-IX-V complex, is critical in hemostasis and arterial thrombosis, binding immobilized von Willebrand factor (vWf) on a damaged vessel walls. Using CHO cells expressing wild type and mutant GP Ibalpha chains, we demonstrated tethering and rolling of these cells on purified vWf under flow conditions. Gain-of-function and loss-of-function mutants have been identified which give insight into the detailed structure-function of this receptor. We also demonstrated that GP Ibalpha can function as a counter-receptor for P-selectin, elucidating a molecular mechanism for unactivated platelet attachment to activated endothelium (which has been demonstrated **in vivo**). Finally, we demonstrated, using insolubilized purified GP Ibalpha and THP-1 monocytic cells or transfected 293 cells, that GP Ibalpha can serve as a counter receptor for the b2 integrin Mac-I under flow, interacting with am I domain, which bears a striking homology to the A domain of vWf. This gives a possible molecular mechanism for co-location of leukocytes and platelets at sites of vascular injury - also as seen **in vivo**.

T7.50

Immobilized Platelets Support Human Colon Carcinoma Cell Tethering, Rolling and Firm Adhesion Under Dynamic Flow Conditions

Owen McCarty, Konstantinos Konstantopoulos
Johns Hopkins University, Chemical Engineering, Baltimore, MD

Accumulating evidence suggests that successful metastatic spread is dependent upon the ability of tumor cells to undergo extensive interactions with platelets. However, the mechanisms mediating tumor cell adhesion to platelets under conditions of flow remain largely unknown. Therefore, this study was designed to analyze the ability of a human colon carcinoma cell line, LS174T, to bind to platelets under flow, and to identify the receptors involved in this process. Immobilized platelets support LS174T cell adhesion at wall shear stresses up to 1.4 dyn/cm2. Our data suggest that platelets primarily recruit LS174T cells through a two-step, sequential process of adhesive interactions that shares common features but is distinct from that elaborated for neutrophils. Platelet P-selectin mediates LS174T cell tethering and rolling in a PSGL-1 and CD24- independent manner. Moreover, platelet GPIIbIIIa integrins appear to be capable of directly capturing LS174T cells from the fluid stream, and also convert instantaneously transient tethers initiated by P-selectin into stable adhesion. This step is at least partially mediated by vWf that bridges platelet GPIIbIIIa with a yet unidentified receptor on the LS174T cell surface via a RGD-dependent mechanism. This cascade of events depicts an efficacious process for colon carcinoma arrest at sites of vascular injury.

T7.51

The Effects of Non-Linear Flow on Cell Aggregation : Role of Spatial and Temporal Variations in Inter-Particle Forces

Harish Shankaran, Sriram Neelamegham
State University of New York at Buffalo, Chemical Engineering, Engineering and Applied Sciences, Buffalo, NY

Cone-plate viscometry is used extensively to study platelet and neutrophil aggregation kinetics. At high shear rates in the viscometer, centrifugal forces result in radial motion of the liquid and hence significant non-linear secondary flow. Numerical solution of the flow in the viscometer, along with theoretical analysis of two-body particle hydrodynamics indicates that the inter-particle normal force varies with position in the viscometer. Cells circulating in suspension are thus subjected to i) time-varying forces and ii) an overall increase in the magnitude of inter-particle forces relative to primary flow. A bimolecular kinetic model was applied to estimate the cell adhesion efficiency under these conditions. Results indicate that secondary flow at **G**=1500 /s causes up to a 40% reduction in adhesion efficiency relative to linear flow. Data from homotypic neutrophil aggregation experiments verify these theoretical predictions, and suggest that secondary flow may alter molecular on and off rates measured in the viscometer. Further, increased inter-cellular forces due to secondary flow, augment the disaggregation kinetics of neutrophils. Overall, our theoretical model combined with coneplate viscometer experiments, maybe a useful tool to study the effects of both spatial and temporal force variations, on the biological function of cells.

7.2P Vascular Cell Cell Adhesive Interactions

T7.52

Temporal Analysis of Fibroblast Traction and Migration in Tissue Equivalents

David Shreiber, Victor Barocas, Paul Enever, Mihir Wagle, Robert Tranquillo
University of Minnesota, Chemical Engineering and Materials Science, Minneapolis, MN

Tissue cells interact mechanically with fibrillar networks by exerting traction which traction results in two primary biomechanical phenomena - migration of the cell and/or compaction of the network. We developed previously experimental methods and complementary theoretical models to estimate these phenomena with two parameters, the random cell motility coefficient, μ, and the cell traction parameter, τ0, for cells in tissue equivalents assuming μ and τ0 were constant in value over time. We have adapted these models to quantify μ and τ0 as functions of time. μ is calculated by regressing experimental mean squared displacement (MSD) data with a generalized least squares analysis. Temporal data is determined by generating MSD data for a continuous subset of time intervals for the displacements and shifting the range of intervals through the range of experimental time points. τ0 is calculated by optimizing a finite element solution to gel compaction. The FEM is based on our anisotropic biphasic theory for tissue equivalents, and is solved with the Control and Optimization (COOPT) software package. COOPT solves a differential-algebraic equation system with piecewise polynomials that are functions of time, allowing the time dependence of τ0 for the optimal fit of the compaction data to be obtained. By employing these two techniques, we can now examine potential relationships between cell traction and cell migration more closely (Fig. 1). Supported by NIH-PO1-GM50150-03S1 grant to RTT.

T7.53

Prostaglandin E_2 (PGE_2) Response to Fluid Flow is Independent of Intracellular Calcium Concentration in Osteoblastic ROS 17/2.8 and RCx16 Cells

Marnie Saunders, Jun You, Clare Yellowley, Henry Donahue, Christopher Jacobs
Pennsylvania State University College of Medicine, Orthopaedics and Rehabilitation, Hershey, PA

PGE_2 has been shown to mediate load-induced bone remodeling in vivo. In vitro, we have demonstrated that PGE_2 production in osteoblastic cell lines increases in response to oscillatory fluid flow (OFF). Here we investigate whether PGE_2 production is dependent upon intracellular calcium concentration ($[Ca^{2+}]i$) as has been suggested. Rat osteoblastic sarcoma cells (ROS 17/2.8) and a transfected ROS cell line exhibiting poor cell-cell coupling (RCx16) were utilized. For PGE_2 quantification, cells were exposed to OFF for 1hour at 1Hz or 2Hz and 20dyne/cm2. Following flow, media was collected for PGE_2 quantification. For $[Ca^{2+}]i$ quantification, cells were loaded with a fluorescent calcium tracer and exposed to 3minutes of OFF at 1Hz and 20dyne/cm2. An image acquisition and analysis

package was used to quantify the signals. Neither ROS nor RCx16 cell lines displayed a calcium response. However, both lines responded to OFF with a significant relative increase in PGE_2 production compared to the no flow controls with responses greater at 2Hz. Moreover, the PGE_2 response of ROS cells was significantly greater than that of RCx16 cells. These finding suggest that PGE_2 production in ROS and RCx16 cells in response to OFF is independent of $[Ca^2+]i$ but dependent upon cell-cell coupling.

T7.54

Particle Diameter Influences Receptor - Ligand Mediated Adhesion Under Flow

Vivek Shinde Patil[1], Craig Campbell[2], Yang Yun[3], Steven Slack[4], *Douglas Goetz*[1]
[1]Ohio University, Chemical Engineering, Athens, OH, [2]University of Memphis, Computer Sciences, Memphis, TN, [3]State University of New York at Stony Brook, Biomedical Engineering, Stoney Brook, NY, [4]University of Memphis, Biomedical Engineering, College of Engineering, Memphis, TN

The diameter of circulating cells which may adhere to the vascular endothelium spans an order of magnitude from ~2 μm (the size of a platelet) to ~20 μm (the potential size of a metastatic cell). Although mathematical models indicate that the adhesion exhibited by a cell will be a function of cell diameter, there have been few experimental investigations into the role of cell diameter in adhesion. Thus, in this study we compared the adhesion of 5 μm and 10 μm diameter P-selectin glycoprotein ligand -1 (PSGL-1) microspheres to P-selectin under in vitro flow conditions. We found that (a) the microsphere diameter influences the rate of attachment in a complex manner, (b) the shear stress required to set in motion a firmly adherent PSGL-1 microsphere was less for the 10 μm microspheres than for the 5 μm microspheres and (c) the rolling velocity of the 10 μm microspheres was greater than the rolling velocity of the 5 μm microspheres. These results suggest that attachment, rolling and firm adhesion are a function of cell diameter and provide experimental proof for theoretical models that indicate a role for cell diameter in adhesion.

T7.55

Analysis of Selectin Binding to Immobilized Glycosphingolipids under Flow Conditions

Monica Burdick, Konstantinos Konstantopoulos
Johns Hopkins University, Chemical Engineering, Baltimore, MD

Selectins are cell-surface proteins capable of mediating tethering and rolling of leukocytes to the inflamed vessel wall. Several glycoconjugates that bind to selectins have been identified, but the natural ligand for Eselectin has yet to be fully elucidated. In this study we provide further evidence that glycosphingolipids constitute major ligands for E- but not Pselectin. To this end, E- or P-selectin expressing CHO cells were perfused over polystyrene-absorbed 2,3-sialyl Lewisx (sLex) conjugated to the sphingolipid ceramide. CHO-E cells tethered extensively and formed slow rolling interactions with the immobilized glycosphingolipid at 1 dyn/cm2. Tethering varied proportionally with ligand density on the substrate and wall shear stress. In contrast, this substrate supported limited and fast CHO-P cell rolling. Using a stochastic model of cell rolling, the step size between successive bond releases from the 2,3-sLex-ceramide conjugate was estimated ~0.3 μm for CHO-E cells and ~8 μm for CHO-P cells. The wait time between these events was 0.1 sec and 0.04 sec for CHO-E and -P cells, respectively. Controlled detachment assays further revealed much stronger adhesive interactions of E- than P-selectin with 2,3-sLex glycosphingolipids. Cumulatively, our data suggest that glycosphingolipids containing 2,3 sLex might act as natural ligands for E- but not P-selectin.

T7.56

CD11b/CD18 Coated Microspheres Adhere to Activated Endothelium via Two Distinct Mechanisms

Vivek Shinde Patil[1], Charles Parkos[2], *Douglas Goetz*[1]
[1]Ohio University, Chemical Engineering, Athens, OH, [2]Emory University, Deparment of Pathology, Atlanta, GA

We have recently demonstrated that 10 micrometer polystyrene microspheres coated with CD11b/CD18 (Mac-1) adhere to IL-1 activated (4 hr) human umbilical vein endothelial cells (HUVEC) via E-selectin under flow. However, pre-treatment of IL-1 HUVEC with a mAb to E-selectin (7A9) did not eliminate all of the adhesion, suggesting an E-selectin independent mechanism. To probe this issue, we pre-treated the CD11b/CD18 microspheres with a mAb (CBRM1/29) that is known to inhibit CD11b/CD18 mediated adhesion. Pre-treatment of the CD11b/CD18 microspheres with CBRM1/29 essentially eliminated the residual adhesion of the CD11b/CD18 microspheres to IL-1 HUVEC pre-treated with 7A9. When IL-1 HUVEC were not pre-treated with 7A9, attachment of CBRM1/29-bound CD11b/CD18 microspheres was only slightly affected. Pre-treatment with CBRM1/29 under these conditions, did, however, convert the population of adherent CD11b/CD18 microspheres from predominantly firmly adherent (~90% firmly adherent) to predominantly rolling (~0% firmly adherent). Taken together, the data indicate that CD11b/CD18 coated microspheres adhere to IL-1 activated HUVEC via two distinct molecular mechanisms: an Eselectin dependent mechanism that mediates attachment and rolling and a mechanism dependent on the CBRM1/29 epitope that mediates, predominantly, firm adhesion. Since these mechanisms mediate different adhesive states, the above data suggest that the mechanisms have distinct kinetics.

T7.57

A Web Site Focused on Explaining the Biology and Physics of Cell Adhesion.

Jao Ou[1], Brian Good[2], Vivek Shinde Patil[2], *Douglas Goetz*[2]
[1]Duke University, Durham, NC, [2]Ohio University, Chemical Engineering, Athens, OH

Collaborations between biologists and engineers have led to significant advances in our understanding of biological systems and the development of novel biotechnologies. These successes have clearly demonstrated the value of educating engineers and biologists who have the ability and desire to work at the interface between biology and engineering. A significant obstacle to training such scientists is that biology and engineering are at somewhat opposite ends of the spectrum. In general, biologists and engineers may be unfamiliar with basic principles from each other's discipline. An additional complication is that rapid advances in certain fields leads to an evolving vocabulary and physical explanation of the biological processes. These changes make it even more difficult for effective communication between the two disciplines. To meet these challenges in the field of cell adhesion, we have developed a web site aimed at facilitating biologists' understanding of the physics of cell adhesion and engineers' understanding of the biology of cell adhesion. This web site serves as a model that could be adapted to other fields that benefit from the close collaboration between biologists and engineers.

T7.58

PSGL-1 Microsphere Adhesion in Vivo

Erin Burch[1], Mohammad Kiani[2], Vivek Shinde Patil[3], *Douglas Goetz*[3]
[1]University of Memphis, Biomedical Engineering, Memphis, TN, [2]University of Tennessee, Biomedical Engineering, Memphis, TN, [3]Ohio University, Chemical Engineering, Athens, OH

We have previously demonstrated that the first 19 amino acids of mature PSGL-1 are sufficient to recreate attachment and rolling on cellular expressed P-selectin in vitro. To determine if this region of PSGL-1 is sufficient to mediate attachment and rolling on P-selectin in vivo, we coated microspheres with a recombinant PSGL-1 construct, 19.ek.Fc, consisting of the first 19 amino acids of mature PSGL-1 linked to an enterokinase cleavage site which in turn is linked to the Fc region of human IgG. Microspheres coated with human IgG or enterokinase liberated human Fc served as negative controls. Murine cremaster muscle was exteriorized and prepared for observation via intravital microscopy. The microspheres were injected and the interaction of the microspheres within the post-capillary venules of the cremaster muscle observed. Intravital microscopy revealed that (a) a significantly greater number of the 19.ek.Fc microspheres rolled compared to the negative control microspheres and (b) a significantly greater number of 19.ek.Fc microspheres were arrested in the microvascualture compared to the number of arrested control microspheres. Combined, the results, along with other supporting in vitro and in vivo data, suggest that the first 19 amino acids of PSGL-1 are sufficient to mediate adhesion to trauma-activated microvascular endothelium.

T7.59

Shear Stress Modulates Platelet-Staphylococcal Interactions

Julia Ross[1], Konstantinos Konstantopoulos[2], Owen McCarty[1], Nehal Mohamed[1]
[1]University of Maryland Baltimore County, Baltimore, MD, [2]Johns Hopkins University, Chemical Engineering, Baltimore, MD

Staphylococcus aureus is a common cause of hospital-acquired infections and is a leading causative organism of bloodstream infection. Once bloodborn, S. aureus causes infective endocarditis and widespread metastatic abscesses. The pathogenesis of infective endocarditis is complex and involves: endocardial damage, inducing platelet and fibrin deposition; adherence of S. aureus to damaged endocardial sites; further deposition of platelets and fibrin onto the damaged, infected endocardium; and endocardial reseeding, either hematogenously or locally. The growth of infected cardiac vegetations is directly linked to the ability of the infecting pathogen to adhere to and aggregate platelets.

The goal of this work was to demonstrate that physiological levels of shear stress modulate staphylococcal-platelet interactions. To simulate events that take place at sites of blood vessel injury, we studied the binding of S. aureus to activated platelet monolayers under shear conditions using a parallel-plate flow chamber and epi-fluorescent videomicroscopy. Results demonstrate reduced staphylococcal adhesion as the shear stress increases, regardless of the bacterial growth phase. We also studied heterotypic aggregation in suspension to simulate interaction events in the bulk flow. Shear increased the percent of platelets bound in heteroaggregates from approximately 2% for static controls to more than 10% after 2 minutes of shear exposure. The results of this work directly support the hypothesis that shear stress modulates S. aureus-platelet interactions.

Appendix 15

T9.26

Modeling of Skeletal Muscle Glycogenolysis

Melissa Lambeth[1], Martin Kushmerick[2]
[1]University of Washington, Dept. of Bioengineering, Seattle, WA, [2]University of Washington, Physiology and Biophysics, School of Medicine, Seattle, WA

Glycogenolysis in skeletal muscle is unique in its ability to meet energetic demands over an extremely broad range of fluxes. This large system capacity requires models to include dynamic information instead of simple steady-state kinetics. We modeled the pathway of 12 glycolytic enzymes with adenylate kinase and creatine kinase on ODE solver software using mammalian kinetic data from the literature. The kinetic model when solved for zero flux gives predicted equilibrium thermodynamic free energies. Important characteristics of the analysis of the model are: a) the model is highly constrained by two sets of conserved moieties: NAD/NADH redox and high-energy phosphate potentials. The redox ratio varies with flux but remains balanced due to the stoichiometry of the network; the second ratio is balanced by the matching of glycolytic ATP synthesis to ATPase. These constraints result in the pathway functioning as two coupled units, above and below fructose-1,6-bisphosphate. b) The model is very sensitive to initial inorganic phosphate concentration. c) The apparent control of the resting system is distributed among several key enzymes besides phosphofructokinase - glycogen phosphorylase, glyceraldehyde dehydrogenase, and 3-phosphoglycerate kinase. Relevant fluxes and concentrations are being measured by NMR spectroscopy experiments.

T9.27

Comparison of NONMEM and NPEM with POP3CM, a new Hierarchical Parametric Empirical Bayes Model, using Levofloxacin Data.

John Lukas C[1], Mitch Watrous[1], George Drusano L[2]
[1]RFPK, Bioengineering, Seattle, WA, [2]Albany Medical College, Department of Medicine and Pharmacology, Albany, NY

Hierarchical models are designed to combine information from different study units in order to better understand the phenomena. They include at least two stages where the within unit and among units variability is assessed. These models are naturally applicable to the pharmacokinetic (PK) setting. Such are NPEM (USC, LAPK), NONMEM (UCSF) and POP3CM (UW, RFPK). The latter two also include a Bayes step, in a further stage, where prior information regarding the distributions of the variabilities and mean parameters can be introduced. Here, results from an NPEM analysis of levofloxacin, (data published in Preston et al., Antimicrob. Agents Chemother., 42, 1998) are re-analyzed with NONMEM (First Order, Conditional and Laplace methods) and POP3CM using a two-compartment oral absorption PK model in Bayesian and non-Bayesian modes. Results for four PK parameters are compared between models independently and with those from NPEM. Using the latter as a standard in non Bayesian runs, the bias estimates for both NONMEM and POP3CM always included zero and precision was always below 15%. ANOVA tests on the three models as factors and student t-tests on NONMEM and POP3CM Bayesian parameter pairs, always had a probability of differences due to chance of at least $p=0.05$.

T9.28

A Barrier Can Cause a Hyperbolic Enzyme to Have Switch-Like Kinetics

Wendy Thomas[1], James Bassingthwaighte[2]
[1]University of Washington, Seattle, WA, [2]Maastricht University (Universiteit Maastricht), Cardiovascular Research Institute Maastricht, Medicine, Seattle, WA

We demonstrate that a barrier separating an enzyme from its substrate can result in an ultrasensitive response. With the current interest in quantifying bioechemical pathways, it becomes increasingly important to understand how enzymes function within an intact cell as well as in a test tube. We present here a novel mechanism through which a barrier such as a cell membrane can cause an enzyme with Michaelis-Menten hyperbolic kinetics to display an arbitrarily steep response to bulk substrate concentrations When a single enzyme utilizes substrate that is supplied externally, and does so quickly relative to the transport rate of the substrate, the apparent Hill coefficient of the enzyme can increase more than tenfold the region between half-maximal and maximal activity. The addition of a lower Km enzyme competing for the same substrate can cause a similar increase in the Hill coefficient of the first enzyme in the region below half-maximal activity. Thus an enzyme that would normally require an 81-fold increase in substrate concentration to switch from 10% to 90% of maximal activity could do the same with only a 2-fold increase in substrate when part of a system involving a membrane and a competing enzyme.

T9.29

Establishment of the Conditions for the Expansion and Purification of Rat Pancreatic Ductal Epithelial Cell Cultures

Michael Boretti, Keith Gooch
University of Pennsylvania, Bioengineering, Philadelphia, PA

During both fetal pancreatic development and adult pancreatic regeneration, ductal epithelial cells (DEC's) differentiate into endocrine cells. The goal of this project is to apply existing understanding of these processes to recapitulate endocrine cell development in vitro and create tissue-engineered islets. As these tissue-engineered islets would be derived from DEC's that have significant proliferative potential, they could greatly increase the number of diabetic recipients served by a given amount of donor tissue. After testing different isolation strategies, collagenase digestion followed by filtering through a size-selective sieve was found to be the most effective means of isolating DEC's. An analysis of different ECM substrates further revealed that DEC's proliferate quite rapidly to form a monolayer when grown on a thick-collagen gel, but not on Matrigel, plastic, or a thin collagen layer. Our research is currently aimed at purifying the progenitor population from contaminating fibroblasts using standard techniques, and we are also experimenting with methods to enhance DEC growth by combining our technique with a fibroblast feeder layer. Future work will investigate candidate growth factors and ECM components under three-dimensional culture conditions to establish the optimal environment for generating tissue-engineered islets.

T9.30

Mathematical Modeling of Angiogenesis: Diffusion, Chemotaxis and Effects of Fibronectin

Vladimir Ajaev
Stanford University, Stanford, CA

Solid tumors cannot grow and develop without formation of a capillary network of blood vessels. This process, known as angiogenesis, is initiated by certain chemicals ('tumor angiogenesis factors') which cause endothelial cells to migrate into the extracellular matrix towards the tumor. Such migration has been a subject of several mathematical models. Most of them, however, either neglect some important effects or seek solutions for geometries which are not relevant experimentally. The purpose of this study is to obtain realistic solutions which can be verified experimentally. The model takes into acccount random diffusion of cells and chemotaxis; to include the effects of fibronectin we use the approach of Anderson and Chaplain (Appl. Math Lett. 12 (1999), p. 121), although other possibilities are also discussed. Solutions indicate limitations to tumor vascularization; mechanisms that limit the migration of endothelial cells are discussed.

T9.31

Frequency Dependent Effects of Oscillating Fluid Flow on Bone Cells

Jun You, Marnie Saunders, Clare Yellowley, Henry Donahue, Christopher Jacobs
The Pennsylvania State University, Department of Orthopaedics and Rehabilitation, Hershey, PA

It is well known that bone cells can sense mechanical loading and alter bone structure to efficiently support the load bearing demands placed upon it. Previously, oscillatory flow induced shear stress was shown to mediate a variety of physiological responses **in vitro**, including increased intracellular calcium concentration ([Ca2+]i) and production of prostaglandin E2 (PGE2). However there is little **in vitro** data to show loading frequency effects on bone cells. Our hypothesis was that over a wide range of loading-induced oscillating flow frequencies bone cells display a frequency dependent response. To test our hypothesis, we developed a high-frequency flow device to deliver a wide range of sinusoidally oscillating flow frequencies while monitoring real time [Ca2+]i and PGE2 production in MC3T3-E1 osteoblastic cells. Our results show that the more stimulatory frequency for [Ca2+]i was 0.1 Hz. However, 0.5-1.0 Hz was more stimulatory of PGE2 production. This suggests that the signaling pathways for [Ca2+]i and PGE2 may be different. Moreover considering viscoelastic properties of cells, our results suggest that bone cell [Ca2+]i response is more dependent on cell membrane deformation whereas PGE2 production is more related to cytosol internal friction.

T9.32

Fluid Flow Induced Intracellular Calcium Signaling Is Shear Stress And Frequency Dependent In Primary Rat Osteoblastic Cells

Seth Donahue, Henry Donahue, Christopher Jacobs
Pennsylvania State University, Orthopaedics and Rehabilitation, Hershey, PA

Bone adaptation is dependent on the magnitude and frequency of mechanical loading in rats. We hypothesized that cytosolic calcium oscillations (spikes) are also dependent on the magnitude and frequency of mechanical loading in primary osteoblastic cells isolated from rat long bones. Fura-2 was used to measure intracellular calcium concentrations in individual cells during a three minute no flow period and three minutes of oscillating fluid flow that produced shear stresses of 1 or 2 Pa at frequencies of 0.2, 1, or 2 Hz. There were spontaneous calcium spikes in 12% of cells during the no flow period. Significantly ($p < 0.0001$) more cells displayed spiking during fluid flow; more cells responded to 2 Pa (70%) than

1 Pa (52%), and to 0.2 Hz (70%) than 2 Hz (49%). The percentage of cells responding was frequency dependent at 1 Pa, but not at 2 Pa. Spike amplitude was dependent on fluid flow frequency, but not shear stress magnitude. Spiking was greater at 0.2 Hz (144 nM) than at 2 Hz (99 nM). Calcium signalling was dependent on the magnitude and frequency of mechanical loading in rat osteoblastic cells; higher magnitude and lower frequency fluid flows were more stimulatory.

T9.33

Tumor Diagnosis using Population Modeling Techniques and MRI Technology

Mary Spilker, Amy Yao, Paolo Vicini
University of Washington, Bioengineering, School of Medicine, Seattle, WA

Tumor diagnosis is one novel application of population modeling techniques. In this work, we apply population modeling techniques to the diagnosis of mammary tumors in animals. Endogenously produced mammary tumors were imaged via dynamic contrast-enhanced MRI after intravenous injection of albumin-(Gd-DTPA)30. Dynamic signal intensity measurements were obtained from blood and tumor tissue and converted to measures proportional to contrast agent concentration. These data were then fitted with a mathematical model of capillary wall permeability, yielding a quantitative measure of capillary permeability of the tumor to albumin-(Gd-DTPA)30. The hypothesis was that the tumor disrupted the endothelial wall to a degree proportional to the malignancy. The permeability model was then embedded in a statistical model of the two subpopulations (benign and malignant tumors). The results allowed us to separate the two subpopulations and correlated very well ($r = 0.80$) with the tumor grade independently determined from histology. The model was able to predict with 89% accuracy whether the tumor was benign or malignant. While these initial results are encouraging, further research is needed to ascertain the power of this technique for diagnostic purposes. Supported by NIH grant P41-RR12609.

Track 10. History, Design, Education, and Engineering Research Centers

10.1 Education

T10.1

Development of a Web-based Teaching Module for Light Propagation in Turbid Media

Conor Kleweno[1], Joseph Walsh[2], Suzanne Olds[2], David Kanter[2], Michael Miller[2]
[1]University of Washington, Biomedical Engineering, Seattle, WA, [2]Northwestern University, Biomedical Engineering, Evanston, IL

The learning of tissue optics is complicated by the numerous models that describe the propagation of light in turbid media. Typically, instructors present a general overview of the models or only one model in great depth, but in-depth comparison of models is difficult and thus limited. This study is one part of a multi-year Engineering Research Center (ERC) project to develop instructional tools on the topic of propagation of light in turbid media. The objective is to create an interactive web site where students can compare and contrast different tissue optical models, examine the light distributions given by the different models, and test strategies for dealing with unanticipated or conflicting results. A computer-based program was developed where the students select the tissue geometry and optical properties, as given by the instructor or dictated by laboratory/clinical conditions, and observe the resulting light distribution for several models. Students perform interactive tasks and, for example, predict then analyze the light distributions generated by the models subsequent to changes in the tissue optical properties. Students with varying levels of tissue optics background were used to assess the success of our learning objectives.

T10.2

Clinical Engineering in Clinical-Care & its Curricular Development

Dhanjoo Ghista
Biomedical Engineering Dept., Hyderabad, Andhra Pradesh India

Role of Clinical Engineering (CLE) in Tertiary-care (today & tomorrow)

The first role entails **monitoring of relevant patient data** concerning organ functional activity, such as by ECG surface mapping to assess heart electrical activity, and detect therefrom the electrical source and/or conduction abnormalities. **Processing and diagnostic analysis of the monitored signals and images** constitutes the next logical role. This is exemplified by power-spectral analysis of HR variability, to characterize autonomic dysfunction. The processed medical data then **enables analysis of organ systems functional processes.** This can include, for instance, intraLV blood flow analysis, to determine intra-LV blood velocity patterns and pressure-gradients, to them compute diagnostic indices of LV resistanceto filing and contractility. **Rehabilitation and Surgical procedures** constitute the fifth BME clinical role. In this category, a novel BME involvement is in surgical simulation, involving presurgical analyses of stress, flow and electrical fields at surgical correction/reconstruction sites, for an optimal surgical procedure. **Artificial organs and Prosthesis design** constitute the sixth role of BME, exemplified by the cardiac pacemaker and artifical heart. **Curricular Revision for Launching CLE** involves teaching integration of engineering-oriented BME disciplines as Organ-systems engineering, applied to clinical specialties.

T10.3

Neural Interfaces Laboratory in Bioengineering

Gregory Clark, Richard Normann, Patick Tresco
University of Utah, Bioengineering, Salt Lake City, UT

Increasingly, bioengineering tools and techniques are being used for the treatment of neural disorders ranging from sensory and motor dysfunction to higher-order phenomena such as epilepsy and depression. This laboratory course provides hands-on training in the engineering and implementation of neural interfaces, and acquaints students with cellular- and systems-level neural properties relevant to these technologies. Specific topics include surgery, electrophysiological stimulation and recording (single neurons, nerves, and brain), cell delivery systems, neural cell culture, biocompatibility, histology, and anatomy (see http://www.bioen.utah.edu/NIL.html). Examples include the following. (1) Students used intracellular recording and stimulation to examine neural accommodation, anode-break excitation, stimulus intensity/duration functions, action potential collision, and synaptic plasticity. (2) Students used tripolar electrodes and quasitrapezoidal stimulation of sciatic nerve (Fang & Mortimer, 1991) to recruit motor units in the normal physiological order, as indicated by amplitudes and kinetics of muscle contractions. (3) Students implanted dopamine-releasing encapsulation devices into rat striatum to alleviate experimental Parkinsonian symptoms. Implants reduced rotational behavior by 75% and were biocompatible. Whitaker Foundation (RAN & GAC) & BEEF Award, Univ. Utah (GAC).

T10.4

From Cells to Systems: A Learning Module for Bioengineering Neural Systems Physiology

John Troy, Brian Reiser, David Kanter, Jaejung Kim, Frank Fisher
Northwestern University, Education & Social Policy, Evanston, IL

Learners of neural systems physiology often find the step from a good understanding of the signaling properties of single neurons to an understanding of how ensembles of neurons process information in interesting ways challenging. We are developing a module based on neural circuits in the visual system to assist students in meeting this challenge. The design team includes biomedical engineers with expertise in systems physiology - one an expert in the area of visual information processing - and learning scientists who bring to the table expertise in the efficient design of educational materials. The objective of this presentation is not primarily to illustrate the module that is being developed, but rather to demonstrate how a partnership between bioengineers and learning scientists can be productive in building optimal educational materials in the field of bioengineering.

This work was supported primarily by the Engineering Research Centers Program of the National Science Foundation under Award Number EEC9876363.

T10.5

A Taxonomy for Bioengineering Systems Physiology

John Troy, Tobias Heidkamp
Northwestern University, Biomedical Engineering, Evanston, IL

We have drafted a taxonomy of the domain of systems physiology within the field of bioengineering. Our objective has been to catalog all aspects of systems physiology that might be included in courses taught in this area of bioengineering. In addition to including an index of topics that might be covered in such courses, the taxonomy includes listings of course materials (e.g. textbooks, laboratory exercises, software packages, internet sites, etc.) that are available for the topics listed, and information on the background a student would need to tackle each topic. The draft taxonomy is being presented here to solicit input from the bioengineering community. When complete, the taxonomy will be internet accessible through the Vanderbilt University, Northwestern University, University of Texas, and Harvard University/Massachusetts Institute of Technology (VaNTH) Engineering Research Center in Bioengineering Educational Technology. We believe that the finished taxonomy will be an invaluable resource for the bioengineering community.

This work was supported in part by the Engineering Research Centers Program of the National Science Foundation under Award Number EEC9876363.

SU182

Fos Family Transcription Factors as Critical Components of Osteogenic Signalling Elicited by Mechanical Loading. D. Inoue,* S. Kido,* T. Matsumoto.* First Department of Internal Medicine, University of Tokushima School of Medicine, Tokushima, Japan.

Mechanical stress is one of the most important physiological osteogenic stimuli and is critical for bone homeostasis as evidenced by severe and rapid bone loss observed in human subjects during space flight as well as immobilization. However, signalling pathways from mechanical loading to bone formation are largely unknown. A transcription factor, c-Fos, has been implicated in this signalling cascade because of its rapid induction by mechanical loading in cells of the osteoblast lineage and its ability to transform osteoblasts when overexpressed in transgenic mice. However, there has been no direct evidence that c-Fos stimulates bone formation. Recent reports have indicated that overexpression of other Fos family members, either delta-FosB, a C-terminal truncated naturally occurring splicing variant of FosB, or Fra-1, causes osteosclerotic changes in transgenic mice, providing *in vivo* evidence that they are capable of enhancing bone formation. Therefore, delta-FosB and Fra-1 may actually mediate osteogenic signals in response to various stimuli such as mechanical loading.

As an initial step to determine roles of Fos family members in the osteogenic response to mechanical loading, we investigated mechanical stress-induced expression of these factors *in vivo*, utilizing a mouse tail suspension model. Seven to nine week-old ICR male mice were tail-suspended for 4 days and then reloaded in rotating cages for 2 hours. Expression of the mRNA for fos family members in periosteum-enriched (Fr.1) and osteocyte-enriched (Fr.2) fractions of the tibiae and femurs was examined at various time points after reloading. RNase protection assay revealed that delta-fosB mRNA was constitutively expressed in Fr.1 and, to a little lesser degree, in Fr.2 at a comparable level to fosB mRNA. Reloading caused a clear-cut induction of both fosB and delta-fosB mRNA expression at 30 min, which reached a peak around 2h and became down-regulated by 8h. Expression of both c-fos and fra-1 mRNA was also enhanced after reloading but with different temporal profiles: c-fos expression reached the maximum at 30 min while fra-1 showed a late peak at 6h, suggesting distinct transcriptional targets for these factors. Consistent with our *in vivo* findings, fluid shear stress also induced delta-fosB expression by a mouse osteoblastic cell line, MC3T3E1, *in vitro*. Furthermore, treatment with human PTH (1-34) also increased expression of both fosB and delta-fosB in MC3T3E1 cells. Nuclear accumulation of delta-fosB proteins was demonstrated by Western blot analysis under these experimental conditions. From these results, we conclude that the Fos family members, particularly delta-FosB and Fra-1, may constitute critical components of downstream signalling events elicited by mechanical loading as well as other osteogenic stimuli such as PTH treatment.

SU183

Investigation of the Glycocalyx of Cultured Bone Cells. G. C. Reilly,* C. R. Jacobs. Orthopaedics and Rehabilitation, Pennsylvania State University College of Medicine, Hershey, PA, USA.

It has been hypothesised that osteocytes posses a hyaluronic acid rich glycocalyx similar to that found on endothelial cells, and that the presence of this type of glycocalyx enhances fluid shear stress levels at the cell surface (Wienbaum et al. J. Biomech 1994, p.339). The glycocalyx has not been characterised for bone cells in vivo or in vitro. We used lectin binding experiments and the critical electrolyte concentration method of Alcian blue staining to investigate the glycocalyx of osteoblast-like cells in culture.

MC3T3-E1, osteoblast-like cells, were cultured in media and 10% FBS for two days prior to experiments. Lectin binding experiments were performed with 3 fluorescently labelled lectins: Concanavalin Agglutinin, Vicia Villosa Agglutinin and Wheat Germ Agglutinin. Cells were incubated for 30 minutes with the lectin alone or the lectin and 0.5 M of an inhibiting sugar: Glucose, N-acetly-D-galactosamine and N-acetyl-D-gluocosamine respectively. All lectins bound well to the cell surface, as viewed under fluorecent microscopy. In each case lectin binding was inhibited by the sugar, indicating the precence of these sugars at the cell surface and lectin specificity for the sugars. Alcian blue stain was dissolved in either 0.1M or 0.5 M $MgCl_2$. At the higher electrolyte ($MgCl_2$) concentration only sulfated proteoglycans are stained and at the lower concentration all sugar groups are stained (Scott and Dorling Histochemie, 1965 p.221). There was no staining at the higher concentration but extensive staining at the lower one, suggesting sulfated proteoglycans are not a major component of the glycocalyx (compare figures A and B below, width of field of view 0.9 mm).

These experiments show that MC3T3 cells have a glycocalyx composed of glycoproteins rich in Glucose, N-acetly-D-galactosamine and N-acetyl-D-gluocosamine, and that sulfated proteoglycans are not present. This supports the hypothesis of an hyaluronic acid rich glycocalyx around bone cells. These results can be used to manipulate the glycocalyx for fluid flow experiments.

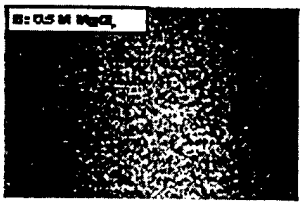

SU184

Prostaglandin Receptor EP4 Mediates the Bone Anabolic Effect

M. Machwate,*[1] S. Harada,[1] C. T. Leu,[1] G. Seedor,[1] M. Labelle,*[2] M. G[illegible] Hutchins,*[2] N. Lachance,*[2] S. B. Rodan,*[1] R. Young,*[2] G. A. Rodan.*[1] [1]Bo[illegible] Osteoporosis Research, Merck Research Laboratories, West Point, PA, USA Chemistry, Merck Frosst, Montreal, PQ, Canada.

PGE2 is a potent inducer of cortical and trabecular bone formation in h[illegible] mals. Although the bone anabolic action of PGE2 is well documented, th[illegible] molecular mechanisms which mediate this effect remain unclear. This study taken to examine the effect of pharmacological inactivation of prostaglandin one of the PGE2 receptors, on PGE2-induced bone formation *in vivo*. We fir[illegible] the ability of an EP4 selective ligand (EP4RA), to act as an antagonist, using th[illegible] osteal cells in which PGE2 increases intracellular cAMP and suppresses apopt[illegible] dose dependently reverses the effect of PGE2 on both intracellular cAMP and[illegible] these cells, suggesting that EP4RA acts as an EP4 antagonist. We next exami[illegible] of EP4RA on PGE2 induction of bone formation in young rats. 5-6 week-o[illegible] treated with PGE2 (6mg/kg/day) in the presence or absence of EP4RA (10m[illegible] 12 days. EP4RA suppressed by 81% the increase in trabecular bone volume[illegible] PGE2. This effect was accompanied by a complete suppression of changes in[illegible] calcin, a 54% reduction in the tetracycline labeled surface and 93% reduction[illegible] trabecular number induced by PGE2. Taken together these findings indicated[illegible] inhibited the bone formation induced by PGE2 and support the hypothesis[illegible] anabolic effects of PGE2 in rats are mediated by the EP4 receptor.

SU185

The Transit Amplifying Mesenchymal Progenitor Cell Compart[illegible] the Stem Cell Compartment, is the Principal Site of Control of O[illegible] Production in Normal and Pathologic Bone Remodeling. G. B. D[illegible] Taguchi, I. Gubrij, C. Smith,* A. M. Parfitt, S. C. Manolagas, R. L. Jilka. Div[illegible] Metab, Center for Osteoporosis and Metabolic Bone Diseases, Central Arkansas Healthcare System, Univ. of Arkansas for Med. Sci., Little Rock, AR, USA.

A continuous supply of osteoclasts and osteoblasts is required for the remo[illegible] bone by the bone multicellular unit (BMU). These cells are ultimately deriv[illegible] hematopoietic and mesenchymal stem cells. Stem cells are normally quiescent bu[illegible] high capacity for self-renewal, and also produce a more differentiated population[illegible] amplifying (TA) progenitors. In contrast to stem cells, TA cells proliferate and g[illegible] lose their ability to self renew as they differentiate. By virtue of their proliferative renewal capacity, early TA cells are well-positioned for the minute-to-minute c[illegible] mature cell production. Indeed, studies in mice have demonstrated that changes remodeling are accompanied by corresponding changes in the number of CFU-G[illegible] progenitor of osteoclasts) and CFU-OB - an undifferentiated population of mese[illegible] osteoblast progenitors. However, the proliferative and self-renewal properties of C[illegible] are not well defined; and the relationship of their self renewal to normal and path[illegible] bone remodeling has not been studied.

We now report that ~90% of CFU-OB from marrow of adult mice are dividing[illegible] as indicated by a reduction in their number following administration of 5-fluoro[illegible] kill dividing cells. Using an *in vitro* replating assay, we also show that CFU-OB by 10-20 fold during the first 11 days of culture, but there is little change in their thereafter. Daughter CFU-OB are identical to the parental cell with respect to the[illegible] generate osteoblast-containing colonies of equivalent size, alkaline phosphatase degree of mineralization, and time of onset of osteocalcin production. These findin[illegible] cate that the majority of CFU-OB are not quiescent stem cells but proliferating TA with a finite self renewal capacity. Further, CFU-OB self-renewal is suppressed by gen and aging, which are known to attenuate remodeling and bone formation. Thus estradiol suppresses the production of new CFU-OB *in vitro* by 2-3 fold, with a m[illegible] effect at 1 nM. In contrast, CFU-OB self-renewal is unaffected by 17β-estradiol in c[illegible] from mice lacking ERα (provided by K. Korach, NIEHS, Research Triangle Park, NC), indicating a receptor-mediated effect of the steroid. In addition, self-renewal of CFU-O[illegible] cultures from 19-month-old C57/BL6 mice, or from the SAMP6 murine model of[illegible] related low turnover osteopenia, is 2-4 fold less than that from 4 month old C57/BL6 or control SAMR1 mice. Hence, we conclude that the TA osteoblast progenitor compartment, not the stem cell compartment, is the principal site of control of osteoblast production in the bone marrow. Because proliferation is logarithmic, small changes in TA osteoblast progenitor self-renewal elicited by estrogen and aging could have potentially large effects on the number of osteoblasts available to the BMU.

M215

Role of Small G Proteins in Parathyroid Hormone Signaling in UMR-106 Osteoblasts. J. M. Radeff,* Z. Nagy, P. H. Stern. Molecular Pharmacology and Biological Chemistry, Northwestern University, Chicago, IL, USA.

Small G proteins mediate many important cellular responses. Small G proteins of the Rho and Arf families are activated by lipid modification and subsequently undergo translocation to membranes. Rho A and Arfs activate phospholipase D (PLD), a membrane enzyme that is stimulated by parathyroid hormone (PTH). PLD hydrolyzes phosphatidylcholine, leading to the production of diacylglycerol, which activates protein kinase C (PKC). The PKC signaling pathway contributes to downstream effects on osteoblasts. The current studies were undertaken to determine the effects of PTH on the small G proteins Rho A and Arf and the role of these small G proteins in PTH-stimulated activation of PKC and PTH effects on interleukin-6 expression. Rho A and Arf translocation were determined by cell fractionation and Western blotting. PKC translocation was assessed by immunofluorescence of the PKC isozyme, PKC-alpha. IL-6 expression was determine using a -224/+11 bp promoter construct in a luciferase assay. Both Rho A and Arf were expressed in the UMR-106 cells. Treatment of UMR-106 osteoblastic cells with PTH (10 nM) caused translocation of both Rho A and Arf from cytosolic to membrane fractions, within 1 minute. Brefeldin A (10 ug/ml), a specific inhibitor of Arfs 1-5, inhibited PTH-stimulated PKC-alpha translocation and PTH- and forskolin-stimulated expression of the IL-6 promoter. *Clostridium difficile* toxin B (4 ng/ml), which inhibits a number of small G proteins including RhoA, inhibited PTH-stimulated PKC-alpha translocation and partially inhibited PTH-stimulated, but not forskolin-stimulated expression of the IL-6 promoter. Neither of the inhibitors showed cell toxicity under the conditions used. The results suggest that small G-proteins contribute to the effects of PTH in osteoblasts.

M216

Investigation of the Signalling Pathways Involved in the Calcium Response of Bone Cells to Oscillating Fluid Flow. G. C. Reilly,* C. E. Yellowley, H. J. Donahue, C. R. Jacobs. Orthopaedics and Rehabilitation, Pennsylvania State University College of Medicine, Hershey, PA, USA.

Bone cells have been shown to respond to pulsatile and oscillating fluid flow with an intracellular calcium (Ca^{2+}) response. Previous work in our laboratory has demonstrated cytostolic release of Ca^{2+} from intracellular stores in response to physiological levels of oscillating fluid flow (You et al. Trans ORS, 2000, 0293). Here we further characterize the Ca^{2+} response of bone cells in terms of the channels and signaling pathways that are involved. MC3T3-E1 cells were cultured on quartz slides and loaded with Fura2, a fluorescent indicator of intracellular Ca^{2+} concentration. The slides were mounted in a parallel plate flow chamber on a fluorescent microscope. Cells were subjected to a 3 minute no flow period and then to oscillating fluid flow at 18ml/min for 3 minutes. To identify Ca^{2+} channels and pathways involved, three drug treatments were performed: neomycin, an IP_3 pathway inhibitor, nifedipine, an L-type Ca^{2+} channel blocker and ryanodine, which depletes ryanodine sensitive Ca^{2+} stores. Drug was applied to the cells for 30 minutes before flow and during the no-flow and flow periods.

Effect of the drug treatments on the percentage of cells responding with an increase in Ca^{2+} (at least 3 slides and 116 cells per group):

	NEOMYCIN		NIFEDIPINE		RYANODINE	
	control	treated	control	treated	control	treated
No Flow	3.1	3.9	6.5	0	4.0	6.9
Flow	35.5	4.2	92.0	0	87.4	81.0

Fluid flow caused a large response in terms of the number of cells exhibiting a Ca^{2+} increase, for all experiments more cells responded in flow controls than in no-flow controls (Chi squared $p<0.0005$). Neomycin and nifedipine reduced the number of cells exhibiting a Ca^{2+} response (significantly fewer than flow controls, Chi squared $p<0.0005$). Ryanodine did not reduce the percentage of cells exhibiting a Ca^{2+} response but the amplitude of the response was reduced (from 50±17nM above background in controls to 30±6nM above background in treated cells), this trend did not achieve statistical significance due to low sample size (t-test on mean amplitude $p = 0.1$). These results suggest that the IP_3 pathway is involved in the Ca^{2+} response to oscillating flow as has been shown for steady and pulsatile flow. There is an indication that the ryanodine sensitive stores are involved, in contrast to experiments on the flow response of chondrocytes (Yellowley *et al.* J. Cell Physiol, 1999, p.402). Surprisingly the nifedipine results suggest a role for the L-type Ca^{2+} channel, contrary to the results of studies on steady flow in bone cells (Hung *et al.* J. Biomechanics, 1996, p1411). However nifedipine sensitive channels have been shown to be important for PGE_2 and NO production by osteoblasts in in vivo loading (Rawlinson *et al.* Bone, 1996, p.609).

M217

Adipose Tissue: Derived Stromal Cells are Multipotent. J. M. Gimble, Franklin,*[1] A. Bond,*[1] D. C. Hitt,*[2] G. R. Erickson,*[3] F. Guilak,*[3] W. Q. Wilkison, C. Halvorsen.*[1] [1]Zen-Bio, Inc., Research Triangle Park, NC, USA, [2]Dept. of University of Oklahoma Health Sciences Center, Oklahoma City, OK, USA, [3]D Orthopaedic Surgery, Duke University Medical Center, Durham, NC, USA.

Bone marrow stromal cells are multipotent and differentiate into adipocytes, cytes, and osteoblasts under appropriate culture conditions. In this study, we exa use of adipose tissue, an accessible, abundant and replenishable organ, as an a source for multipotent stromal cells. Stromal cells were isolated from human adipo specimens by collagenase digestion, centrifugation, and adherence to plastic culture in a selective medium. Cells were induced with adipogenic, chondrogenic or o agents and examined by histochemical and molecular methods. In response to ind amethasone and a thiazolidinedione ligand for the peroxisome proliferator activa tory, the stromal cells exhibited the morphologic characteristics of adipocytes. Th adipocytes secreted leptin and expressed the lineage specific gene markers aP2, li lipase, and CAAT/enhancer binding protein α. When cultured in a three-dimensiona matrix, the stromal cells expressed gene markers consistent with chondrocyte diffe in a time dependent manner; these included collagens type II and VI, aggrecan and teins. The presence of transforming growth factor β increased expression of these m response to dexamethasone and vitamin D3, the stromal cells displayed an osteobl type characterized by mineralization of the extracellular matrix, increased alkali phatase activity, increased osteocalcin secretion, and expression of osteopontin, o and bone morphogenetic protein mRNAs. Together, these findings indicate that a sue-derived stromal cells can serve as an alternative to bone marrow-derived stroma tissue engineering applications.

The presenter is a salaried employee of Zen-Bio, Inc. which supported the rese

M218

IL-1 Regulation of Osteoblastic Differentiation in Murine Bone M and Primary Osteoblastic Cultures. M. Tomita, Y. Okada, C. Alander, J. L. G. Raisz, C. C. Pilbeam. Medicine, University of Connecticut Health Farmington, CT, USA.

We compared effects of IL-1 on markers of osteoblastic differentiation in marrow cells (MSC) from long bones and in primary osteoblastic cells (POB) from neonatal of C57Bl/6 X 129 mice. For MSC cultures, cells were plated at 1.5 million / well dishes, and for POB cultures, cells were plated 40,000 / well. To assess osteogenic ation, we compared alkaline phosphatase (ALP) staining with total cell counterst crystal violet (CV); determined ALP activity; assessed mineralization by von Koss and measured mRNAs for ALP, osteocalcin, and type 1 collagen (COL1A1). Ten t of culture with IL-1 (10 ng/ml) did not significantly affect the area of ALP or CV s the ALP/CV ratio. However, IL-1 decreased ALP activity by more than 80%; inhibited mRNA expression for ALP, osteocalcin, and COL1A1; and blocked miner IL-1 also stimulated osteoclast formation in the center of ALP stained colonies and increased RANKL mRNA expression. All effects of IL-1 were mediated by the IL-1 type 1 (IL-1R1), since IL-1 had no effects on MSC cultured from mice with the IL-1 disrupted (IL-1R1-/-). The only difference between IL-1R1-/- and wild type MSC was a 30% decrease in ALP activity in untreated IL-1R1-/- MSC compared to wild t days of culture. In POB cultures, IL-1 (10 ng/ml) decreased COL1A1 mRNA expr day 8, abrogated osteocalcin mRNA expression on day 14 and 21 and blocked miner at day 21. Cell numbers did not differ between IL-1 treated cultures and controls. I to its effects on MSC, IL-1 increased ALP staining and increased ALP activity 5-f day POB cultures. At 14 days of culture there was no difference in ALP activity o between IL-1 treated and control cultures. Based on its inhibition of COL1A1 and cin mRNA expression and its abrogation of mineralized matrix formation, IL-1 i inhibitor of osteoblastic differentiation in both MSC and POB cultures. However, inhibition of osteogenic capacity is not predicted by ALP staining in MSC cultu either ALP staining or ALP activity in POB cultures.

Appendix 18

Characterisation of the glycocalyx of bone cells in order to investigate fluid flow effects

G.C. Reilly, C.E. Yellowley, C.R. Jacobs

Musculoskeletal Research Laboratory, Department of Orthopaedics and Rehabilitation, Penn State College of Medicine, 500 University Drive, PO Box 850- MC H089, Hershey, PA 17033, U.S.A.

Introduction

The glycocalyx is a cell coat composed of glycoproteins and proteoglycans. It has been hypothesised that the glycocalyx contributes toward the ability of bone cells to detect and respond to load-induced fluid flow [1]. However, there is no evidence that there is a glycocalyx around bone cells cultured *in vitro* or around osteocytes *in vivo*, though there is some evidence that proteoglycans are present in the space between the osteocyte membrane and the mineralised tissue boundary [2]. Our long term goal is to investigate the role of the glycocalyx in the response of bone cells *in vitro* to fluid flow. In this study we characterised the glycocalyx of cultured cells and developed a strategy for manipulating its structure. The information gained will contribute to elucidating the role of the glycocalyx in the response of bone cells to mechanical stimuli.

Materials and methods

Lectin binding:

Lectins are proteins which bind specifically to glycocalyx carbohydrates [3]. Fluorescently labelled lectins (Table 1) were dissolved in cell culture medium to a concentration of 50 µg/ml. To demonstrate that the labelled lectins were staining particular sugars, competitive binding tests were performed with specific inhibiting carbohydrates, which were added to the medium at concentrations of 0.2M or 0.5M (Table 1). Osteoblast-like cells derived from mouse calvaria (MC3T3-E1) cells were plated onto slides and incubated with 1 ml of a lectin or the lectin plus its inhibiting sugar and examined under epifluorescence.

Table 1. Lectins used and their inhibiting sugars.

Lectin	Inhibiting sugar
Concanavalin A (Con A)	Glucose
Vicia Villosa Agglutinin (VVA)	N-acetyl-D-galactosamine
Wheat Germ Agglutinin (WGA)	N-acetyl-D-glucosamine

Enzyme effects:

To further elucidate the composition of the glycocalyx, MC3T3-E1 cells were treated with enzymes that digest specific carbohydrate bonds [3]. Plated cells were incubated for 30 mins in the presence or absence of enzymes in the following concentrations: 800 units per ml (U/ml) hyaluronidase, (digests bonds found in hyaluronic acid, chondroitin and chondroitin sulphates) 2.5 U/ml chondroitinase ABC (digests bonds found in chondroitin sulphate) or 0.5 U/ml neuraminidase (liberates sialic acid). Cells were fixed in 3.7% formalin and stained with 0.1% alcian blue in 0.25 M sodium acetate buffer. Alcian blue is a cationic dye which stains proteoglycans, and therefore cell glycocali, because they are negatively charged [3].

Results

All the cells stained with labelled lectin fluoresced brightly and fluorescence was markedly reduced in the presence of an inhibiting sugar (Fig. 1) in a dose dependant fashion. The inhibition effect was strongest for Con A. Enzyme treatment and alcian blue staining showed a reduction in staining for cells treated with hyaluronidase and neuraminidase but no reduction for chondroitinase ABC.

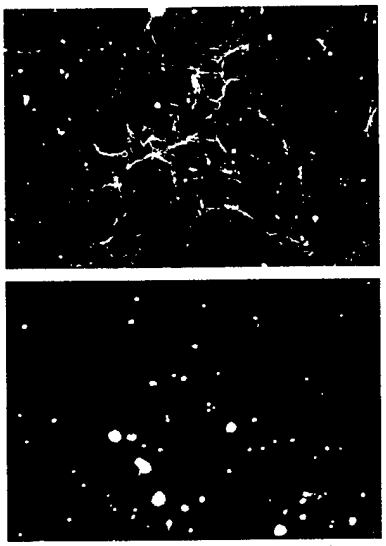

Fig 1: Epifluorescence micrographs of a monolayer of MC3T3-E1 cells incubated with labelled Con A (top) staining brightly and with labelled Con A plus 0.5M glucose (bottom), clearly showing less staining. Field of view 490 µm wide.

Discussion and conclusions

Using lectin staining and enzyme treatment we have demonstrated the presence of a glycocalyx in the MC3T3-E1 osteoblast-like cell line. This is the first direct investigation of the glycocalyx structure in bone cells. The degradation of the glycocalyx by hyaluronidase and neuraminidase suggest that hyaluronic acid and sialic acid groups are present in the glycocalyx of these cells. This is particularly interesting as the theory of Weinbaum et al. [1] suggests an important role for hyaluronic acid in linking the glycosaminoglycan chains to the cell membrane. Interestingly Chondroitinase ABC did not show a reduction in alcian blue staining, which one would have expected if the bone proteins decorin and biglycan (which both contain chondroitin sulphate) formed a large component of the glycocalyx.

The information we have obtained will be crucial to *in vitro* fluid flow studies in which the effect of the glycocalyx is to be examined. Furthermore the technique can be used to compare the composition of the glycocalyx of *in vitro* cultured cells with that of osteocytes *in situ*.

References

[1] S. Weinbaum, S.C. Cowin and Y. Zeng (1994) J. Biomech. 27: 339-360. [2] Y. M. H. F. Sauren, R. H. P. Mieremet, C. G. Groot and J. P. Scherft (1992) The Anatomical Record 232: 36-44. [3] K. A. Haldenby, D.C. Chappell, C. P. Winlove, K. H. Parker and J.A. Firth (1994) J. Vasc. Res. 31: 2-9.

Acknowledgements

This work was supported by the Wittaker Foundation and U.S. Army grant DAMD17-98-1-8509.

MECHANOSENSITIVITY OF RAT OSTEOBLASTIC CELLS DECREASES WITH AGE

Seth W. Donahue, Christopher R. Jacobs, Henry J. Donahue

Musculoskeletal Research Laboratory, Department of Orthopaedics and Rehabilitation, Pennsylvania State University, Hershey, PA 17033

Introduction: Bone adaptation is dependent on the magnitude and frequency of mechanical loading.[2] The ability of long bones, including those of the rat, to adapt to mechanical loading declines with age.[3] *In vitro* experimentation has shown that intracellular calcium spiking is an early signaling response of osteoblastic cells to mechanical loading.[1] We hypothesized that cytosolic calcium oscillations are dependent on the magnitude and frequency of mechanical loading in primary osteoblastic cells isolated from rat long bones. We also hypothesized that intracellular calcium signaling is dependent on the age of the rat from which cells are isolated.

Methods: Osteoblastic cells were isolated from the periosteal surface of long bones from young (4 months) and old (24 months) rats by collagenase digestion. Cells were grown to confluence, then plated on quartz microscope slides at a concentration that reached 70% confluence on the day of experimentation. Fura-2 was used to measure intracellular calcium concentrations in individual cells. Microscope slides were mounted in a parallel plate flow chamber and the cells' fluorescence intensity was digitized during a three minute no flow period and three minutes of oscillating fluid flow that produced shear stresses of 1 or 2 Pa at frequencies of 0.2, 1, or 2 Hz. A calcium oscillation of greater than 50 nM was considered a response.

Results: Resting intracellular calcium concentrations were 20-50 nM. There were spontaneous calcium oscillations in 12% of cells from young rats and in 9% of cells from old rats during the no flow period. Significantly ($p < 0.0001$) more cells displayed calcium oscillations during fluid flow. Cells from young rats (61%) were significantly ($p = 0.026$) more responsive than cells from old rats (41%). The percentage of cells responding was neither frequency nor rate dependent in cells from old rats. However, calcium oscillations in cells from young rats were both frequency and rate dependent. More cells responded to 2 Pa (70%) than 1 Pa (52%). More cells responded to 0.2 Hz (70%) than 2 Hz (49%).

Discussion: Calcium oscillations were dependent on the magnitude and frequency of mechanical loading in osteoblastic cells isolated from young rats; higher magnitude and lower frequency fluid flows were most stimulatory. Osteoblastic cells from old rats were significantly less responsive to mechanical loading than cells from young rats. *In vivo*, rat long bone adaptation to mechanical loading is also magnitude and frequency dependent,[2] and impaired with age.[3] This suggests that intracellular calcium signaling may be an important component of

mechanotransduction in bone. Bone adaptation to mechanical loading may be mediated by the coordinated actions of a network of bone cells including osteoblasts, osteocytes, and bone lining cells. The decreased mechanoresponsiveness of bone cells from older rats may help explain why adaptation is impaired in older rats.

References:

1. Jacobs, C. R., Yellowley, C. E., Davis, B. R., Zhou, Z., Cimbala, J. M., and Donahue, H. J. Differential effect of steady versus oscillating flow on bone cells. J Biomech 31:969-76; 1998.

2. Turner, C. H., and Forwood, M. R. Bone adaptation to mechanical forces in the rat tibia. In: A. Odgard and H. Weinans, Eds. Bone Structure and Remodeling. River Edge, NJ: World Scientific Publishing Co.; 1995; 65-77.

3. Turner, C. H., Takano, Y., and Owan, I. Aging changes mechanical loading thresholds for bone formation in rats. J Bone Miner Res 10:1544-9; 1995.

Acknowledgements:

This work was supported by grants from the U. S. Army (DAMD17-98-1-8509) and the NIH (RO1AG13087).

BED-Vol. 43, 1999 Advances in Bioengineering
ASME 1999

PHYSIOLOGICAL LEVELS OF SUBSTRATE DEFORMATION ARE LESS STIMULATORY TO BONE CELLS COMPARED TO FLUID FLOW

Jun You, Clare E. Yellowley, Henry J. Donahue and Christopher R. Jacobs
The Musculoskeletal Research Laboratory
Department of Orthopaedics and Rehabilitation
The Pennsylvania State University College of Medicine
Hershey, Pennsylvania 17033

ABSTRACT

It is believed that bone cells can sense mechanical loading and alter bone external shape and internal structure to efficiently support the load bearing demands placed upon it. However, the mechanism by which bone cells sense and respond to their mechanical environment is still poorly understood. In particular, the load-induced signals to which bone cells respond, e.g. fluid flow, substrate deformation, electrokinetic effects etc., are unclear. Furthermore, there are few studies focused on the effects of physiological strain (strain< 0.5%, Burr, 1996; Owan, 1997) on bone cells. The goal of this study was to investigate cytosolic Ca^{2+} mobilization (a very early signaling event) in response to different substrate strains (physiological or supra-physiological strains), and to distinguish the effects of substrate strain from those of fluid flow by applying precisely controlled strain without induced fluid flow. In addition, we quantified the effect of physiologically relevant fluid flow (Cowin, 1995) and substrate stretch on the expression of mRNA for the bone matrix protein osteopontin (OPN). A computer controlled stretch device was employed to apply different substrate strains, 0.1%, 1%, 5% and 10%. A parallel plate flow chamber was used to test cell responses to steady and oscillating flows (20dyn/cm^2, 1Hz). Our data demonstrate that physiological strain (<0.5%) does not induce $[Ca^{2+}]_i$ responses in primary rat osteoblastic cells (ROB) *in vitro*. However, there was a significant ($p<0.05$) increase in the number of responding cells at supra-physiological strains of 1, 5, and 10% suggesting that the cells were capable of a biological response. Similar results for human fetal osteoblastic cells (hFOB 1.19) and osteocyte-like cells (MLO-Y4) were obtained. Furthermore, compared to physiological substrate deformation, physiological fluid flow induced greater $[Ca^{2+}]_i$ responses for hFOB cells, and these $[Ca^{2+}]_i$ responses were quantitatively similar to those obtained for 10% substrate strain. Moreover we found no change in osteopontin mRNA expression after 0.5% strain stretch. Conversely, physiological oscillating flow (20dyn/cm^2, 1Hz) caused a significant increase in osteopontin mRNA. These data suggest that, relative to fluid flow, substrate deformation may play less of a role in bone cell mechanotransduction.

METHODS

Cell Culture

We utilized three kinds of bone cells in this study. Primary rat subperiosteal osteoblastic cells (ROB) were obtained from long bones of four-month-old male Fischer-344 rats. Cells were cultured in Dulbecco's modified Eagle medium (DMEM) containing 20% FBS and 1% penicillin and streptomycin. Human fetal osteoblastic cells (hFOB 1.19) were grown in DMEM with nutrient mixture F-12 supplemented with 10% FBS and 1% penicillin/streptomycin. Osteocyte-like cells (MLO-Y4) were cultured in alpha modified essential medium supplemented with 5% FBS and 5% CS. In stretch experiments ROB and hFOB cells were grown on fibronectin coated silicone membranes to enhance adhesion. The coating for MLO-Y4 cells was type I collagen. For the flow experiments, bone cells were cultured on quartz glass slides.

Experimental Approach

Our substrate deformation stretch apparatus consisted of a silicone membrane and a computer controlled ZETA 6104 motor-driven micrometer. One end of the membrane was fixed to the microscope stage and the other end was connected to the micrometer. The motor can perform precise micro-motions (1μm) to apply the desired mechanical strain. Local strains in the substrate were verified by tracking optical markers to confirm that the substrate to which cells attached was accurately deformed. A parallel plate flow chamber was used to applied fluid flow (Jacobs, 1998). The flow rate was quantified with an ultrasonic flowmeter. Cytosolic Ca^{2+} concentration ($[Ca^{2+}]_i$) was quantified using Fura-2 AM. Basal $[Ca^{2+}]_i$ was sampled for 0.5 min followed by 0.5 min of mechanical stretch. For substrate deformation we first induced strains of 0.1% for 0.5 min followed by a 3 min rest period then 1% strain, rest, 5%, rest, 10%, and then rest. Bathing media consisted of Tyrode's saline solution with 2% FBS. Image acquisition and analysis software was used to capture and convert fluorescent signals into real time $[Ca^{2+}]_i$ values. $[Ca^{2+}]_i$ data were analyzed during the no-stretch rest period only. A cell was considered responsive if the maximum change in $[Ca^{2+}]_i$ following the

stretch period was at least 20% over the average oscillation in $[Ca^{2+}]_i$ in the baseline record. Quantitative real time PCR was used to measure the relative changes in mRNA level of osteopontin right before or 72 hours after mechanical stimulation.

RESULTS

The fraction of cells responding with an increase in $[Ca^{2+}]_i$ at different substrate strains is shown in *Figure 1*. The data were obtained from three cell types, ROB (dotted bar), MLO-Y4 (gray bar)

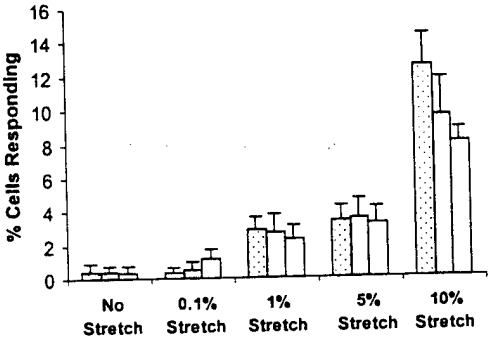

Figure 1

and hFOB (white bar). Each group included 6 individual experiments and roughly 250 total of cells. Less than 1% of cells responded to physiologically relevant strains (0.1%) a value not significantly different from non-strained controls ($p>0.05$) for all these three cell types. However, there was a significant ($p<0.05$) increase in the number of responding cells at supra-physiological strains of 1, 5, and 10% suggesting that the cells were capable of a significant response. Compared to physiological substrate deformation, physiologically relevant fluid flow induced greater $[Ca^{2+}]_i$ responses for hFOB cells (*Figure 2*). Osteopontin mRNA expression levels in hFOB were

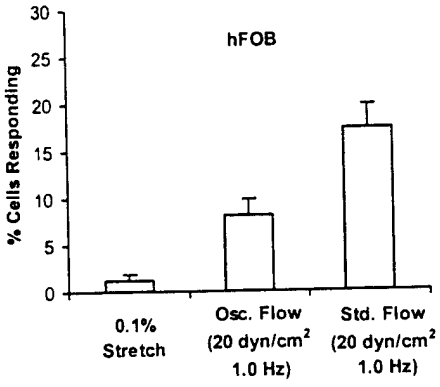

Figure 2

quantified after 0.5% substrate stretch and physiological flow (20 dyne/cm^2, 1Hz). There was no change in osteopontin mRNA expression after 0.5% stretch (*Figure 3*). However physiological oscillating flow increased osteopontin mRNA expression.

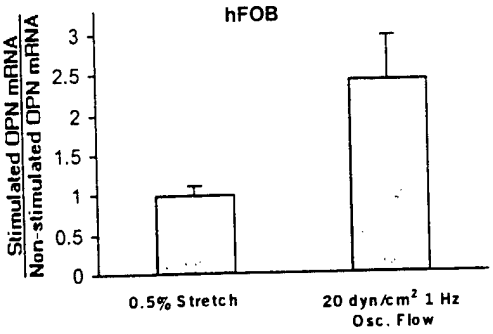

Figure 3

DISCUSSION

A precisely controlled cell stretch device was employed to assess the $[Ca^{2+}]_i$ response of osteoblastic cells to different mechanical strains (0.1% - 10%). Our data demonstrate that physiological strain (<0.5%) does not induce Ca^{2+} responses in three types of bone cells *in vitro*. Larger strains (1-5%) induced a response but only in approximately 5% of total cells. When the strain reached 10%, the $[Ca^{2+}]_i$ responses for bone cells significantly increased. These data support the concept that there may be a threshold for bone cell response to mechanical strain *in vitro*. This threshold appears to be between 5% and 10%. However physiological oscillating flow (20 dyn/cm^2, 1Hz) induced $[Ca^{2+}]_i$ responses which were quantitatively similar to those for 10% substrate strain. Furthermore, the expression of the bone matrix protein, osteopontin, was investigated for physiological stretch and flow. Physiological substrate deformation did not alter osteopontin mRNA expression, but oscillating flow did. These data suggest that, relative to fluid flow, substrate deformation may play less of a role in bone cell mechanotransduction.

ACKNOWLEDGEMENTS

This work was supported by the Whitaker Foundation, NIH RR11769 & AG13087 and The U.S. Army.

REFERENCES

Burr, D. B., Milgrom, C., Fyhrie, D., Forwood, M. R., Nyska, M., Finestone, A., Hoshaw, S., Saiag, E., and Simkin, A., 1996, "In vivo measurement of human tibial strains during vigorous activity," *Bone*, Vol. 18 pp. 405-410.

Cowin, S. C., Weinbaum, S. and Zeng, Y., 1995, "A case for bone canaliculi as the anatomical site of strain generated potentials," *J. Biomech*, Vol. 28 pp. 1281-1297.

Jacobs, C. R., Yellowley, C. E., Davis, B. R., Zhou, Z., Cimbala, J. M. and Donahue, H. J., 1998, "Differential effect of steady versus oscillating flow on bone cells," *J. Biomech*, Vol. 31 pp. 969-976.

Owan, I., Burr, D. B., Turner, C. H., Qiu, J., Tu, Y., Onyia, J. E. and Duncan, R. L., 1997, "Mechanotransduction in bone: osteoblasts are more responsive to fluid forces than mechanical strain," *Amer. J. Physiol.* Vol. 273 C810-C815.

DIFFERENTIAL EFFECT OF OSCILLATING FLUID FLOW ON CYTOSOLIC CALCIUM AND PROSTAGLANDIN IN OSTEOBLASTIC ROS 17/2.8 CELLS

+*Saunders, M M; *You, J; *Yellowley, C E; *Jacobs, C R; *Donahue, H J
+*Musculoskeletal Research Laboratory, Department of Orthopaedics and Rehabilitation, Pennsylvania State University College of Medicine, Hershey, PA 17033.
Dept. of Orthopaedics and Rehabilitation, Hershey Medical Center, 500 University Drive, Hershey, PA 17033, (717) 531-6696, Fax: (717) 531-7583,
msaunder@ortho.hmc.psu.edu

Introduction: It has been previously established that bone adapts to mechanical loading and that this adaptation may play a significant role in pathologic diseases such as osteoporosis. Although the specific mechanisms by which load-induced signals are transduced are unknown, it has been suggested that these signal transduction pathways include biophysical signals such as fluid flow, mechanical stretch, electrokinetic effects and chemotransport. In support of fluid flow as a potent bone cell stimulator which transduces mechanical signals, we and others have previously shown that fluid flow can increase cytosolic calcium concentration ($[Ca^{2+}]_i$) and prostaglandin E_2 (PGE_2) response in osteoblastic and osteocytic cells (1,2). Furthermore, Ajubi, et al. demonstrated that, in osteocytic cells, the PGE_2 response to fluid flow was dependent upon cytosolic Ca^{2+} mobilization. Interestingly, Hung, et al. demonstrated that fluid flow-induced Ca^{2+} responses varied among osteoblastic cell lines. For instance, the rat osteoblastic sarcoma cell line ROS 17/2.8 (ROS) did not respond to fluid flow with an increase in $[Ca^{2+}]_i$ (3). Since cytosolic Ca^{2+} mobilization has been postulated as a second messenger for fluid-induced PGE_2 synthesis in many cell types, we examined the effect of fluid flow on $[Ca^{2+}]_i$ and PGE_2 in ROS cells.

Methods:

Cultures: ROS cells were grown to confluence in polyethylene petri dishes. Cells were maintained in Ham's F12 (phenol red free) supplemented with 10% fetal bovine serum and 1% penicillin/streptomycin at 37°C.

Ca^{2+} Imaging: Preconfluent slides of cells were loaded with 10μL (10μM) fura2-AM, incubated for 45 minutes, washed and inverted on the flow chamber. For steady flow the chamber was connected to a Harvard syringe pump; for oscillatory flow the chamber was connected to a materials testing system via tubing and syringes to deliver a 1Hz sine wave and a shear stress of 20 dyne/cm^2 for 3 minutes preceded by a 1 minute no flow baseline control (1). An image acquisition and analysis software package was used to capture the images and convert the fluorescent signals into ratios which reflect $[Ca^{2+}]_i$.

PGE_2 Assays: Preconfluent slides of cells were inverted on the parallel plate flow chamber and connected to a materials testing system which delivered an oscillatory flow utilizing either a 1 or 2Hz sine wave at 20 dyne/cm^2. Cells were exposed to flow for 1 hour following which media from the inlet and outlet ports of the chamber were collected for PGE_2 analysis using a commercially available assay kit (BioTrak). 1mL of aliquoted media from each chamber was placed in a 2mL tube and frozen at -80°C until assaying of the supernatant.

Results: Calcium imaging was completed on thirty plates of cells (>2000 individual cells). Neither exposure to steady nor oscillatory flow resulted in an increase in $[Ca^{2+}]_i$ in ROS cells (Figure 1) which is in agreement with previous findings (3). To further substantiate the findings and eliminate the possibility that the cells were not viable or that the dye was not functioning, cells were exposed to 10μL of the calcium ionophore, 4-Bromo-Calcium (50μM). In all cases, exposure to the ionophore resulted in a strong increase in $[Ca^{2+}]_i$. This suggests that the failure of ROS cells to respond to fluid flow with an increase in $[Ca^{2+}]_i$ was not a function of technique nor due to a dysfunction in the ability of ROS cells to regulate cytosolic Ca^{2+} homeostasis. Indeed, previous studies have shown that ROS cells have a robust cytosolic Ca^{2+} response to several extracellular signals including parathyroid hormone, vitamin D, ATP and bradykinin, suggesting that they have the machinery to respond to extracellular signals, other than fluid flow, with an increase in $[Ca^{2+}]_i$. Interestingly, while exposure to fluid flow failed to increase $[Ca^{2+}]_i$ in ROS, it did stimulate an increase in PGE_2 (Figure 2). Oscillating flow at 1 (85.2±14.9) and 2 Hz (104.3±17.2) stimulated a 6-fold and 8-fold increase in PGE_2 over the control (12.5±1.9), respectively. There was no significant difference between the responses at 1 and 2 Hz.

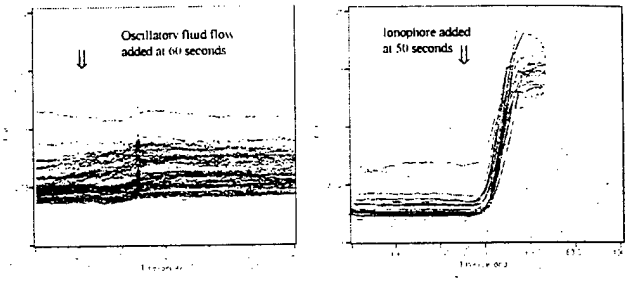

Figure 1. (Left) Typical Ca^{2+} response curve from a 1 minute baseline and 3 minute flow regime. (Right) The ionophore, 4-Bromo-Calcium, was added to the plated cells and a Ca^{2+} response recorded.

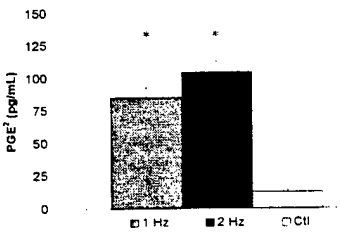

*Figure 2. PGE_2 response of ROS 17/2.8 cells to 1 hour of oscillatory flow at 1 Hz and 2 Hz with a shear stress of 20 dyne cm^2. * Significantly greater than the no-flow control, $p < 0.05$ by t-test.*

Discussion: Although fluid flow has been shown to increase $[Ca^{2+}]_i$ in other osteoblastic cell lines, it did not elicit a Ca^{2+} response in ROS cells even when cells were exposed to oscillating flow which bone cells are more likely to experience *in vivo*. Importantly, fluid flow does stimulate PGE_2 release in ROS cells suggesting that cytosolic Ca^{2+} mobilization is not a critical second messenger in transducing the effects of fluid flow on PGE_2 release. For instance, other second messengers, such as cAMP, may transduce the fluid flow signal into a prostaglandin response in ROS cells. Our results suggest that caution should be taken when extrapolating the effects of biophysical signals, even from one osteoblastic cell line to another. Furthermore, the differential effect of fluid flow on cytosolic Ca^{2+} and downstream effects in ROS cells may prove to be a powerful tool in dissecting mechanotransduction pathways in bone cells.

References: 1)Jacobs C.R. *et al.*, 1998 J. Biomechanics; 2)Ajubi N.E. *et al.*, 1999 Amer. J. Physiol.; 3)Hung C.T. *et al.*, 1996 J. Biomechanics

Acknowledgments: The authors would like to acknowledge Zhiyi Zhou for technical assistance. This work was supported by Army grant DAMD17-98-1-8509, NIH AG 15107 and the Whitker Foundation.

MECHANOTRANSDUCTION IN BONE CELLS VIA OSCILLATING FLOW

-*You, J; **Zhen, X; *Yellowley, C E; *Chen, Q; *Donahue, H J, *Jacobs, C R

+*Musculoskeletal Research Laboratory, Dept. of Orthopaedics & Rehabilitation, Penn State University, Hershey, Pennsylvania. Dept. of Orthopaedics, P.O. Box 850, Hershey, PA 17033, 717-531-4819, Fax: 717-531-7583, jyou@ortho.hmc.psu.edu

INTRODUCTION

External mechanical loading of bone results in a variety of biophysical signals that may affect cellular metabolism and gene expression. Recently one of these physical signals, lacunar-canalicular fluid flow, has been shown to induce a variety of physiological responses linked to bone maintenance, including increased paracrine factor release and gene transcription *in vitro*. However, none of these studies applied oscillating fluid flow, which is what occurs physiologically. Moreover, the biochemical pathways between the mechanical signal (fluid flow) and the biological response (gene transcription) are unclear. The overall goal of this study is to demonstrate that oscillating flow is a potentially important physical signal for bone cells. To achieve this goal, we selected three well-known biological response variables including immediate, intermediate and long timeframe responses. Intracellular calcium, a known second messenger transducing extracellular signals to the cell interior, was our first immediate response variable. Mitogen-activated protein kinases (MAPK) are important for regulating cell differentiation and apoptosis by transmitting extracellular signals to the nucleus. Therefore MAPK were our second intermediate outcome variables. Recently strong evidence suggests that osteopontin (OPN) is an important factor in loading induced bone remodeling. Thus, we quantified OPN mRNA levels as a long timeframe response to oscillating flow. Another goal of this study is to study the relationship between these variables using pharmacological agents.

METHODS

Cell culture and fluid flow chamber: The mouse osteoblast cell line MC3T3-E1 was cultured in α-MEM containing 10% FBS and maintained in 5% CO_2 at 37°C. The fluid flow chamber employed in this study is a parallel plate design. A flow delivery device generated 1Hz sinusoidaly oscillating flow (peak shear stress 2N/m^2). Calcium imaging: Cytosolic Ca^{2+} concentration ($[Ca^{2+}]_i$) was quantified using Fura-2 AM. Basal $[Ca^{2+}]_i$ was sampled for 3 min followed by 3 min of oscillating flow. Bathing media consisted of α-MEM medium with 2% FBS. Image acquisition and analysis software was used to capture and convert fluorescent signals into real-time $[Ca^{2+}]_i$ values (MetaFluor, West Chester, PA). A cell was considered responsive if the peak increase in $[Ca^{2+}]_i$ following the oscillating flow period was at least two-fold greater than that of the average baseline level. MAPK activity assay: There are three major MAPK, p38 MAPK, ERK (extracellular signal regulated protein kinase) and JNK (Jun-N-terminal kinase). 100 μg lysate protein from either control or flowed cells was immunoprecipitated with anti-p38 MAPK, anti-ERK2 or anti-JNK1 antibody overnight. Immunocomplex was collected and the kinase reaction was then conducted in a kinase reaction buffer containing substrates myelin basic protein (for p38 MAPK or ERKs) or c-Jun (for JNK) in presence of [grama-32P] ATP. The reaction mix was subjected to SDS-PAGE. Phosphorylation of substrates was subjected to autoradiogram. Osteopontin mRNA Analysis: Quantitative real-time reverse transcriptase PCR was employed to quantify changes in steady-state osteopontin mRNA levels before and after oscillating flow. Pharmacological agents: The effect of fluid flow on OPN mRNA levels was examined in the presence of thapsigargin, which inhibits the ATP-dependent Ca^{2+} pump of intracellular stores and causes Ca^{2+} discharge, gadolinium chloride, a putative stretch-activated channel blocker, the p38 inhibitor SB203580 or the ERK inhibitor PD98059.

RESULTS

We found oscillating flow stimulates a variety of physiological responses. First, within thirty seconds of starting oscillating flow (peak shear stress 2N/m^2, 1Hz), 59.1±4.6% of cells increased $[Ca^{2+}]_i$ which was significantly different from no flow period (8.9±1.6%). Secondly, two of three MAPK activities were elevated during a two-hour oscillating flow. p38 activity reached a maximum at 30 min and returned to initial levels 90 min after the onset of oscillating flow (*figure 1*). ERK activity at 60 min reached a peak and returned to its non-flow value at 90 min. However, we could not detect a change in JNK activity during 90 min flow stimulation. Third, the long timeframe biological response, OPN mRNA level, was increased approximately four-fold 24 hours after a two-hour oscillating flow stimulation (*figure 2*). Finally, to elucidate the relationship between these variables, different pharmacological blockers were utilized during the flow stimulation. Gadolinium (Gd^{3+}) (10 μM) did not block the oscillating flow-induced increase in OPN mRNA level expression. However thapsigargin (Thapsi.) (50 nM) completely blocked the flow effect on OPN mRNA. Both p38 inhibitor SB203580 (SB) and ERK inhibitor PD98059 (PD) largely attenuated (80%) the flow effect on OPN mRNA. The presence of both inhibitors (SB+PD) completely abolished the effect of flow on OPN mRNA levels.

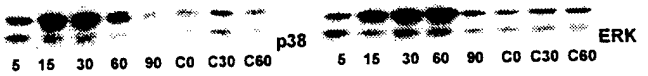

Figure 1. Time courses for p38 and ERK activation during oscillating flow. (C0, C30 and C60 represent control [no flow] time points at 0, 30 and 60 min respectively).

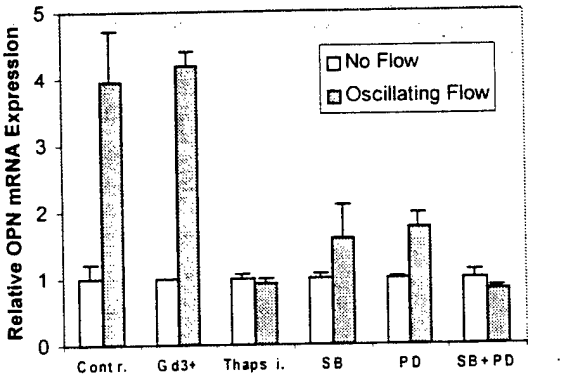

Figure 2. The effects of different pharmacological agents on OPN mRNA levels in response to oscillating flow (peak shear stress 2N m^2, 1Hz). Control was no pharmacological agent present.

DISCUSSION

We have shown that oscillating flow as a biophysical signal induces a variety of physiological responses, including immediate ($[Ca^{2+}]_i$), intermediate (MAPK activity) and long timeframe (OPN mRNA) responses. This strongly suggests that oscillating flow is an important physiological physical signal in bone cell mechanotransduction. Our thapsigargin results indicate $[Ca^{2+}]_i$ is essential for gene transcription, i.e. OPN mRNA expression. However, gadolinium has no effect on OPN mRNA expression which implies that activation of stretch-activated channels is not required. The MAPK blocking data show that there are two possible pathways for oscillating flow to effect OPN gene transcription involving p38 and ERK activities but not JNK. Absence of either of the two will dramatically temper the effects of oscillating flow. In conclusion, oscillating flow as a physiological signal induces intracellular calcium release which is required for OPN mRNA expression involving p38 and ERK, MAPK pathways.

ACKNOWLEDGMENTS

This work was supported by the Whitaker Foundation, NIH RR11769, AG13087, and The Department of Defense Research and Materiel Command.

**Dept. of Pharmacology & Physiology, MCP-Hahneman School of Medicine, Drexel University, Philadelphia, PA 19129.

FLUID FLOW INDUCED CALCIUM MOBILIZATION IS FREQUENCY DEPENDENT

+*You, J; *Yellowley, C E; *Donahue, H J; *Jacobs, C R

+*Musculoskeletal Research Laboratory, Dept. of Orthopaedics and Rehabilitation, Penn State University, Hershey, Pennsylvania. Dept. of Orthopaedics, P.O. Box 850, Hershey, PA 17033, 717-531-4819, Fax: 717-531-7583, jyou@ortho.hmc.psu.edu

INTRODUCTION

It is well known that bone cells can sense mechanical loading and alter bone external shape and internal structure to efficiently support the load bearing demands placed upon it. Recently, fluid flow has been shown to mediate a variety of physiological responses *in vitro*, including increased intracellular calcium concentration and production of prostaglandin E_2, nitric oxide, alkaline phosphatase, collagen type I and osteopontin (1,2,3 and 4). Therefore it is believed that fluid flow is an important biophysical signal in mechanotransduction. However, most investigators have applied steady or pulsing flow profiles rather than more physiological oscillating flow. Also it is controversial which frequencies are most important to bone mechanotransduction, particularly for high frequencies (above 5 Hz). Our hypothesis is that over the wide range of oscillating flow frequencies experienced physiologically bone cells would exhibit a frequency dependent response. To test our hypothesis, we developed a high-frequency flow delivery device to deliver a wide range of sinusoidaly oscillating flow frequencies (0.1Hz to 10Hz) while monitoring real time intracellular calcium mobilization. The second goal of this study is to characterize the response in terms of shear stress and culture stage.

METHODS

Cell culture and fluid flow chamber: The mouse osteoblastic cell line MC3T3-E1 was cultured in alpha-MEM containing 10% FBS and maintained in 5% CO_2 at 37°C. MC3T3-E1 cells have a reproducible phenotype with a distinct proliferative stage and, on reaching confluence, a differentiated stage in which osteoblastic markers such as alkaline phosphatase are expressed. The fluid flow chamber we employed in this study was a parallel plate flow chamber modified to accept quartz glass microscope slides required for the fluorescent imaging technique (5). High frequency flow delivery device: A small servopneumatic loading frame with a high frequency response (EnduraTec, Eden Prairie, MN) was employed as our high frequency flow delivery source. A Hamilton glass syringe was mounted in the loading frame which generated displacement commands resulting in the desired sinusoidaly oscillating flow profile. An ultrasonic flowmeter (Transonic Systems Inc., Ithaca, NY) was utilized to ensure that high frequency flow profiles were accurately delivered to the flow chamber. Calcium imaging: Cytosolic Ca^{2+} concentration ($[Ca^{2+}]_i$) was quantified using Fura-2 AM. Basal $[Ca^{2+}]_i$ was sampled for 3 min followed by 3 min of oscillating flow (peak shear stress 2N/m^2, from 0.1Hz--10Hz). Bathing media consisted of alpha-MEM medium with 2% FBS. Image acquisition and analysis software was used to capture and convert fluorescent signals into real-time $[Ca^{2+}]_i$ values (MetaFluor, West Chester, PA). A cell was considered responsive if the peak increase in $[Ca^{2+}]_i$ following the oscillating flow period was at least two-fold greater than that of the average baseline level.

RESULTS

The fraction of cells responding with an increased $[Ca^{2+}]_i$ to sinusoidaly oscillating flow (peak shear stress 2N/m^2) at different frequencies (0.1Hz to 10Hz) is shown in figure 1. From 0.5Hz to 2.5Hz, the percentage of cells responding increased when the frequency was increased. Beyond 2.5Hz (high frequencies), cell responses decreased, but the cells still exhibited the capacity to respond to oscillating flow. Also the time lag between flow onset and a response observed in a majority of cells was significantly longer at 10Hz relative to lower frequencies. The most stimulatory frequencies were at the low end of range, around the range 0.1Hz. We also found that responding cell numbers were significantly increased when the peak shear stress was elevated from 1N/m^2 to 4N/m^2. Almost 100% of cells responded when peak shear stress reached 4N/m^2. Moreover the fraction of MC3T3 cells responding was observed to depend on stage of differentiation (1, 2 or 3 days culture). The longer the time in culture, the more cells responded.

DISCUSSION

To our knowledge these are the first experiments to examine the effect of high frequency oscillating flow on bone cells. We found bone cells can sense high frequency oscillating flow which may occur due to *in vivo* muscle contraction and impact loads. In a certain frequency range (0.5Hz to 2.5Hz), the fraction of MC3T3-E1 cells responding with an increased $[Ca^{2+}]_i$ became greater when the frequency of oscillating flow increased. This trend agrees with *in vivo* results (6), i.e. dynamic loading can increase bone formation, and suggests that shear stress rate contributes to fluid flow responsiveness. However at very low or high frequencies the $[Ca^{2+}]_i$ responses could not be explained in this way. One possibility is that due to the viscoelastic behavior of the cell membrane, deformation in response to oscillating shear stress at very low frequencies is extremely large, conversely at high frequencies the cell membrane experiences small deformation, and thus need a longer time to sense the extracellular flow motion. The varied calcium responses for a wide range of frequencies reflected many factors involved in bone cell sensitivity. In conclusion, our data indicate that the $[Ca^{2+}]_i$ response to oscillating flow is shear stress and frequency dependent.

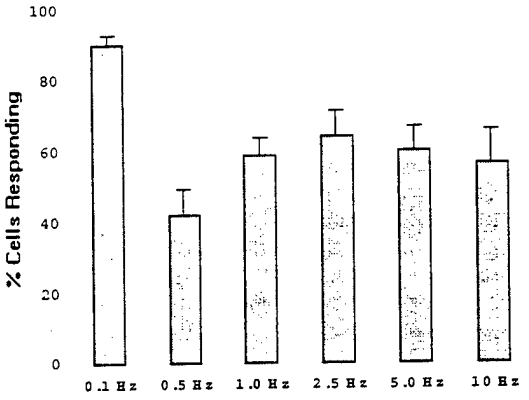

Figure 1. Fraction of MC3T3 cells responding with an increase in $[Ca^{2+}]_i$ at different frequencies.

REFERENCES

1) Hung C.T. *et al.* 1995 Clin. Orthop.; 2) Ajubi N.E. *et al.* 1999 Amer. J. Physiol.; 3) Smalt R. *et al.* 1997 Amer. J. Physiol.; 4) Pavalko F.M. *et al.* 1998 Amer. J. Physiol.; 5) Jacobs C.R. *et al.* 1998 J. Biomech; 6) Turner C.H .*et al.* 1994 FASEB.

ACKNOWLEDGMENTS

This work was supported by the Whitaker Foundation, NIH RR11769, AG13087, and The Department of Defense Research and Materiel Command.